



**US Army Corps
of Engineers®**
Engineer Research and
Development Center

Mid-Bay Islands Hydrodynamics and Sedimentation Modeling Study, Chesapeake Bay

Walter J. Dinicola, Edward T. Fulford,
Mathew R. Henderson, Nicholas C. Kraus, Lihwa Lin,
Ram K. Mohan, Mark Reemts, Ann R. Sherlock,
Jane M. Smith, and Oner Yucel
Edited by Nicholas C. Kraus

August 2006



Front cover image courtesy of NASA: <http://www.chesapeakebayimages.com/history.htm>

Mid-Bay Islands Hydrodynamics and Sedimentation Modeling Study, Chesapeake Bay

Lihwa Lin, Nicholas C. Kraus, Ann R. Sherlock, and Jane M. Smith

*Coastal and Hydraulics Laboratory
U.S. Army Engineer Research and Development Center
3909 Halls Ferry Road
Vicksburg, MS 39180-6199*

Edward T. Fulford and Oner Yucel

*Andrews, Miller, and Associates, Inc.
508 Maryland Avenue
Cambridge, MD 21613*

Walter J. Dinicola, Mathew R. Henderson, Ram K. Mohan, and Mark Reemts

*Blasland, Bouck & Lee, Inc.
326 First Street, Suite 200
Annapolis, MD 21403*

Edited by Nicholas C. Kraus

Final report

Approved for public release; distribution is unlimited

Prepared for U.S. Army Corps of Engineers, Baltimore District
10 South Howard Street, Baltimore, MD 21201
and
Maryland Port Administration
2310 Broening Highway, Baltimore, MD 21224

Under Contract to Maryland Environmental Service
259 Najoles Road, Millersville, MD 21108

ABSTRACT: James Island and Barren Island, in Maryland waters, are among the few remaining eastern shore islands in mid-Chesapeake Bay. Both islands are eroding at a rapid rate due to wave and storm action, as well as to relative sea level rise. These two islands are considered as potential candidate restoration sites as a beneficial use of clean dredged material from the Baltimore Harbor and Channels Federal Navigation Project. The island restoration project requires the construction of protective dikes to contain the dredged material. The restoration work should provide efficient protection to the existing islands, shelter sandy beaches and the shoreline from severe erosion, and improve water quality and surrounding environment for submerged aquatic vegetation. This report describes establishment and operation of a suite of numerical models to evaluate alternative designs as an initial study for restoration and modification of James Island and Barren Island. The predicted wave climate along the mainland shore was also estimated for the alternatives. Both typical and storm hydrodynamic conditions were assessed. In support of the numerical modeling, sediment samples were taken and bathymetric surveys made in key areas, together with assemblage of relevant data sets such as aerial photographs of the shoreline, wind, and presence and vulnerability of submerged aquatic vegetation. Data from the modeling and other data sets assembled and collected were compiled on a DVD.

DISCLAIMER: The contents of this report are not to be used for advertising, publication, or promotional purposes. Citation of trade names does not constitute an official endorsement or approval of the use of such commercial products. All product names and trademarks cited are the property of their respective owners. The findings of this report are not to be construed as an official Department of the Army position unless so designated by other authorized documents.

Contents

Preface	xi
Conversion Factors	xii
1—Introduction.....	1
Background	1
Study Approach.....	5
2—Island Restoration and Design Conditions.....	7
Island Restoration.....	7
James Island Alternatives.....	8
Barren Island Alternatives.....	10
Normal Tide and Large Storm Conditions	10
3—Wave Transformation	13
Wave Transformation Modeling	13
STWAVE model description	13
Wave model inputs	15
Wave Model Results for Shoreline Impacts	19
James Island	19
Barren Island.....	26
Summary	26
4—Hydrodynamic and Sediment Transport Models	32
Hydrodynamic Modeling	32
Sediment Transport Model.....	42
5—Evaluation of Alternatives	47
Response to Waves.....	47
Current Velocity Comparison	48
James Island	56
Barren Island.....	57
Sedimentation.....	58

James Island	62
Barren Island.....	63
Summary	63
References.....	65
Appendix A—Data Acquisition and Baseline Monitoring	A1
Data Acquisition.....	A1
Existing Data Assessment	A2
Sediment type at James Island and Barren Island.....	A2
Chesapeake Bay wind data	A8
Existing hydrographic surveys.....	A14
Aerial photograph	A14
Baseline Coastal Monitoring	A14
Sediment sampling.....	A14
Navigational channels.....	A34
Shoaling	A37
Hydrographic survey.....	A42
Historical shoreline position	A43
Appendix B—Evaluation of Additional James Island Alternatives	B1
James Island Alternatives	B1
Wave Transformation.....	B2
Hydrodynamic and Sediment Transport Modeling	B3
Hydrodynamic modeling with ADCIRC	B3
Hydrodynamic and sediment transport modeling with M2D.....	B7
Hydrodynamics	B7
Sedimentation	B9
Evaluation of Alternatives.....	B11
Current Velocity Comparison	B12
Sedimentation	B13
Summary	B14
Appendix C—Evaluation of Additional Barren Island Alternatives	C1
Study Approach.....	C2
Evaluation of Barren Islands Alts BI-1 to BI-6.....	C2
SAV History at Barren Island	C3
SAV Tolerance	C7
Literature search	C7
UMCES coordination	C10
Alts BI-1 to PI-6 Performance.....	C11
Development and Modeling of Alts BI-7 and BI-8.....	C19
Modeling of Barren Island Alts BI-7 and BI-8	C22
Hydrodynamic Modeling	C22
Current Velocity Comparison	C25
Wave Modeling	C27
Wave Height Comparison	C28

Summary	C29
Conclusions and Recommendations.....	C30

List of Figures

Figure 1. Chesapeake Bay map.....	2
Figure 2. Location map of study area	4
Figure 3. James Island Alts JI-1 through JI-6	9
Figure 4. Barren Island Alts BI-1 through BI-6.....	11
Figure 5. Wave transmission simulations for Hurricane Isabel for breakwater crest elevation of 5.2 ft mtl.....	18
Figure 6. Wave transmission simulations for Hurricane Isabel for breakwater crest elevation of 3.2 ft mtl.....	18
Figure 7. Wave height difference in feet, Alt - existing, northeast grid	20
Figure 8. Wave height difference in feet, Alt – existing, south grid.....	20
Figure 9. Wave height difference in feet, Alt – existing, west grid.....	21
Figure 10. Wave height difference in feet, Alt – existing, northwest grid	21
Figure 11. Wave height difference in feet, future without-project, - existing, northeast grid.....	22
Figure 12. Wave height difference in feet, future without-project – existing, south grid.....	22
Figure 13. Wave height difference in feet, future without-project – existing, west grid	23
Figure 14. Wave height difference in feet, future without-project – existing, northwest grid.....	23
Figure 15. Alongshore wave height variation for James Island existing condition, future without-project, and alternative, northeast grid....	24
Figure 16. Alongshore wave height variation for James Island existing condition, future without-project, and alternative, south grid	24
Figure 17. Alongshore wave height variation for James Island existing condition, future without-project, and alternative, west grid	25
Figure 18. Alongshore wave height variation for James Island existing condition, future without-project, and alternative, northwest grid... .	25

Figure 19.	Wave height difference in feet, Alt BI-1 – existing, northwest grid	27
Figure 20.	Wave height difference in feet, Alt BI-1 – existing, southeast grid .	27
Figure 21.	Wave height difference in feet, Alt BI-2 – existing, west grid.....	28
Figure 22.	Wave height difference in feet, future without-project – existing, northwest grid.....	28
Figure 23.	Wave height difference in feet, future without-project – existing, southwest grid	29
Figure 24.	Wave height difference in feet, future without-project – existing, west grid	29
Figure 25.	Alongshore wave height variation for Barren Island existing condition, future without-project, and Alt BI-1 through BI-6, northwest grid.....	30
Figure 26.	Alongshore wave height variation for Barren Island existing condition, future without-project, and Alt BI-1 through BI-6, southeast grid.....	30
Figure 27.	Alongshore wave height variation for Barren Island existing condition, future without-project, and Alt BI-1 through BI-6, west grid	31
Figure 28.	Regional ADCIRC mesh resolution and shoreline.....	33
Figure 29.	Mid-Bay ADCIRC mesh bathymetry with overbank extensions	33
Figure 30.	Local mesh bathymetry for existing and future without-project conditions	34
Figure 31.	Volume difference for existing and future without-project conditions	34
Figure 32.	NOAA meteorological stations	35
Figure 33.	Measured wind speed and direction at sta 8571892 and 8577330 ...	36
Figure 34.	Measured water level at sta 8571892 and 8577330.....	36
Figure 35.	Measured and calculated water levels at James Island at Gauge JI1385.....	37
Figure 36.	Calculated maximum current fields at James Island under normal tide condition.....	37
Figure 37.	Calculated maximum current fields at Barren Island under normal tide condition.....	38
Figure 38.	Calculated maximum current field at Alt JI-1 under normal tide condition.....	38
Figure 39.	Calculated maximum current field at Alt BI-1 under normal tide condition.....	39
Figure 40.	Hurricane Isabel storm track and a snap-shot of wind field and pressure field at 1800 GMT, 18 September.....	40

Figure 41.	Maximum current fields at James Island during Hazel with and without wave forcing condition	40
Figure 42.	Water level comparison during Hurricane Hazel.....	41
Figure 43.	Water level comparison during Hurricane Isabel.....	42
Figure 44.	Bed change at James Island from Hurricane Hazel.....	44
Figure 45.	Bed change at Barren Island from Hurricane Hazel	44
Figure 46.	Bed change at James Island, Alt JI-3 from Hurricane Hazel	45
Figure 47.	Bed change at James Island, Alt JI-3 from NE20	45
Figure 48.	Bed change at Barren Island, Alt BI-5 from Hurricane Hazel	46
Figure 49.	Bed change at Barren Island, Alt BI-5 from NE20	46
Figure 50.	James Island comparison locations	50
Figure 51.	Barren Island comparison locations	50
Figure A1.	James Island existing boring locations.....	A3
Figure A2.	Barren Island existing boring locations	A4
Figure A3.	Wind data collection locations	A9
Figure A4.	Thomas Point NDBC station wind rose	A11
Figure A5.	CBOS buoy wind rose	A12
Figure A6.	Barren Island NOAA station wind rose	A13
Figure A7.	James Island grab sample locations	A16
Figure A8.	Barren Island grab sample locations	A17
Figure A9.	James Island sediment classification.....	A18
Figure A10.	Barren Island sediment classification.....	A19
Figure A11.	Honga River Federal navigation channel.....	A35
Figure A12.	James Island private watermen channel	A36
Figure A13.	Honga River channel alignments	A37
Figure A14.	Honga River channel, selected shoaling study sections.....	A39
Figure A15.	James Island and Barren Island hydrographic survey area, June 2005	A42
Figure A16.	James Island aerial photograph coverage, 24 July 2005	A43
Figure A17.	Barren Island aerial photograph coverage, 24 July 2005	A44
Figure A18.	James Island shoreline position baselines	A46
Figure A19.	James Island shoreline position and changes	A47
Figure A20.	Taylors Island shoreline position and changes.....	A48
Figure A21.	Hoopers Neck shoreline position and changes.....	A49
Figure A22.	Barren Island shoreline position baselines	A50

Figure A23.	Barren Island shoreline position and changes	A51
Figure A24.	Meekins Neck shoreline position and changes	A52
Figure A25.	Upper Hoopers shoreline position and changes	A53
Figure B1.	James Island alignment Alts 7, 8, and 9	B2
Figure B2.	Example ADCIRC grid refinement in channel	B4
Figure B3.	Predicted tidal ranges during 1-15 January in the James Island region	B5
Figure B4.	Alt JI-8 maximum current field, normal tide	B6
Figure B5.	Alt JI-9 maximum current field, normal tide	B6
Figure B6.	Alt JI-7 M2D model grid	B7
Figure B7.	Alt JI-7 maximum current field, NE33	B9
Figure B8.	Alt JI-7 M2D sedimentation results	B10
Figure B9.	James Island key locations	B12
Figure C1.	Estimated Barren Island SAV areal extent 1971-2004	C3
Figure C2.	Barren Island SAV in 2000	C4
Figure C3.	Barren Island SAV in 2002	C5
Figure C4.	Barren Island SAV in 2004	C6
Figure C5.	Modeling data output points	C12
Figure C6.	Average calculated maximum current velocity in SAV area	C18
Figure C7.	Average calculated maximum wave height in SAV area	C18
Figure C8.	Barren Island Alt BI-7	C20
Figure C9.	Barren Island Alt BI-8	C21
Figure C10.	Alt BI-7 M2D bathymetry	C23
Figure C11.	Alt BI-7 M2D grid	C23
Figure C12.	Alt BI-7 NE20 time-step 45	C24
Figure C13.	Alt BI-8 Hazel time-step 45	C25
Figure C14.	Barren Island output data locations	C26

List of Tables

Table 1.	James Island Alternatives	8
Table 2.	Barren Island Alternatives	10

Table 3.	Peak Water Levels at James Island and Barren Island.....	12
Table 4.	Bathymetry Grid Specifications.....	15
Table 5.	Waves and Water Levels Simulated in STWAVE for James Island..	16
Table 6.	Waves and Water Levels Simulated in STWAVE for Barren Island	17
Table 7.	James Island Save Locations.....	49
Table 8	Barren Island Save Locations	49
Table 9.	Calculated Maximum Current Speed at James Island Under Normal Tide Conditions	51
Table 10.	Calculated Maximum Current Speed at Barren Island Under Normal Tide Conditions	51
Table 11.	Calculated Maximum Current Speed at James Island During Hurricane Hazel	52
Table 12.	Calculated Maximum Current Speed at James Island During Hurricane Isabel	52
Table 13.	Calculated Maximum Current Speed at James Island During NE20	53
Table 14.	Calculated Maximum Current Speed at James Island During NE33	53
Table 15.	Calculated Maximum Current Speed at Barren Island During Hurricane Hazel	54
Table 16.	Calculated Maximum Current Speed at Barren Island During Hurricane Isabel	54
Table 17.	Calculated Maximum Current Speed at Barren Island During NE20	55
Table 18.	Calculated Maximum Current Speed at Barren Island During NE33	55
Table 19.	Calculated Bed Elevation Change at James Island During Hurricane Hazel	58
Table 20.	Calculated Bed Elevation Change at James Island During Hurricane Isabel	59
Table 21.	Calculated Bed Elevation Change at James Island During NE20.....	59
Table 22.	Calculated Bed Elevation Change at James Island During NE33.....	60
Table 23.	Calculated Bed Elevation Change at Barren Island During Hurricane Hazel	60
Table 24.	Calculated Bed Elevation Change at Barren Island During Hurricane Isabel.....	61
Table 25.	Calculated Bed Elevation Change at Barren Island During NE20	61
Table 26.	Calculated Bed Elevation Change at Barren Island During NE33	62
Table A1.	Existing Borings – James Island	A5

Table A2.	Existing Borings – Barren Island	A7
Table A3.	BWI Airport Annual Extreme Wind Speed	A10
Table A4.	James Island Sample Classification Log.....	A20
Table A5.	Barren Island Sample Classification Log	A27
Table A6.	CEM Sample Sediment Characterization	A32
Table A7.	Honga River Shoaling Analysis.....	A38
Table A8.	Honga River Section 1 Shoaling Analysis.....	A40
Table A9.	Honga River Section 2 Shoaling Analysis.....	A41
Table A10.	Summary of Average Annual Shoreline Change for Various Time Periods	A54
Table A11.	James Island Shoreline Change	A55
Table A12.	Taylors Island Shoreline Change.....	A56
Table A13.	Hoopers Neck Shoreline Change.....	A57
Table A14.	Barren Island Shoreline Change	A58
Table A15.	Meekins Neck Shoreline Change.....	A59
Table A16.	Upper Hoopers Shoreline Change	A60
Table B1.	James Island Model Run Save Locations	B11
Table B2.	Calculated Maximum Current Speed at James Island	B13
Table B3.	Calculated Bed Elevation Change at James Island	B14
Table C1.	Barren Island Alternatives	C3
Table C2.	SAV Tolerances.....	C11
Table C3.	Barren Island Alternatives	C13
Table C4.	Barren Island Alternative Plan Evaluation Matrix	C15
Table C5.	Barren Island Alternatives	C19
Table C6.	Calculated Maximum Current Speed at Barren Island During Hurricane Hazel.....	C26
Table C7.	Calculated Maximum Current Speed at Barren Island During NE20.....	C27
Table C8.	Calculated Maximum Wave Heights at Barren Island During Hurricane Hazel.....	C28
Table C9.	Calculated Maximum Wave Heights at Barren Island During NE20.....	C28
Table C10.	Barren Island Alternatives	C30

Preface

This report was produced for the U.S. Army Corps of Engineers, Baltimore District (NAB), and Maryland Port Administration (MPA) under contract with the Maryland Environmental Service. Work was performed by Andrews, Miller & Associates, Inc. (AMA), Blasland, Bouck & Lee, Inc. (BBL), and the U.S. Army Engineer Research and Development Center (ERDC), Coastal and Hydraulics Laboratory (CHL). Ms. Karen Nook Riches, civil engineer, was the NAB Point of Contact and lead technical review for NAB; and Mr. Scott Johnson and Ms. Stacey S. Blersh were the NAB Project Manager and Study Manager, respectively, of the Mid-Chesapeake Bay Island Ecosystem Restoration Feasibility Study. Dr. Stephen E. Storms was the MPA Project Manager and technical reviewer. Ms. Stephanie E. Lindley, Environmental Specialist, and Ms. Karen A. Cushman, Project Manager, were the MES Project Managers and technical reviewers. Dr. Nicholas C. Kraus, Senior Scientist Group, CHL, was the ERDC Project Manager and technical editor of this report.

Chapters 1, 2, 4, and 5 of this report were prepared by Dr. Lihwa Lin, research physical scientist, CHL, Coastal Engineering Branch (CEB), and Dr. Kraus. Chapter 3 was prepared by Dr. Jane M. Smith and Ms. Ann R. Sherlock, research hydraulic engineers, CHL, Coastal Processes Branch. Appendix A was prepared by Mr. Walter J. Dinicola, senior project engineer; Dr. Ram K. Mohan, Vice President; Mr. Mathew R. Henderson, senior engineer; and Mr. Mark Reemts, engineer in training, BBL; and by Mr. Edward T. Fulford, President, and Dr. Oner Yucel, senior coastal engineer, AMA. Appendix B was prepared by the aforementioned staff of BBL. Appendix C was prepared by the aforementioned staff of AMA. Ms. J. Holley Messing, CEB, completed word processing and formatting.

COL Richard B. Jenkins was Commander and Executive Director of ERDC. Dr. James R. Houston was Director.

Conversion Factors, Non-SI to SI Units of Measurement

Non-SI units of measurement used in this report can be converted to SI units as follows:

Multiply	By	To Obtain
acres	4,046.873	square meters
cubic feet	0.02831685	cubic meters
cubic yards	0.7645549	cubic meters
feet	0.3048	meters
knots (international)	0.5144444	meters per second
miles (U.S. statute)	1.609347	kilometers
square feet	0.09290304	square meters
square miles	2,589,998	square meters

1 Introduction

James Island and Barren Island, located in the state of Maryland waters, are among the few remaining eastern shore islands in the mid-Chesapeake Bay. Both islands are eroding at a rapid rate due to wave and storm action, as well as to relative sea level rise that has occurred in the last century. These two islands are considered potential candidate restoration sites as a beneficial use of clean dredged material from the Baltimore Harbor and Channels Federal Navigation Project. The island restoration project requires the construction of protective dikes to contain the dredged material. The restoration work should provide efficient protection to the existing islands, shelter sandy beaches and the shoreline from severe erosion, and improve water quality and the surrounding environment for submerged aquatic vegetation (SAV).

The state of Maryland and the U.S. Army Engineer District, Baltimore (hereafter, Baltimore District), are undertaking studies to determine the technical, economic, and environmental feasibility of protecting, restoring, and creating aquatic intertidal wetland and upland habitat for fish and wildlife at Mid-Chesapeake Bay islands as a beneficial use of clean sediments dredged from the Baltimore Harbor and Channels Federal Navigation Project. James Island and Barren Island are among 105 islands identified under the Dredged Material Management Plan.

This report describes establishment and operation of a suite of numerical models to evaluate alternative designs as a reconnaissance or initial study for restoration and modification of James Island and Barren Island. In addition to evaluation and optimization of design of the islands, the predicted wave climate on the mainland shore was also estimated for the various alternatives considered, as well as changes in conditions at SAV areas, and increased sedimentation in a Federal channel and a private waterman navigation channel located in the study areas. Both normal bay hydrodynamic conditions and storm conditions were assessed. Sediment sampling and bathymetry surveys in key areas of the study were conducted, together with assemblage of relevant data sets such as aerial photographs of the shoreline, wind, and presence and vulnerability of SAV.

Background

Chesapeake Bay is one of the most productive marine ecosystems and the largest estuary in the United States, extending more than 150 miles from its seaward end at the Atlantic Ocean to the bayward end at the entrance to the

Chesapeake and Delaware (C&D) Canal (Figure 1). It serves as a nursery ground for many commercially and noncommercially important species. The bay and its tributaries have a surface area of approximately 4,500 square miles.¹ Water depths in the bay average 20 ft with a maximum depth reaching 175 ft (Schubel and Pritchard 1987). The drainage area of the bay is approximately 64,000 square miles. Fresh water enters the bay from more than 150 major rivers and streams at approximately 80,000 cu ft/sec. Ocean tides enter the bay through the Atlantic Ocean entrance and C&D Canal. The mean range of tides in the bay varies from approximately 1 ft on the western shore to 3 ft at the Atlantic Ocean entrance and in the C&D Canal.

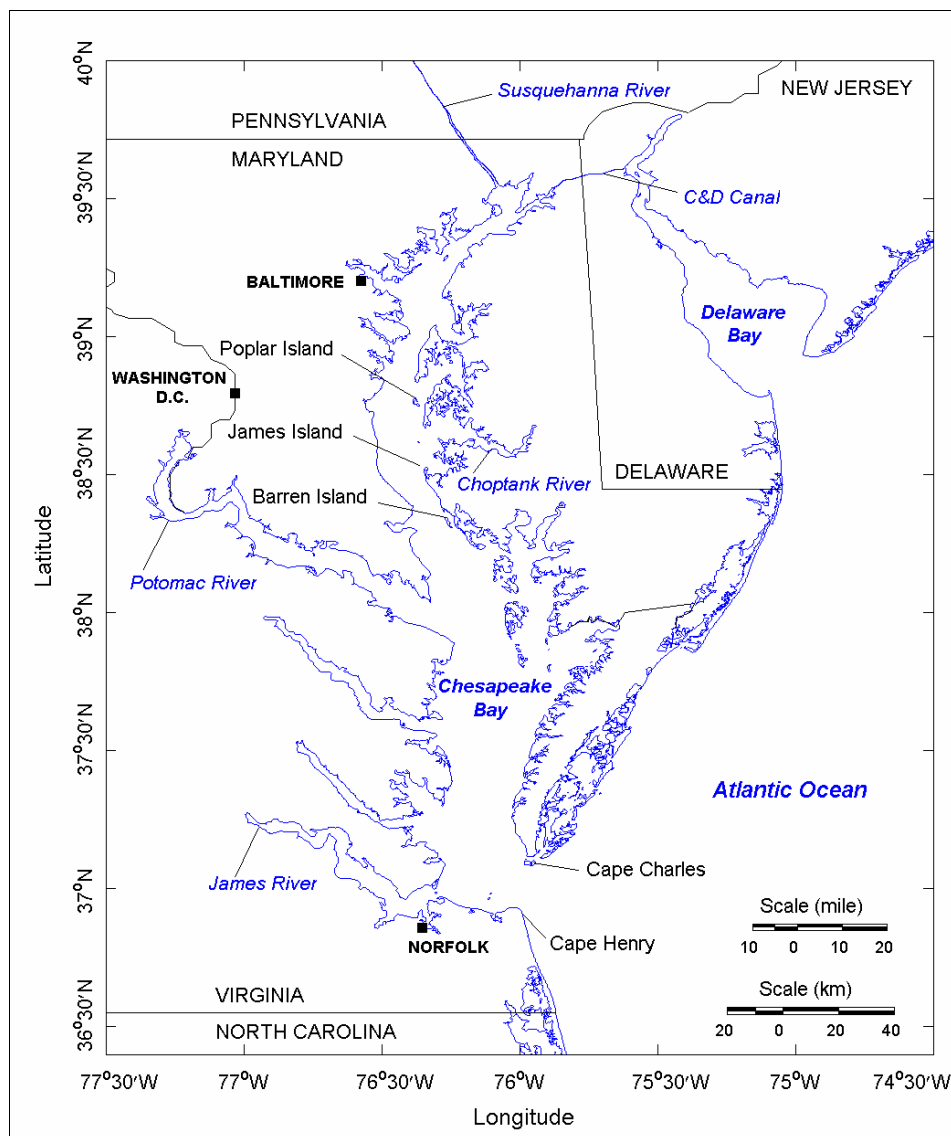


Figure 1. Chesapeake Bay map

¹ A table of conversion factors from non-SI units to SI units of measurement can be found on page xii.

In the last century, rising sea level and frequent flooding have caused extensive erosion to many islands in the bay. According to the National Oceanic and Atmospheric Administration (NOAA), National Ocean Service (NOS), the bay water level has been rising more than 3 mm/year on average for a total of about 1 ft during the last 100 years. As a result, many islands are disappearing, the low-lying land along the bay is turning into open water, and other stretches are flooding. An accelerated sea level rise could eliminate most of the bay's marshes and beaches. The loss of these habitats would be harmful to birds, fish, oysters, and other aquatic life and wildlife.

To address the threat of losing more marsh, beaches and islands, a coalition of Federal, state and nongovernmental agencies has initiated studies and programs to restore critical wetlands and streams and important fisheries habitat throughout the bay. For example, the Poplar Island Environmental Restoration Project, launched in 1998, is a \$427 million restoration project that involves placing material dredged from shipping channels to the previously rapidly vanishing Poplar Island. The island is located 15 miles south-southeast of Annapolis, MD, along the east side of Chesapeake Bay (Figure 2). Use of this dredged material for island and beach restoration is considered beneficial because of the need for sediment as a resource. In Chesapeake Bay, there are eight major ports (Cape Charles, Norfolk, Newport News, Hopewell, Richmond, and Alexandria in Virginia; and Baltimore and Cambridge in Maryland) and a long ship channel extending from the Atlantic Ocean entrance to the C&D Canal, with many local channels leading to major ports. Channels approaching these ports require more than 15 million cu yd of maintenance dredging annually. Most dredged sediments are clean silt and sand suitable for the beneficial use in island and wetland restoration projects.

Baltimore is the chief port on the upper portion of Chesapeake Bay. Channels serving the port require removal of about 3.2 million cu yd/year of dredged material. The placement of dredged material is a continuous and challenging task for the port. As a joint effort, the Maryland Port Administration (MPA) and the Baltimore District have conducted the Poplar Island Environmental Restoration Project (Melby et al. 2005) to reconstruct the island to its approximate size in 1847 using uncontaminated sediment dredged from Baltimore Harbor and approaching channels. Based on the projected capacity of all placement sites in the bay, it would be advantageous to develop additional sites by year 2010.

Chesapeake Bay is typically divided into three regions; Upper Bay, from the Susquehanna River to the Chesapeake Bay Bridge, MD; Mid Bay from the Chesapeake Bay Bridge, MD, to the mouth of the Potomac River; and Lower Bay, from the Potomac River to the Atlantic Ocean. The division of the bay into three zones is not completely arbitrary, but is aligned with the character of the land, rivers, and the Bay waters of each region. Mid Bay includes the eastern half of the Chesapeake Bay from the Chester River to the Maryland-Virginia state line. The salinity of the water in the Mid Bay is transitional and subjected to a great fluctuation between the fresher Upper Bay and salty Lower Bay.

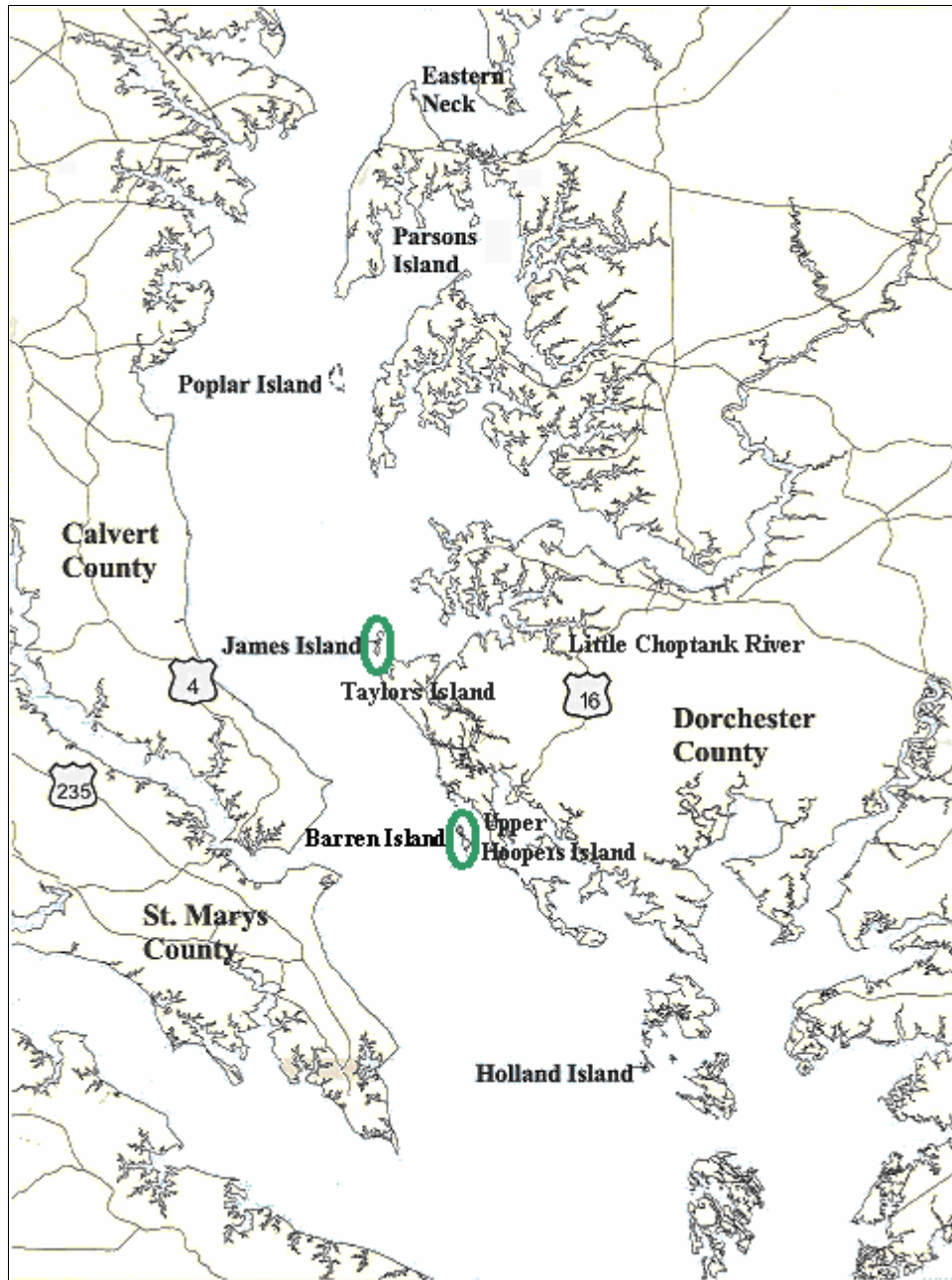


Figure 2. Location map of study area

Water circulation in Mid Bay is controlled by the tide, as well as by wind and waves either from Upper Bay or from Lower Bay. High water level, strong currents, and large waves occur more often in the Mid Bay as a result of frequent subtropical storms (northeasters) and tropical events (tropical storms, hurricanes). Therefore, vanishing marshes, beaches, and wetlands are a natural outcome for islands without adequate protection in the Mid Bay. Among these islands that are in danger of disappearing, Poplar Island is already under a restoration project. James Island and Barren Island are now considered as potential restoration sites. James Island is located in Mid Bay at the mouth of the Little Choptank River,

approximately 17 miles south of Poplar Island (Figure 2). Barren Island is located south and west of Taylors Island and Upper Hoopers Island, approximately 12 miles south-southeast of James Island (Figure 2). The emergent area and volume of these two islands have been rapidly decreasing in the last decade, and the islands may soon disappear if no protection efforts are taken.

Study Approach

The MPA and the Baltimore District are co-sponsoring studies of the technical, economic, and environmental feasibility of protecting, restoring, and creating aquatic intertidal wetland and upland habitat for fish and wildlife at Mid-Chesapeake Bay islands as a beneficial use of clean sediment dredged from the Baltimore Harbor and Channels Federal Navigation Project. James Island and Barren Island are among those identified as potential restoration sites after the Poplar Island Expansion. The study described in this report was performed by the U.S. Army Engineer Research and Development Center (ERDC), Coastal and Hydraulics Laboratory (CHL), and consultants to MES, under contract to MPA [Andrews, Miller & Associates, Inc. (AMA), and Blasland, Bouck & Lee, Inc. (BBL)] to evaluate a number of alternative alignments at James Island and Barren Island restoration sites.

This study had the following goals, with emphasis on storms that would produce the maximum change in physical environmental conditions at the sites:

- a. Perform wave modeling for James Island and Barren Island.
- b. Perform circulation modeling in combination with wave modeling for James Island to establish preliminary tidal gut configurations.
- c. Perform circulation modeling in combination with wave modeling for Barren Island to assess alternatives for protecting the islands and providing flushing within them.
- d. Investigate sediment transport patterns at and around James Island and Barren Island, including sediment shoaling at neighboring navigation channels.
- e. Evaluate engineering merits of environmental impacts of alternative island alignments.

Alternative designs and information for restoration and modification of James Island and Barren Island were defined in close coordination with MPA and the Baltimore District. Operation of wave, circulation, and sediment transport models was conducted for normal tides and four representative extra-tropical and tropical storms. Results from numerical models were analyzed for preliminary evaluation of alternative designs and their impacts on the mainland shoreline, adjacent Federal and private navigation channels, and environmental resources including SAV, oyster bars, and nursery grounds.

For the present study, alternative design of islands considered and storms chosen are discussed in Chapter 2. The wave modeling techniques for James Island and Barren Island are presented in Chapter 3. The circulation model and sediment transport calculation method are described in Chapter 4. The

evaluation and optimization of alternatives based on model results in addition to conclusions and recommendations are given in Chapter 5. This chapter is followed by the references.

This report contains three appendices. Appendix A documents data acquired in this study and the baseline monitoring conducted. Appendices B and C describe additional numerical simulations of hydrodynamics and sediment transport identified as the study progressed and made apart from those covered in the main text of the report for James Island and Barren Island, respectively. Data sets acquired from literature review and physical monitoring, as well as information generated as part of the numerical modeling, were assembled and delivered on DVD media to the sponsors as part of this study.

2 Island Restoration and Design Conditions

James Island and Barren Island are considered as two primary sites in Mid-Chesapeake Bay for wetland and upland restoration by placement of clean sediment dredged from Baltimore Harbor and Channels Federal Navigation Project. Both islands, serving as home to a large wildlife population, are presently eroding at a rapid rate, attributed to storm action and relative sea level rise in the last century (Cronin 2005).

Since the mid-19th century, James Island has diminished from more than 1,300 acres to about 550 acres by the late 1990s.² At present, James Island exists as a group of three small islands with a total surface area of 72 acres above mean tide level (mtl). The continuing erosion has threatened to destroy wetlands and valuable bay grass habitat that the island protects. Barren Island probably had an area of nearly 1,000 acres in the mid 1600s and now is less than 200 acres above mtl.³ Barren Island has been undergoing an initial protection project with the placement of geotubes and dikes along with dredged sediment along its north end for shoreline protection and wetland recreation (http://restoration.noaa.gov/htmls/cwc_case.html).

Island Restoration

Present study efforts for restoration of James Island and Barren Island mainly concern (a) restoration of the island upland and wetland habitat through beneficial use of dredged material, (b) formulation of plans to address problems related to protecting island habitat, wetlands, and SAV, and (c) recommendation of cost-effective solutions for implementation of the project to restore island ecosystem habitat and address dredged material management options. Placement of dredged material at the James Island and Barren Island sites is intended to recreate wetlands and uplands and restore habitats that have been declining for a wide range of species. The sediment removed annually from the approach channels to Baltimore Harbor, approximately 3.2 million cu yd/year, is the main source of material intended for the island restoration. Because James Island is geographically closer to the channels, it is more economical to place the dredged material at James Island than at Barren Island. For Barren Island restoration and

² From the World Wide Web: www.bayjournal.com/article.cfm?article=1093.

³ From the World Wide Web: www.bayjournal.com/article.cfm?article=1116.

protection, it appears more feasible to access material dredged locally from the nearby Honga River Channel.

James Island Alternatives

Alternative alignments for protecting, restoring, and creating wetlands at James Island and Barren Island were investigated in a feasibility study developed concurrently with the present study. For James Island, wetland and upland development of approximately 1,800 acres located west of the existing island was proposed based on the use of clean dredged material from Chesapeake Bay approach channels and environmental benefits from creating and protecting island habitat, the existing island, and SAV. The alignment layout is bounded by James Island to the east, deep water to the west, a natural oyster bar to the north, and a local navigation channel to the south.

The uplands (approximately 932 acres) are located on the northern side, and the wetlands (approximately 1,400 acres) are located on the southern side. The total baseline perimeter dike is 45,235 ft long. The designed upland development should prevent flooding under typical water-level (nonstorm) conditions while effectively flushing the wetlands through primary tidal channels. The design wetland elevation is +1.5 ft mean lower low water (mllw). The dike elevation along the upland perimeter is +25 ft mllw. The wetland dike elevation is +10 ft mllw along western and southern sides, +8 ft mllw along eastern sides, and +6 ft mllw for the interior dike along primary tidal channels.

Six James Island alternatives with three primary tidal channel configurations and two different channel widths were investigated in the present study (Table 1). The primary tidal channel is connected to the bay at the east side of the wetland for maximum protection of the channel. All of these alternatives have a turning basin in the upland southwestern corner with an access channel connecting to the main navigation channel. An unmarked channel used by local watermen exists between the existing James Island and Taylors Island (cf. Appendix A). The alignments of these alternatives are shown in Figure 3.

Table 1
James Island Alternatives

Alternative	Description
JI-1	150-ft-wide y-shaped primary channel.
JI-2	150-ft-wide fork-shaped primary channel.
JI-3	150-ft-wide y-shaped primary channel and a 4-acre bird island at the south channel opening to the bay. The channel around the bird island is 75 ft wide.
JI-4	300-ft-wide y-shaped primary channel.
JI-5	150-ft-wide c-shaped primary channel.
JI-6	300-ft-wide c-shaped primary channel and a 4-acre bird island at the south channel opening to the bay. The channel around the bird island is 150 ft wide.

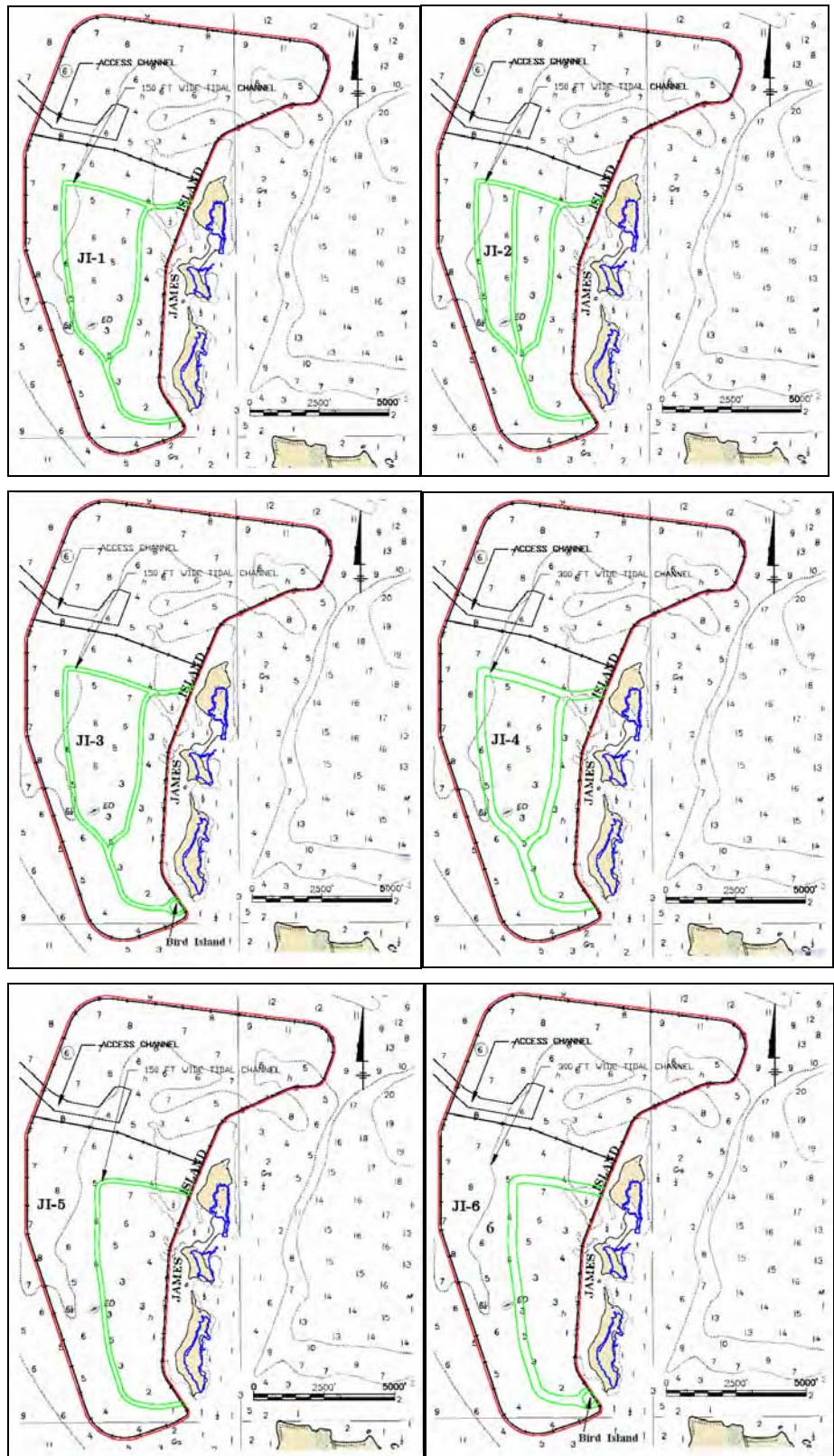


Figure 3. James Island Alts JI-1 through JI-6

Barren Island Alternatives

The proposed Barren Island project emphasizes protection of the existing island and SAV east and south of the island through construction of breakwaters and raising the existing shore protection structure. The design for the protection of the existing island includes a new northern breakwater/sill at +4 ft mllw (3,840 ft), a raised existing northwestern breakwater at +4 ft mllw (4,900 ft), and a new western breakwater at +4 ft mllw (5,915 ft).

The design for additional protection of SAV includes a new southern breakwater that extends southeastward from the island into the bay. The restoration should not increase sediment shoaling in the Honga River Channel that is located to the north and northeast of Barren Island. Six alternatives with four south breakwater configurations and two different south breakwater crest elevations are investigated in the present study (Table 2, Figure 4).

Table 2
Barren Island Alternatives

Alternative	Description
BI-1	8,166-ft-long south breakwater at +6 ft mllw.
BI-2	5,915-ft-long south breakwater at +6 ft mllw.
BI-3	8,166-ft-long south breakwater at +4 ft mllw.
BI-4	5,915-ft-long south breakwater at +4 ft mllw.
BI-5	8,166-ft-long south breakwater at +4 ft mllw with 400-ft segments and 200-ft gaps.
BI-6	8,166-ft-long south breakwater at +4 ft mllw with 500-ft segments and 100-ft gaps.

Normal Tide and Large Storm Conditions

The primary source of the tide in Chesapeake Bay is the progression of the ocean tide through the southern entrance from the Atlantic Ocean. A secondary source is through the C&D Canal from the ocean tide that progresses through Delaware Bay. The characteristics of the actual tide that takes place in the bay depend on the width, depth, and configuration of the estuarine basins and tributaries. The tide in the bay is unusual because one complete wavelength of a semidiurnal tide almost matches the length of the long axis of the bay. That is, when one high tide is reaching the northern end of the bay, the next high tide is just entering the bay near the Chesapeake Bay Bridge Tunnel.

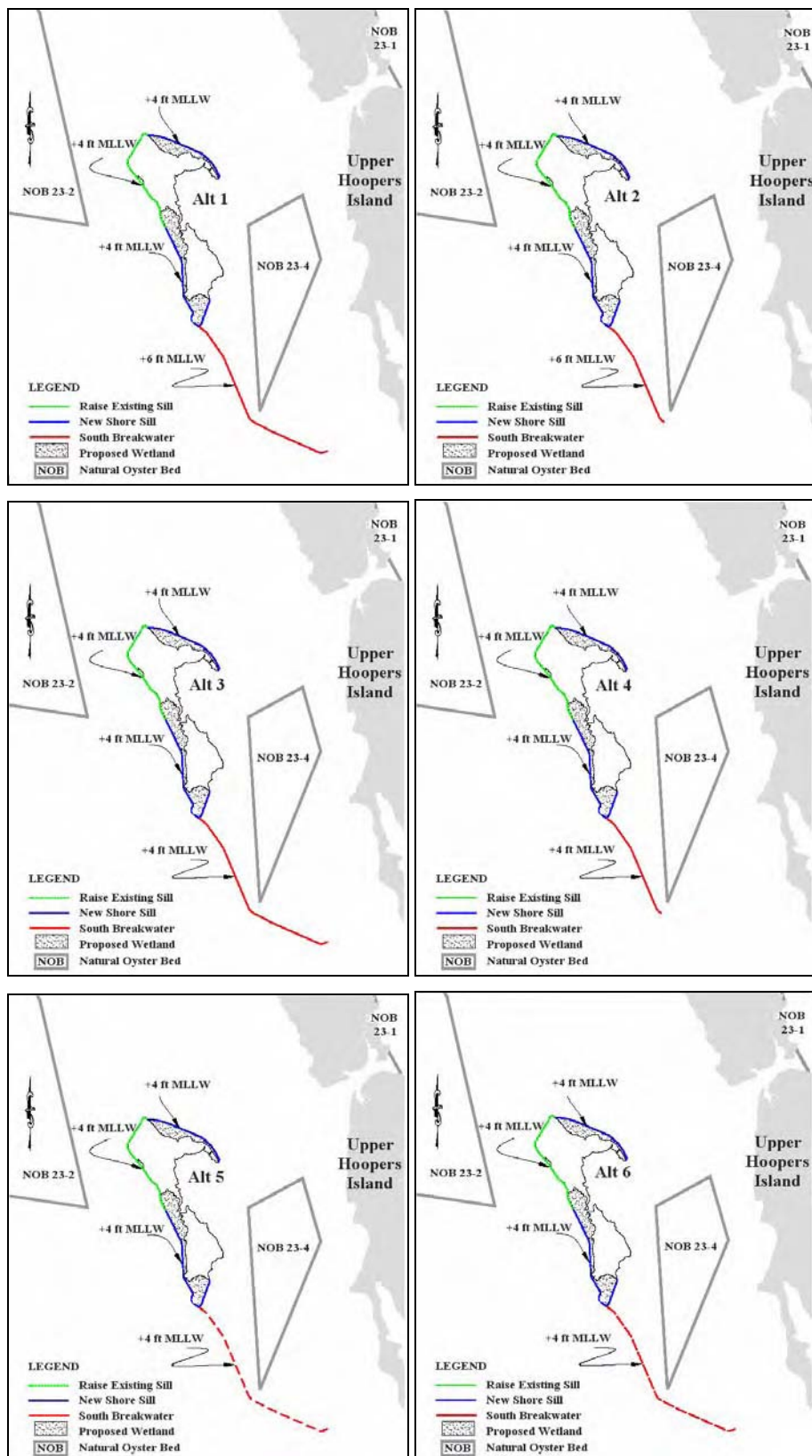


Figure 4. Barren Island Alts BI-1 through BI-6

Water level fluctuations in Chesapeake Bay are dominated by the semidiurnal tide. The mean range of tide (the elevation difference between mean high water and mean low water) in the bay varies from 2.8 ft at the Atlantic Ocean entrance, gradually decreasing to 1 ft near Annapolis, MD, in Mid Bay, and then increasing to nearly 2 ft near Chesapeake City, MD, at the northern end of the bay. The ranges of tide in the tributaries on the western and eastern sides of the bay show significant increases proceeding up the rivers. For example, in the Potomac River, the range of tide near the entrance is just about 1 ft, whereas the range of tide at Washington, DC, is just over 2.6 ft.

Water level in Chesapeake Bay is susceptible to strength and duration of wind speed and direction, barometric pressure changes, and runoff. Higher water level can be produced by changing wind direction to the orientation of the basin during a meteorological event. For example, a local squall line may cause significant change in local water level for a short duration, whereas a large-scale storm can alter the water level in the entire bay for several days. In Chesapeake Bay, relatively frequent meteorological patterns are also seen to significantly alter the water level. A moderate seasonal variation in water level, higher in the summer and lower in the winter, is usually observed in the bay. Therefore, non-astronomical factors, such as the configuration of the shoreline, local bathymetry, and meteorological influences all contribute in altering the water level.

For the island restoration project, it is essential to investigate both normal tide and large meteorological influences for the identified alternatives. In the meteorological case, two strong historical hurricanes, the 1954 Hazel and 2003 Isabel, and two moderate northeasters that occurred in March 1984 and March 1993, were selected for this investigation after examination of many storms. Hurricane Hazel and Hurricane Isabel are categorized as those of a 100-year event that can cause extreme high water levels in the bay. On the other hand, the March 1984 and March 1993 northeasters represent spring and winter moderate storms often seen on a yearly basis. Table 3 presents calculated maximum water levels at James and Barren Islands, respectively, from these four storms (Melby et al. 2005). For Hurricane Hazel and Hurricane Isabel, the calculated maximum water level at James Island and Barren Island ranges from 5 to 5.6 ft, mtl. For the March 1984 and March 1993 northeasters [referred to as NE20 and NE33, respectively, as identified by Melby et al. (2005)], the maximum water level at the two islands range from 2.5 to 2.9 ft mtl, much smaller than water levels associated with strong hurricanes.

Table 3
Peak Water Levels¹ at James Island and Barren Island, ft (mtl)

Storm	James Island	Barren Island
Hurricane Hazel, 1954	5.6	5.0
Hurricane Isabel, 2003	5.5	5.5
Northeaster, March 1984 (NE20)	2.9	2.8
Northeaster, March 1993 (NE33)	2.5	2.5

¹ Calculated maximum water level at existing island.

3 Wave Transformation

In a previous study, wave generation and transformation were modeled to supply information for design of shore protection for the proposed James Island and Barren Island projects (Melby et al. 2005). In the present study, additional wave transformation modeling was performed to assess impacts of the island designs on adjacent shorelines and provide wave input to calculate circulation and sediment transport. This chapter describes the wave transformation model STWAVE, model inputs and outputs, and model results.

Wave Transformation Modeling

Numerical model simulations of wave transformation in Chesapeake Bay were required to provide the relative difference in wave parameters in the local region and at the shoreline for the existing James Island and Barren Island configurations, the planned island alternatives, and estimated future conditions if projects are not constructed. This section describes the STWAVE model, model inputs, and sample model results. STWAVE was forced with directional wave spectra based on typical wave height, period, and direction combinations. The simulations include representative wave and tidal levels, and simulation of two hurricanes (Hazel and Isabel) and two northeasters (NE20 and NE33) summarized in Table 3.

STWAVE model description

The numerical model STWAVE (Smith et al. 2001) was used to transform waves to the project sites. STWAVE numerically solves the steady-state conservation of spectral action balance along backward-traced wave rays:

$$(C_{ga})_x \frac{\partial}{\partial x} \frac{C_a C_{ga} \cos(\mu - \alpha) E(f, \alpha)}{\omega_r} + (C_{ga})_y \frac{\partial}{\partial y} \frac{C_a C_{ga} \cos(\mu - \alpha) E(f, \alpha)}{\omega_r} = \sum \frac{S}{\omega_r} \quad (1)$$

where

C_{ga} = absolute wave group celerity

x, y = spatial coordinates; subscripts indicate x and y components

C_a = absolute wave celerity

- μ = current direction
- α = propagation direction of spectral component
- E = spectral energy density
- f = frequency of spectral component
- ω_r = relative angular frequency (frequency relative to the current)
- S = energy source/sink terms

The source terms include wind input, nonlinear wave-wave interactions, dissipation within the wave field, and surf-zone breaking. The terms on the left-hand side of Equation 1 represent wave propagation (refraction and shoaling), and the source terms on the right-hand side of the equation represent energy growth or decay in the spectrum.

The assumptions made in STWAVE are as follows:

- a. Mild bottom slope and negligible wave reflection.
- b. Spatially homogeneous offshore wave conditions.
- c. Steady waves, currents, and winds.
- d. Linear refraction and shoaling.
- e. Depth-uniform current.
- f. Negligible bottom friction.

STWAVE is a half-plane model, meaning that only waves propagating toward the coast are represented. Waves reflected from the coast or waves generated by winds blowing offshore are neglected. Wave breaking in the surf zone limits the maximum wave height based on the local water depth and wave steepness:

$$H_{m0_{\max}} = 0.1L \tanh kd \quad (2)$$

where

- H_{m0} = zero-moment wave height
- L = wavelength
- k = wave number
- d = water depth

STWAVE is a finite-difference model and calculates wave spectra on a rectangular grid with square grid cells. The model outputs zero-moment wave height, peak wave period (T_p), and mean wave direction (α_m) at all grid points and two-dimensional (2-D) spectra at selected grid points.

Wave model inputs

The inputs required to execute STWAVE are as follows:

- a. Bathymetry grid (including shoreline position and grid size and resolution).
- b. Incident frequency-direction wave spectrum on the offshore grid boundary.
- c. Current field (optional).
- d. Tide elevation, wind speed, and wind direction (optional).

Bathymetry grids. The James Island and Barren Island model grids from the previous study were extended to include the full shoreline section of interest. The same underlying bathymetry was used for each grid, but the grid orientation was changed so the input wave direction was less than 60 deg relative to the x-axis of the grid. The grid specifications are given in Table 4. The grid origin is given in MD State Plane coordinates. The grid orientation is the orientation of the grid x-axis measured counterclockwise from East (Surface-water Modeling System (SMS) interface default). The grid naming convention indicates the approximate incident wave direction. The bathymetry for each grid was interpolated from the ADCIRC bathymetry grid, so the models are consistent. Depths are relative to mtl. Each grid was developed for the existing island configuration and then modified for the island alternatives. The James NE and S grids are the same grids with the origin redefined (rotated 180 deg), and the James NW and W grids are the same grids with the origin redefined (rotated 270 deg). Alts BI-5 and BI-6 required finer grid spacing to resolve the segmented breakwaters. Alts BI-5 and BI-6 grids have the same origin and cover the same domain as the base grid (150-ft resolution), but have higher resolution (50 and 25 ft, respectively).

Table 4
Bathymetry Grid Specifications

Grid	X Origin ft	Y Origin ft	Δx ft	Orientation deg	X Cells	Y Cells
James NE	1,486,470.71	343,645.08	150	255	373	268
James NW	1,467,265.00	333,926.00	150	287	373	328
James S	1,510,820.00	279,197.00	150	75	373	268
James W	1,483,623.20	280,420.75	150	17	328	373
Barren NW	1,494,430.00	242,245.00	150	337	295	211
Barren NW Alt BI-5	1,494,430.00	242,245.00	50	337	885	633
Barren NW Alt BI-6	1,494,430.00	242,245.00	25	337	1,770	1,266
Barren W	1,520,230.00	219,690.00	150	20	145	285
Barren W Alt BI-5	1,520,230.00	219,690.00	50	20	435	855
Barren W Alt BI-6	1,520,230.00	219,690.00	25	20	870	1,710
Barren SE	1,531,110.00	202,800.00	150	80	411	232
Barren SE Alt BI-5	1,531,110.00	202,800.00	50	80	1,233	696
Barren SE Alt BI-6	1,531,110.00	202,800.00	25	80	2,466	1,392

Input wave spectra and water levels. Input wave spectra are required to drive STWAVE on the offshore grid boundary. The definition of offshore changes for each grid, and it is the boundary across which the waves are propagating. Parametric spectral shapes are used to generate the input spectral. The wave energy is distributed in frequency using the TMA spectral shape with a spectral peakedness parameter of 3.3 (Bouws et al. 1985) and in direction using a $\cos^4(\alpha - \alpha_m)$ distribution, where α_m is the mean wave direction. The input spectra have 25 frequencies, starting with 0.05 Hz and incrementing by 0.02 Hz. The directional resolution is 5 deg. The wave parameters run to investigate shoreline impacts for each grid are summarized in Table 5 for James Island and Table 6 for Barren Island. These wave and water level parameters were chosen in coordination with the Baltimore District and are representative of the conditions generated in the previous study (Melby et al. 2005). These parameters do not represent specific storms, but cover the range of conditions. The 1.6-ft, 3-sec waves run without surge for each island and direction are typical conditions. The higher waves and surges represent moderate and strong storm conditions. Statistical analysis on return periods was not performed. Note that the largest waves are produced from hurricanes (generally from the south) and northeasters (producing waves out of the northwest because of the alignment of the bay).

The water depths at the grid input boundary are approximately 60 ft for James NE and S, 100 ft for James NW, and 45 ft for James W. The water depths at the grid input boundary are approximately 100 ft for Barren NW and W and 60 ft for Barren SE. Additionally, Hurricanes Hazel (October 1954) and Isabel (September 2003) and Northeasters 20 (March 1984) and 33 (March 1993) were simulated. These storm waves were used to drive wave-induced currents and sediment transport as discussed in Chapter 4. They were also consulted to investigate SAV survivability (Appendix C).

Table 5
Waves and Water Levels Simulated in STWAVE for James Island

Grid	Grid Shore Normal, deg	Wave Angle, deg	Water Level, ft (mtl)	Wave Height, ft	Wave Period, sec
James NE	15	30	2	5.0	5
			2	3.0	4
			0	1.6	3
James S	195	170	5	10.0	7
			4	7.0	6
			2	3.0	4
			0	1.6	3
James W	253	270	3	4.0	4
			0	1.6	3
James NW	343	343	2	7.0	5
			2	4.0	4
			0	1.6	3

Table 6 Waves and Water Levels Simulated in STWAVE for Barren Island					
Grid	Grid Shore Normal, deg	Wave Angles, deg	Water Level, ft (mtl)	Wave Height, ft	Wave Period, sec
Barren NW	293	340	3	6.5	5
			2	3.0	4
			0	1.6	3
Barren SE	190	170	5	14.0	7
			4	10.0	6
			3	6.0	5
			2	3.0	4
			0	1.6	3
Barren W	250	260	3	3.0	3
			0	1.6	3

Winds and currents. Local wind and currents were not included within the STWAVE domains.

Wave diffraction. STWAVE includes simplified, phase-averaged wave diffraction that allows wave energy to spread behind structures (Smith et al. 2001). Wave energy is also spread behind structures through the directional distribution of wave energy included in the model.

Wave transmission. STWAVE does not include the process of wave transmission through rubble-mound structures, but transmission is significant for the low-crested breakwaters under consideration for the southern end of Barren Island. Wave transmission for Hurricane Hazel and Hurricane Isabel was estimated by reference to guidance from the *Coastal Engineering Manual* (Headquarters, U.S. Army Corps of Engineers (HQUSACE) 2002) (Figure II-7-19) based on transformed wave heights at the toe of the structure and estimates of freeboard (crest elevation above the mean water level), including the surge calculated from the ADCIRC simulations. Then, the structure crest elevation was modified in STWAVE to simulate transmission (lowering the modeled crest elevation allows more wave energy to pass over the structure at elevated water levels, representing the transmission over and through the structure in storms). Figures 5 and 6 show comparisons of transmission for Hurricane Isabel for Alt BI-1 with a crest elevation of +6 ft mllw (+5.2 ft mtl) and Alt BI-3 with a +4 ft mllw (+3.2 ft mtl), respectively. Reducing the crest elevation in the model to an elevation of +2 ft mtl provides the closest comparison to transmission results predicted by the *Coastal Engineering Manual* for the actual +5.2 ft crest elevation (Alt BI-1). For the +3.2 ft crest elevation, the optimal crest reduction was found to be +1 ft mtl. Thus, the crest elevations of the southern breakwater were modified to represent transmission in all Barren Island simulations.

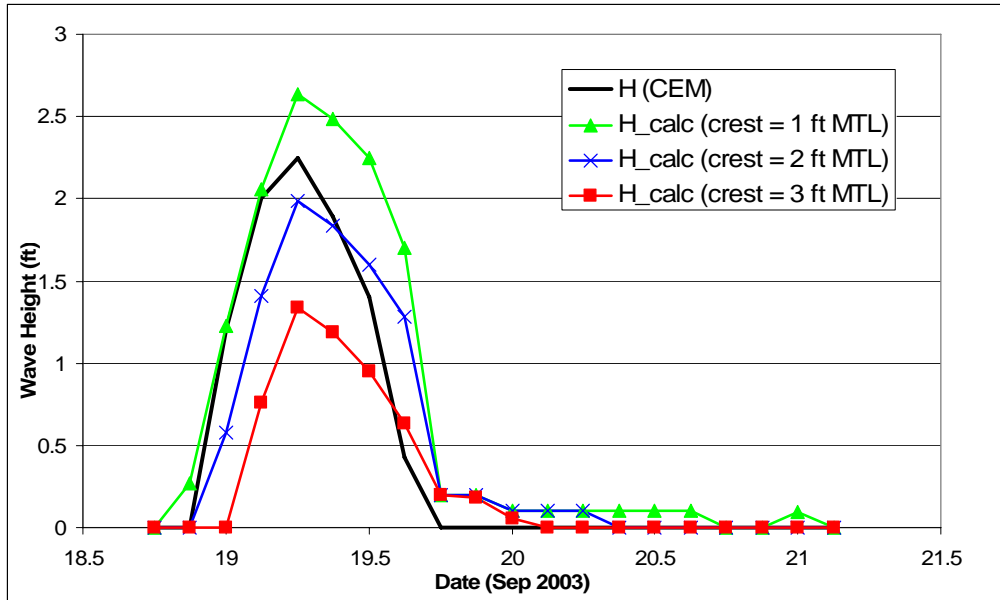


Figure 5. Wave transmission simulations for Hurricane Isabel for breakwater crest elevation of 5.2 ft mtl (6 ft mllw)

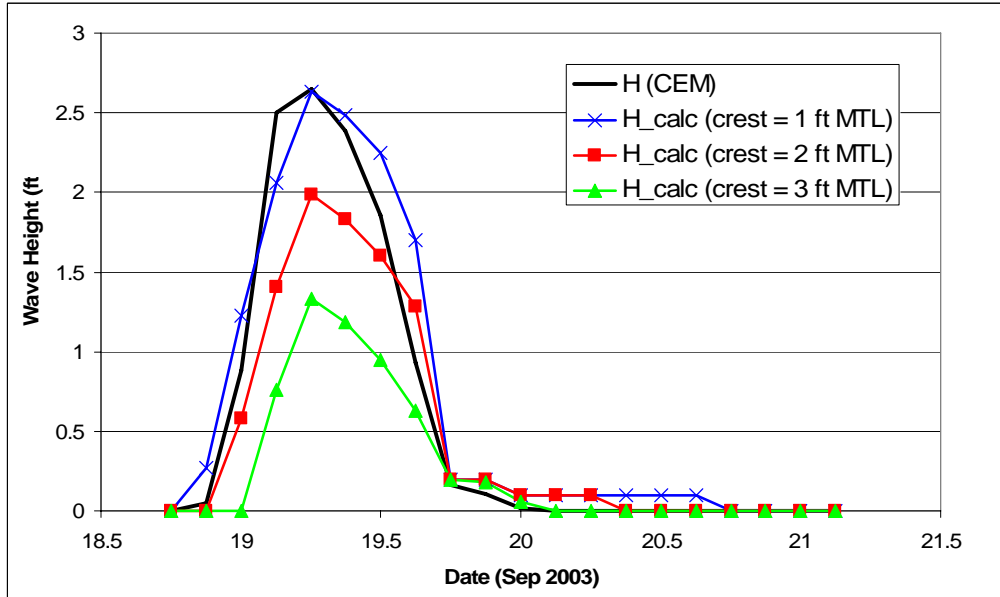


Figure 6. Wave transmission simulations for Hurricane Isabel for breakwater crest elevation of 3.2 ft mtl (4 ft mllw)

Wave Model Results for Shoreline Impacts

Model results to evaluate shoreline impacts are presented in two formats. First, color contour plots of the wave height differences are presented. These plots show the wave heights for selected alternative minus the existing condition, so negative values indicate a reduction in wave height. Blue indicates no difference and red indicates the maximum difference. Note that the scales vary from figure to figure. Land is represented in brown. Figures are provided for the maximum wave condition for each grid orientation in Tables 3 and 4. The lower wave conditions produced similar patterns. Next, plots of the wave height for the existing condition, all alternatives, and an estimate of the future condition without the projects are provided for points along the shoreline. These points are in a water depth of approximately 7 ft away from the islands, and 3-4 ft in the shallow areas in the lee of the islands. The locations of these points are shown as red squares in wave height difference figures. The first point (Point 1) is the most northerly point on each grid and the last point (Point 20) is the most southerly point. The future without-project bathymetries were estimated as erosion of the islands to the surrounding bathymetry elevation.

James Island

All the James Island alternatives have the same external island planform and, therefore, produce the same wave transformation. Figures 7-10 show the wave height differences between the alternatives and the existing condition for the maximum incident wave height for each of the four incident wave directions (northeast, south, west, and northwest grids) and Figures 11-14 show the height differences between the future no-project and the existing conditions for the same wave conditions.

As expected, the maximum differences occur in the lee of the island (relative to the wave direction). James Island is relatively far from the shore, so the impact of the proposed island alternative on the shoreline is relatively small. Figures 15-18 show the alongshore distribution of the wave height for the existing condition, future without-project, and Alts JI-1 through JI-6 (3-7-ft water depth). The island reduces the maximum wave height near the shore by as much as 2 ft. No increases in wave height along the shoreline occurred due to implementation of the alternatives. The future without-project wave heights near the shore are similar to the existing condition, with small increases in height over limited areas.

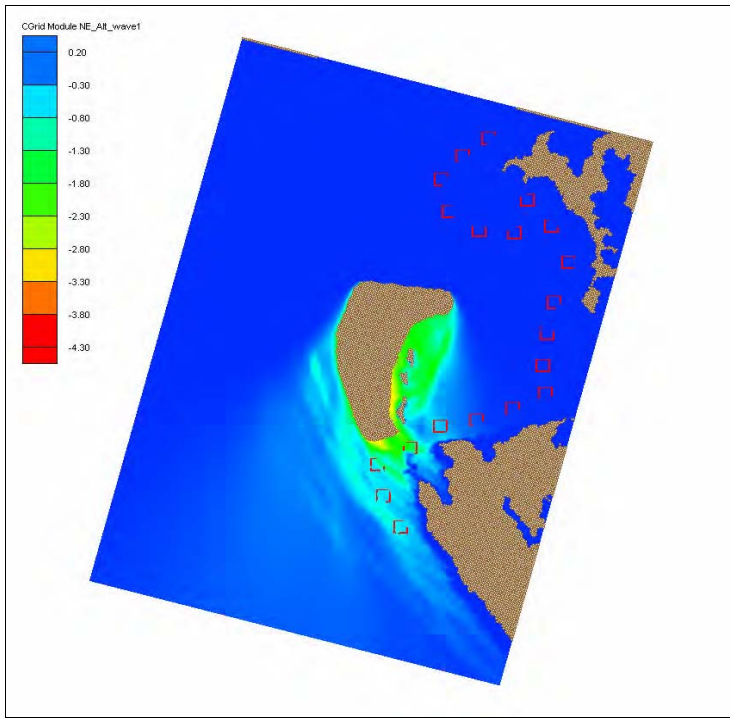


Figure 7. Wave height difference in feet (Alt – existing). Northeast grid, $H = 5.0$ ft, $T = 5$ sec, water level = 2 ft (mtl), wave direction = 30 deg

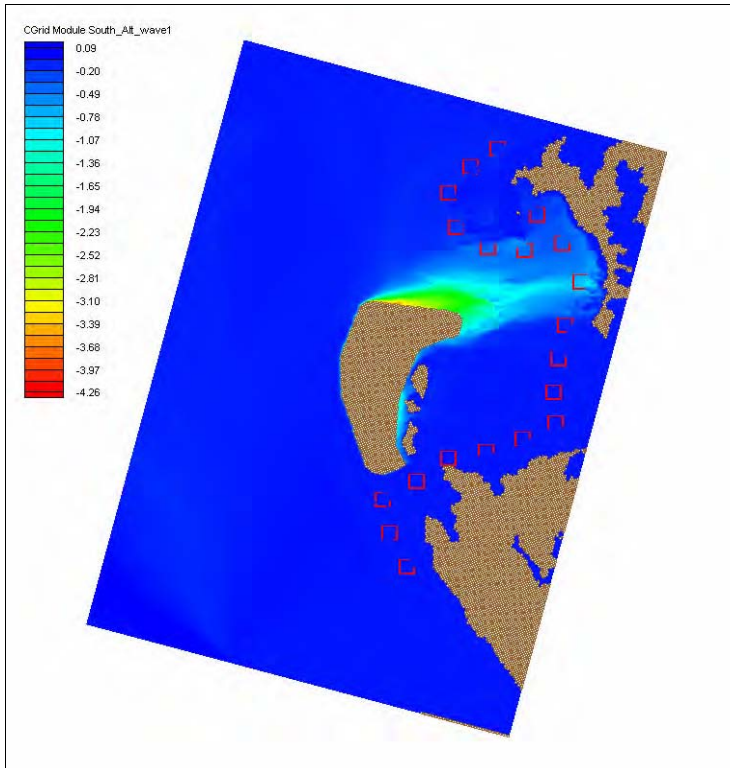


Figure 8. Wave height difference in feet (Alt – existing). South grid, $H = 10$ ft, $T = 7$ sec, water level = 5 ft (mtl), wave direction = 170 deg

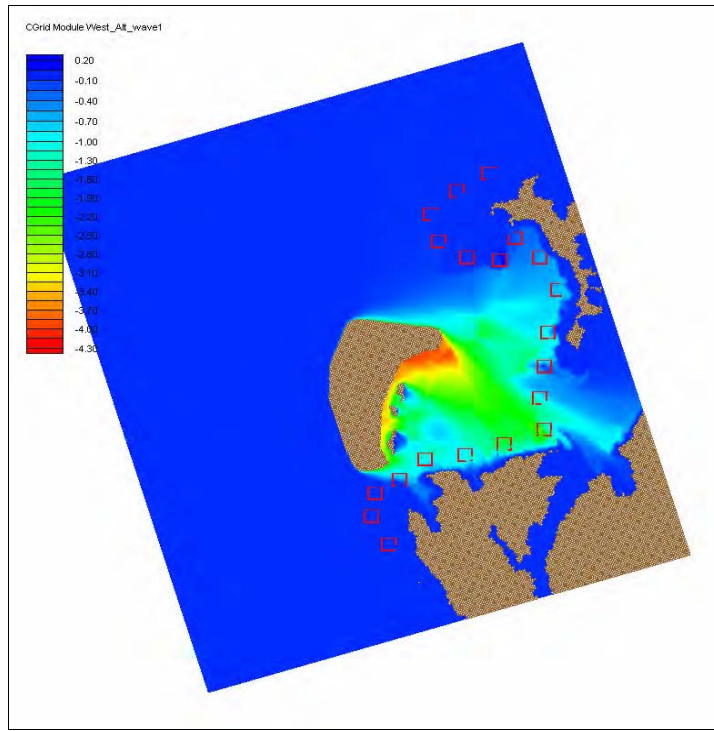


Figure 9. Wave height difference in feet (Alt – existing). West grid, $H = 4$ ft, $T = 4$ sec, water level = 4 ft (mtl), wave direction = 270 deg

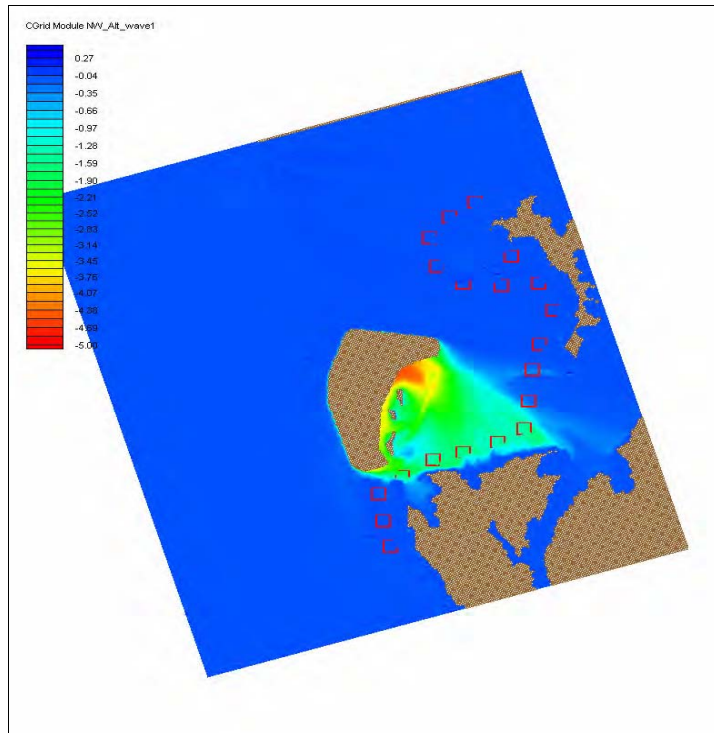


Figure 10. Wave height difference in feet (Alt – existing). Northwest grid, $H = 7$ ft, $T = 5$ sec, water level = 2 ft (mtl), wave direction = 343 deg

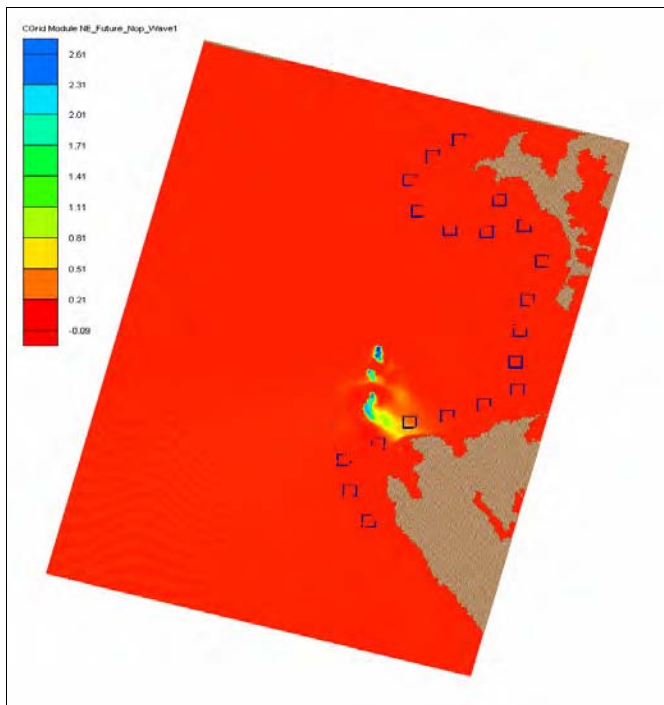


Figure 11. Wave height difference in feet (future without-project – existing).
Northeast grid, $H = 5$ ft, $T = 5$ sec, water level = 2 ft (mtl), wave direction = 30 deg

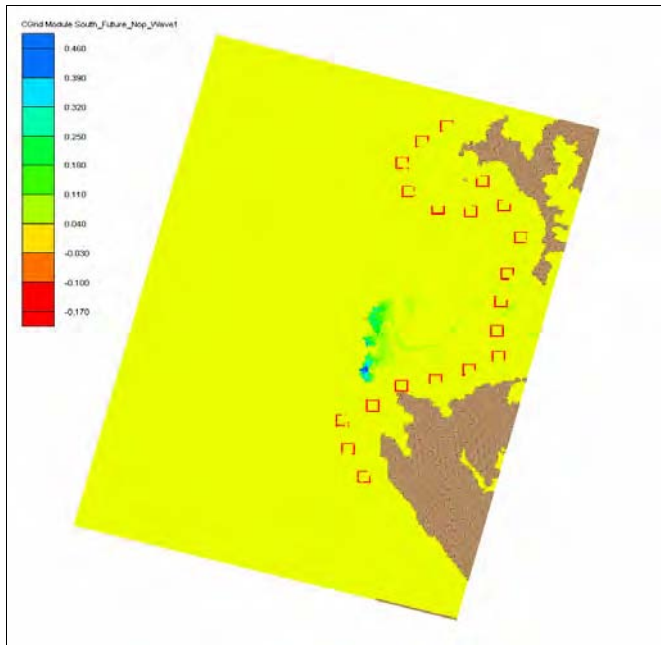


Figure 12. Wave height difference in feet (future without-project – existing).
South grid, $H = 10$ ft, $T = 7$ sec, water level = 5 ft (mtl), wave direction = 170 deg

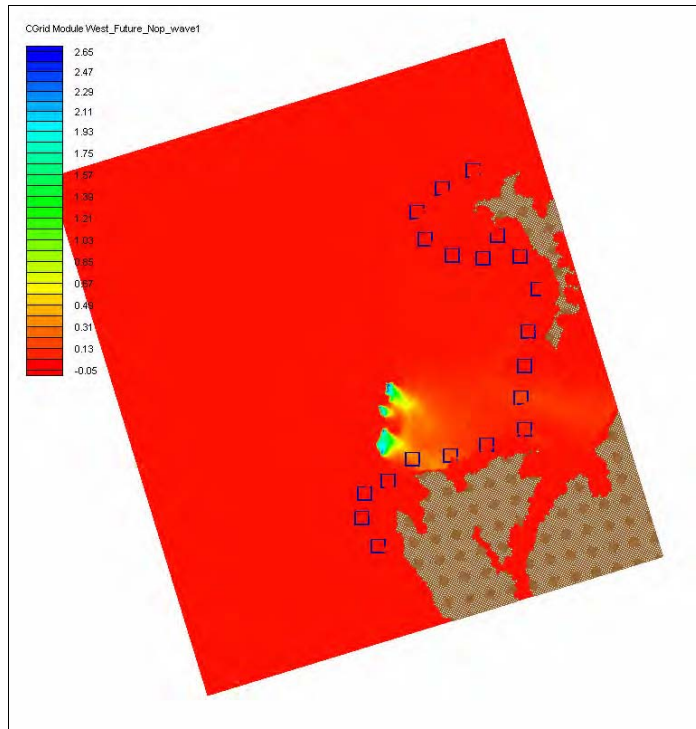


Figure 13. Wave height difference in feet (future without-project – existing). West grid, $H = 4$ ft, $T = 4$ sec, water level = 3 ft (mtl), wave direction = 270 deg

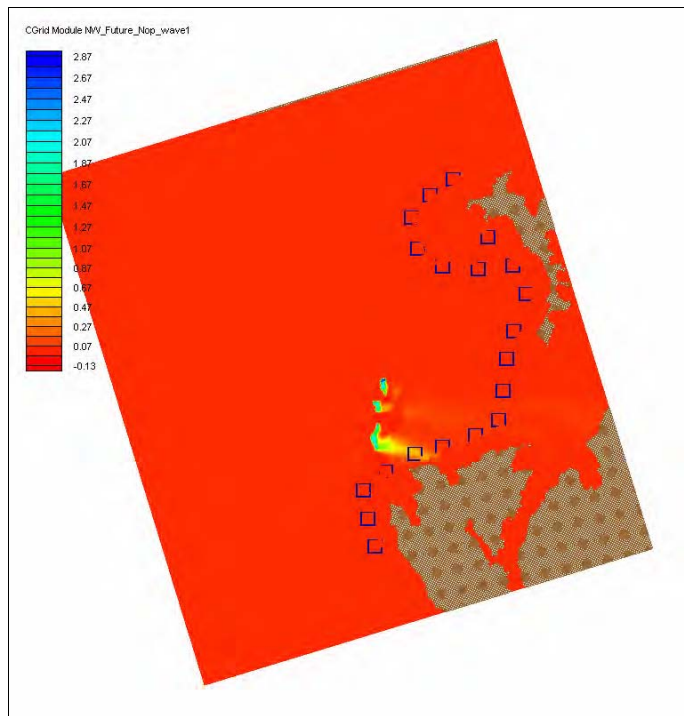


Figure 14. Wave height difference in feet (future without-project – existing). Northwest grid, $H = 7$ ft, $T = 5$ sec, water level = 2 ft (mtl), wave direction = 343 deg

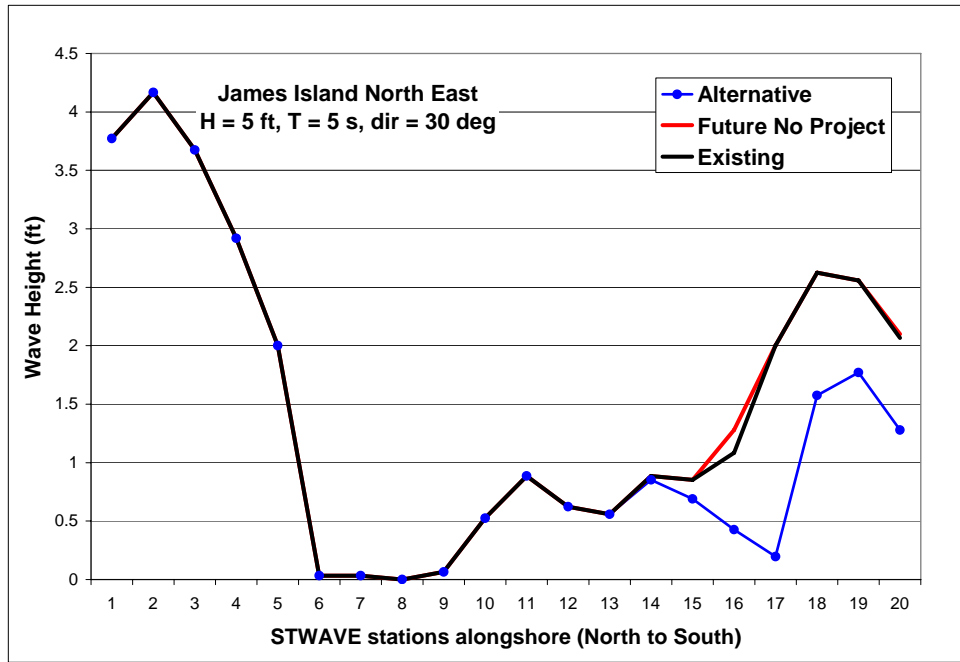


Figure 15. Alongshore wave height variation for James Island existing condition, future without-project, and alternative. Northeast grid, $H = 5$ ft, $T = 5$ sec, water level = 2 ft (mtl), wave direction = 30 deg

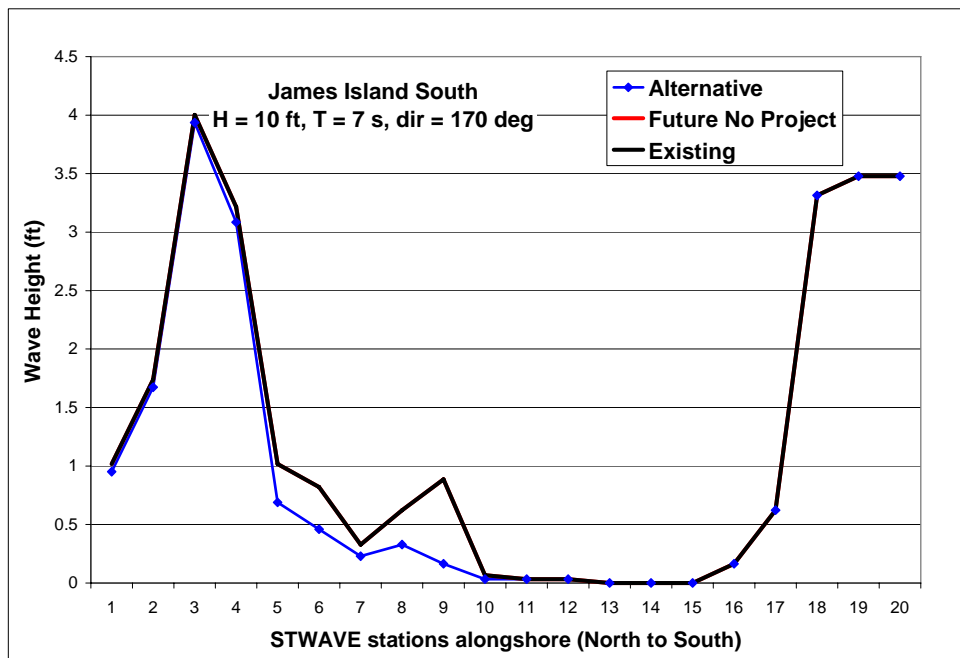


Figure 16. Alongshore wave height variation for James Island existing condition, future without-project, and alternative. South grid, $H = 10$ ft, $T = 7$ sec, water level = 5 ft (mtl), wave direction = 170 deg

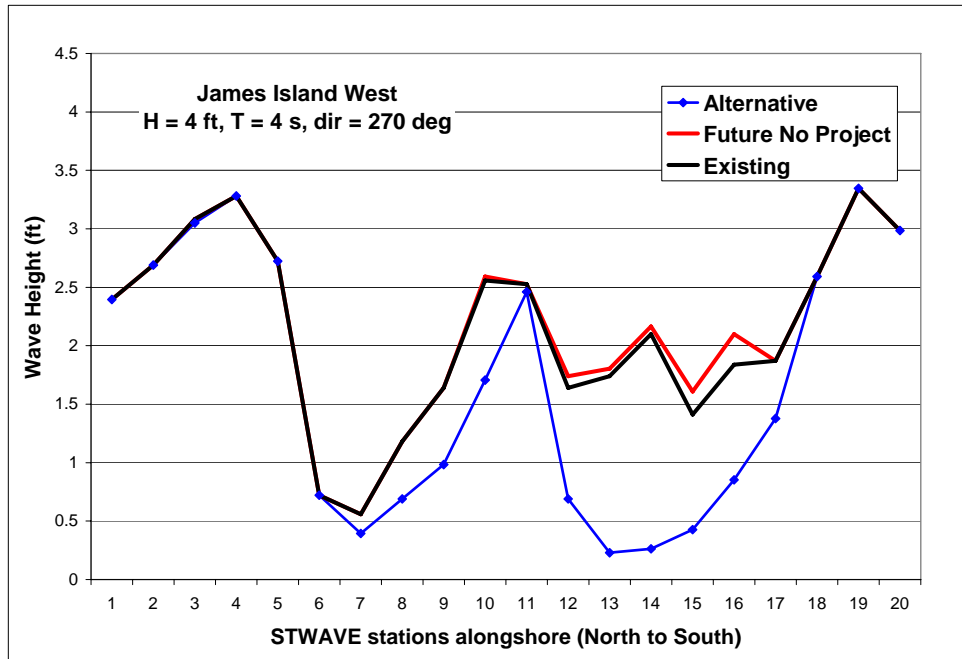


Figure 17. Alongshore wave height variation for James Island existing condition, future without-project, and alternative. West grid, $H = 4 \text{ ft}$, $T = 4 \text{ sec}$, water level = 3 ft (mtl), wave direction = 270 deg

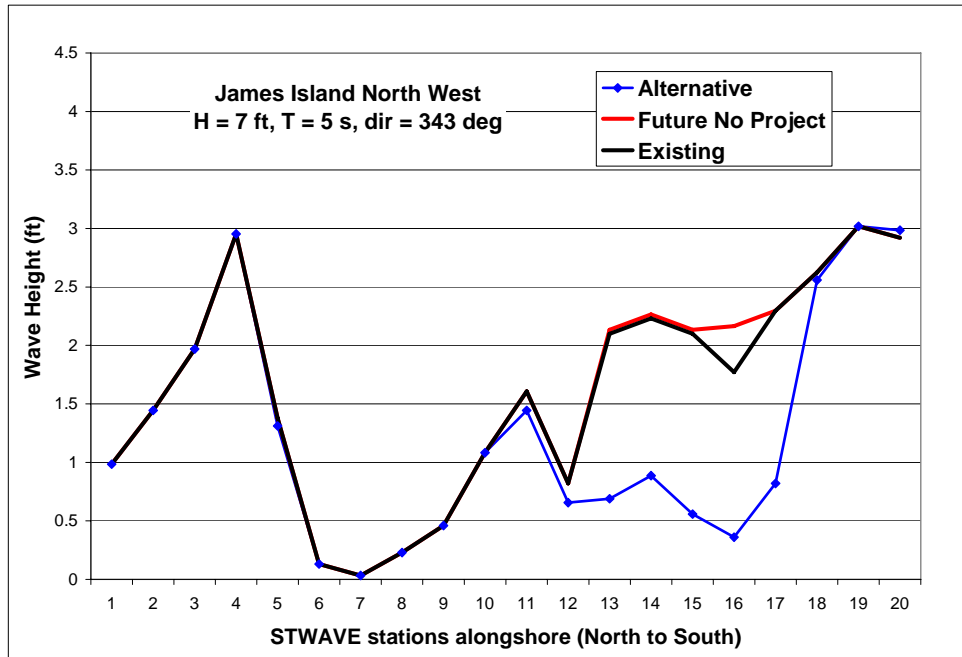


Figure 18. Alongshore wave height variation for James Island existing condition, future without-project, and alternative. Northwest grid, $H = 7 \text{ ft}$, $T = 5 \text{ sec}$, water level = 2 ft (mtl), wave direction = 343 deg

Barren Island

Alts BI-1 though BI-6 required modifications to the bathymetry grid and independent simulations. Figures 19-21 show the wave height differences between Alt BI-1 and the existing condition for the maximum incident wave height for each of the three incident wave directions (northwest, southeast, and west, grids) and Figures 22-24 show the wave height differences between the future without-project and existing conditions for the same wave conditions. As expected, the maximum differences occur in the lee of the south breakwater. Barren Island is relatively close to shore compared to James Island, so the impact of the proposed island alternative on the shoreline is greater. Figures 25-27 show the alongshore distribution of the wave height for the existing condition, future without-project, and Alts BI-1 though BI-6 (3-7-ft water depth). The alternatives reduce the maximum wave height near the shore by up to 4 ft. No increases in wave height along the shoreline occurred due to implementation of the alternatives.

The future without-project wave heights near the shoreline are significantly different than the existing condition. Wave heights at the shore could increase up to 3 ft if the island degrades, thus posing a significant risk by increasing shoreline erosion and potential destruction of SAV habitat. Alt BI-1 provides the greatest reduction in wave height at the shoreline because it has the greatest length and highest crest elevation (+6 ft mllw). Alt BI-3 provides the next highest protection (crest elevation of +4 ft mllw), followed by Alts BI-5 and BI-6 (segmented breakwaters) and Alts BI-2 and BI-4 (crest elevations of +6 and +4 ft mllw, but shorter breakwater length). Alt BI-5 has a crest elevation of +4 ft mllw and 200 ft breakwater gaps, and Alt BI-6 has a +4 ft mllw crest with 100-ft gaps. These two alternatives provide approximately the same wave reduction at the shoreline.

Summary

Modifications to wave transformation due to the James Island and Barren Island alternatives were modeled for two hurricanes, two northeasters, and representative wave conditions with the wave model STWAVE. The James Island alternatives expand the footprint of the island and reduce the wave height in the lee of the island by 1-2 ft. The future without-project condition increases the wave height at the shoreline slightly. Barren Island alternatives include six breakwater extensions to the south of the island. Alt BI-1 and Alt BI-3 reduce the wave height 2-3 ft at the shoreline in the lee of the island (greater reduction for Alt BI-1 with the greater breakwater crest height). Alts BI-2 and BI-4 (shorter overall breakwater length) provide approximately 0.5 ft less reduction in wave height than Alts BI-1 and BI-3 and the reduction is over a smaller region. Alts BI-5 and BI-6 are segmented breakwaters. They provide approximately 0.5 ft less reduction in wave height than Alts BI-1 and BI-3, but over a similar region. The future without-project condition results in a 2-4-ft increase in wave height at the shoreline, thus having the potential to adversely impact SAV habitats, as well as the shoreline. None of the alternatives considered for James Island and Barren Island increased the wave height at the shore.

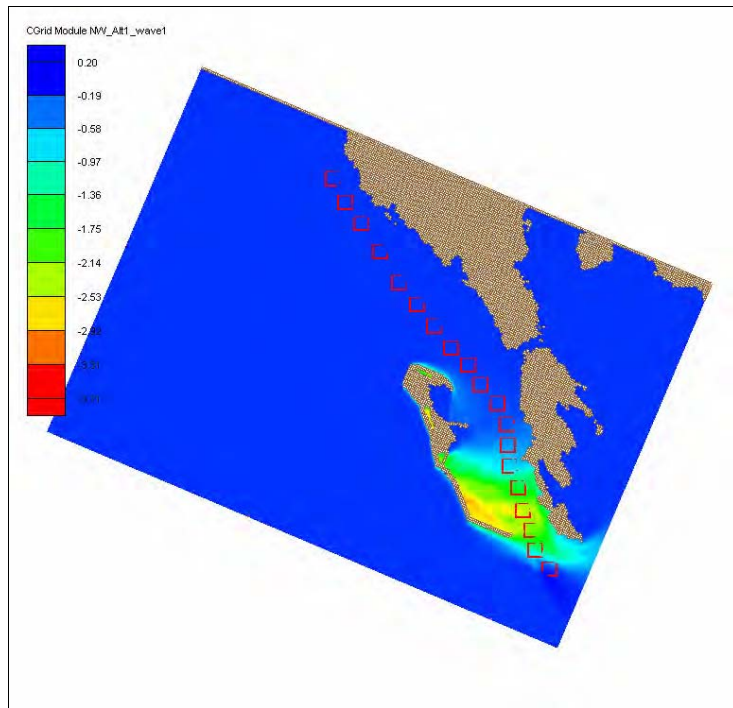


Figure 19. Wave height difference in feet (Alt Bl-1 – existing). Northwest grid, $H = 6.5$ ft, $T = 5$ sec, water level = 3 ft (mtl), wave direction = 330 deg

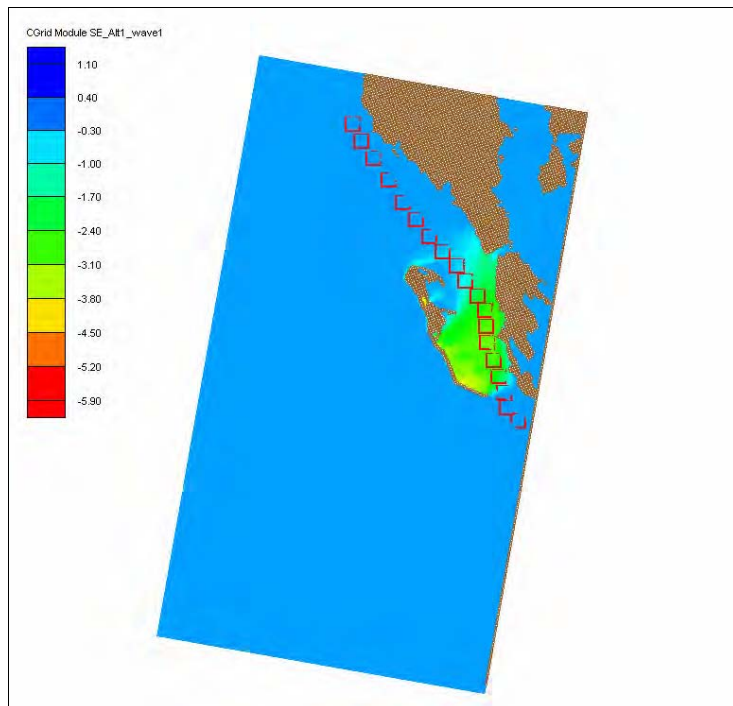


Figure 20. Wave height difference in feet (Alt Bl-1 – existing). Southeast grid, $H = 14$ ft, $T = 7$ sec, water level = 5 ft (mtl), wave direction = 170 deg

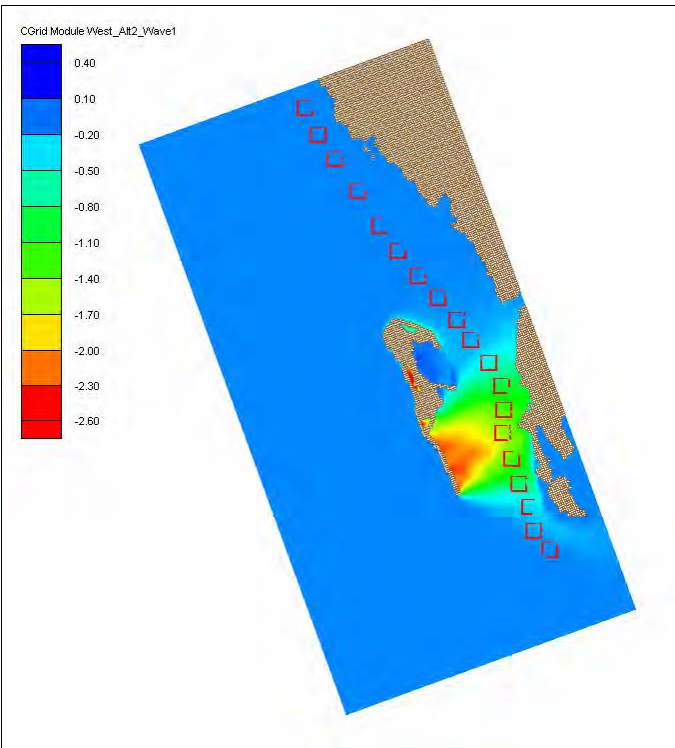


Figure 21. Wave height difference in feet (Alt BI-2 – existing). West grid, H = 3 ft, T = 3 sec, water level = 3 ft (mtl), wave direction = 260 deg

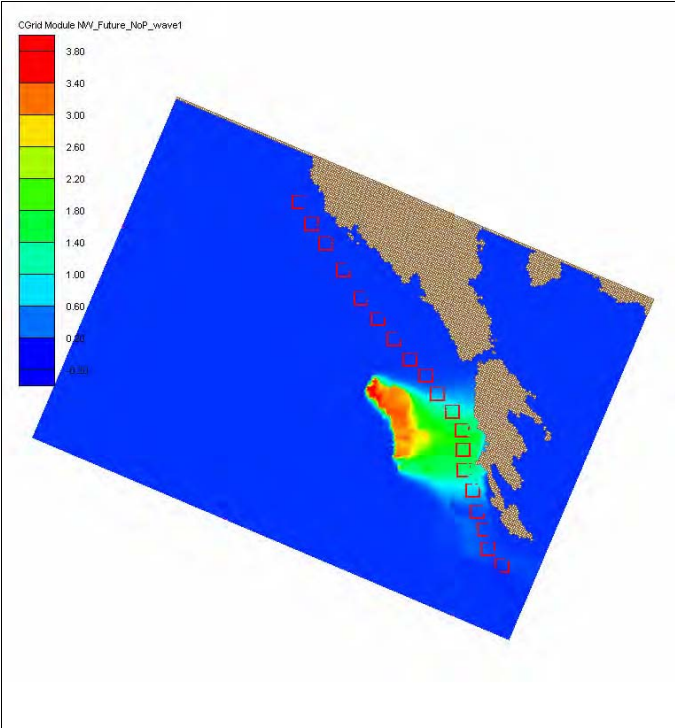


Figure 22. Wave height difference in feet (future without-project – existing). Northwest grid, H = 6.5 ft, T = 5 sec, water level = 3 ft (mtl), wave direction = 340 deg

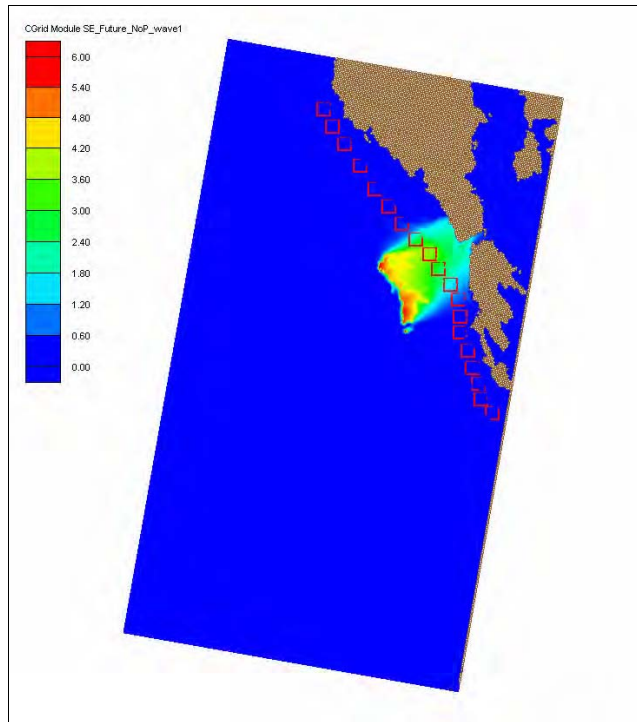


Figure 23. Wave height difference in feet (future without-project – existing).
 Southeast grid, $H = 14$ ft, $T = 7$ sec, water level = 5 ft (mtl), wave direction = 170 deg

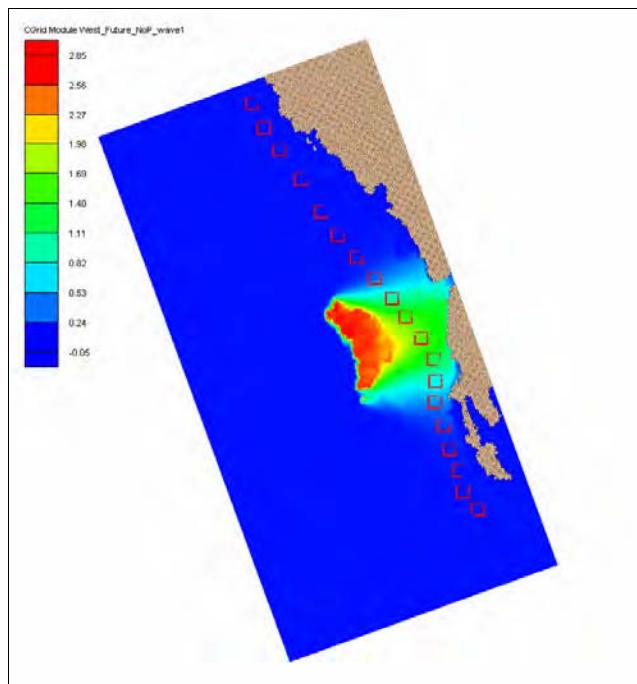


Figure 24. Wave height difference in feet (future without-project – existing). West grid, $H = 3$ ft, $T = 3$ sec, water level = 3 ft (mtl), wave direction = 260 deg

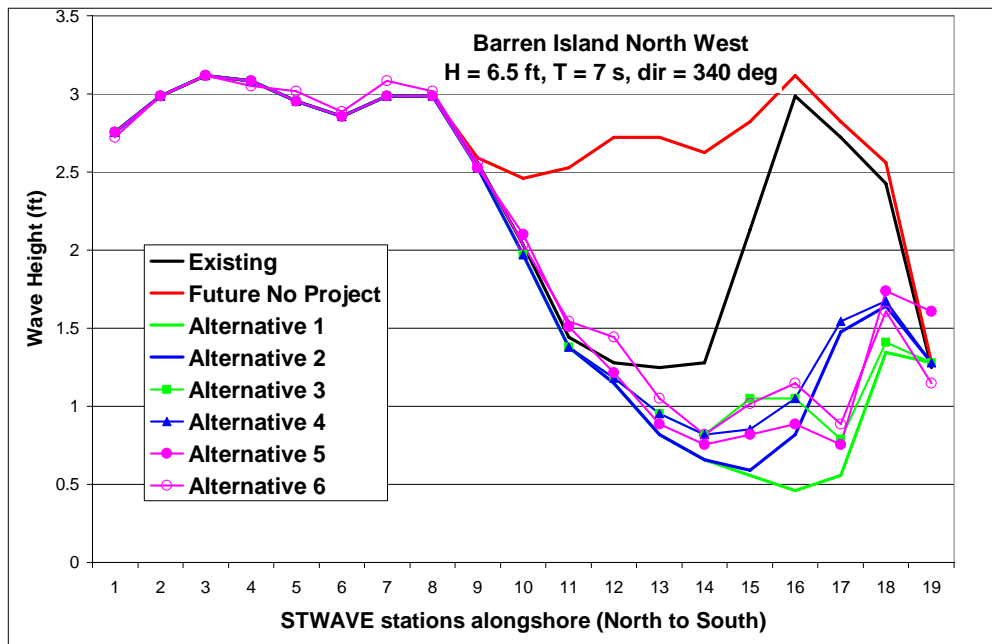


Figure 25. Alongshore wave height variation for Barren Island existing condition, future without-project, and Alt BI-1 through BI-6. Northwest grid, H = 6.5 ft, T = 5 sec, water level = 3 ft (mtl), wave direction = 340 deg

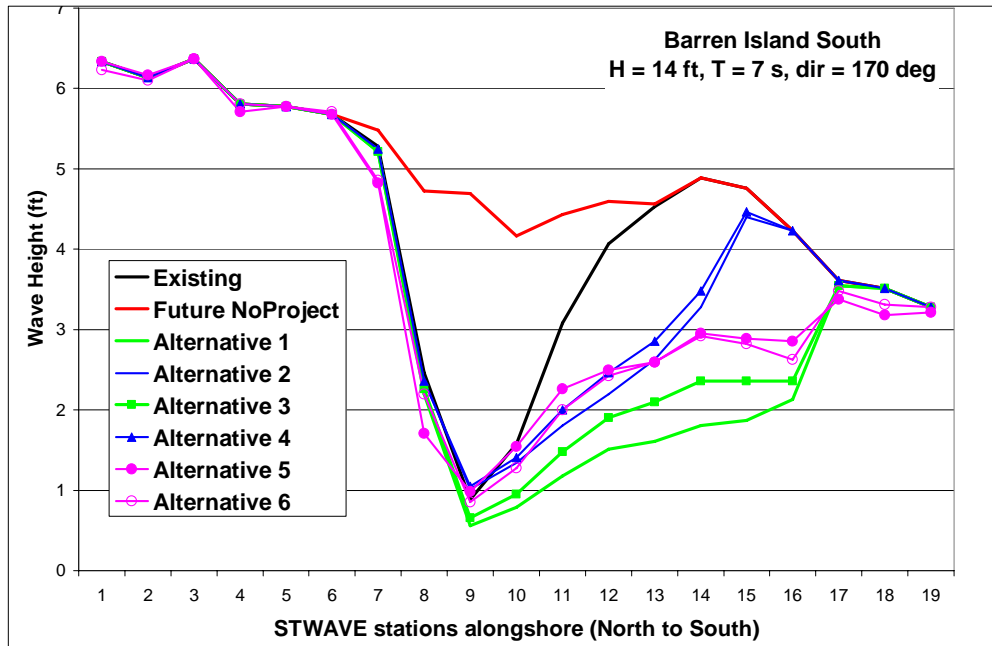


Figure 26. Alongshore wave height variation for Barren Island existing condition, future without-project, and Alt BI-1 through BI-6. Southeast grid, H = 14 ft, T = 7 sec, water level = 5 ft (mtl), wave direction = 170 deg

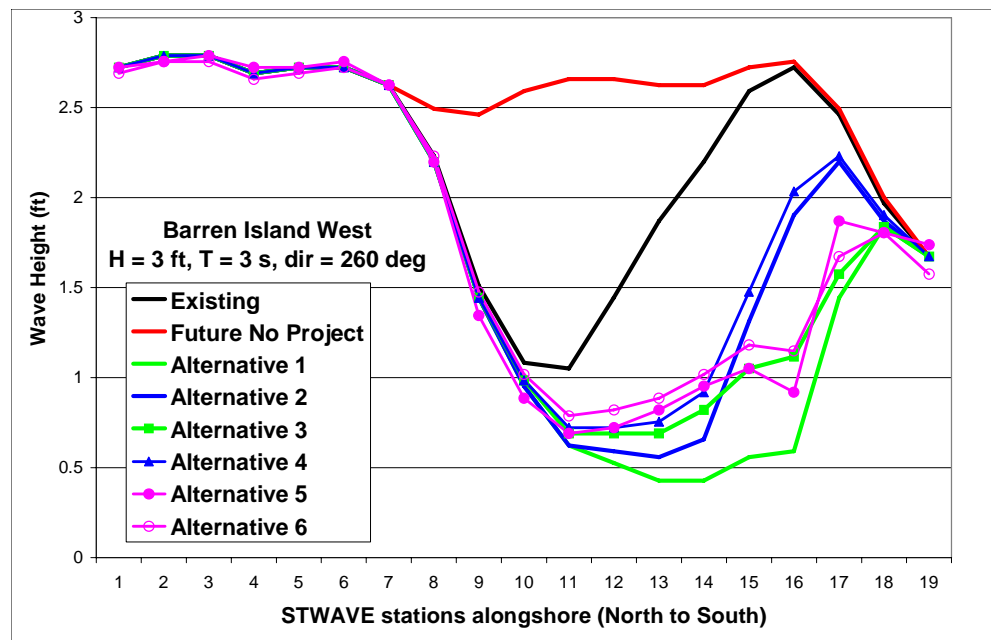


Figure 27. Alongshore wave height variation for Barren Island existing condition, future without-project, and Alt BI-1 through BI-6. West grid, H = 3 ft, T = 3 sec, water level = 3 ft (mtl), wave direction = 260 deg

4 Hydrodynamic and Sediment Transport Models

Hydrodynamic modeling and sediment transport modeling were conducted to investigate the environmental impact of alternative island alignments. The hydrodynamic modeling determines the influences of alternatives on water level and current velocity in the vicinity of islands, and the sediment modeling predicts the accretion and erosion of bay bottom in the surrounding area. The model used for the hydrodynamic calculation is a depth-integrated, 2-D finite element circulation model ADCIRC (Luettich et al. 1992), and the sediment transport model is based on the Van Rijn method (1984a, 1984b, 1984c), implemented in an advection-diffusion approach.

Hydrodynamic Modeling

The hydrodynamic model ADCIRC solves the equations of motion for a moving fluid on a rotating earth. It serves as the USACE regional oceanographic and storm surge model as certified by the Federal Emergency Management Agency for storm surge modeling. The model is formulated with hydrostatic pressure and Boussinesq approximations on a finite-element mesh. ADCIRC can be run either as a 2-D depth-integrated model or as a three-dimensional (3-D) model. Water-surface elevation is calculated from the depth-integrated continuity equation in the Generalized Wave-Continuity Equation form. Velocity is calculated from either the 2DDI or 3-D momentum equations. All nonlinear terms are retained in these equations. The model can be forced with water-surface elevation, normal flow, tidal potential at the mesh boundary, and water-surface stresses generated by winds, waves, and atmospheric pressures.

A regional scale ADCIRC mesh developed in the previous Mid-Bay Poplar Island project (Melby et al. 2005) was adopted in the present study. This mesh was refined in James Island and Barren Island areas using recent hydrographic survey data (June 2005) provided by AMA (Appendix A). The mesh also includes low land topography data to +10 m, mean tide level, from U.S. Geologic Survey Global 30 Arc-Second Elevation Data Set (<http://www1.gsi.go.jp/geowww/globalmap-gsi/gtopo30/README.html>). The numerical mesh was developed for ADCIRC to represent present-day (2005) conditions. The mesh has a minimum resolution of 20 m around the James Island and Barren Island area and a maximum cell size of 500 m in the open ocean. Figures 28 and 29

show the regional mesh and local scale bathymetry grid for James Island and Barren Island areas, respectively.

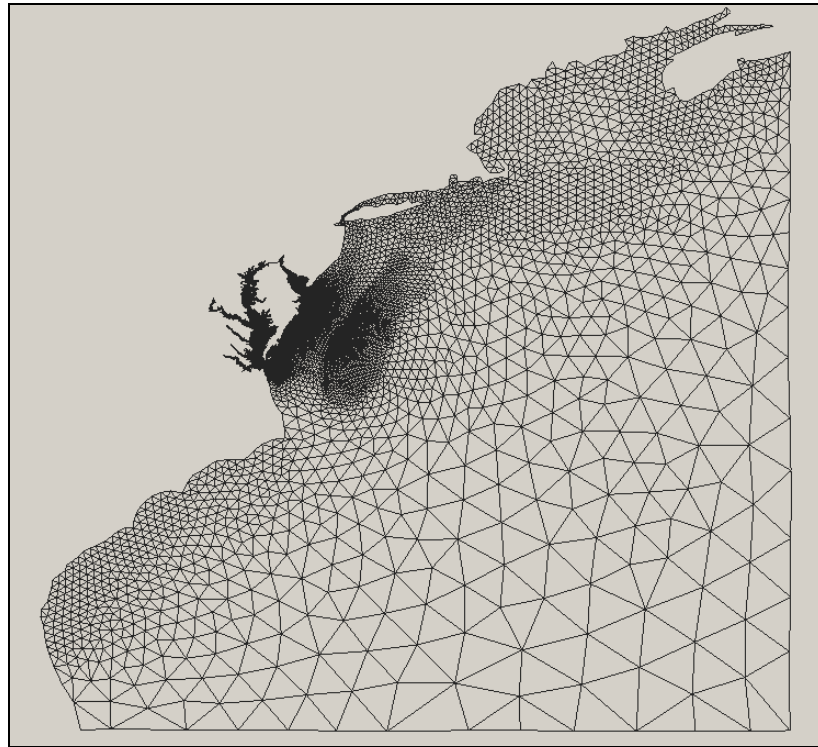


Figure 28. Regional ADCIRC mesh resolution and shoreline

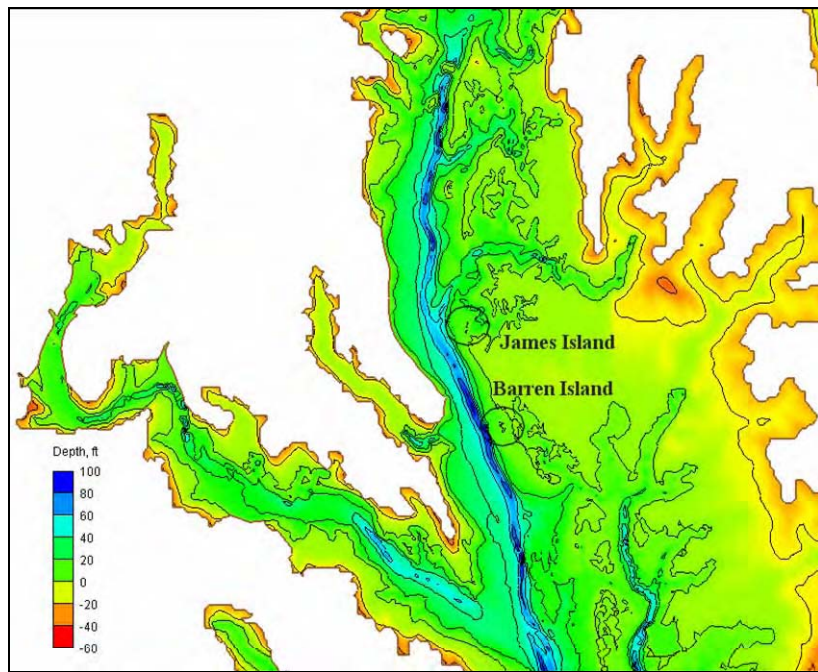


Figure 29. Mid-Bay ADCIRC mesh bathymetry with overbank extensions

Hydrodynamic simulations were conducted for the existing island condition, each of the alternative island alignments, and the future without-project condition. The future without-project condition assumes that both James Island and Barren Island disappear completely as a result of natural erosion under severe storms that occur frequently in the bay. Both islands were removed in the numerical mesh and replaced by water depth interpolated linearly from the surrounding bed. Figure 30 shows the local scale mesh bathymetry at James Island and Barren Island for the existing islands and future without-project conditions. The volume difference between the existing and the future without-project condition is 0.64 million cu yd at James Island and 1.13 million cu yd at Barren Island (Figure 31).

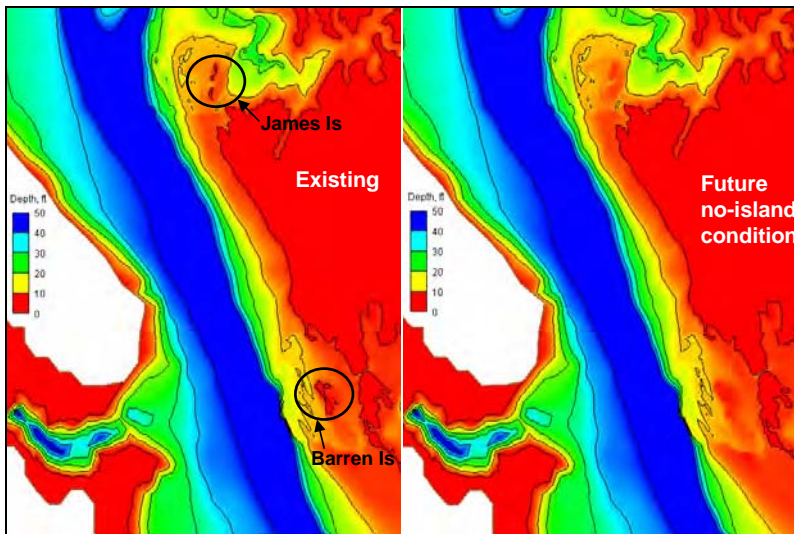


Figure 30. Local mesh bathymetry for existing and future without-project conditions

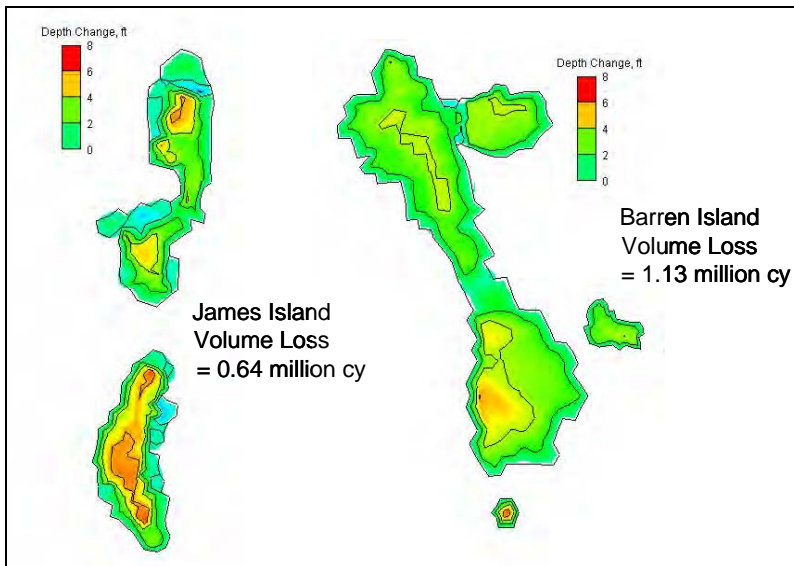


Figure 31. Volume difference for existing and future without-project conditions

Model simulation cases included a normal tide and four historical storms. The normal tide case covers a 2-week period of 1-15 January 2005. During this 2-week period, the wind was light over the bay as observed at several NOAA meteorological stations in the Mid-Bay area (Figure 32). Figure 33 shows measured wind speed and direction at sta 8571892 (Cambridge, Choptank River, MD) and sta 8577330 (Solomons Island, MD). The water level data collected at these NOAA stations is also available for the same period. Figure 34 shows measured water levels at sta 8571892 and 8577330. These wind and water level data show that the water level is effectively responsive to the change in wind direction, especially at locations near the shore and in the shallow tributaries.

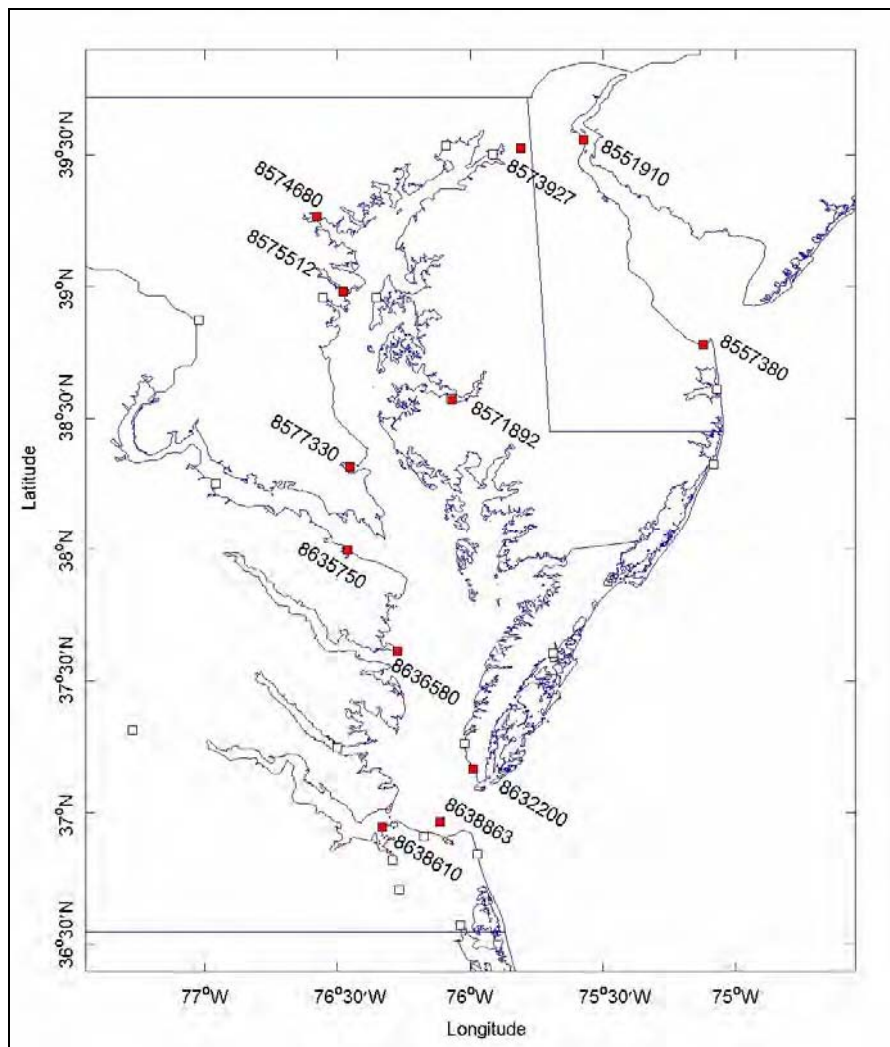


Figure 32. NOAA meteorological stations

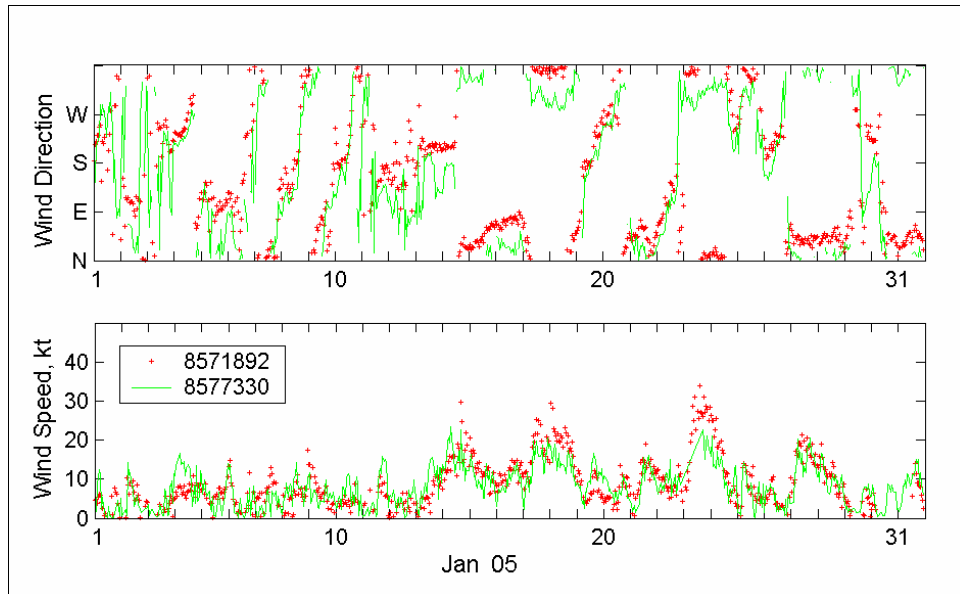


Figure 33. Measured wind speed and direction at sta 8571892 and 8577330

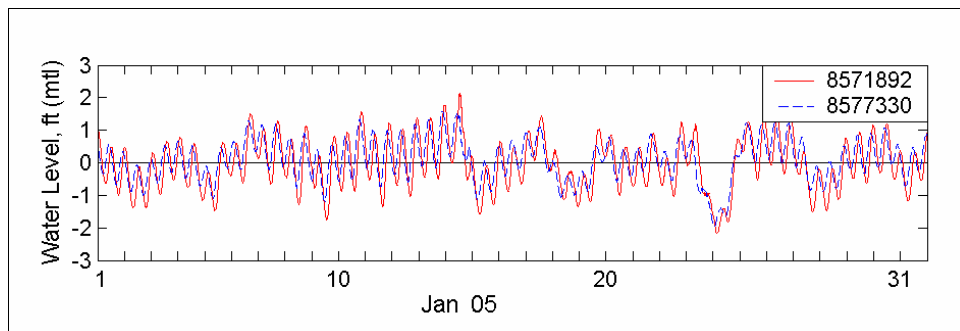


Figure 34. Measured water level at sta 8571892 and 8577330

The simulation for the normal tide case was conducted only for existing islands and for Alts JI-1 and BI-1 to demonstrate the rather weak tidal current condition in the vicinity of islands. The time-step in ADCIRC was 1 sec for the existing condition, and 0.25 sec for the Alt 1 simulation. Figure 35 compares calculated and measured water levels at James Island under the normal tide condition. The calculated water level compares well to the measurements. Figures 36 and 37 show corresponding maximum current conditions in the vicinity of existing James Island and Barren Island, respectively. For the existing condition, the current magnitude is small, with the maximum speed at 0.9 ft/sec in both island locations. Figures 38 and 39 show corresponding maximum current fields for Alts JI-1 and BI-1, respectively. For Alt JI-1, the strongest current, approximately 1.5 ft/sec, is calculated at the southeast corner of the alternative island alignment near the tidal channel entrance. In the tidal channel, the calculated maximum current speed is around 0.9 ft/sec. For Alt BI-1, the largest current magnitude, approximately 1.5 ft/sec, is seen at the northeast corner of the existing island.

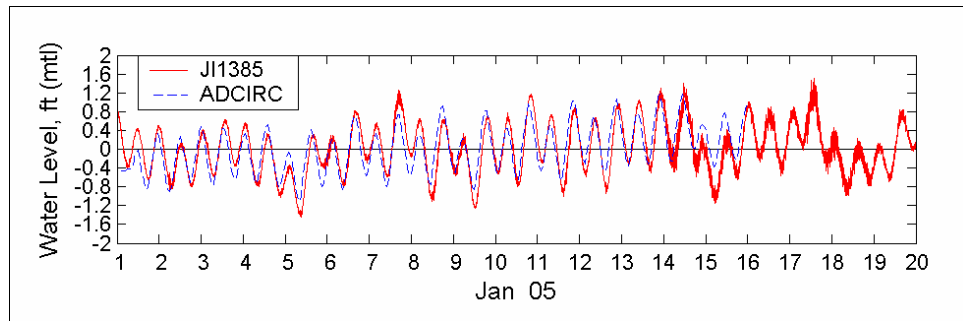


Figure 35. Measured and calculated water levels at James Island at Gauge JI1385

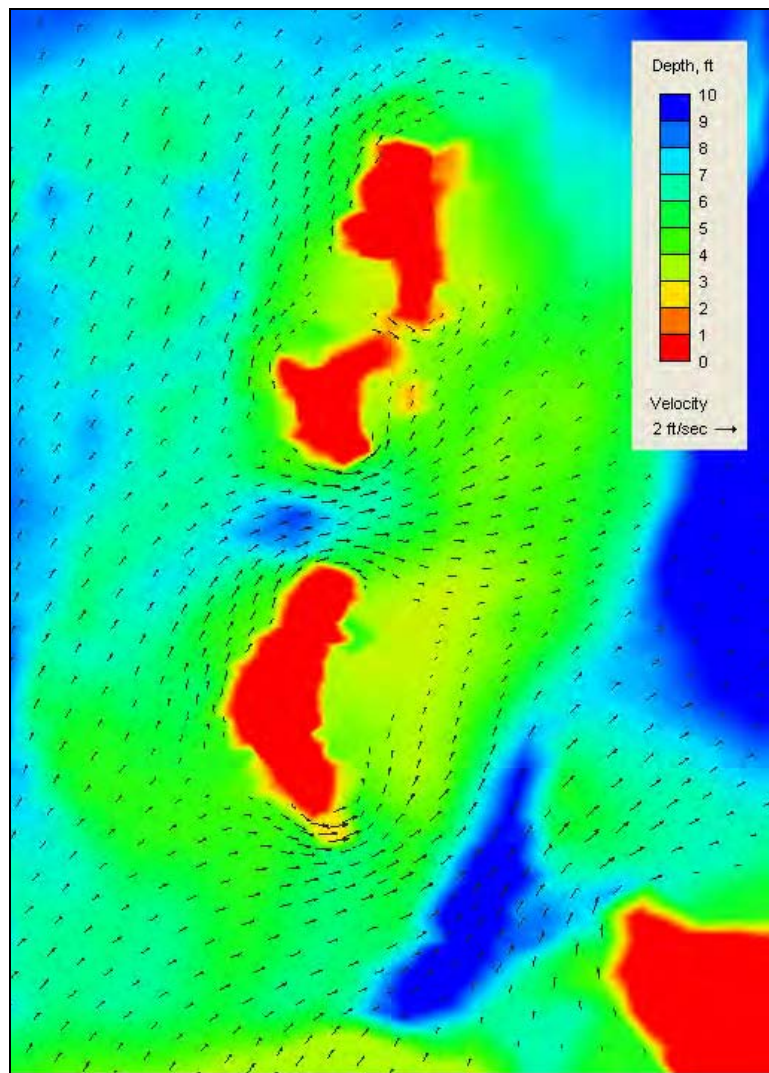


Figure 36. Calculated maximum current fields at James Island under normal tide condition

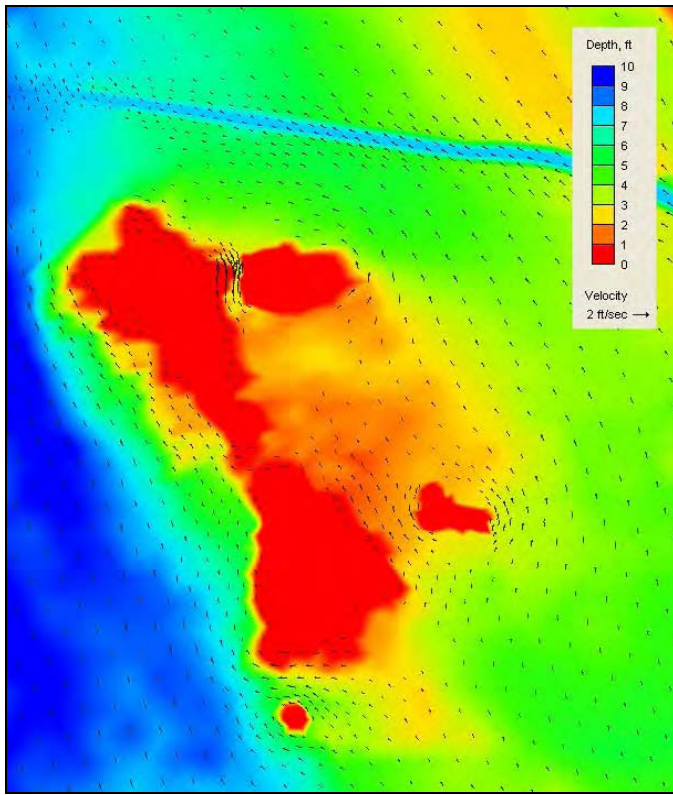


Figure 37. Calculated maximum current field at Barren Island under normal tide condition

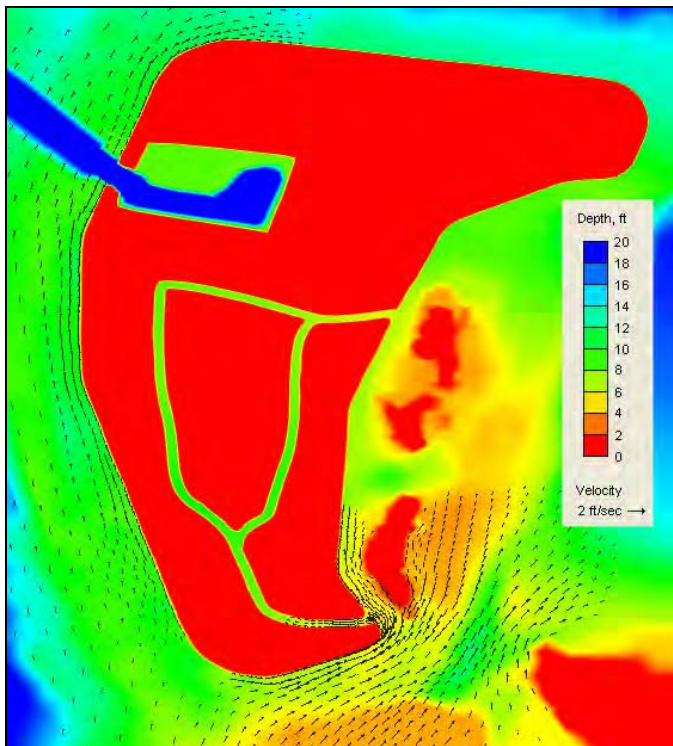


Figure 38. Calculated maximum current field at Alt JI-1 under normal tide condition

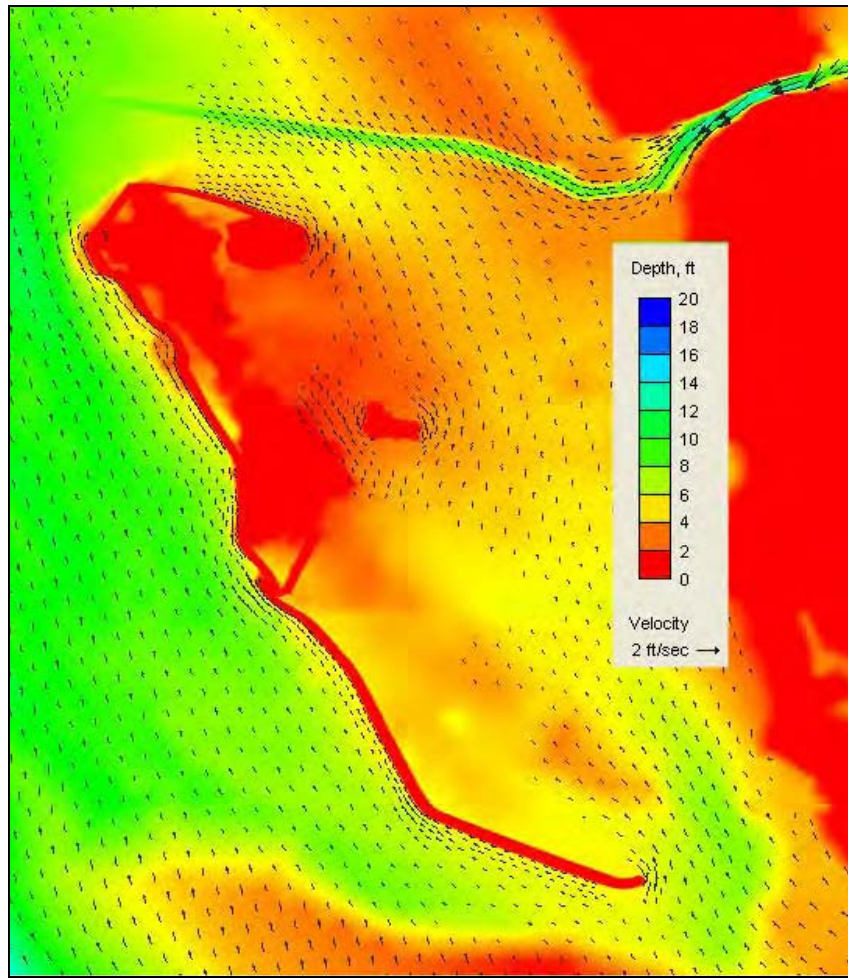


Figure 39. Calculated maximum current field at Alt BI-1 under normal tide condition

Four historical storms were selected for the hydrodynamics and sediment transport modeling. These four storms include two strong hurricanes, 1954 Hazel and 2003 Isabel, and two moderate northeasters, March 1984 and March 1993. For these hurricanes and northeast storms, both surface wind and pressure fields developed from the previous Mid-Chesapeake Bay and Poplar Island study (Melby et al. 2005) were input, together with the surface wave forcing and tidal potentials at the ocean boundary, to the hydrodynamic model. Figure 40 shows an example of the surface wind and pressure field during Hurricane Isabel. The surface wind-wave forcing was also included as input to the hydrodynamic and sediment transport models. Wave field and wave-induced surface shear stress information were precalculated by STWAVE in local areas covering James Island and Barren Island for individual storms and for each alternative island alignment. Figure 41 compares calculated current fields during the maximum water level for Hurricane Isabel at James Island (existing condition) with and without wave forcing. With wave forcing, the change in current magnitude and direction was significant around the island perimeter. Therefore, wave forcing was applied together with the surface wind and pressure input to the ADCIRC model in the present study.

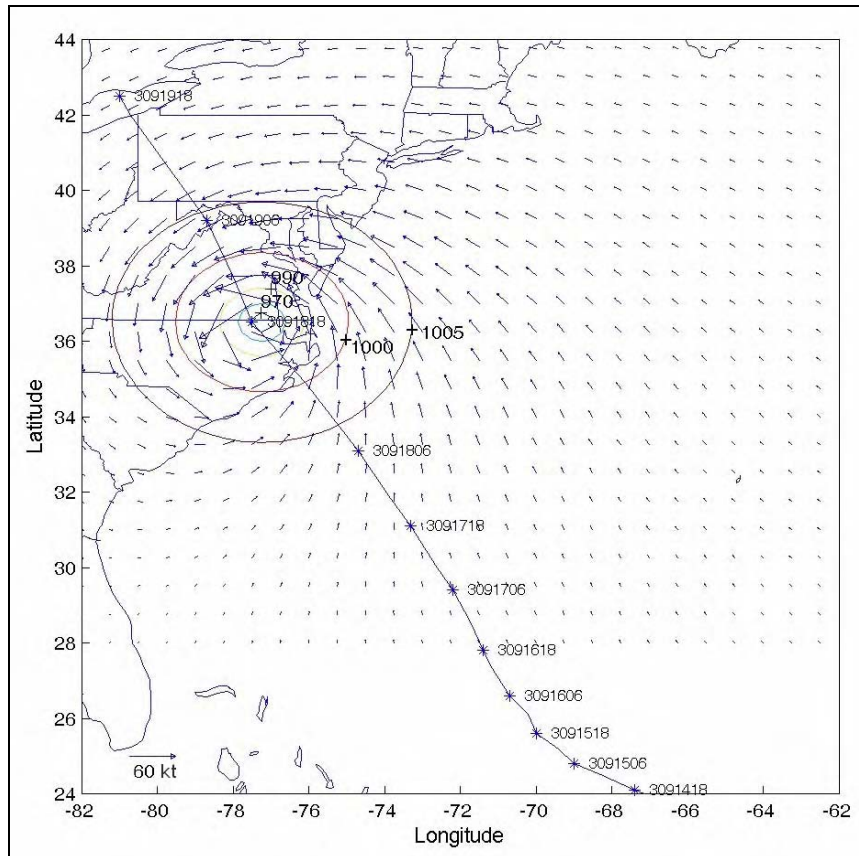


Figure 40. Hurricane Isabel (2003) storm track, wind field (knot), and pressure field (mb) at 1800 GMT, 18 September

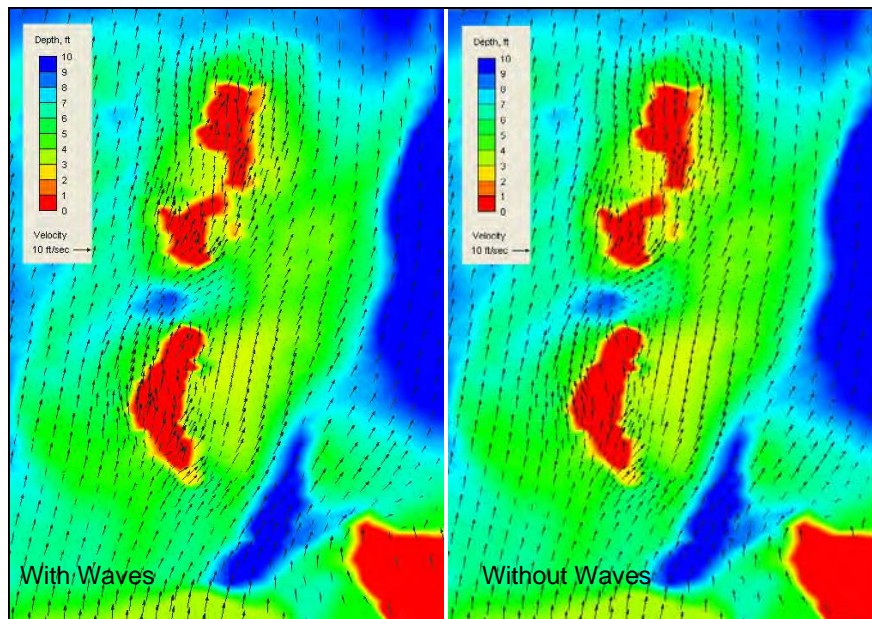


Figure 41. Maximum current fields at James Island during Hurricane Hazel with and without wave forcing condition

Figures 42 and 43 show the calculated water level comparison at the east and west sides of James Island and Barren Island (existing condition) during Hurricane Hazel and Hurricane Isabel. The high water level calculated at James Island and Barren Island during Hurricane Hazel and Hurricane Isabel reaches almost 6 ft mtl. The maximum water level at James Island during these two hurricanes is about the same at the east and west sides of the island, indicating that the storm water can circulate more freely around the island. On the other hand, the maximum wave level at the west side of Barren Island is higher than the east side, indicating that some storm water can be trapped between the island and the neighbored Taylors Island and Upper Hoopers Island to the east. For both the Hurricane Hazel and Hurricane Isabel simulations, the calculated peak water level on the east side of Barren Island is about 5 percent higher than on the west side as a result of strong winds and large waves impounding storm water from the south and southwest. For the northeasters, storm water impoundment to the east of Barren Island is insignificant because the strong wind and large waves originate mainly from either the north or the northwest.

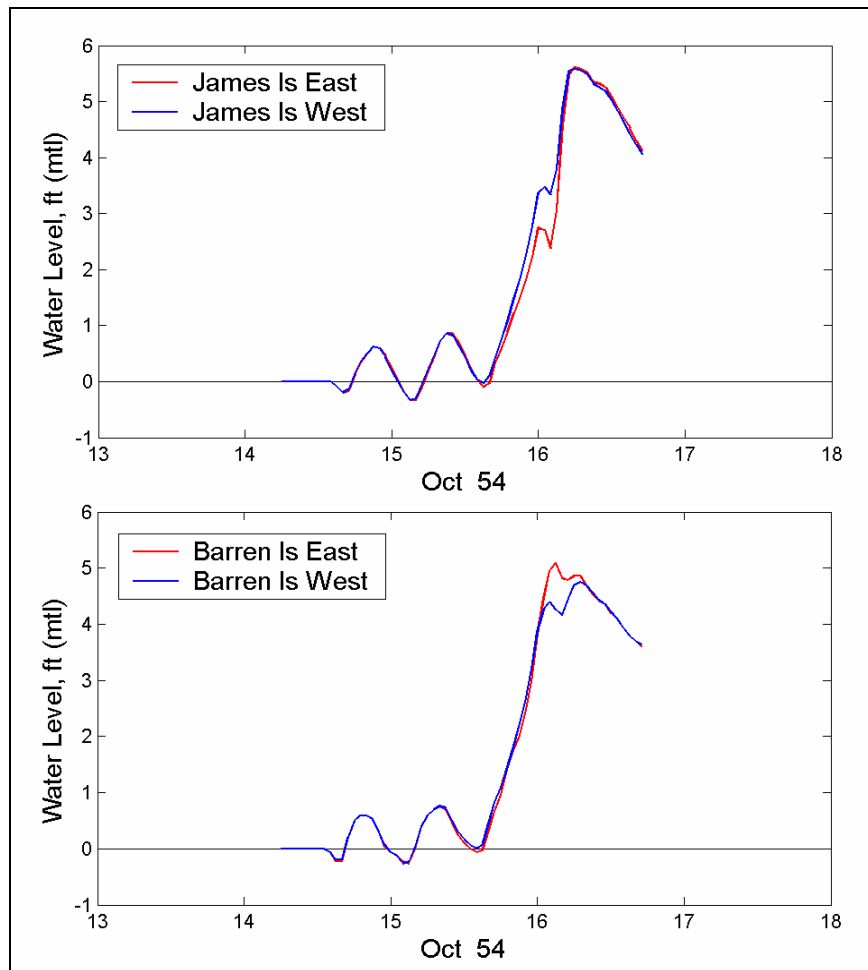


Figure 42. Water level comparison during Hurricane Hazel

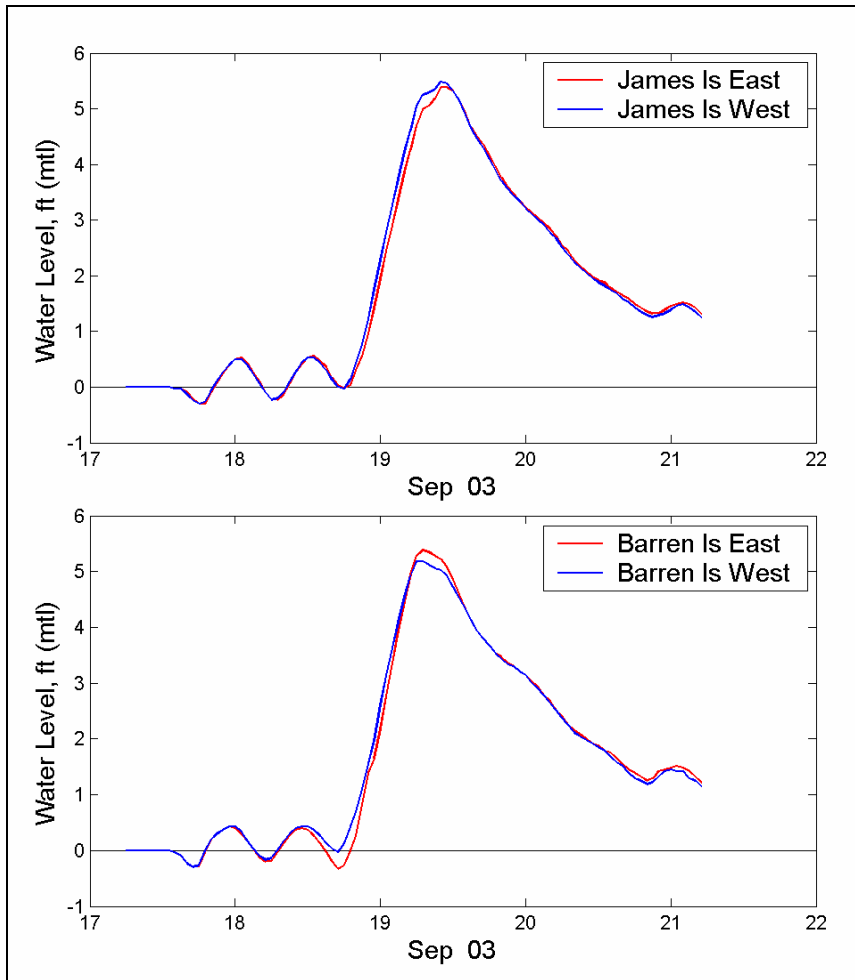


Figure 43. Water level comparison during Hurricane Isabel

Sediment Transport Model

Sediment in Chesapeake Bay can be moved by the current, or by waves, or by both a current and waves acting together. The sediment is transported by the basic processes of entrainment, transportation, and deposition. Entrainment occurs as a result of the bottom friction exerted on the bay bed by currents and waves. Sediment transport can take place by grains moving along the bed or away from the bed into suspension. The former is known as bed-load transport, and the latter is suspended-load transport. Bed-load transport is usually the dominant mode for weak flows and large grains (coarser than 2 mm), whereas suspended-load transport is dominant for strong and turbulent flows and smaller grains (finer than about 0.2 mm). In a typical marine or estuarine area, sediment transport likely involves mixed bed load and suspended load. Deposition of sediment occurs if grains come to rest in bed-load transport, or by settling out of suspension. Depending on the difference in transport rates at which sediment is entering or leaving the area, net accretion or erosion of the bed can occur, and these processes were represented in the modeling.

In the present study, a sediment model was applied to predict the pattern of accretion and erosion in the study area. The sediment transport rate calculated in the model is valid for the sand range (0.062 to 2 mm) through the transport formulas, including bed load and suspended load, developed by Van Rijn (1993). The sediment transport rate is a vector quantity over the 2-D bed plane and is defined as the change of sediment volume per unit time passing though a water column of unit width perpendicular to the flow direction. The transport rate is calculated through introduction of bed shear stresses induced by currents and waves exerted on the bottom sediment.

The hydrodynamic forcing (water level, current, and waves) for the sediment transport model was precalculated. The sediment transport simulation then employed the same finite element mesh as the ADCIRC model. Sediment fluxes were calculated at each element face to determine the sediment quantity transported in and out of each element, based on the transport direction and magnitude.

The sediment transport simulation for the Mid-Bay project involved non-erodible levee structures (armored with rock post-construction). In the situation of a storm condition, all or portions of these structures can be overtapped by high water depending on the height of the levee and the predicted surge level. For elements representing these structures, sediment deposition was permitted, but erosion was only allowed if there had been previous deposition. This procedure prevents unphysical erosion below the original levee elevation for the non-erodible structural condition. Erosion of the interior 6-ft sand dikes was not permitted.

Each sediment transport simulation requires an initial bathymetry, grain size information, and hydrodynamic forcing (water level, current, and waves). The sediment transport model can support multiple grain sizes. However, for the screening level analysis completed in the present study, a single grain size of 0.2 mm representing the average sediment size the James Island and Barren Island was specified. Figures 44 and 45 demonstrate calculated sediment accretion and bed erosion patterns at James Island and Barren Island, respectively, under Hurricane Hazel. Erosion appears on the surface and along the perimeter of James Island and Barren Island as a result of inundation of these two islands during the peak surge condition.

Figures 46 and 47 show sediment accretion and erosion patterns for Alt JI-3 during Hurricane Hazel and NE20. Sediment accretion and erosion appear to be more significant along the bay side levee of Alt JI-5 under the stronger Hurricane Hazel than NE20. It is noted that the pattern of accretion and erosion reverses on the north and south sides of the access channel for Hurricane Hazel and NE20 indicating opposite sand transport directions across the access channel during these two storms. Figures 48 and 49 show calculated sediment accretion and erosion for Alt BI-5 during Hurricane Hazel and NE20. There is more accretion and erosion at shore protection structures and breakwaters where stronger wave-current and wave-structure interactions occur. Bed erosion is significant at the south breakwater, where the current is strong surrounding segmented breakwater elements. Sediment transport simulations for Barren Islands Alts BI-1 through BI-6 generally show less sediment accretion or erosion along the Honga River Channel, especially between Taylors Island and Upper Hoopers Island. This trend is opposite to the future without-project condition, where the erosion

becomes significant along the bay side shoreline and Honga River Channel because Barren Island does not exist to provide the protection to Taylors Island and Upper Hoopers Island.

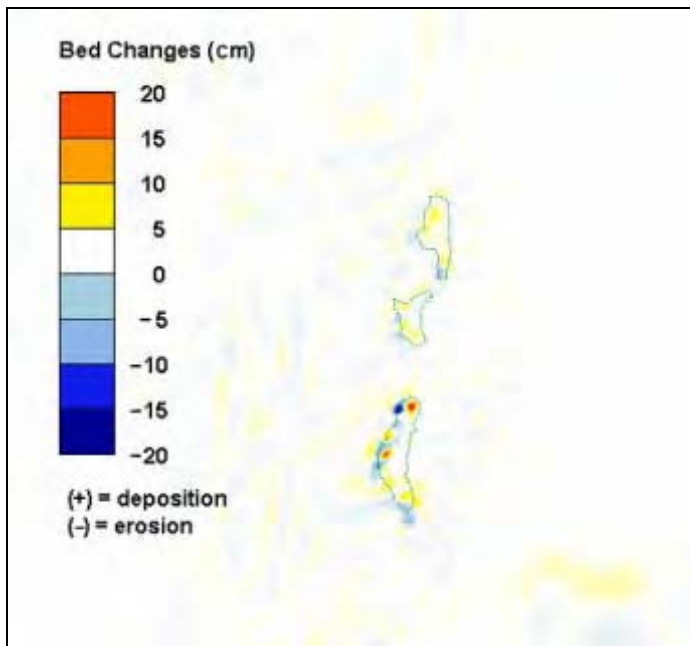


Figure 44. Bed change at James Island from Hurricane Hazel

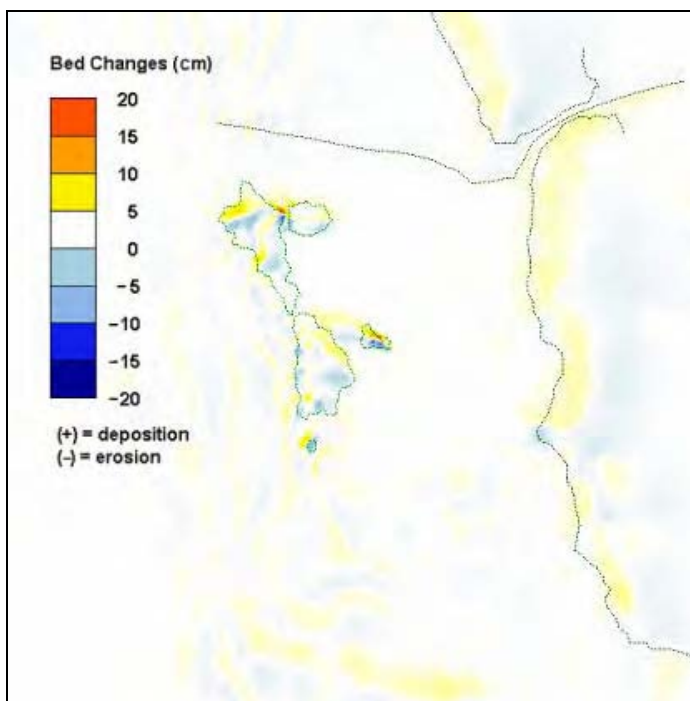


Figure 45. Bed change at Barren Island from Hurricane Hazel

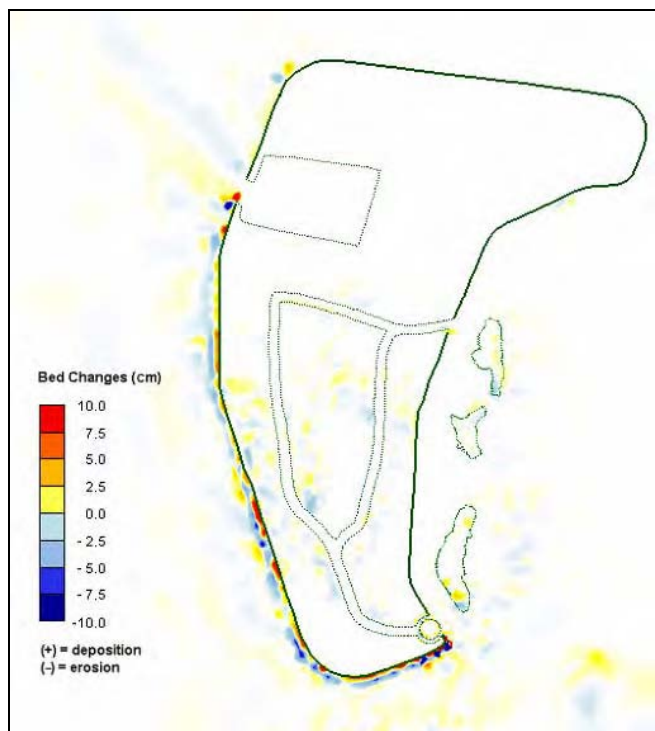


Figure 46. Bed change at James Island, Alt JI-3, from Hurricane Hazel

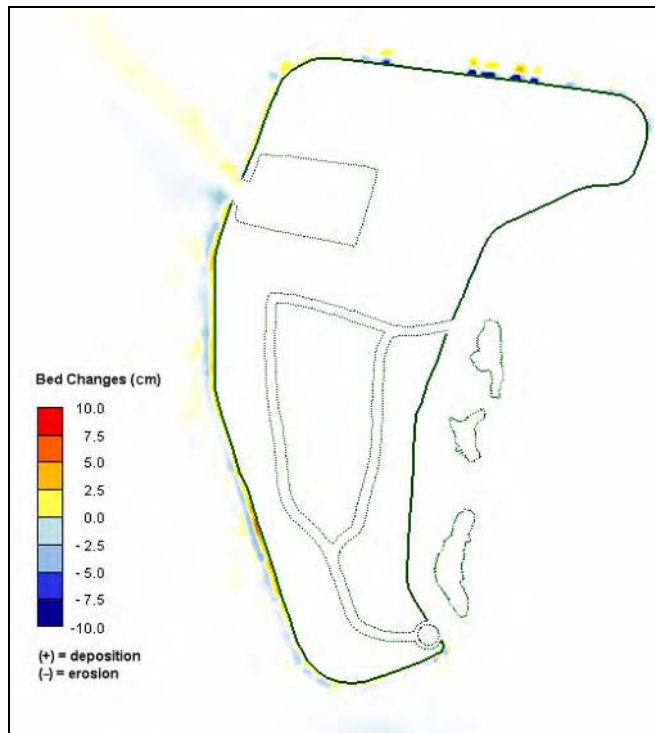


Figure 47. Bed changes at James Island, Alt JI-3, from NE20

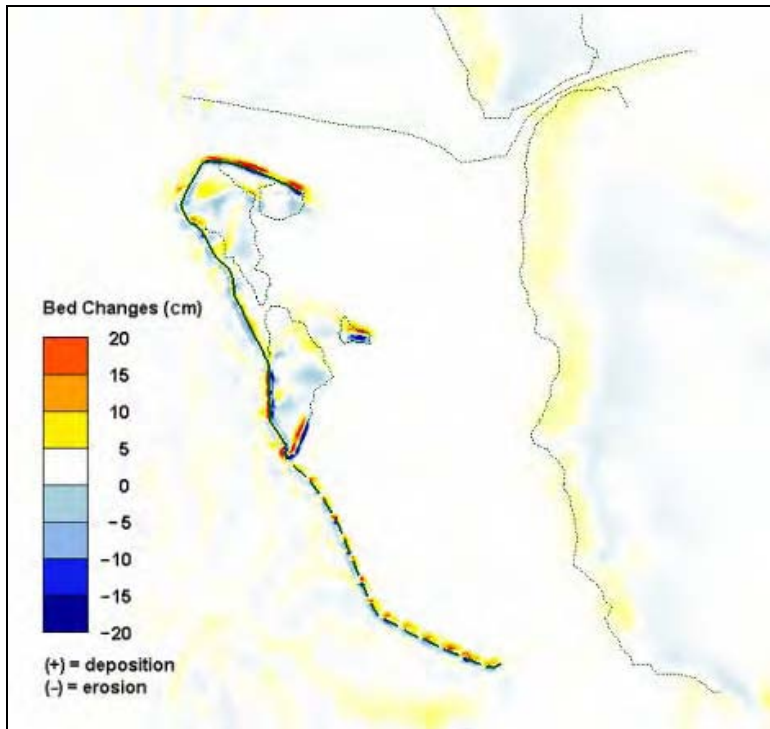


Figure 48. Bed change at Barren Island, Alt BI-5, from Hurricane Hazel

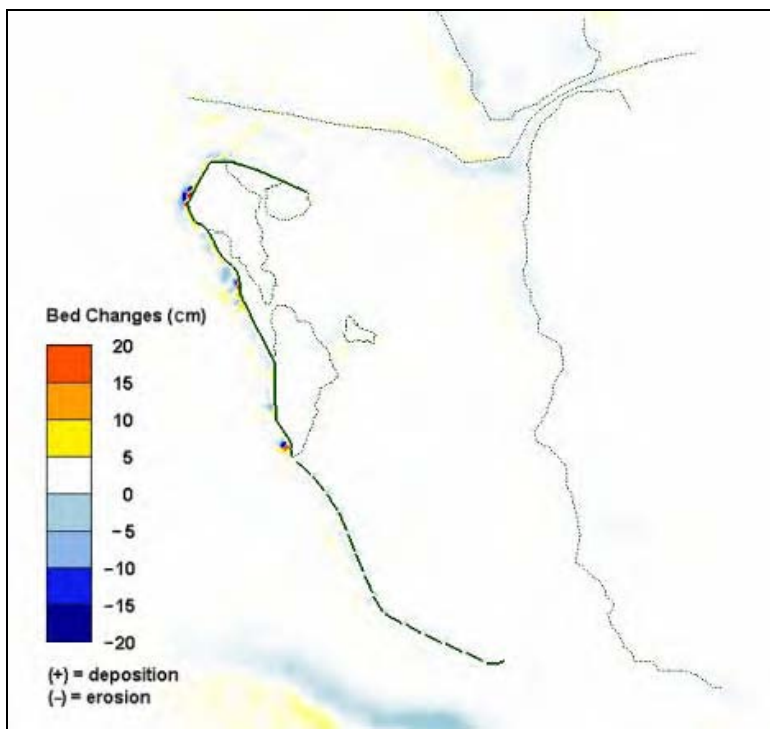


Figure 49. Bed change at Barren Island, Alt BI-5, from NE20

5 Evaluation of Alternatives

Evaluation of the James Island and Barren Island alternatives encompasses diverse subjects such as physical processes for assessing environmental impacts, engineering design, construction cost, recreational use, and other aspects such as real estate and cultural benefits. In the present study, components of the evaluation address waves, hydrodynamics (circulation and sediment transport) in support of engineering and environmental studies. The hydrodynamics and sediment transport were evaluated for a normal tide condition and four historical storms (Table 3) consisting of two strong (100+ year compatible) hurricanes (1954 Hazel and 2003 Isabel) and two moderate northeasters (NE20 and NE33).

The evaluation covers analysis of the existing island condition and future without-project condition, assuming that the existing James Island and Barren Island will erode completely if island restoration does not take place. Results from wave, hydrodynamic, and sediment transport simulations are compared to evaluate conditions for the engineering alternatives with respect to the adjacent islands, including sediment erosion in tidal guts and sediment shoaling in local channels.

Response to Waves

Chapter 3 describes numerical modeling of wave transformation for the James Island and Barren Island alternatives, existing condition, and future without-project condition. The wave results were examined to evaluate the nearshore (close to shore) wave climate associated with the individual alternatives. The nearshore waves were evaluated for a range of characteristic conditions. Additionally, two hurricanes (Hazel and Isabel) and two northeaster storms were simulated. Wave model results were input to drive the circulation and sediment transport models described in Chapter 4. The storm simulation results are available to specialists such as ecologists for assessing survivability of SAV in the areas sheltered by different alternatives.

James Island alternatives expanded the footprint of the island and reduced the wave height in the lee of the island by 1-2 ft. The future without-project condition (submerged island) increased the wave height at the shoreline slightly. The Barren Island alternatives include six breakwater extensions to the south of the island. Alts BI-1 and BI-3 reduced the wave height 2-3 ft at the shoreline in the lee of the island (greater reduction for Alt BI-1 with the greater breakwater crest height). Alts BI-2 and BI-4 (shorter overall breakwater length) provided approximately 0.5 ft less reduction in wave height than Alts BI-1 and BI-3, and

the reduction was over a smaller region. Alts BI-5 and BI-6 pertain to segmented breakwaters. They provided approximately 0.5 ft less reduction in wave height than Alts BI-1 and BI-3, but over a similar region. Increasing the length and crest elevation of the Barren Island breakwaters reduced wave energy in their lee. The future without-project condition increased the nearshore wave height 2-4 ft for Barren Island, thus potentially increasing shore erosion. None of the alternatives considered for James Island and Barren Island increased the nearshore wave height.

Current Velocity Comparison

The current velocity calculated from the hydrodynamic model allows evaluation and comparison of the individual alternatives. The current velocity was evaluated at key locations selected to identify conditions that might alter water quality and be a concern to environmental resources such as oyster beds and SAV. Tables 7 and 8 present easting and northing coordinates (MD State Plane) of the identified key locations at James Island and Barren Island, respectively. Among the locations selected for James Island, Points 1 and 12 are located in the local navigation channel. Points 5 and 8 represent the tidal gut entrance locations. Points 7 and 9 are located in the tidal gut channel. Points 2 and 3 are located in the neighboring oyster bed ground. Point 4 is located in the SAV area.

For Barren Island, Points 2 to 8, and 10 are located in the SAV area, and Points 9, 11, and 13 are located in the oyster bed. Points 14 and 15 are located in the north island cut (northward-most tidal gut). Points 16 and 17 are located in the up-wave side and lee side, respectively, of the south breakwater. Point 1 is located in the south local channel, and Point 12 is located in the Honga River Channel at the Tar Bay entrance. Figures 50 and 51 show the comparison location points for James Island and Barren Island, respectively (Alts JI-6 and BI-6 serve as the background bottom topography).

The response of the current field to the presence of each alternative was investigated for both normal tide and storm conditions. The normal tide simulation covered the 2-week period 1-15 January 2005. The simulation was conducted only for the existing island configuration and for Alts JI-1 and BI-1 to investigate sedimentation patterns (erosion and deposition) in a typical, frequent weak current. The calculation results were analyzed for the first 12-day period of the simulation because the wind was relatively weak in this period and became stronger afterward. Tables 9 and 10 present the maximum current velocity values from the normal tide analysis at comparison points for both islands and Alts JI-1 and Alt BI-1, respectively. These tables show that the current velocity is not strong and similar for the existing condition and Alt 1 for both islands, with a maximum speed of 2.1 ft/sec at the southeast corner of Alt JI-1 (Point 13) and 2 ft/sec at the north island cut of Alt BI-1 (Point 15). The stronger current at the southeast corner of Alt JI-1 occurs because of the sharp turning angle of the current between the south tidal gut outlet and open bay. The stronger current at the north island cut of Alt BI-1 occurs because of the increase in water surface gradient during high tide at the narrow cut. The calculated current velocity is similar in magnitude to the results from two previous numerical model studies by Moffatt & Nichol Engineers (2002, 2004) that investigated the current field

under normal tide for James Island and Barren Island for several different alternative alignments.

Table 7
James Island Save Locations

Location	Easting, ft	Northing, ft
1	1,503,685.827	304,923.294
2	1,508,416.896	312,049.5079
3	1,500,881.824	320,596.2927
4	1,502,676.969	309,755.1837
5	1,501,389.862	304,992.7822
6	1,498,119.882	303,393.7336
7	1,498,537.27	306,209.4816
8	1,501,737.73	312,605.6759
9	1,498,258.99	313,127.0997
10	1,495,058.53	313,439.9606
11	1,495,291.995	316,450.1312
12	1,500,916.47	303,225.9514
13	1,501,402.231	304,382.5459
14	1,501,761.549	305,303.0184
15	1,500,937.008	304,818.5696
16	1,500,618.438	305,018.0446

Table 8
Barren Island Save Locations

Location	Easting, ft	Northing, ft
1	1,531,352.428	234,510.8596
2	1,529,207.874	236,213.9108
3	1,528,176.575	237,928.248
4	1,527,378.707	239,325.689
5	1,526,812.041	244,400.853
6	1,533,207.316	236,718.0774
7	1,532,177.756	238,192.6837
8	1,530,727.526	240,194.1273
9	1,529,799.77	241,406.0367
10	1,529,077.986	244,985.1706
11	1,529,299.049	240,747.769
12	1,531,982.612	248,266.0761
13	1,518,821.522	250,722.4409
14	1,524,838.583	246,663.3858
15	1,524,906.168	246,087.5984
16	1,527,136.155	237,959.3176
17	1,527,016.076	237,691.601

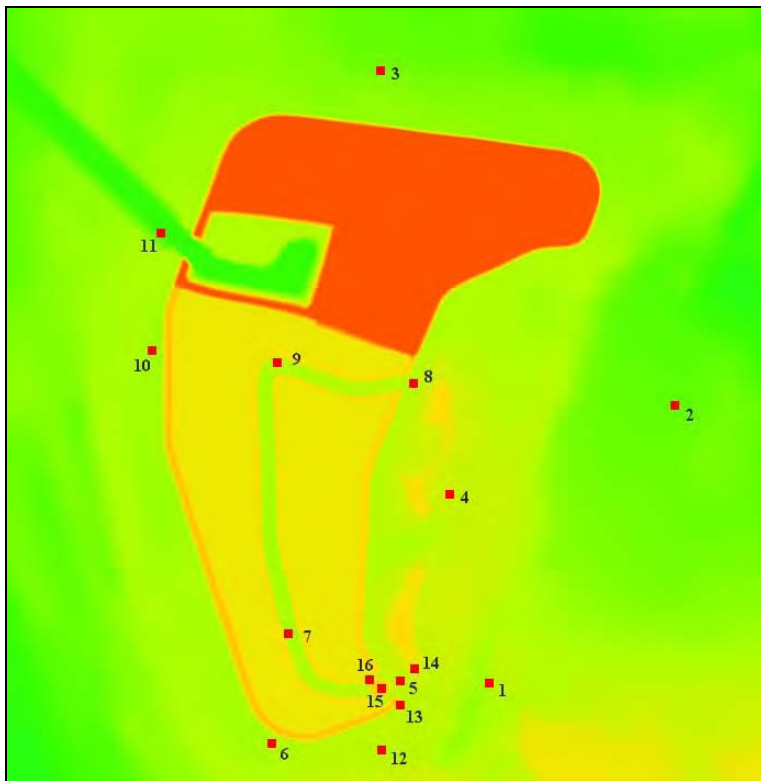


Figure 50. James Island comparison locations (JI-6)

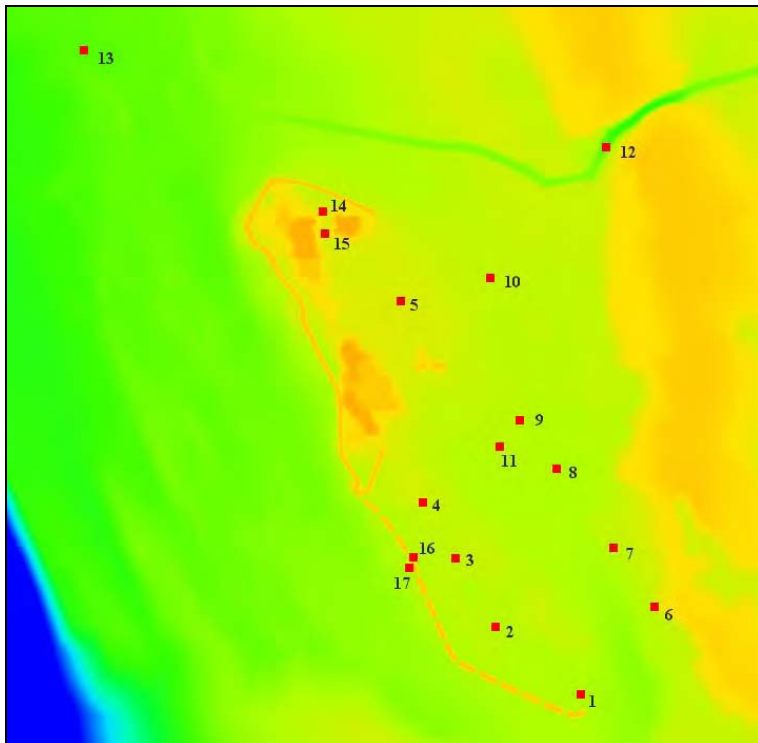


Figure 51. Barren Island comparison locations (BI-6)

Table 9
Calculated Maximum Current Speed (ft/sec) at James Island Under Normal Tide Condition

Location	Existing	Alt JI-1
1	1.97	1.94
2	0.36	0.20
3	0.82	0.59
4	1.08	0.79
5	1.28	1.28
6	1.34	0.66
7	1.28	0.52
8	1.71	0.88
9	1.41	0.20
10	1.38	1.57
11	0.95	0.49
12	1.11	1.80
13	1.18	2.13
14	0.00	0.00
15	0.92	0.72
16	0.79	0.00

NOTE: A '0' velocity indicates the 'no-current' (dry) condition.

Table 10
Calculated Maximum Current Speed (ft/sec) at Barren Island Under Normal Tide Condition

Location	Existing	Alt BI-1
1	1.15	1.15
2	1.08	0.69
3	0.98	0.75
4	0.85	0.69
5	0.92	0.89
6	1.15	1.18
7	0.98	0.98
8	0.98	0.89
9	0.95	0.92
10	1.15	1.15
11	0.62	0.56
12	1.90	1.87
13	0.82	0.82
14	0.85	0.82
15	0.92	2.03
16	0.56	0.10
17	0.56	0.23

Table 11**Calculated Maximum Current Speed (ft/sec) at James Island During Hurricane Hazel**

Location	Existing	Future	JI-1	JI-2	JI-3	JI-4	JI-5	JI-6
1	3.31	3.31	3.31	3.31	3.31	3.31	3.31	3.31
2	1.41	1.41	1.67	1.71	1.61	2.00	1.90	1.97
3	3.28	0.98	1.25	1.21	1.18	1.67	1.71	1.48
4	3.48	3.51	3.38	3.38	3.38	3.38	3.38	3.38
5	3.28	3.31	3.31	3.35	3.35	3.31	3.31	3.35
6	3.31	3.28	3.28	3.28	3.28	3.28	3.28	3.28
7	3.28	3.28	2.59	3.28	3.25	3.28	3.28	2.82
8	3.31	3.31	3.31	3.31	3.31	3.31	3.31	3.31
9	3.28	3.28	1.67	1.97	1.90	1.80	0.59	0.75
10	3.28	3.28	3.28	3.28	3.28	3.28	3.28	3.28
11	3.28	3.28	2.43	2.46	2.40	3.02	3.02	3.02
12	3.31	3.31	3.31	3.28	3.28	3.28	3.31	3.31
13	3.31	3.31	3.48	3.44	3.54	3.51	3.58	3.51
14	6.14	6.40	4.10	4.13	3.94	5.61	5.51	5.58
15	3.31	3.31	3.31	3.31	0.00	3.31	3.28	0.00
16	3.31	3.35	0.03	0.07	3.35	1.28	1.21	3.31

Note: A '0' velocity magnitude indicates the 'no-current' (dry) condition.

Table 12**Calculated Maximum Current Speed (ft/sec) at James Island During Hurricane Isabel**

Location	Existing	Future	JI-1	JI-2	JI-3	JI-4	JI-5	JI-6
1	2.69	2.66	3.25	3.28	3.28	3.28	3.28	3.28
2	1.02	1.18	1.18	1.18	1.15	1.18	1.18	1.18
3	1.74	1.71	0.98	0.89	0.89	0.75	0.75	0.75
4	3.15	2.92	2.49	2.49	2.53	2.49	2.49	2.49
5	1.84	2.49	3.51	3.25	3.31	3.25	3.25	3.02
6	2.79	2.92	2.66	2.17	2.53	2.17	2.17	2.17
7	2.82	2.89	2.30	2.20	1.90	1.08	0.82	0.66
8	2.82	2.66	3.35	2.00	3.41	1.77	1.87	1.80
9	2.69	2.69	2.00	0.82	1.87	1.21	0.75	0.62
10	2.76	2.79	3.28	3.28	3.28	3.28	3.28	3.28
11	2.59	2.59	1.54	1.61	1.54	1.61	1.61	1.61
12	2.53	2.66	3.02	3.22	3.12	3.22	3.18	3.22
13	2.30	2.56	3.31	3.31	3.31	3.31	3.31	3.31
14	4.00	3.05	3.87	3.54	3.54	3.51	3.48	3.51
15	2.23	2.66	3.31	1.94	0.00	1.71	2.17	0.00
16	2.36	2.76	0.43	0.10	3.35	0.07	0.07	2.46

Note: A '0' velocity magnitude indicates the 'no-current' (dry) condition.

Table 13
Calculated Maximum Current Speed (ft/sec) at James Island During NE20

Location	Existing	Future	JI-1	JI-2	JI-3	JI-4	JI-5	JI-6
1	1.48	1.35	1.51	1.67	1.51	1.51	1.51	1.51
2	0.36	0.52	0.36	0.36	0.39	0.36	0.36	0.36
3	1.08	1.02	0.82	0.85	0.82	0.82	0.82	0.82
4	1.18	1.41	0.92	0.92	0.92	0.92	0.92	0.92
5	1.31	1.35	1.48	1.61	1.44	1.44	1.48	1.44
6	1.48	1.51	1.25	1.38	1.25	1.25	1.25	1.25
7	1.64	1.38	0.66	0.75	0.49	0.59	0.59	0.46
8	1.51	2.03	1.21	1.21	1.15	1.25	1.21	1.21
9	1.48	1.57	0.26	0.16	0.16	0.20	0.56	0.36
10	1.48	1.41	1.97	2.00	1.97	1.97	1.97	1.97
11	1.41	1.38	0.62	0.62	0.62	0.62	0.62	0.62
12	1.18	1.57	1.90	2.13	1.90	1.90	1.90	1.90
13	1.12	1.28	2.43	2.43	2.40	2.46	2.43	2.40
14	0.00	1.67	0.00	0.00	0.00	0.00	0.00	0.00
15	1.35	1.74	0.85	0.95	0.00	0.92	0.75	0.00
16	1.44	1.84	0.00	0.00	1.18	0.00	0.00	0.95

Note: A '0' velocity magnitude indicates the 'no-current' (dry) condition.

Table 14
Calculated Maximum Current Speed (ft/sec) at James Island During NE33

Location	Existing	Future	JI-1	JI-2	JI-3	JI-4	JI-5	JI-6
1	1.61	1.74	1.61	1.61	1.84	1.57	1.61	1.61
2	0.30	0.39	0.26	0.26	0.30	0.26	0.26	0.26
3	0.82	1.21	0.56	0.56	0.56	0.56	0.56	0.56
4	1.35	1.54	0.62	0.62	0.62	0.62	0.62	0.62
5	1.51	0.95	1.44	1.44	1.44	1.41	1.41	1.41
6	0.98	1.02	1.48	1.48	1.51	1.51	1.48	1.51
7	0.95	1.02	0.62	0.66	0.49	0.59	0.56	0.46
8	1.57	1.25	0.72	0.72	0.69	0.75	0.72	0.66
9	1.31	1.25	0.26	0.16	0.20	0.23	0.52	0.36
10	1.21	1.21	1.12	1.12	1.08	1.12	1.12	1.12
11	1.18	1.12	0.49	0.49	0.52	0.49	0.49	0.49
12	1.44	1.21	1.90	1.90	1.94	1.94	1.90	1.90
13	1.35	1.21	2.10	2.10	2.53	2.00	2.10	1.80
14	0.00	1.64	0.00	0.00	0.00	0.00	0.00	0.00
15	1.21	1.05	0.89	0.95	0.00	0.98	0.79	0.00
16	1.18	1.08	0.00	0.00	1.25	0.00	0.00	1.02

Note: A '0' velocity magnitude indicates the 'no-current' (dry) condition.

Table 15**Calculated Maximum Current Speed (ft/sec) at Barren Island During Hurricane Hazel**

Location	Existing	Future	BI-1	BI-2	BI-3	BI-4	BI-5	BI-6
1	3.31	3.31	3.25	3.28	3.28	3.28	3.31	3.22
2	3.31	3.31	3.18	3.28	2.95	3.28	3.31	2.33
3	3.31	3.31	3.28	3.31	3.28	3.31	3.31	2.49
4	3.31	3.31	3.28	3.28	3.25	3.31	3.28	3.31
5	3.35	3.02	3.31	3.31	3.31	3.35	3.35	3.35
6	3.44	3.48	3.41	3.41	3.41	3.44	3.44	3.38
7	3.31	3.31	3.48	3.28	3.28	3.31	3.31	3.31
8	3.31	3.31	3.28	3.28	3.28	3.28	3.31	3.28
9	3.28	3.31	3.31	3.28	3.28	3.31	3.28	3.31
10	3.31	3.31	3.28	3.28	3.31	3.31	3.28	3.31
11	3.31	3.31	3.31	3.28	3.28	3.31	3.28	3.28
12	3.28	3.28	3.28	3.28	3.28	3.28	3.28	3.28
13	3.28	3.28	3.28	3.28	3.28	3.28	3.28	3.28
14	3.97	3.44	3.90	3.94	3.71	3.87	3.87	3.87
15	3.51	3.35	3.48	3.44	3.41	3.38	3.51	3.48
16	3.31	3.28	0.59	0.59	3.64	3.87	3.97	7.09
17	3.31	3.28	1.25	1.25	3.74	3.81	5.64	7.87

Table 16**Calculated Maximum Current Speed (ft/sec) at Barren Island During Hurricane Isabel**

Location	Existing	Future	BI-1	BI-2	BI-3	BI-4	BI-5	BI-6
1	3.28	3.28	2.99	3.12	3.28	3.22	2.72	2.82
2	3.28	3.28	1.90	2.43	2.76	2.89	2.89	1.84
3	3.15	3.28	2.36	2.62	2.72	2.66	2.72	1.97
4	2.82	3.22	2.46	2.53	2.49	2.43	2.46	3.28
5	3.28	3.28	3.02	2.95	3.15	2.89	2.89	3.08
6	3.15	3.22	3.15	3.02	3.05	3.08	2.72	2.72
7	3.22	3.28	3.15	2.99	3.15	3.12	3.05	2.99
8	2.89	3.22	2.79	2.79	2.85	2.79	2.72	2.56
9	2.69	2.99	2.69	2.72	2.72	2.69	2.66	2.62
10	2.95	2.99	3.08	3.18	3.05	3.08	3.12	3.28
11	2.62	3.02	2.56	2.62	2.59	2.56	2.56	2.46
12	3.28	3.28	3.28	3.28	3.28	3.31	3.28	3.28
13	2.79	2.89	2.82	2.82	2.79	2.79	2.76	2.72
14	3.61	3.25	3.44	3.48	3.44	3.48	3.51	3.54
15	3.38	3.15	3.81	3.38	3.51	3.38	3.38	3.41
16	3.08	3.22	1.97	0.49	2.89	2.82	3.15	7.35
17	3.08	3.18	1.35	1.25	3.28	3.28	5.25	6.76

Table 17
Calculated Maximum Current Speed (ft/sec) at Barren Island During NE20

Location	Existing	Future	BI-1	BI-2	BI-3	BI-4	BI-5	BI-6
1	1.12	1.12	1.94	1.05	1.84	1.18	1.28	1.38
2	1.28	1.21	1.08	1.05	1.02	1.41	1.08	1.05
3	1.44	1.31	1.12	0.98	1.05	1.28	1.18	1.21
4	1.74	1.25	0.92	0.75	0.82	0.95	1.35	1.31
5	1.05	1.31	0.82	0.95	0.82	0.92	1.02	1.02
6	2.07	1.25	1.41	1.51	1.35	1.51	1.35	1.51
7	1.38	1.41	1.31	1.08	1.28	1.48	1.38	1.44
8	1.61	1.35	1.28	1.18	1.21	1.51	1.48	1.48
9	1.90	1.57	1.51	1.21	1.51	1.71	1.84	1.80
10	1.35	1.05	1.12	1.35	1.12	1.25	1.25	1.28
11	1.71	1.41	1.35	1.12	1.35	1.54	1.61	1.61
12	3.28	3.12	3.31	2.72	3.28	3.31	3.28	3.28
13	1.12	1.18	1.12	1.18	1.12	1.15	1.18	1.15
14	1.67	1.28	0.33	0.33	0.33	0.26	0.30	0.30
15	1.80	1.21	0.16	0.39	0.20	0.23	0.36	0.23
16	1.28	1.15	0.16	0.13	0.16	0.20	0.33	0.16
17	1.31	1.12	0.95	0.95	1.12	1.12	1.02	0.52

Table 18
Calculated Maximum Current Speed (ft/sec) at Barren Island During NE33

Location	Existing	Future	BI-1	BI-2	BI-3	BI-4	BI-5	BI-6
1	0.66	0.82	2.33	0.82	0.98	0.82	1.05	1.41
2	0.89	1.41	1.28	1.41	0.49	1.48	1.31	1.41
3	1.15	2.03	1.21	1.12	0.46	1.15	1.64	1.67
4	1.38	2.43	0.79	0.75	0.39	0.79	1.84	1.67
5	0.52	1.54	0.89	0.46	0.52	0.49	0.62	0.75
6	1.35	0.72	0.89	0.92	0.69	0.92	0.79	0.98
7	0.95	1.18	1.25	1.35	0.52	1.31	1.18	1.48
8	1.35	2.40	1.41	1.02	0.59	1.05	2.07	2.10
9	1.94	2.10	1.21	1.51	0.56	1.54	1.54	1.61
10	1.54	1.54	1.38	1.38	0.69	1.38	1.38	1.28
11	1.64	2.07	1.02	1.28	0.52	1.31	1.61	1.57
12	3.31	3.28	3.28	3.28	2.89	3.28	3.28	3.28
13	0.85	0.92	0.92	0.85	0.82	0.89	0.95	0.95
14	0.79	1.35	0.46	0.23	0.30	0.43	0.23	0.23
15	1.15	1.21	1.90	0.26	0.43	1.84	0.33	0.43
16	0.95	1.71	0.20	0.16	0.10	0.20	0.49	0.26
17	0.98	1.57	0.49	0.49	0.56	0.56	0.75	0.36

For the simulated storms, the calculated maximum current velocity has a much greater magnitude for the hurricanes (Hazel and Isabel) as compared to the northeasters (NE20 and NE33) and the normal tide condition, for both the existing condition and the alternative configurations. The calculated maximum current velocity from the two northeasters is similar to that of the the normal tide condition at the SAV and oyster bed areas. Tables 11 to 18 present the maximum current velocity at comparison locations for the storms and the individual James Island and Barren Island alternatives.

James Island

For the James Island alternative evaluation, the maximum current velocity was overall strong during Hurricanes Hazel and Isabel (large hurricanes) in the existing condition, the future without-project condition, and for all six alternatives, because the low-lying island area was partially or completely submerged under the peak storm surge. In the case of Hurricanes Hazel and Isabel for all alternatives, the current velocity was stronger at the tidal gut south channel (Point 7) than at the north channel (Point 9) because more water entered the lower wetland through the south tidal gut. For the northeasters NE20 and NE33, the current velocity was stronger at the tidal gut north channel (Point 9) than the south channel (Point 7) because more water flowed into the wetland through the north tidal gut. The current velocity during these northeasters was weak in the tidal gut (Points 7 and 9) as compared to the existing island condition. The current magnitude in the existing condition was similar to the future without-project condition for both hurricanes and northeasters.

With a bird island present at the tidal gut south entrance (Alts JI-3 and JI-6), the maximum current velocity weakened in the tidal gut south channel (Point 7) because of increased friction. However, the current velocity was stronger at the narrower channel around the bird island (Point 16). On the other hand, the current velocity also became stronger in the local channel (Points 1 and 12) for all six alternatives other than the existing island condition because of the narrower water exchange area between James and Taylors Islands for the local channel.

The behavior of the individual alternatives with respect to the velocity is summarized as follows:

Alt JI-1. The maximum current velocity can become strong at the tidal gut channel and entrance area (Points 5, 7, 8, 9, 14, and 15) in a hurricane with high storm surge (e.g., Hurricane Isabel). The current velocity was generally stronger in the local channel (Points 1 and 12), with the current magnitude similar to other alternatives, as compared to the existing island condition. A strong current also occurred at the southeast corner of the island alternative because of the sharp turning angle of the flow between the south tidal gut outlet and open bay. In the case of a northeaster, the current at all key locations overall was not strong, similar to the current magnitude in other alternatives.

Alt JI-2. The maximum current velocity was similar to that in Alt JI-1. The maximum current can also become stronger at the tidal gut channel and entrance area (Points 5, 7, 8, 9, 14 and 15) in a hurricane (e.g., Hurricane Hazel).

Alt JI-3. The maximum current velocity was similar to that in Alts JI-1 and JI-2. However, with a bird island present in the tidal gut south entrance, the maximum current was stronger around the bird island (Point 16) in a hurricane with high storm surges (e.g., Hurricane Hazel). In contrast, the current in the tidal gut (Points 7 and 9) was generally weaker than for the other alternatives in a northeaster because of increased friction at the bird island periphery.

Alt JI-4. The maximum current velocity was similar to that in Alt JI-1. However, the current in the south end of the existing island (Point 14) can become strong in a hurricane (e.g., Hurricane Hazel). The current velocity was reduced in the tidal gut and at the north entrance (Points 7, 8, and 9) as a result of wider channel section.

Alt JI-5. The maximum current velocity was similar to that in Alt JI-4. Because the c-shaped tidal gut cross section is smaller (150 ft wide) and the current velocity in the channel similar to that of Alt JI-4, the flow discharge in the tidal gut was the weakest among all six alternatives.

Alt JI-6. The maximum current velocity was similar to that in Alt JI-3. The current velocity at the tidal gut and around the bird island (Points 7, 8, 9, and 16) was weaker than that in Alt JI-3 because of the wider channel section. The current in the south end of the existing island (Point 14) can become strong in a hurricane (e.g., Hurricane Hazel).

Barren Island

For the Barren Island alternatives, the calculated maximum current velocity was strong during Hurricane Hazel and Hurricane Isabel, because the existing island and alternatives were either partially or completely submerged under the peak storm surge. The current velocity in the existing island case was similar to the future without-project condition. The current velocity can become strong at the low-crested south breakwater (Points 16 and 17), especially in a hurricane. The effect of the individual alternatives on the current velocity is summarized as follows.

Alt BI-1. The maximum current velocity was similar to that in the existing island condition. However, the current magnitude was reduced significantly at the high-crested south breakwater (Points 16 and 17), especially in a northeaster storm. The current can become strong at the tip of south breakwater (Point 1) during a northeaster because of the sharp turning of the current flow.

Alt BI-2. The maximum current velocity was similar to that in Alt BI-1. However, the current flow becomes weaker south of the short south breakwater (Point 1) in the northeaster.

Alt BI-3. The maximum current velocity was similar to that in Alt BI-1. However, the current flow is stronger at the low-crested south breakwater (Points 16 and 17).

Alt BI-4. The maximum current velocity was similar to that in Alt BI-2. However, the current flow is stronger at the low-crested short south breakwater (Points 16 and 17).

Alt BI-5. The maximum current velocity was similar to that in Alt BI-3. However, the current flow was strong at the segmented south breakwater (Points 16 and 17) during the hurricanes.

Alt BI-6. The maximum current velocity was similar to that in Alt BI-4. However, the current flow becomes strong at the segmented short south breakwater (Points 16 and 17) during the hurricanes.

Sedimentation

Sedimentation is evaluated as the change of the bottom elevation surrounding the island and at the tidal guts and navigation channels. Results from the sediment transport simulations are evaluated at the same location as in the current velocity comparison. The evaluation results are presented only for the storms because the calculated bottom elevation change was negligibly small under the normal tide condition as compared to the storms. In the case of the normal tide, locally generated wind waves are small and, therefore, sediment movement is insignificant under the weak tidal current.

The sediment transport simulation shows that the bottom elevation change is greater for hurricanes as compared to northeasters. Bottom erosion will take place in areas with strong currents and gradients in the current, whereas sediment shoaling occurs next to erosion areas where the current is diminished. Tables 19 through 26 present the calculated bottom elevation change (positive values denote accretion and negative values denote erosion) at locations selected for the evaluation of James Island and Barren Island alternatives (Figures 40 and 41).

Table 19
Calculated Bed Elevation Change (cm) at James Island During Hurricane Hazel

Location	Existing	Future	JI-1	JI-2	JI-3	JI-4	JI-5	JI-6
1	-0.10	-0.10	-0.20	-0.20	-0.20	-0.20	-0.20	-0.20
2	0.00	0.00	0.00	0.00	0.00	0.00	0.00	0.00
3	0.10	0.20	0.00	0.00	0.00	0.00	0.00	0.00
4	-0.40	-1.00	-0.10	-0.10	-0.10	-0.10	-0.10	-0.10
5	-0.10	0.00	0.60	0.50	0.60	0.40	0.60	0.50
6	0.20	0.20	0.50	0.50	0.60	0.60	0.60	0.70
7	0.30	0.30	-0.10	-0.20	-0.10	0.00	0.00	0.00
8	0.20	0.00	0.10	0.10	0.10	0.00	0.00	0.00
9	0.00	0.00	0.00	0.00	0.00	0.00	-0.10	0.00
10	0.00	0.00	-1.00	-1.00	-1.00	-1.00	-1.00	-1.00
11	-0.10	-0.10	0.10	0.10	0.10	0.10	0.10	0.10
12	0.00	0.00	-0.10	-0.10	-0.10	0.00	-0.10	0.00
13	-0.10	0.00	-10.60	-10.40	-10.50	-11.50	-11.50	-10.90
14	-4.80	-2.20	-6.80	-4.30	-2.00	-7.90	-7.90	-7.50
15	0.20	0.10	0.10	0.00	0.00	-0.20	-0.20	0.00
16	-0.40	-0.40	0.00	0.00	-1.20	0.20	0.20	-0.30

NOTE: Positive values denote accretion, and negative values denote erosion.

Table 20
Calculated Bed Elevation Change (cm) at James Island During Hurricane Isabel

Location	Existing	Future	JI-1	JI-2	JI-3	JI-4	JI-5	JI-6
1	0.00	0.10	-0.10	0.00	0.00	0.00	0.00	0.00
2	0.00	0.00	0.00	0.00	0.00	0.00	0.00	0.00
3	0.00	0.00	0.00	0.00	0.00	0.00	0.00	0.00
4	-0.20	-0.40	0.00	0.00	0.00	0.00	0.00	0.00
5	0.00	-0.20	0.20	0.40	0.20	0.40	0.50	0.30
6	-0.10	-0.10	0.10	0.00	0.00	0.00	-0.10	0.00
7	0.10	0.10	0.00	-0.10	-0.20	0.00	0.00	0.00
8	0.00	0.30	-0.10	0.00	-0.10	0.00	0.00	0.00
9	0.10	0.10	0.00	-0.10	0.00	0.00	0.00	0.00
10	0.00	0.00	0.20	0.30	0.30	0.30	0.20	0.30
11	0.00	0.00	0.10	0.10	0.10	0.10	0.10	0.10
12	0.10	0.10	-0.20	-0.20	-0.10	-0.20	-0.20	-0.20
13	0.20	0.30	-9.95	-9.52	-9.53	-9.45	-9.65	-9.35
14	-3.50	0.50	-3.20	-1.80	-2.50	-1.80	-1.80	-1.80
15	0.10	0.10	0.00	0.10	0.00	0.00	0.20	0.00
16	-0.20	-0.20	-0.10	0.00	-5.30	0.00	0.00	0.10

NOTE: Positive values denote accretion, and negative values denote erosion.

Table 21
Calculated Bed Elevation Change (cm) at James Island During NE20

Location	Existing	Future	JI-1	JI-2	JI-3	JI-4	JI-5	JI-6
1	0.00	0.00	0.00	0.00	0.00	0.00	0.00	0.00
2	0.00	0.00	0.00	0.00	0.00	0.00	0.00	0.00
3	0.00	0.00	0.00	0.00	0.00	0.00	0.00	0.00
4	0.10	0.90	0.00	0.00	0.00	0.00	0.00	0.00
5	0.10	0.20	0.00	0.00	0.00	0.00	0.00	0.00
6	0.10	0.20	0.10	0.10	0.10	0.10	0.10	0.10
7	-0.10	0.00	0.00	0.00	0.00	0.00	0.00	0.00
8	0.00	0.30	0.00	0.00	0.00	0.00	0.00	0.00
9	0.00	-0.20	0.00	0.00	0.00	0.00	0.00	0.00
10	0.00	0.10	-0.60	-0.60	-0.60	-0.60	-0.60	-0.60
11	0.00	-0.10	0.10	0.10	0.10	0.10	0.10	0.10
12	0.00	0.00	-0.10	-0.10	0.00	0.00	-0.10	-0.10
13	0.00	-0.10	-3.30	-3.40	-3.20	-3.30	-3.30	-3.10
14	-0.50	-2.00	0.10	0.10	0.10	0.10	0.10	0.10
15	0.00	-0.10	0.00	0.00	0.00	0.00	0.00	0.00
16	0.10	-0.20	0.00	0.00	0.00	0.00	0.00	0.00

NOTE: Positive values denote accretion, and negative values denote erosion.

Table 22**Calculated Bed Elevation Change (cm) at James Island During NE33**

Location	Existing	Future	JI-1	JI-2	JI-3	JI-4	JI-5	JI-6
1	0.00	0.10	0.00	0.00	0.00	0.00	0.00	0.00
2	0.00	0.00	0.00	0.00	0.00	0.00	0.00	0.00
3	0.00	0.00	0.00	0.00	0.00	0.00	0.00	0.00
4	0.00	0.30	0.00	0.00	0.00	0.00	0.00	0.00
5	0.00	0.00	0.00	0.00	0.00	0.00	0.00	0.00
6	0.00	0.00	0.00	0.00	0.00	0.00	0.00	0.00
7	0.00	0.00	0.00	0.00	0.00	0.00	0.00	0.00
8	0.00	0.00	0.00	0.00	0.00	0.00	0.00	0.00
9	-0.10	0.00	0.00	0.00	0.00	0.00	0.00	0.00
10	0.00	0.00	0.00	0.00	0.00	0.00	0.00	0.00
11	0.00	0.00	0.00	0.00	0.00	0.00	0.00	0.00
12	0.00	0.00	0.00	0.00	0.00	0.00	0.00	0.00
13	0.00	0.00	-0.20	-0.20	-0.20	-0.20	-0.20	-0.20
14	-0.10	-0.50	0.00	0.00	0.00	0.00	0.00	0.00
15	0.00	0.00	0.00	0.00	0.00	0.00	0.00	0.00
16	0.00	0.00	0.00	0.00	0.00	0.00	0.00	0.00

NOTE: Positive values denote accretion, and negative values denote erosion.

Table 23**Calculated Bed Elevation Change (cm) at Barren Island During Hurricane Hazel**

Location	Existing	Future	BI-1	BI-2	BI-3	BI-4	BI-5	BI-6
1	-0.10	-0.10	0.00	0.00	0.10	0.00	0.00	0.00
2	0.20	0.10	0.00	0.40	0.00	0.10	0.00	0.00
3	0.10	0.00	0.00	0.00	0.00	0.00	0.20	0.00
4	-0.10	-0.10	0.00	0.00	0.00	0.00	-0.10	0.00
5	0.00	-0.20	0.00	0.00	0.00	0.00	0.00	0.00
6	0.10	0.10	0.20	-0.10	0.20	0.10	0.20	0.30
7	0.20	0.20	0.00	0.30	0.00	0.20	0.00	0.00
8	0.00	0.00	0.00	0.00	0.00	0.10	0.00	0.00
9	-0.10	0.30	0.00	0.00	0.00	0.00	0.00	0.00
10	0.00	-0.30	0.00	0.00	0.00	0.00	0.10	0.00
11	0.00	-0.40	0.00	0.00	0.00	0.00	-0.10	0.00
12	0.00	0.00	0.00	0.00	0.00	0.00	0.00	0.00
13	0.00	0.00	0.00	0.00	0.00	0.00	-0.10	0.00
14	15.30	-0.90	1.20	1.10	1.00	1.40	8.50	8.30
15	0.60	-0.10	0.20	0.40	0.00	0.00	-2.90	-0.60
16	0.20	0.20	-0.10	-0.10	1.00	0.50	20.10	8.00
17	0.00	-0.10	1.10	0.70	-1.20	-0.10	-15.70	-32.70

NOTE: Positive values denote accretion, and negative values denote erosion.

Table 24
Calculated Bed Elevation Change (cm) at Barren Island During Hurricane Isabel

Location	Existing	Future	BI-1	BI-2	BI-3	BI-4	BI-5	BI-6
1	-0.20	-0.10	0.00	0.10	0.10	0.10	0.00	0.00
2	0.30	0.30	0.00	0.20	0.00	0.10	-0.10	0.00
3	-0.20	-0.20	0.00	0.00	0.00	0.00	0.00	0.10
4	-0.20	-0.30	0.00	0.00	0.00	-0.10	0.00	-0.20
5	0.00	0.20	0.30	0.00	0.10	0.00	0.00	0.00
6	0.20	0.20	0.20	0.30	0.20	0.20	0.30	0.40
7	0.30	0.30	0.00	0.20	0.00	-0.10	-0.10	0.00
8	0.00	0.00	0.00	0.00	0.00	0.00	0.00	0.00
9	0.10	0.00	0.00	0.00	0.00	0.00	0.00	0.00
10	0.10	0.20	0.00	0.00	0.00	0.00	0.00	0.00
11	0.10	0.10	0.00	0.00	0.00	0.00	0.00	0.00
12	-0.10	-0.30	-0.20	-0.10	-0.20	-0.10	-0.10	-0.10
13	0.00	0.00	0.00	0.00	0.00	0.00	0.00	0.00
14	58.50	-1.90	-3.40	1.30	0.00	0.90	3.70	4.20
15	1.80	0.70	9.00	0.60	2.80	-0.20	-3.30	-1.40
16	-0.30	-0.40	-0.10	0.00	-3.40	-2.30	23.00	32.60
17	-0.20	-0.30	0.70	1.10	4.70	2.00	-17.00	-42.40

NOTE: Positive values denote accretion, and negative values denote erosion.

Table 25
Calculated Bed Elevation Change (cm) at Barren Island During NE20

Location	Existing	Future	BI-1	BI-2	BI-3	BI-4	BI-5	BI-6
1	-0.10	0.00	-0.10	-0.10	-0.10	-0.10	0.00	0.00
2	-0.20	0.00	0.00	0.00	0.00	0.00	0.00	0.00
3	0.10	0.00	0.00	0.00	0.00	0.00	0.00	0.10
4	-0.10	0.00	0.00	0.00	0.00	0.00	0.00	0.00
5	0.00	0.00	0.00	-0.10	0.00	0.00	0.00	0.00
6	-0.20	0.00	0.00	-0.10	0.00	-0.10	0.00	0.00
7	0.10	0.00	0.00	0.00	0.00	0.00	0.00	0.00
8	0.00	0.00	0.00	0.00	0.00	0.00	0.00	0.00
9	0.00	0.00	0.00	0.00	0.00	0.00	0.00	0.00
10	0.00	0.00	0.00	0.00	0.10	0.10	0.10	0.10
11	0.00	0.00	0.00	0.00	0.00	0.00	0.00	0.00
12	-0.10	0.00	-0.20	-0.20	-0.20	-0.20	-0.40	-0.30
13	-0.10	0.00	-0.10	-0.10	-0.10	-0.10	-0.10	-0.10
14	0.20	0.00	0.00	0.00	0.00	0.00	0.00	0.00
15	0.10	0.00	0.00	0.00	0.00	0.00	0.00	0.00
16	0.20	0.00	0.00	0.00	0.00	0.00	0.90	0.90
17	0.00	0.00	0.20	0.20	0.30	0.30	1.20	-0.10

NOTE: Positive values denote accretion, and negative values denote erosion.

Table 26**Calculated Bed Elevation Change (cm) at Barren Island During NE33**

Location	Existing	Future	BI-1	BI-2	BI-3	BI-4	BI-5	BI-6
1	0.00	0.00	0.00	0.00	0.00	0.00	0.00	0.00
2	0.00	0.00	0.00	0.00	0.00	0.00	0.00	0.00
3	-0.10	0.10	0.00	0.00	0.00	0.00	0.00	0.00
4	0.10	0.00	0.00	0.00	0.00	0.00	0.00	0.00
5	0.00	0.00	0.00	0.00	0.00	0.00	0.00	0.00
6	-0.10	0.00	0.00	0.00	0.00	0.00	0.00	0.00
7	0.00	0.00	0.00	0.00	0.00	0.00	0.00	0.00
8	0.00	0.00	0.00	0.00	0.00	0.00	0.00	0.00
9	0.00	0.00	0.00	0.00	0.00	0.00	0.00	0.00
10	0.00	0.00	0.00	0.00	0.00	0.00	0.00	0.00
11	0.00	0.00	0.00	0.00	0.00	0.00	0.00	0.00
12	-0.10	-0.50	-0.20	-0.10	-0.10	-0.20	-0.10	-0.10
13	0.00	0.00	0.00	0.00	0.00	0.00	0.00	0.00
14	0.00	0.00	0.00	0.00	0.00	0.00	0.00	0.00
15	-0.10	0.00	0.00	0.00	0.00	0.00	0.00	0.00
16	0.00	0.00	0.00	0.00	0.00	0.00	0.40	0.40
17	0.00	0.00	0.00	0.00	0.00	0.00	0.20	0.10

NOTE: Positive values denote accretion, and negative values denote erosion.

James Island

For the James Island alternatives, the greatest bed erosion occurred at the southeast corner of the alternative island (Point 13) and at the southern end of the existing island (Point 14). There was sediment accretion and erosion along the east and south sides of the alternative island (Points 6 and 10). Mild sediment shoaling also occurred in the access channel (Point 11). The evaluation of sedimentation for the individual James Island alternative is summarized as follows:

Alt JI-1. Sediment erosion was significant at the southeast corner of the alternative island (Point 13) as a result of the strong current (and gradient) in the area. The southern end of the existing island (Point 14) can erode extensively in a hurricane (e.g., Hurricane Hazel). There was mild erosion in the local channel (Points 1 and 12) corresponding to the increased current velocity at the channel.

Alt JI-2. The bottom change pattern was similar to that in Alt JI-1. The erosion at the southern end of the existing island was not as severe as in Alt JI-1 under a hurricane.

Alt JI-3. The bed change pattern was similar to that in Alt JI-1. However, more erosion can occur in the south tidal gut around the bird island under a hurricane.

Alt JI-4. The bed change pattern was similar to that in Alt JI-1. The sedimentation was smaller in the tidal gut and at the north entrance (Points 7, 8, and 9) than in Alt JI-1.

Alt JI-5. The bed change pattern was similar to that in Alt JI-4.

Alt JI-6. The bed change pattern was similar to that in Alts JI-4 and JI-5.

Barren Island

For the Barren Island alternatives, the strongest sediment shoaling appeared at the north island tidal channel cut (Points 14 and 15) as a result of sediment being eroded from the existing island and carried by the current to the channel. For the existing island, sediment shoaling at the north island tidal channel cut can be strong in a hurricane (e.g., Hurricane Isabel). The greatest erosion occurred at the up-wave side of the low-crest south breakwater (Points 16 and 17) for the hurricanes. Evaluation of sedimentation for the individual Barren Island alternative is summarized as follows:

Alt BI-1. Sedimentation in the lee side (sheltered area) of the island (Points 1 to 12) was overall minor. Sediment shoaling in the north island tidal channel cut (Points 14 and 15) was much smaller than in the existing island condition. There was mild sediment shoaling at the high-crest south breakwater (Points 16 and 17) as a result of the weaker current at the breakwater.

Alt BI-2. The sedimentation pattern was similar to that in Alt BI-1. However, some sediment deposition occurred east of the short south breakwater (Points 2, 6, and 7).

Alt BI-3. Bottom change was similar to that in Alt BI-1. However, both sediment accretion and erosion were more significant at the low-crested south breakwater (Points 16 and 17).

Alt BI-4. Bottom change was similar to that in Alt BI-3. However, both sediment accretion and erosion at the short and low-crest south breakwater (Points 16 and 17) were not as significant as in Alt BI-3.

Alt BI-5. Bottom change was similar to that in Alt BI-3. However, both sediment shoaling and erosion can become more significant in the north island tidal cut channel (Points 14 and 15) in a hurricane (e.g., Hurricane Hazel). More sediment deposition and erosion appeared at the segmented south breakwater (Points 16 and 17).

Alt BI-6. Bottom change was similar to that in Alt BI-5. However, both sediment deposition and erosion were more significant at the segmented short south breakwater than in Alt BI-5.

Summary

Results from wave, hydrodynamic, and sediment transport numerical simulation models were analyzed to evaluate the performance of James Island and Barren Island plan view alternatives from engineering assessments. For the James Island alternatives, the wave height reduction was found to be approximately 1-2 ft on the lee of the island, as compared to the existing configuration and future without-project condition, for four severe storms. With respect to current velocity and sediment transport, no major performance differences were found among the alternatives (Alts JI-1 to JI-6). In the absence

of protective structures (such as riprap dikes), significant erosion can occur at the southeast corner of the alternative island and at the south end of the existing island in a hurricane. If a bird island is present at the tidal gut south entrance, erosion under a hurricane was predicted to be greater at the bird island (Point 16) for a narrow tidal channel (Alt JI-3) as compared to a wider tidal channel (Alt JI-6).

Bed erosion of as much as 10 to 20 cm was calculated to occur in the local channel (Points 1 and 12) for all alternatives in a hurricane because of the increased gradients in current velocity. Similarly, channel erosion of 10 to 20 cm can occur at the narrower tidal gut in a hurricane for Alts JI-1 to JI-3 because of increased current magnitude. For all alternative configurations, accretion of 20 to 60 cm was calculated to occur at the tidal gut south entrance (Point 5) under a hurricane as a result of scour of the tidal gut channel and erosion at the south end of the existing island, as well as erosion at the southeast corner of the island alternative. Sediment accumulation at the tidal gut south entrance can be minimized by reducing the erosion at the south end of the existing island and southeast corner of the island alternative with protective structures.

For the Barren Island alternatives, Alts BI-1 and BI-3 have a longer south breakwater and provide the greatest wave height reduction, reaching 2-3 ft in the lee of the island for the four storms evaluated. The future without-project condition results in a 2-4 ft increase in wave height at the mainland nearshore. With respect to current velocity and sediment transport, no significant performance differences were found among the existing configuration and alternatives (Alts BI-1 to BI-6) at locations distant from the site (Points 6 to 13). The influence of the alternatives is localized in the area at and near the south breakwater (Points 1 to 5).

For the four storm conditions, the maximum current velocity at the Honga River Tar Bay entrance (Point 12) was always strong, approximately 3.3 ft/sec, regardless of the existing configuration or future without-project or the island alternatives. As a result, the Honga River Tar Bay entrance usually experiences bed erosion of 10 to 50 cm during severe storms. The predicted erosion is slightly greater for the future with-project condition than for the existing configuration and the alternatives. Alts BI-3 and BI-4, with a low-crest south breakwater, are likely to induce relatively greater current velocities during storms, causing potentially significant temporary erosion at the breakwaters. Segmented breakwaters (Alts BI-5 and BI-6) can create a similar condition with strong current around the segmented breakwater element, causing either sediment deposition or erosion at the structures, depending on the direction of the current. The strong current at the north island cut (Points 14 and 15) in a hurricane can also cause extensive bed erosion or accretion at various locations along and near this cut.

References

- Bouws, E., Gunther, H., Rosenthal, W., and Vincent, C. L. (1985). "Similarity of the wind wave spectrum in finite depth waves; 1. Spectral form." *Journal of Geophysical Research* 90(C1), 975-986.
- Chesapeake Bay Program. (2000). *Chesapeake Bay submerged aquatic vegetation water quality and habitat-based requirements and restoration targets: A second synthesis*. Printed by the U.S. Environmental Protection Agency, Washington, DC.
- Cronin, W. B. (2005). *The disappearing islands of the Chesapeake*. The John Hopkins University Press, Baltimore and London, 200 p.
- E2CR, Inc. (2002a). "Geotechnical reconnaissance study for James Island, Chesapeake Bay, MD," prepared for Roy F. Weston, Inc., West Chester, PA.
- E2CR, Inc. (2002b). "Geotechnical reconnaissance study for Barren Island, Chesapeake Bay, MD," prepared for Roy F. Weston, Inc., West Chester, PA.
- Headquarters, U.S. Army Corps of Engineers. (2002). *Coastal Engineering Manual*, EM 1110-2-1100, Washington, DC.
- Luettich, R. A., Westerink, J. J., and Scheffner, N. W. (1992). "ADCIRC: An advanced three-dimensional circulation model for shelves, coasts, and estuaries. Report 1: Theory and methodology of ADCIRC-2DDI and ADCIRC-3DL," Dredging Research Program Technical Report DRP-92-6, U.S. Army Engineer Waterways Experiment Station, Vicksburg, MS.
- Melby, J. A., Thompson, E. F., Cialone, M. A., Smith, J. M., Borgman, L. E., Demirbilek, Z., Hanson, J. L., Lin, L. (2005). "Life-cycle analysis of Mid Bay and Poplar Island projects, Chesapeake Bay, Maryland," ERDC/CHL TR-05-12, Coastal and Hydraulics Laboratory, U.S. Army Engineer Research and Development Center, Vicksburg, MS.
- Militello, A., Reed, C. W., Zundel, A. K., and Kraus, N. C. (2004). "Two-dimensional depth-averaged circulation model M2D: Version 2.0, Report 1: Technical documentation and user's guide," Contract Report ERDC/CHL TR-04-2, Coastal and Hydraulics Laboratory, U.S. Army Engineer Research and Development Center, Vicksburg, MS.
- Moffatt & Nichol Engineers. (2002). "James Island reconnaissances study – hydrodynamics and sedimentation modeling," final report prepared for Maryland Port Administration, Baltimore, MD, and Maryland Environmental Services, Millersville, MD.

- Moffatt & Nichol Engineers. (2004). "Barren Island reconnaissance study – hydrodynamics and sedimentation modeling," final report prepared for the U.S. Army Engineer District, Baltimore, MD.
- Schubel, J. R., and Prichard, D. W. (1987). "A brief physical description of the Chesapeake Bay, in contaminant problems and management of living Chesapeake Bay resources," S. K. Majumdar, L. W. Hall, Jr., and H. M. Austin (eds.), 1-32, Pennsylvania Academy of Science, Philadelphia, PA.
- Smith, J. M., Sherlock, A. R., and Resio, D. T. (2001). "STWAVE: Steady-state spectral wave model user's manual for STWAVE, Version 3.0," Special Report ERDC/CHL SR-01-1, Coastal and Hydraulics Laboratory, U.S. Army Engineer Research and Development Center, Vicksburg, MS.
- U.S. Army Corps of Engineers. (2005). "Integrated Mid-Chesapeake Bay Island ecosystem restoration feasibility report and environmental impact statement (EIS)," Baltimore, MD.
- Van Rijn, L. C. (1984a). "Sediment transport: Part 1: Bed load transport." *Journal of the Hydraulics Division, Proceedings* 110 (HY10), ASCE, 1,431-56.
- Van Rijn, L. C. (1984b). "Sediment transport: Part II: Suspended load transport." *Journal of the Hydraulics Division, Proceedings* 110 (HY11), ASCE, 1,613-41.
- Van Rijn, L. C. (1984c). "Sediment transport: Part III: Bed forms and alluvial roughness." *Journal of the Hydraulics Division, Proceedings* 110 (HY12), ASCE, 1,733-54.
- Van Rijn, L. C. (1993). *Principles of sediment transport in rivers, estuaries, and coastal seas*. Aqua Publications, Amsterdam.
- Weston Solutions, Inc. (2002). "Reconnaissance of the proposed environmental restoration project near Barren Island, Dorchester County, Maryland," prepared for Maryland Environmental Service, Millersville, MD.

Appendix A

Data Acquisition and Baseline Monitoring

This chapter summarizes coastal engineering data gathered as part of the Coastal Monitoring and Modeling Support task undertaken by Blasland, Bouck & Lee, Inc. (BBL), and Andrews, Miller & Associates, Inc. (AMA), at James Island and Barren Island. Collected information encompassed pre-existing data and preliminary investigations to develop baseline monitoring for the regions surrounding James Island and Barren Island. This work was undertaken by the Maryland Port Administration (MPA) and the U.S. Army Corps of Engineers, Baltimore District (hereafter, Baltimore District), through the Maryland Environmental Service (MES).

Data Acquisition

Existing data assembled to support the coastal modeling effort included:

- a. Sediment type within the vicinity of James Island and Barren Island.
- b. Wind data.
- c. Review of dredging frequency of nearby navigational (Federal) channels, as well as estimated shoaling rates of the channels (based on available hydrographic surveys).
- d. Available hydrographic surveys.
- e. Aerial photography.

Data collection and monitoring information assembled for the coastal modeling tasks included:

- a. Thirty sediment grab samples collected at each island at the time of the bathymetric surveys. Sediment grain size distributions (GSDs) and characteristics were determined for each sample using standard sieve and hydrometer analyses.
- b. Identification of locations and characteristics of navigational channels, and calculation of associated historical shoaling rates.
- c. Hydrographic surveys conducted at James Island and Barren Island.

- d. High spatial resolution aerial imagery obtained for both islands.
- e. Historical shoreline position data developed for the island shorelines and mainland shorelines east of James Island and Barren Island using available historical aerial photography and the latest high spatial resolution imagery.

Existing Data Assessment

Sediment type at James Island and Barren Island

E2CR, Inc. completed a geotechnical investigation for both James Island and Barren Island over the winter of 2001 as part of a reconnaissance study conducted by the MPA (E2CR 2002a, 2002b)¹. The geotechnical studies involved several aspects including a field investigation with cone penetrometer tests (CPT), borings, and laboratory testing for determination of sediment characteristics. Twenty-two borings and four CPTs were made around James Island (Figure A1), extending between 27.5 and 70 ft below water level and 18 borings were made in the vicinity of Barren Island (Figure A2), extending between 35 and 70 ft.

A feasibility study was conducted by the U.S. Army Corps of Engineers (USACE) to further evaluate the potential for James Island and Barren Island to undergo restoration activities (USACE 2005). Sixty-two borings in the vicinity of James Island (Figure A1) and an additional 27 borings around Barren Island (Figure A2) were collected by the USACE to investigate the subsurface conditions along proposed dike and channel alignments. These borings were collected during the summer of 2004. Additional sampling involved collection of undisturbed samples of clay and silt for laboratory testing, which included triaxial strength testing, unconfined compression testing, and consolidation testing. On-site testing included grain size analysis, Atterberg Limits, and water contents.

¹ References cited in this appendix are contained in the reference section of the main text of this report.

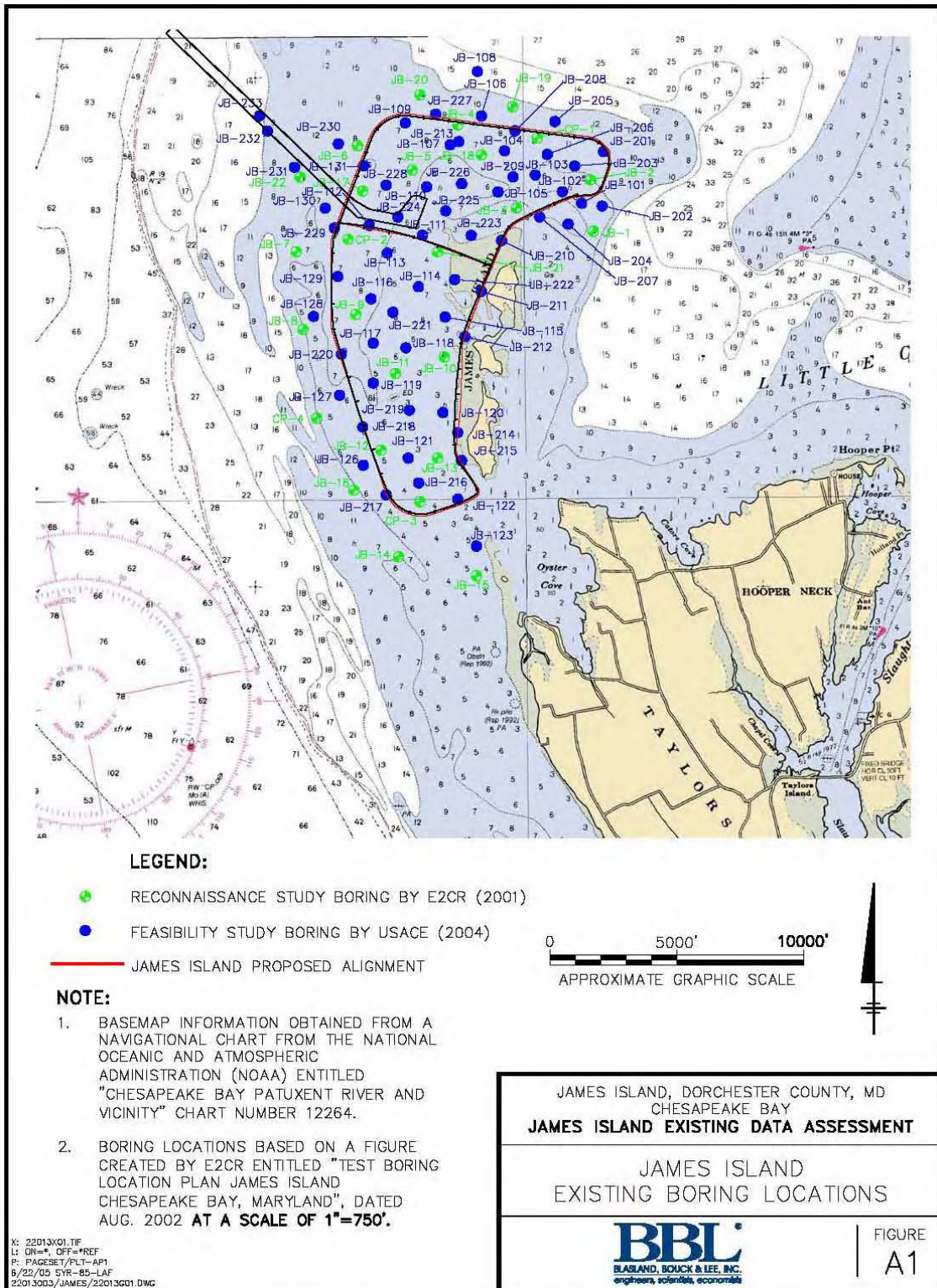


Figure A1. James Island existing boring locations

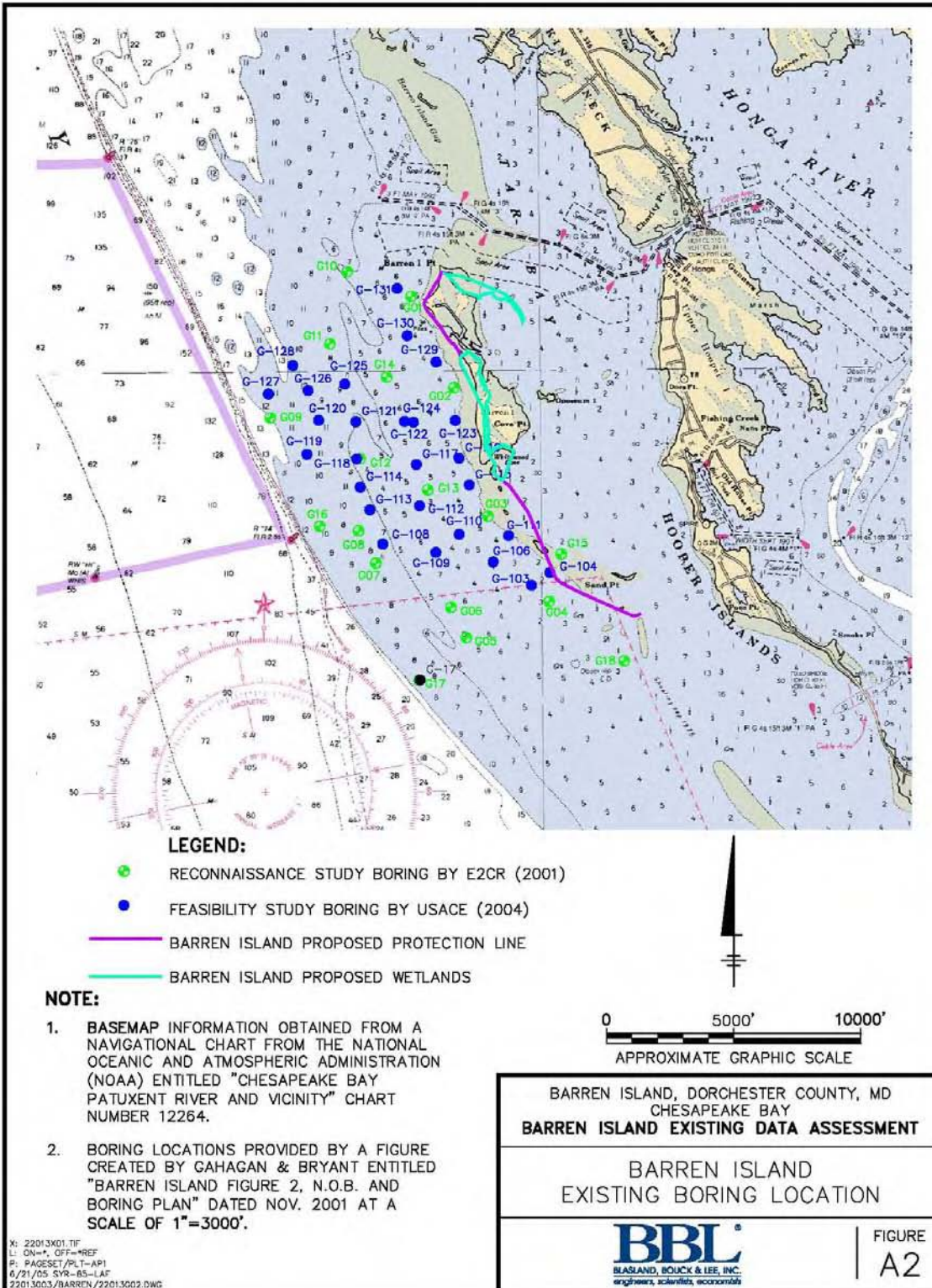


Figure A2. Barren Island existing boring locations

Tables A1 and A2 list information on the borings collected as part of the Reconnaissance and Feasibility Studies at James Island and Barren Island. Each table lists boring ID, location coordinates (X, Y) in Maryland State Plane, North American Datum 1983 (NAD83) (ft), the phase of study from when the boring was conducted, and the organization that collected the samples.

Table A1
Existing Borings - James Island

Boring ID	X Coordinate	Y Coordinate	Study Phase	Performed By
CP-1	1,503,547.73	318,451.27	RECON (2001)	E2CR
CP-2	1,496,094.74	314,458.80	RECON (2001)	E2CR
CP-3	1,498,937.64	304,093.73	RECON (2001)	E2CR
CP-4	1,494,865.38	307,395.20	RECON (2001)	E2CR
JB-1	1,505,768.86	314,771.88	RECON (2001)	E2CR
JB-2	1,505,653.61	316,806.50	RECON (2001)	E2CR
JB-3	1,502,733.88	315,693.22	RECON (2001)	E2CR
JB-4	1,500,426.62	318,975.34	RECON (2001)	E2CR
JB-5	1,498,623.21	317,190.39	RECON (2001)	E2CR
JB-6	1,496,471.83	318,150.12	RECON (2001)	E2CR
JB-7	1,494,051.53	313,965.71	RECON (2001)	E2CR
JB-8	1,494,320.46	310,894.58	RECON (2001)	E2CR
JB-9	1,496,404.59	311,488.89	RECON (2001)	E2CR
JB-10	1,499,890.99	309,807.78	RECON (2001)	E2CR
JB-11	1,497,970.12	309,155.17	RECON (2001)	E2CR
JB-12	1,497,393.85	306,122.43	RECON (2001)	E2CR
JB-13	1,499,622.07	305,815.31	RECON (2001)	E2CR
JB-14	1,498,085.37	301,911.52	RECON (2001)	E2CR
JB-15	1,501,158.77	301,170.23	RECON (2001)	E2CR
JB-16	1,496,322.51	304,550.34	RECON (2001)	E2CR
JB-17	1,496,665.92	316,358.37	RECON (2001)	E2CR
JB-18	1,501,354.38	317,787.88	RECON (2001)	E2CR
JB-19	1,502,580.77	319,690.26	RECON (2001)	E2CR
JB-20	1,498,938.22	320,165.86	RECON (2001)	E2CR
JB-21	1,499,629.15	313,959.74	RECON (2001)	E2CR
JB-22	1,494,210.62	316,907.99	RECON (2001)	E2CR
JB-101	1,505,302.92	315,875.03	FEASIBILITY (2004)	USACE
JB-102	1,504,544.64	316,334.80	FEASIBILITY (2004)	USACE
JB-103	1,503,475.02	316,994.63	FEASIBILITY (2004)	USACE
JB-104	1,502,268.25	317,946.89	FEASIBILITY (2004)	USACE
JB-105	1,502,009.86	316,326.38	FEASIBILITY (2004)	USACE
JB-106	1,501,352.45	319,326.19	FEASIBILITY (2004)	USACE
JB-107	1,500,121.21	318,184.27	FEASIBILITY (2004)	USACE
JB-108	1,501,196.79	321,075.21	FEASIBILITY (2004)	USACE
JB-109	1,498,351.10	319,051.73	FEASIBILITY (2004)	USACE
JB-110	1,499,195.47	316,528.65	FEASIBILITY (2004)	USACE
JB-111	1,499,034.34	314,615.49	FEASIBILITY (2004)	USACE
JB-112	1,496,933.66	315,005.21	FEASIBILITY (2004)	USACE
JB-113	1,497,640.74	313,907.53	FEASIBILITY (2004)	USACE
JB-114	1,498,874.04	312,580.94	FEASIBILITY (2004)	USACE
JB-115	1,499,923.73	311,384.60	FEASIBILITY (2004)	USACE
JB-116	1,497,002.00	312,105.00	FEASIBILITY (2004)	USACE

(Continued)

Table A1 (Concluded)

Boring ID	X Coordinate	Y Coordinate	Study Phase	Performed By
JB-117	1,497,089.00	310,349.00	FEASIBILITY (2004)	USACE
JB-118	1,498,374.64	310,169.67	FEASIBILITY (2004)	USACE
JB-119	1,497,088.98	308,774.60	FEASIBILITY (2004)	USACE
JB-120	1,499,839.55	307,610.57	FEASIBILITY (2004)	USACE
JB-121	1,498,469.29	305,810.17	FEASIBILITY (2004)	USACE
JB-122	1,500,420.56	304,195.40	FEASIBILITY (2004)	USACE
JB-123	1,501,157.41	302,339.30	FEASIBILITY (2004)	USACE
JB-126	1,496,698.53	305,534.58	FEASIBILITY (2004)	USACE
JB-127	1,495,764.92	308,299.91	FEASIBILITY (2004)	USACE
JB-128	1,494,733.74	311,408.54	FEASIBILITY (2004)	USACE
JB-129	1,495,692.30	312,983.30	FEASIBILITY (2004)	USACE
JB-130	1,495,196.58	315,680.91	FEASIBILITY (2004)	USACE
JB-131	1,496,710.41	317,360.76	FEASIBILITY (2004)	USACE
JB-201	1,506,169.82	317,914.86	FEASIBILITY (2004)	USACE
JB-202	1,506,114.23	315,769.76	FEASIBILITY (2004)	USACE
JB-203	1,505,037.75	317,350.08	FEASIBILITY (2004)	USACE
JB-204	1,504,776.58	315,051.71	FEASIBILITY (2004)	USACE
JB-205	1,504,254.11	319,104.57	FEASIBILITY (2004)	USACE
JB-206	1,503,953.76	317,807.45	FEASIBILITY (2004)	USACE
JB-207	1,503,646.08	315,336.79	FEASIBILITY (2004)	USACE
JB-208	1,502,683.59	318,738.99	FEASIBILITY (2004)	USACE
JB-209	1,502,601.52	316,917.44	FEASIBILITY (2004)	USACE
JB-210	1,502,150.97	314,405.28	FEASIBILITY (2004)	USACE
JB-211	1,501,346.99	312,396.39	FEASIBILITY (2004)	USACE
JB-212	1,500,708.18	310,611.29	FEASIBILITY (2004)	USACE
JB-213	1,500,461.97	318,308.12	FEASIBILITY (2004)	USACE
JB-214	1,500,417.52	306,825.65	FEASIBILITY (2004)	USACE
JB-215	1,500,576.56	305,713.99	FEASIBILITY (2004)	USACE
JB-216	1,498,881.69	304,831.82	FEASIBILITY (2004)	USACE
JB-217	1,497,597.14	304,367.44	FEASIBILITY (2004)	USACE
JB-218	1,496,671.99	307,041.74	FEASIBILITY (2004)	USACE
JB-219	1,498,511.45	307,702.24	FEASIBILITY (2004)	USACE
JB-220	1,495,833.03	309,919.01	FEASIBILITY (2004)	USACE
JB-221	1,497,863.95	311,572.22	FEASIBILITY (2004)	USACE
JB-222	1,500,302.52	312,864.33	FEASIBILITY (2004)	USACE
JB-223	1,500,949.54	314,609.02	FEASIBILITY (2004)	USACE
JB-224	1,498,059.71	315,336.92	FEASIBILITY (2004)	USACE
JB-225	1,499,949.27	315,572.99	FEASIBILITY (2004)	USACE
JB-226	1,500,577.22	316,649.85	FEASIBILITY (2004)	USACE
JB-227	1,499,548.39	319,394.13	FEASIBILITY (2004)	USACE
JB-228	1,497,597.81	316,598.19	FEASIBILITY (2004)	USACE
JB-229	1,495,559.61	314,904.49	FEASIBILITY (2004)	USACE
JB-230	1,495,711.12	318,223.74	FEASIBILITY (2004)	USACE
JB-231	1,493,985.41	317,301.20	FEASIBILITY (2004)	USACE
JB-232	1,492,918.73	318,730.33	FEASIBILITY (2004)	USACE
JB-233	1,492,612.62	319,335.20	FEASIBILITY (2004)	USACE

Table A2
Existing Borings - Barren Island

Boring ID	X	Y	Study Phase	Performed By
G-1	1,522,379.54	246,553.30	RECON (2001)	E2CR
G-2	1,524,057.91	242,955.25	RECON (2001)	E2CR
G-3	1,525,389.96	237,897.72	RECON (2001)	E2CR
G-4	1,527,803.88	234,536.55	RECON (2001)	E2CR
G-5	1,524,539.00	233,144.18	RECON (2001)	E2CR
G-6	1,523,941.32	234,304.76	RECON (2001)	E2CR
G-7	1,520,981.28	236,047.34	RECON (2001)	E2CR
G-8	1,520,306.49	237,310.57	RECON (2001)	E2CR
G-9	1,516,828.51	241,768.80	RECON (2001)	E2CR
G-10	1,519,862.00	247,534.75	RECON (2001)	E2CR
G-11	1,519,172.22	244,688.60	RECON (2001)	E2CR
G-12	1,520,360.39	240,157.76	RECON (2001)	E2CR
G-13	1,523,028.88	238,928.70	RECON (2001)	E2CR
G-14	1,521,405.78	243,377.04	RECON (2001)	E2CR
G-15	1,528,281.10	236,403.93	RECON (2001)	E2CR
G-16	1,518,774.71	237,498.76	RECON (2001)	E2CR
G-17	1,522,725.63	231,436.06	RECON (2001)	E2CR
G-18	1,530,731.35	232,187.48	RECON (2001)	E2CR
G-103	1,527,109.94	235,174.26	FEASIBILITY (2004)	USACE
G-104	1,527,831.17	235,675.89	FEASIBILITY (2004)	USACE
G-106	1,525,603.91	236,092.66	FEASIBILITY (2004)	USACE
G-108	1,521,254.28	236,796.11	FEASIBILITY (2004)	USACE
G-109	1,523,345.18	236,468.91	FEASIBILITY (2004)	USACE
G-110	1,524,264.06	237,174.36	FEASIBILITY (2004)	USACE
G-111	1,526,209.19	237,129.48	FEASIBILITY (2004)	USACE
G-112	1,522,700.75	238,304.92	FEASIBILITY (2004)	USACE
G-113	1,520,749.43	238,137.57	FEASIBILITY (2004)	USACE
G-114	1,520,367.71	239,034.90	FEASIBILITY (2004)	USACE
G-115	1,524,662.66	239,130.06	FEASIBILITY (2004)	USACE
G-116	1,524,255.68	240,178.88	FEASIBILITY (2004)	USACE
G-117	1,522,576.11	239,932.66	FEASIBILITY (2004)	USACE
G-118	1,520,231.29	240,156.74	FEASIBILITY (2004)	USACE
G-119	1,518,269.42	240,333.45	FEASIBILITY (2004)	USACE
G-120	1,518,729.06	241,672.43	FEASIBILITY (2004)	USACE
G-121	1,520,195.82	241,613.22	FEASIBILITY (2004)	USACE
G-122	1,522,459.20	241,590.82	FEASIBILITY (2004)	USACE
G-123	1,524,108.19	241,664.80	FEASIBILITY (2004)	USACE
G-124	1,522,108.26	241,628.47	FEASIBILITY (2004)	USACE
G-125	1,519,761.63	243,107.01	FEASIBILITY (2004)	USACE
G-126	1,518,313.44	242,842.66	FEASIBILITY (2004)	USACE
G-127	1,516,752.64	242,709.04	FEASIBILITY (2004)	USACE
G-128	1,517,716.02	243,829.38	FEASIBILITY (2004)	USACE
G-129	1,523,348.45	243,975.33	FEASIBILITY (2004)	USACE
G-130	1,522,216.64	245,008.22	FEASIBILITY (2004)	USACE
G-131	1,521,819.31	246,866.46	FEASIBILITY (2004)	USACE

Chesapeake Bay wind data

Wind data were collected from a variety of locations throughout Chesapeake Bay for comparison to and possible input to the models. Locations at Baltimore-Washington International Airport (BWI), Thomas Point, a buoy in the Mid-Bay region between James Island and Barren Island, and a temporary National Oceanic and Atmospheric Administration (NOAA) station set up on Barren Island, allowed good coverage of the region of interest surrounding James Island and Barren Island. Wind data from BWI were collected by Weston Solutions, Inc., for 1951 through 1982 for extremal analysis (Weston Solutions, Inc. 2002). Thomas Point is a NOAA National Data Buoy Center (NDBC) location, sta TPLM2. Wind data were collected for 7 years (January 1993 through the end of 2000). The Mid-Bay buoy is operated by the Chesapeake Bay Observing System (CBOS); data were collected from June 1995 to July 2003. The station on Barren Island was a temporary NOAA station (ID No. 8571579). This station was installed in December 2001 and recorded wind speed from January 2002 through most of April 2003. Patuxent Naval Air Station wind data were evaluated through other conceptual design projects, but were not analyzed here due the completeness of the BWI wind data set that was ultimately used. Figure A3 shows the location of each wind station relative to James Island and Barren Island.

Wind information for BWI Airport was analyzed to determine yearly extreme wind speeds from 1951 through 1982 (Table A3). Wind roses were generated using the data gathered from the other three wind stations. Data were plotted at 10-deg intervals, displaying average wind speed frequency over the duration of each station's recorded data interval. Figures A4 through A6 show the wind rose diagram for each of these stations.

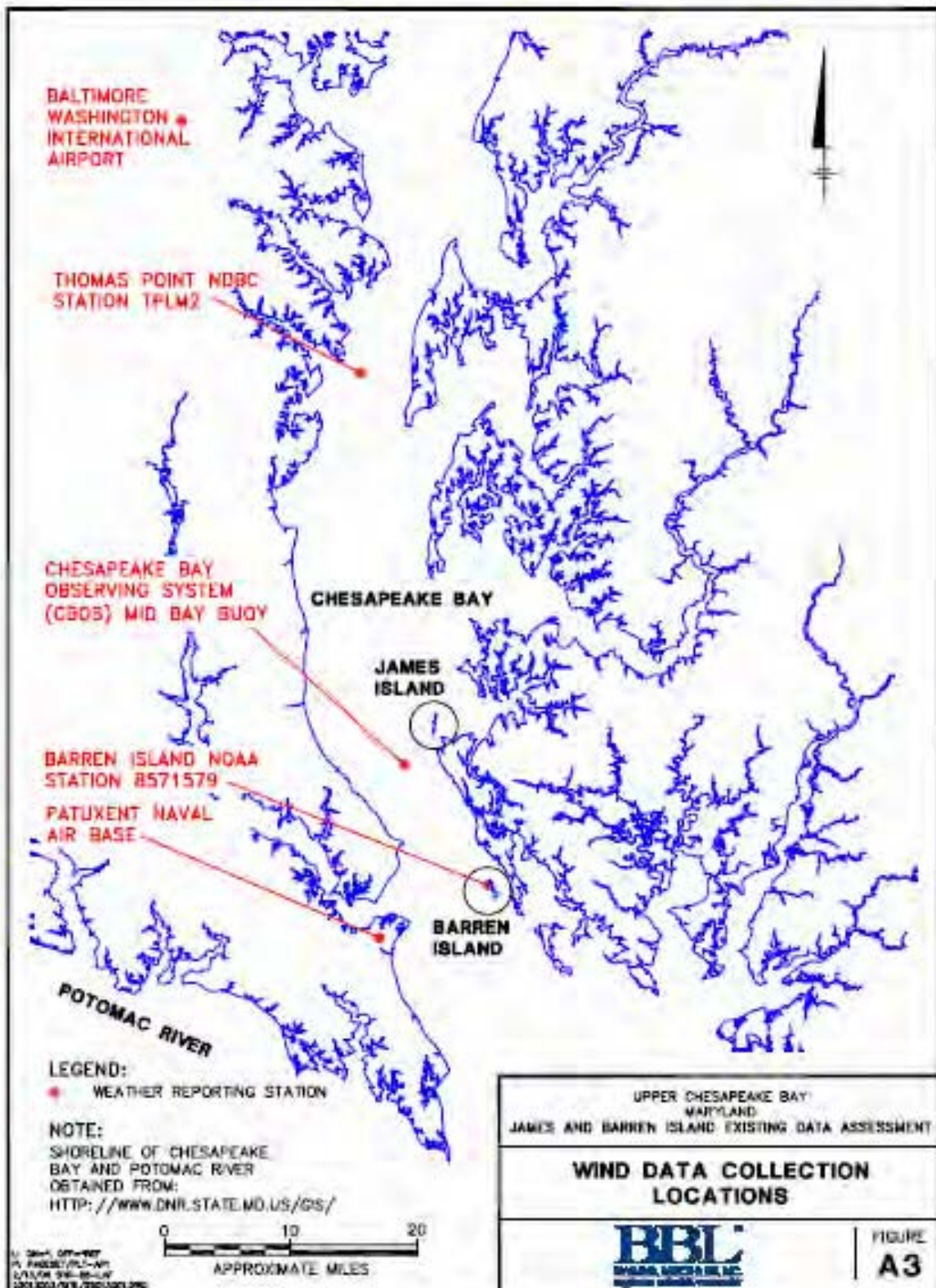


Figure A3. Wind data collection locations

Table A3**BWI Airport Annual Extreme Wind Speed (Weston Solutions, Inc. 2002)**

Year	N	NE	E	SE	S	SW	W	NW
Wind Direction								
1951	24	41	27	34	39	29	42	46
1952	66	25	47	66	41	66	46	43
1953	20	28	22	27	34	39	47	43
1954	31	27	22	60	28	39	57	44
1955	21	43	29	28	43	53	40	43
1956	29	34	25	24	28	34	56	40
1957	29	53	35	33	33	30	46	46
1958	30	52	25	33	37	43	40	43
1959	28	26	20	27	23	38	46	43
1960	26	38	28	27	25	35	40	53
1961	45	28	28	29	24	70	41	54
1962	56	41	28	17	25	36	42	61
1963	38	32	18	34	25	28	44	60
1964	34	31	23	24	47	23	48	61
1965	36	26	28	34	36	54	44	44
1966	32	25	29	24	47	43	50	48
1967	30	29	25	39	27	46	53	43
1968	45	30	36	26	19	45	48	50
1969	28	21	20	34	26	45	45	53
1970	28	28	18	21	39	34	48	60
1971	31	45	26	18	21	41	39	58
1972	28	25	35	26	20	41	41	41
1973	40	26	26	38	26	35	49	33
1974	32	23	46	29	33	33	45	41
1975	40	26	21	24	25	38	54	45
1976	31	18	20	28	32	28	45	54
1977	32	31	19	28	26	25	49	48
1978	39	28	36	28	19	52	33	45
1979	32	25	27	36	32	32	45	47
1980	33	27	18	32	20	32	45	50
1981	24	24	19	26	23	28	41	42
1982	31	20	23	23	29	34	40	48

NOTE: Data adjusted to 10-m (32.8 ft) elevation.

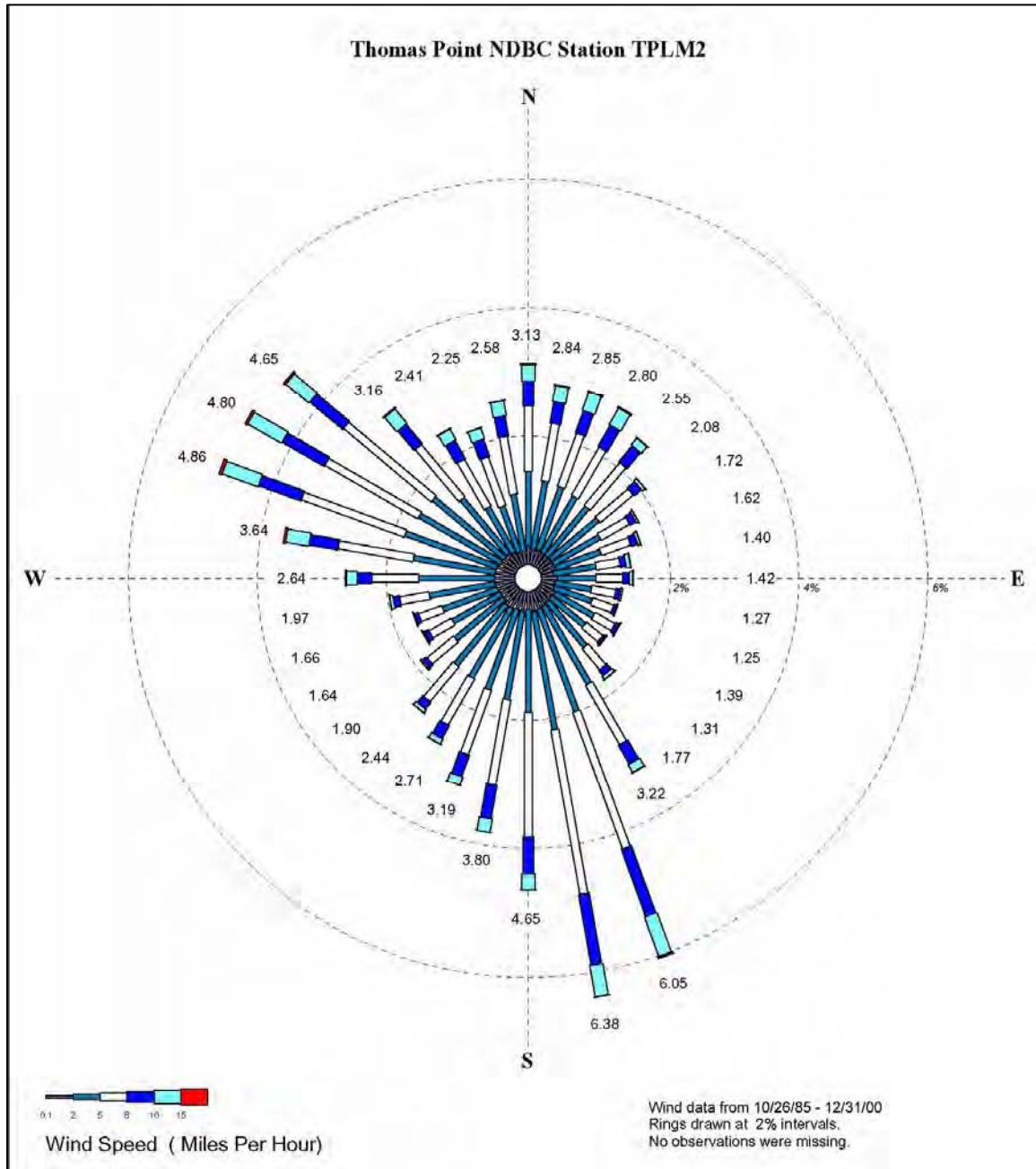


Figure A4. Thomas Point NDBC station wind rose

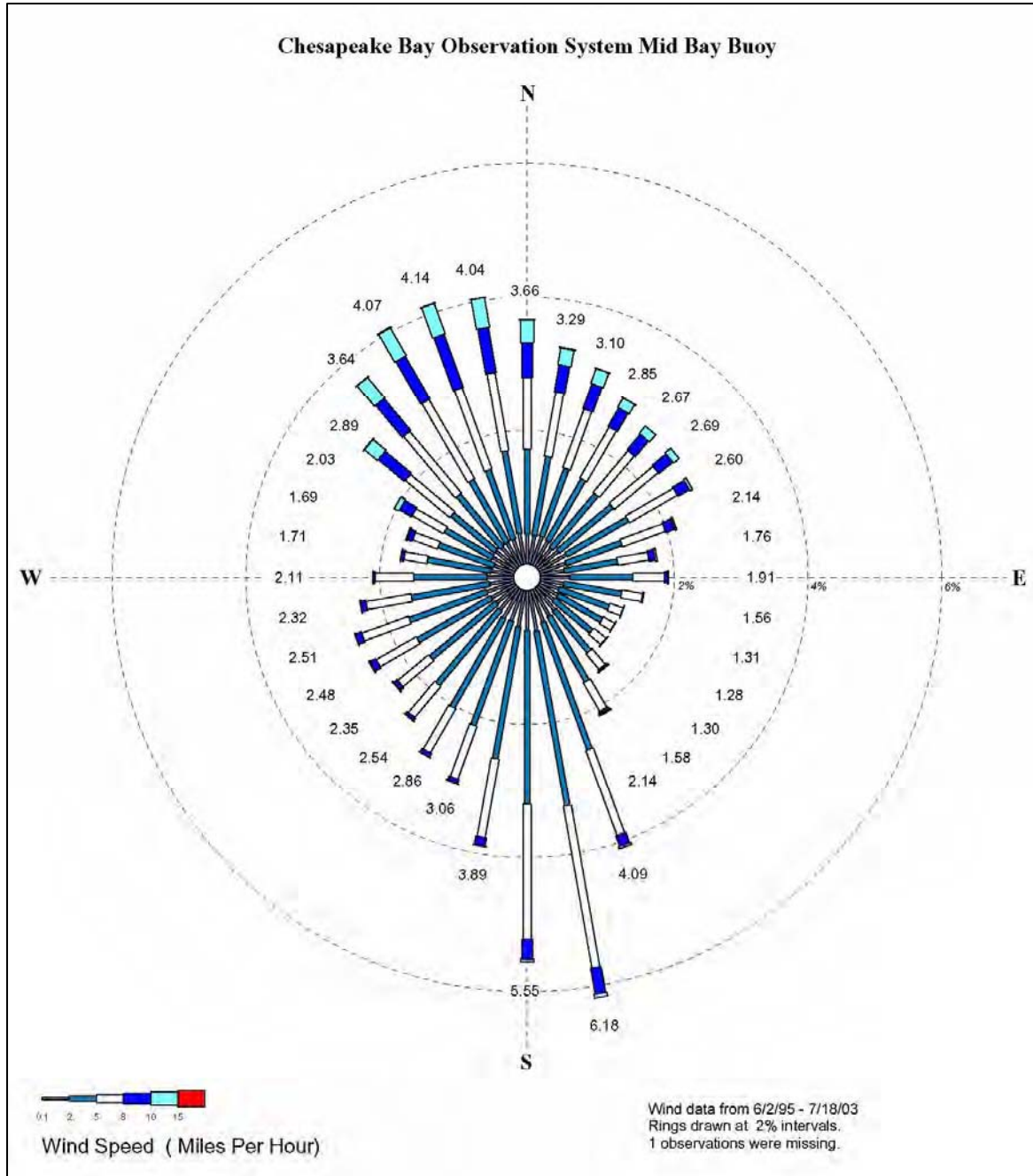


Figure A5. CBOS buoy wind rose

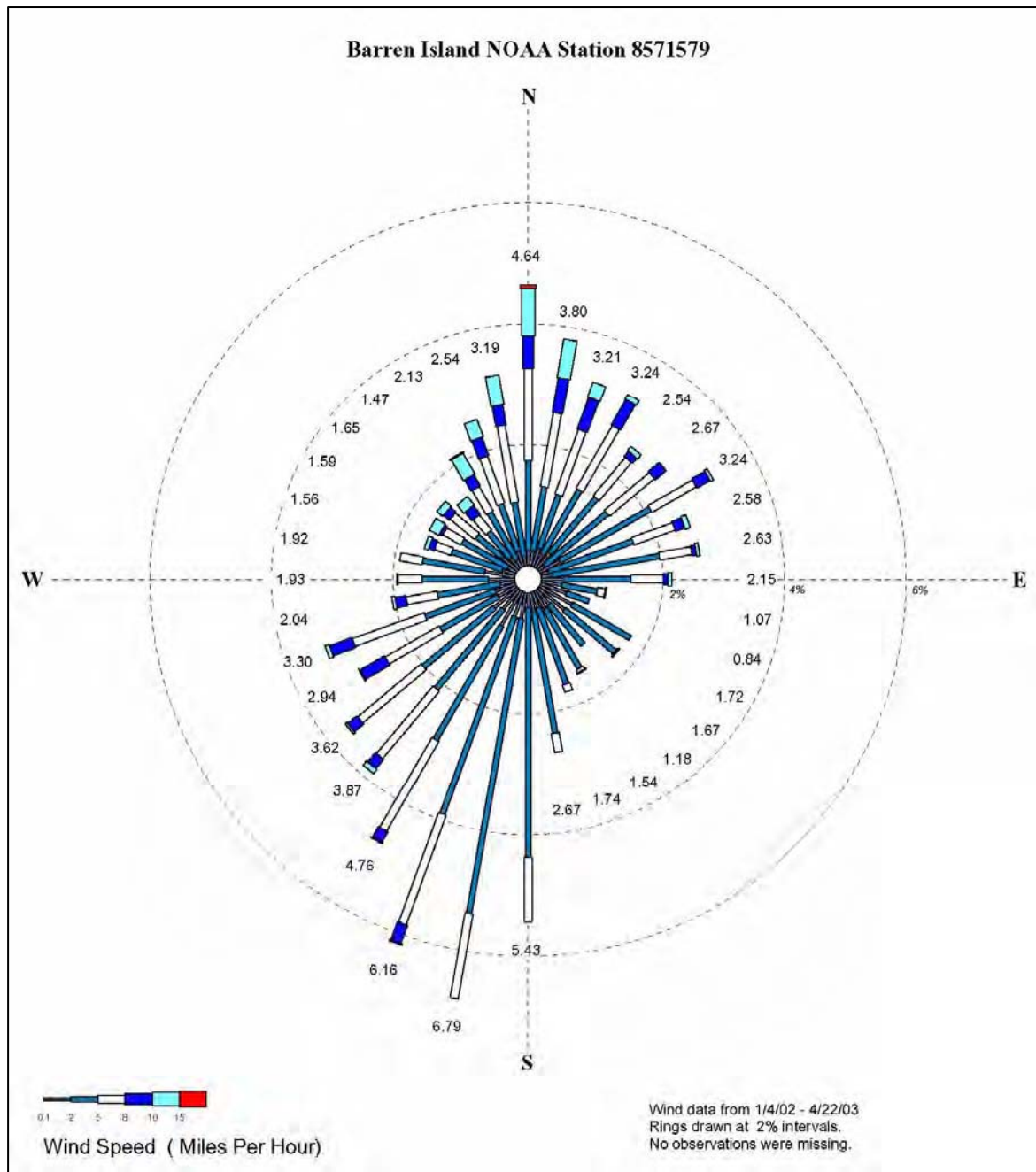


Figure A6. Barren Island NOAA station wind rose

Existing hydrographic surveys

Hydrographic survey data sets available for the James Island and Barren Island areas are as follows:

- a. National Ocean Service (NOS) Digital Elevation Models and corresponding navigational charts for the Chesapeake Bay. Vertical and horizontal data are referenced to mean lower low water (mllw) based on the 1960 to 1978 tidal epoch and the Maryland State Plane, NAD83, respectively.
- b. Hydrographic survey of Barren Island, MD, performed by Ocean Surveys, Inc., of Old Saybrook, CT, on 6-9 February and 20-23 February 2005. Vertical and horizontal data are referenced to mllw based on the 1960 to 1978 tidal epoch and the Maryland State Plane, NAD83, respectively.
- c. Hydrographic survey of James Island, MD, performed by Ocean Surveys, Inc., on 8-12 January 2005. Vertical data are referenced to North American Vertical Datum 1988 (NAVD88). Horizontal data are referenced to the Maryland State Plane.

Aerial photography

An investigation of the available aerial photography for the James Island and Barren Island areas identified yearly aerial photographs from 1987 to 2004 that were obtained by the Virginia Institute of Marine Science (VIMS) in Gloucester, VA. These photographs were obtained as a part of the submerged aquatic vegetation monitoring program conducted by VIMS. The photographs provide an excellent source of shoreline data, as they are high resolution and were obtained as close as possible to mean low water. Digital copies of the photographs are available as a 12.5-micron resolution scan written to a CD-ROM at a cost of \$335.00 for each year from the following vendor:

Air Photographics, Inc.
2115 Kelly Island Road
Martinsburg, WA 25401
1-800-624-8993

For the Mid-Bay Island study, digital photographs of James Island and Barren Island were obtained from Air Photographics, Inc., for 1989, 1999, and 2004. Additional aerial photographs were made available from the U.S. Army Engineer District, Baltimore, for March 2004 and January 2005.

Baseline Coastal Monitoring

Sediment sampling

Chesapeake Environmental Management (CEM) was subcontracted by BBL to collect grab samples in the vicinity of James Island and Barren Island to determine the composition of surficial sediments. Thirty samples were collected

in July 2005 at each island location. Locations of grab sample collection are shown on Figures A7 and A8.

These sediment samples, in conjunction with the existing boring samples and laboratory tests collected and run by E2CR and the Baltimore District, were analyzed to classify the top 6 in. of sediment in the regions around James Island and Barren Island. This information was used to generate Thiessen polygon maps of the sediment types in each area based on the spatial location of samples. Figures A9 and A10 show the surficial sediment types, as classified in the Unified Soil Classification System (USCS). Tables A4 and A5 provide individual sample and boring details in regards to the sediment type, USCS classification, and median grain size, D_{50} , if applicable to the individual sample. Tables A4 and A5 combine the results of the E2CR, Baltimore District, and CEM sampling for comparison. Additional details from the grab sample testing results are contained in Table A6: bulk density, percentages of different sediment sizes, and other sediment classifications are included.

In the vicinity of James Island, the typical median grain size was found to be 0.28 mm, whereas sediments near Barren Island showed a smaller median size of 0.23 mm. Both regions contained a majority of poorly graded sands and silty sands/sand-silt mixtures.

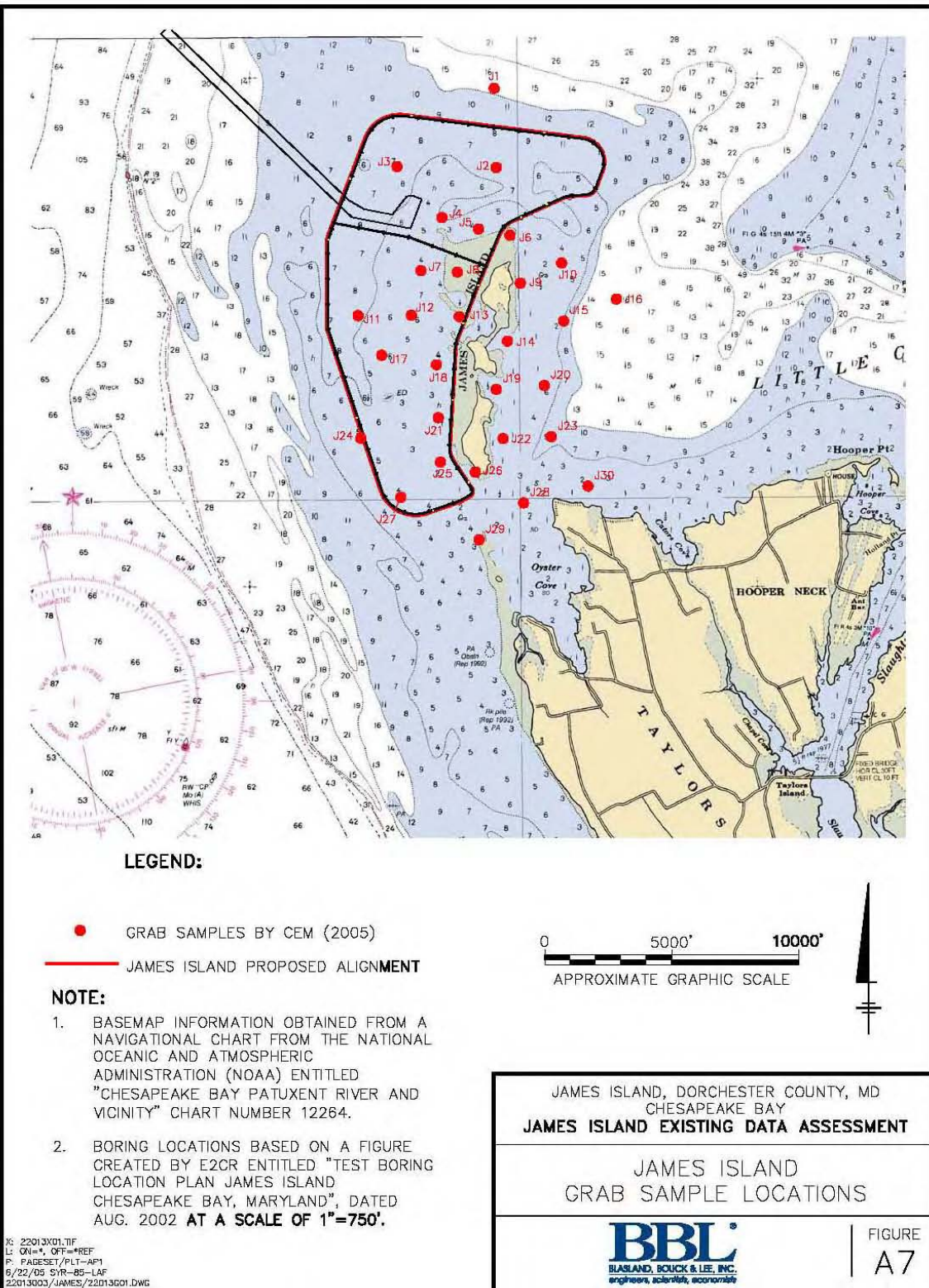


Figure A7. James Island grab sample locations

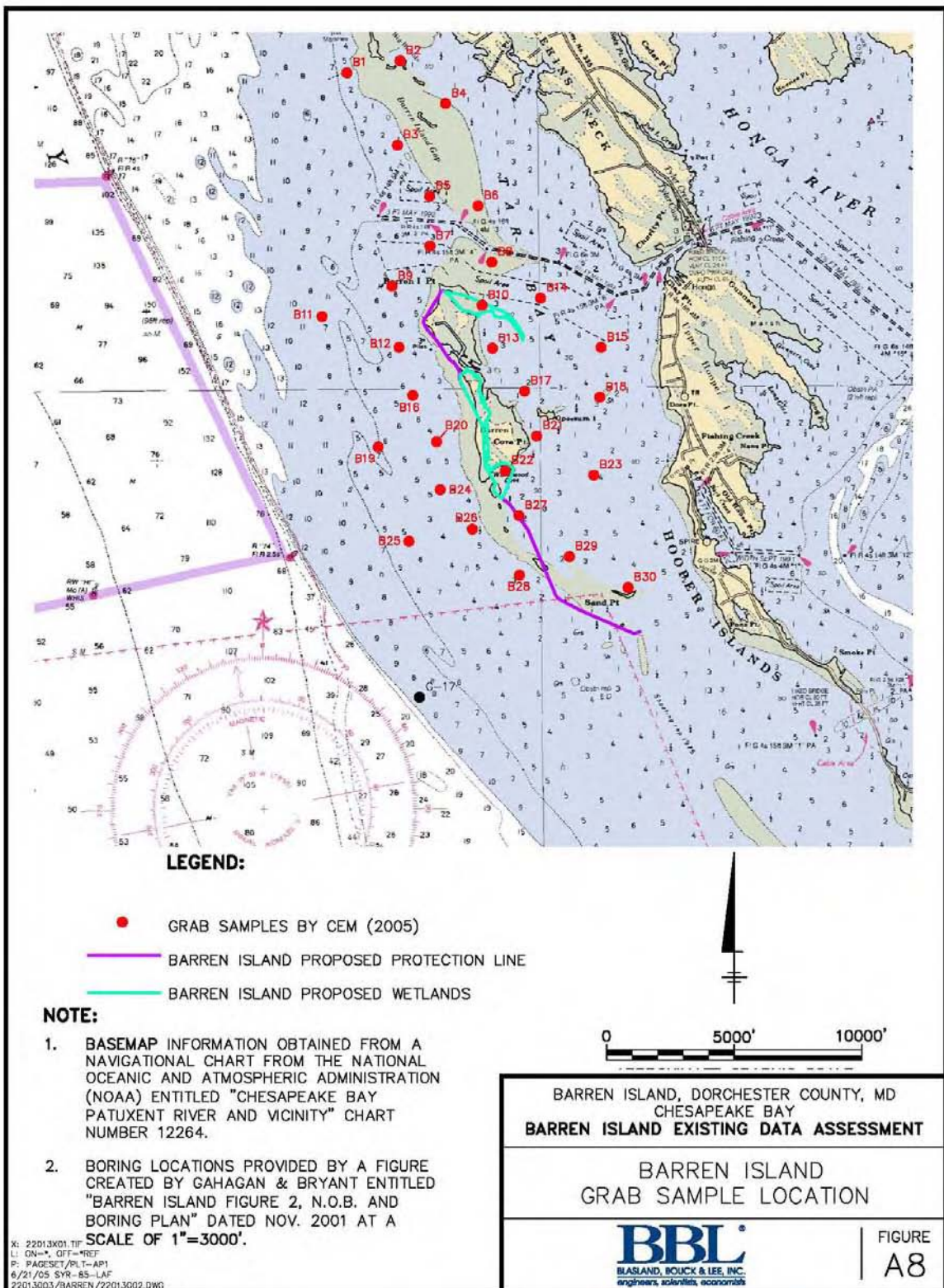


Figure A8. Barren Island grab sample locations

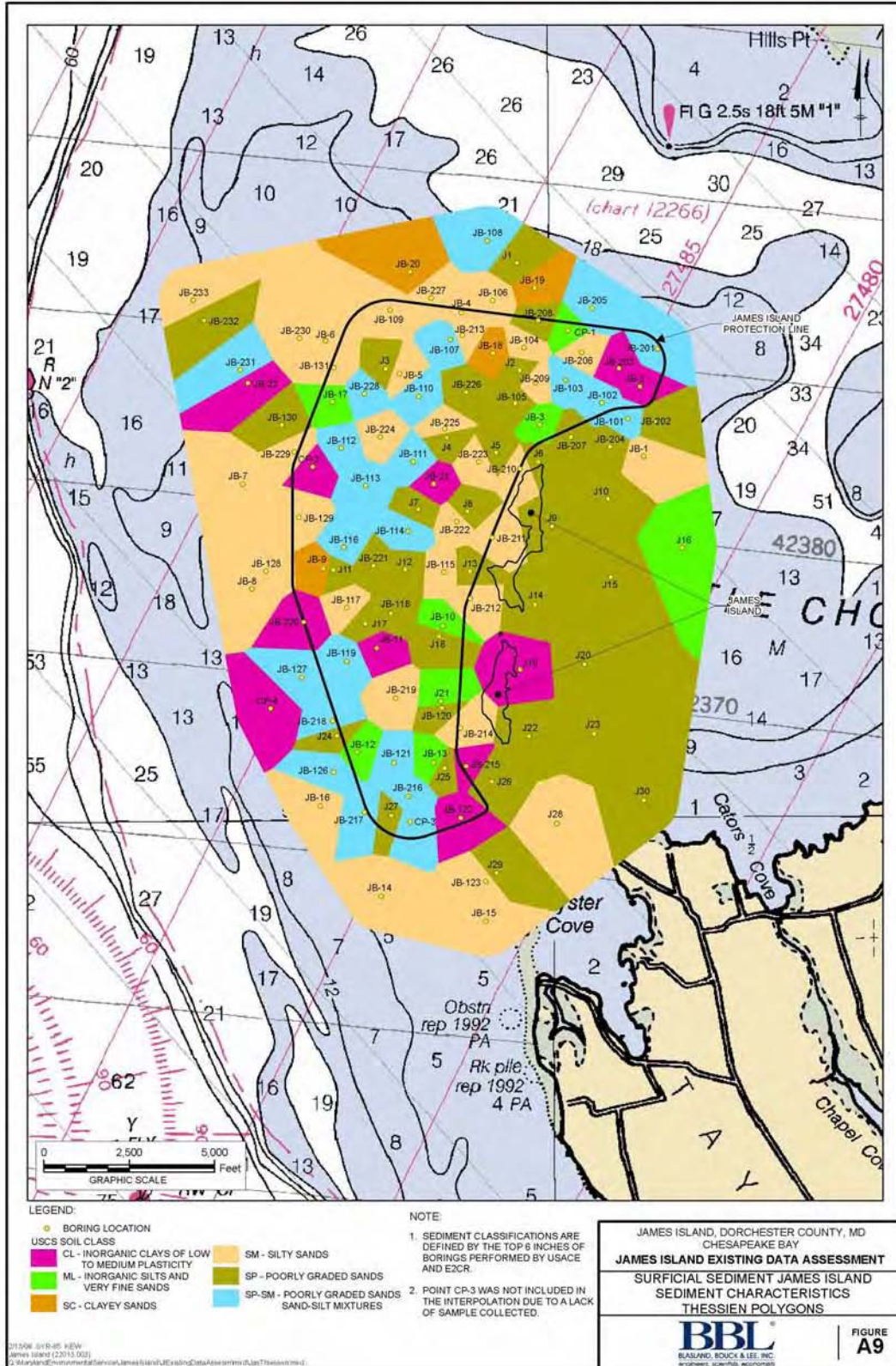


Figure A9. James Island sediment classification (USCS)

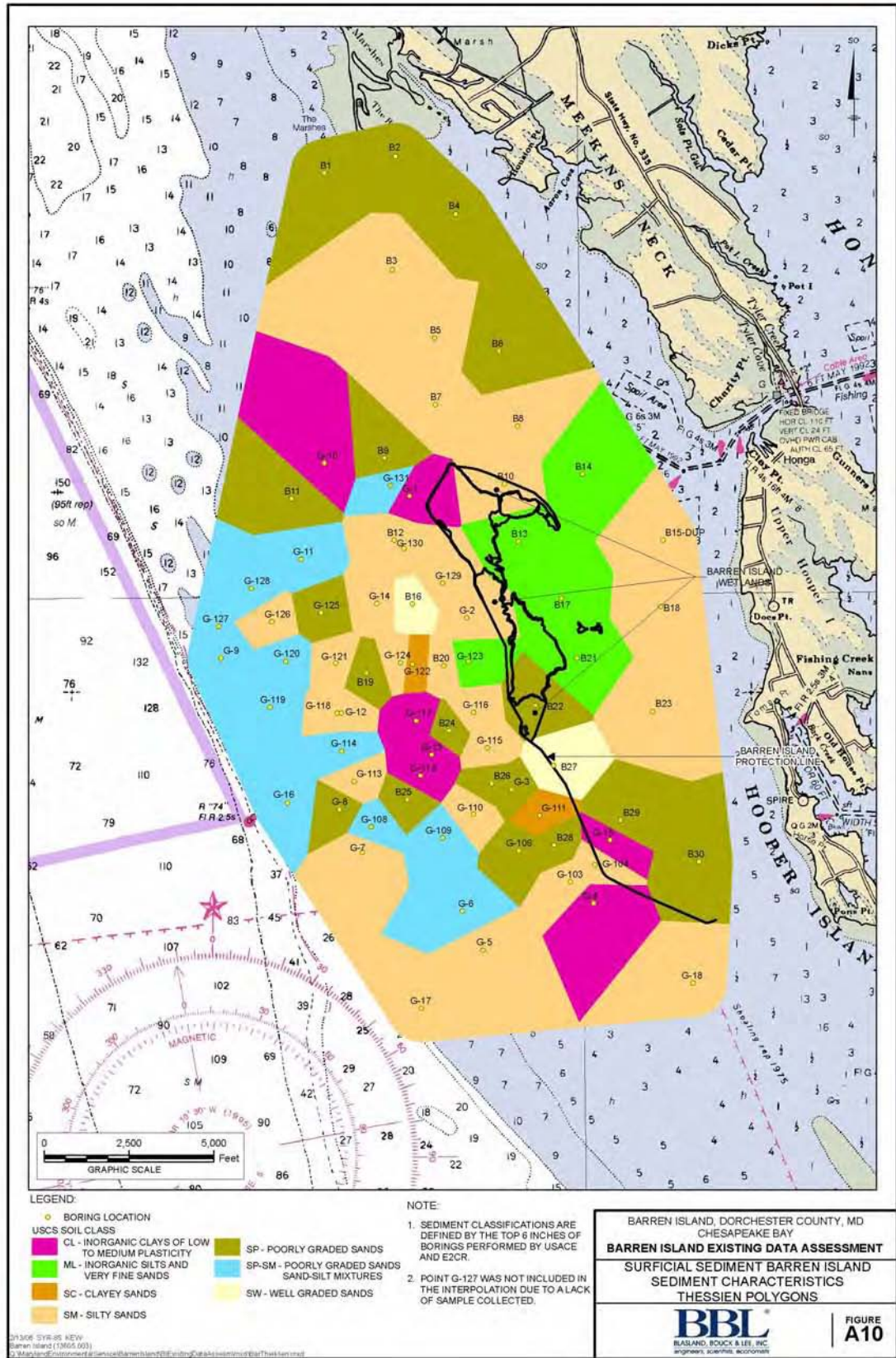


Figure A10. Barren Island sediment classification (USCS)

Table A4
James Island Sample Classification Log

Sample ID	X Coordinate	Y Coordinate	Study Phase	Company	Top 6-in. Classification	USCS Classification	D ₅₀ (mm)	Grain Size Description
JB-11	1,497,970.12	309,155.17	RECON (2001)	E2CR	Greenish gray, moist, sandy clay (CL)	CL		
CP-4	1,494,865.38	307,395.20	RECON (2001)	E2CR	Greenish gray, moist, silty clay	CL		
CP-2	1,496,094.74	314,458.80	RECON (2001)	E2CR	Gray, moist, sandy clay	CL		
JB-21	1,499,629.15	313,959.74	RECON (2001)	E2CR	Dark gray, moist, silty clay	CL		
JB-22	1,494,210.62	316,907.99	RECON (2001)	E2CR	Dark gray, moist, fine to med. sand, trace silty and shell frags	CL		
JB-2	1,505,653.61	316,806.50	RECON (2001)	E2CR	Greenish gray, moist, silty clay, little sand, trace shell frags (CL)	CL		
JB-12	1,497,393.85	306,122.43	RECON (2001)	E2CR	Dark gray, moist, silty fine sand, trace shell frags	ML		
JB-10	1,499,890.99	309,807.78	RECON (2001)	E2CR	Dark gray, moist, silty sand, trace shell frags	ML		
JB-13	1,499,622.07	305,815.31	RECON (2001)	E2CR	Brownish gray, moist, fine to med. sand, little silty, trace shell frags	ML		
JB-17	1,496,665.92	316,358.37	RECON (2001)	E2CR	Dark gray fine to med. sand, trace silt and shell frags	ML		
JB-3	1,502,733.88	315,693.22	RECON (2001)	E2CR	Orange brown, moist, silty fine sand, trace shell frags	ML		
CP-1	1,503,547.73	318,451.27	RECON (2001)	E2CR	Gray silty sand	ML		
JB-9	1,496,404.59	311,488.89	RECON (2001)	E2CR	Light green, moist, clayey sand, trace gravel (SC)	SC		
JB-20	1,498,938.22	320,165.86	RECON (2001)	E2CR	Brownish gray, moist, silty sand with a 6-in. layer of silty clay, trace shell frags on the top	SC		
JB-19	1,502,580.77	319,690.26	RECON (2001)	E2CR	Dark gray, moist, silty fine to med. sand, with a layer of orange brown, silty fine to med. sand at the bottom	SC		
JB-18	1,501,354.38	317,787.88	RECON (2001)	E2CR	Dark gray, moist, fine to med. sand, trace silt and shell frags	SC		
JB-14	1,498,085.37	301,911.52	RECON (2001)	E2CR	Dark gray, moist, fine sand, trace silt and shell frags	SM		
JB-15	1,501,158.77	301,170.23	RECON (2001)	E2CR	Dark gray, moist, fine to med. sand, trace silt	SM		
JB-16	1,496,322.51	304,550.34	RECON (2001)	E2CR	Dark brownish gray, moist, fine sand, trace shell frags and silt (SM)	SM		

(Sheet 1 of 7)

Table A4 (Continued)

Sample ID	X Coordinate	Y Coordinate	Study Phase	Company	Top 6-in. Classification	USCS Classification	D ₅₀ (mm)	Grain Size Description
JB-8	1,494,320.46	310,894.58	RECON (2001)	E2CR	Dark gray, moist, silty fine to med. sand, trace shell frags (SM)	SM		
JB-7	1,494,051.53	313,965.71	RECON (2001)	E2CR	Dark gray, moist, fine to med. sand, trace silty, little shell frags (SM)	SM		
JB-1	1,505,768.86	314,771.88	RECON (2001)	E2CR	Dark reddish gray, moist, silty fine sand, trace shell (SM)	SM		
JB-6	1,496,471.83	318,150.12	RECON (2001)	E2CR	Dark gray, moist, fine sand, trace silty and shell frags (SM)	SM		
JB-5	1,498,623.21	317,190.39	RECON (2001)	E2CR	Dark gray, moist, fine sand, trace silty and shell frags (SM)	SM		
JB-4	1,500,426.62	318,975.34	RECON (2001)	E2CR	Dark gray, moist, fine to med. sand, trace shell frags (SM)	SM		
CP-3	1,498,937.64	304,093.73	RECON (2001)	E2CR	NA			
JB-122	1,500,420.56	304,195.40	FEASIBILITY (2004)	USACE	Very moist, olive brown, soft, lean clay, w/sand and shells (CL) PPR 0.0'-1.5': 2.5, 1.0, 1.0	CL		
JB-203	1,505,037.75	317,350.08	FEASIBILITY (2004)	USACE	Wet, dark gray, very soft lean clay (CL)	CL		
JB-215	1,500,576.56	305,713.99	FEASIBILITY (2004)	USACE	Wet, dark gray, soft lean clay (CL)	CL		
JB-220	1,495,833.03	309,919.01	FEASIBILITY (2004)	USACE	Wet, light olive gray, soft sandy lean clay w/shells (CL)	CL		
JB-120	1,499,839.55	307,610.57	FEASIBILITY (2004)	USACE	Wet, olive brown and yellowish brown, sandy silt w/trace shells (ML)	ML		
JB-104	1,502,268.25	317,946.89	FEASIBILITY (2004)	USACE	Wet, olive brown and gray, silty fine sand w/shells (SM)	SM	0.18	Measured at top 6 in.
JB-106	1,501,352.45	319,326.19	FEASIBILITY (2004)	USACE	Wet, olive gray, silty fine sand w/shells (SM)	SM	0.2	Measured at top 6 in.
JB-109	1,498,351.10	319,051.73	FEASIBILITY (2004)	USACE	Wet, olive gray, silty fine-med. sand w/shells (SM)	SM		
JB-115	1,499,923.73	311,384.60	FEASIBILITY (2004)	USACE	Wet, dark gray, silty very fine sand w/trace of shells (SM)	SM		
JB-117	1,497,089.00	310,349.00	FEASIBILITY (2004)	USACE	Wet, very dark gray, silty fine sand w/shells (SM)	SM		
JB-123	1,501,157.41	302,339.30	FEASIBILITY (2004)	USACE	Wet, dark gray, silty fine sand w/trace shells (SM)	SM		

(Sheet 2 of 7)

Table A4 (Continued)

Sample ID	X Coordinate	Y Coordinate	Study Phase	Company	Top 6-in. Classification	USCS Classification	D ₅₀ (mm)	Grain Size Description
JB-128	1,494,733.74	311,408.54	FEASIBILITY (2004)	USACE	Wet, very dark gray, poorly graded silty fine sand w/shells (SM)	SM	0.2	Measured at top 6 in.
JB-129	1,495,692.30	312,983.30	FEASIBILITY (2004)	USACE	Wet, dark gray, silty fine sand w/shells (SM)	SM		
JB-131	1,496,710.41	317,360.76	FEASIBILITY (2004)	USACE	Wet, olive gray and yellowish brown, silty fine sand w/shells (SM)	SM	0.18	Measured at top 6 in.
JB-206	1,503,953.76	317,807.45	FEASIBILITY (2004)	USACE	Wet, gray, silty fine sand w/trace shells (SM)	SM		
JB-209	1,502,601.52	316,917.44	FEASIBILITY (2004)	USACE	Wet, dark gray, silty fine sand w/shells (SM)	SM		
JB-210	1,502,150.97	314,405.28	FEASIBILITY (2004)	USACE	Wet, light brownish gray, silty fine sand w/trace shells (SM)	SM		
JB-211	1,501,346.99	312,396.39	FEASIBILITY (2004)	USACE	Wet, light olive brown silty fine sand (SM)	SM		
JB-212	1,500,708.18	310,611.29	FEASIBILITY (2004)	USACE	Wet, gray, silty fine sand (SM)	SM		
JB-213	1,500,461.97	318,308.12	FEASIBILITY (2004)	USACE	Wet, black, silty fine sand w/shells (SM)	SM		
JB-214	1,500,417.52	306,825.65	FEASIBILITY (2004)	USACE	Wet, light olive brown, silty very fine sand (SM)	SM		
JB-219	1,498,511.45	307,702.24	FEASIBILITY (2004)	USACE	Wet, dark gray and yellowish brown, silty fine sand w/shells (SM)	SM		
JB-222	1,500,302.52	312,864.33	FEASIBILITY (2004)	USACE	Wet, dark gray, poorly graded med. silty sand w/shells (SM)	SM	0.21	Measured at top 6 in.
JB-223	1,500,949.54	314,609.02	FEASIBILITY (2004)	USACE	Wet, dark grayish brown, silty fine sand w/shells (SM)	SM		
JB-224	1,498,059.71	315,336.92	FEASIBILITY (2004)	USACE	Wet, yellowish brown and black, silty fine sand w/shells (SM)	SM		
JB-225	1,499,949.27	315,572.99	FEASIBILITY (2004)	USACE	Wet, black and olive brown, silty fine sand w/shells (SM)	SM		
JB-229	1,495,559.61	314,904.49	FEASIBILITY (2004)	USACE	Wet, light yellowish brown, silty med. to fine sand w/trace of gravel and shell frags (SM)	SM		
JB-230	1,495,711.12	318,223.74	FEASIBILITY (2004)	USACE	Wet, dark gray, silty med. to fine sand w/shells (SM)	SM		
JB-233	1,492,612.62	319,335.20	FEASIBILITY (2004)	USACE	Moist, dark gray, silty med. to fine sand w/shells (SM)	SM		

(Sheet 3 of 7)

Table A4 (Continued)

Sample ID	X Coordinate	Y Coordinate	Study Phase	Company	Top 6-in. Classification	USCS Classification	D ₅₀ (mm)	Grain Size Description
JB-227	1,499,548.39	319,394.13	FEASIBILITY (2004)	USACE	Wet, gray, silty med. to fine sand w/trace of shell frags (SM/SP-SM)	SM		
JB-105	1,502,009.86	316,326.38	FEASIBILITY (2004)	USACE	Wet, light yellowish brown, poorly graded fine sand (SP)	SP	0.28	Measured at top 6 in.
JB-118	1,498,374.64	310,169.67	FEASIBILITY (2004)	USACE	Moist, olive brown, poorly graded sand w/silt and shells (SP)	SP	0.3	Measured at top 6 in.
JB-130	1,495,196.58	315,680.91	FEASIBILITY (2004)	USACE	Wet, dark gray, poorly graded, fine sand w/shells (SP)	SP	0.28	Measured at top 6 in.
JB-202	1,506,114.23	315,769.76	FEASIBILITY (2004)	USACE	Wet, dark gray, poorly graded fine sand w/trace shells (SP)	SP	0.19	Measured at top 6 in.
JB-204	1,504,776.58	315,051.71	FEASIBILITY (2004)	USACE	Wet, very dark gray, poorly graded fine sand w/shells (SP)	SP		
JB-207	1,503,646.08	315,336.79	FEASIBILITY (2004)	USACE	Wet, dark gray, poorly graded fine-med. sand w/shells (SP)	SP		
JB-208	1,502,683.59	318,738.99	FEASIBILITY (2004)	USACE	Wet, dark gray, poorly graded fine sand w/trace shells (SP)	SP		
JB-221	1,497,863.95	311,572.22	FEASIBILITY (2004)	USACE	Wet, black, poorly graded fine sand w/shells (SP)	SP		
JB-226	1,500,577.22	316,649.85	FEASIBILITY (2004)	USACE	Wet, dark gray, poorly graded fine sand w/shells (SP)	SP		
JB-232	1,492,918.73	318,730.33	FEASIBILITY (2004)	USACE	Wet, dark gray, poorly graded sand w/silt and shells (SP)	SP	0.26	Measured at top 6 in.
JB-101	1,505,302.92	315,875.03	FEASIBILITY (2004)	USACE	Wet, gray, poorly graded fine sand w/silt and trace shell frags (SP-SM)	SP-SM	0.16	Measured at top 6 in.
JB-102	1,504,544.64	316,334.80	FEASIBILITY (2004)	USACE	Wet, gray, poorly graded fine sand w/silt and trace shell frags (SP-SM)	SP-SM		
JB-103	1,503,475.02	316,994.63	FEASIBILITY (2004)	USACE	Wet, gray, poorly graded fine sand w/trace shell frags (SP-SM)	SP-SM	0.18	Measured at top 6 in.
JB-107	1,500,121.21	318,184.27	FEASIBILITY (2004)	USACE	Wet, dark gray, poorly graded med. sand w/silt and shells (SP-SM)	SP-SM		
JB-108	1,501,196.79	321,075.21	FEASIBILITY (2004)	USACE	Wet, light gray, poorly graded fine sand w/silt and shells (SP-SM)	SP-SM	0.21	Measured at top 6 in.
JB-110	1,499,195.47	316,528.65	FEASIBILITY (2004)	USACE	Wet, very dark gray, poorly graded fine sand w/silt and shells (SP-SM)	SP-SM		
JB-111	1,499,034.34	314,615.49	FEASIBILITY (2004)	USACE	Wet, light olive brown and black, poorly graded fine sand w/silt and shells (SP-SM)	SP-SM	0.25	Measured at top 6 in.

(Sheet 4 of 7)

Table A4 (Continued)

Sample ID	X Coordinate	Y Coordinate	Study Phase	Company	Top 6-in. Classification	USCS Classification	D ₅₀ (mm)	Grain Size Description
JB-112	1,496,933.66	315,005.21	FEASIBILITY (2004)	USACE	Wet, dark gray, poorly graded, fine sand w/silt and shells (SP-SM)	SP-SM	0.2	Measured at top 6 in.
JB-113	1,497,640.74	313,907.53	FEASIBILITY (2004)	USACE	Wet, light olive brown, poorly graded fine sand w/silt and shells (SP-SM)	SP-SM	0.21	Measured at top 6 in.
JB-114	1,498,874.04	312,580.94	FEASIBILITY (2004)	USACE	Wet, gray, poorly graded fine sand w/silt and shells (SP-SM)	SP-SM	0.18	Measured at top 6 in.
JB-116	1,497,002.00	312,105.00	FEASIBILITY (2004)	USACE	Wet, very dark gray, poorly graded, med. sand w/silt and shells (SP-SM)	SP-SM		
JB-119	1,497,088.98	308,774.60	FEASIBILITY (2004)	USACE	Wet, olive brown, poorly graded sand w/trace shells frags (SP-SM)	SP-SM		
JB-121	1,498,469.29	305,810.17	FEASIBILITY (2004)	USACE	Wet, light olive brown, poorly graded, fine sand w/silt (SP-SM)	SP-SM		
JB-126	1,496,698.53	305,534.58	FEASIBILITY (2004)	USACE	Wet, dark gray, poorly graded, med. sand w/silt and shells (SP-SM)	SP-SM		
JB-127	1,495,764.92	308,299.91	FEASIBILITY (2004)	USACE	Wet, grayish brown, poorly graded, med. sand w/silt and shells (SP-SM)	SP-SM		
JB-201	1,506,169.82	317,914.86	FEASIBILITY (2004)	USACE	Wet, dark gray, poorly graded fine sand w/silt and shells (SP-SM)	SP-SM		
JB-205	1,504,254.11	319,104.57	FEASIBILITY (2004)	USACE	Wet, dark gray, poorly graded fine sand w/silt and shells (SP-SM)	SP-SM		
JB-216	1,498,881.69	304,831.82	FEASIBILITY (2004)	USACE	Wet, very dark gray, poorly graded fine sand w/silt and shells (SP-SM)	SP-SM	0.25	Measured at top 6 in.
JB-217	1,497,597.14	304,367.44	FEASIBILITY (2004)	USACE	Wet, black, poorly graded fine sand w/silt and shells (SP-SM)	SP-SM		
JB-218	1,496,671.99	307,041.74	FEASIBILITY (2004)	USACE	Wet, dark gray, poorly graded fine sand w/silt and shells (SP-SM)	SP-SM	0.29	Measured at top 6 in.
JB-231	1,493,985.41	317,301.20	FEASIBILITY (2004)	USACE	Wet, dark gray, poorly graded sand w/silt and shells (SP-SM)	SP-SM		
JB-228	1,497,597.81	316,598.19	FEASIBILITY (2004)	USACE	Wet, dark gray, poorly graded med. to fine sand w/trace of silt and shell frags (SP-SM/SP)	SP-SM		
J19	1,502,147.53	308,535.70	Modeling Analysis (2005)	CEM	Clayey-silt	CL	0.02	Grab samples
J16	1,506,885.37	312,097.15	Modeling Analysis (2005)	CEM	Sandy-silt	ML	0.03	Grab samples
J28	1,503,224.82	304,039.72	Modeling Analysis (2005)	CEM	Silty-sand	SM	0.08	Grab samples

(Sheet 5 of 7)

Table A4 (Continued)

Sample ID	X Coordinate	Y Coordinate	Study Phase	Company	Top 6-in. Classification	USCS Classification	D ₅₀ (mm)	Grain Size Description
J1	1,502,061.17	320,419.86	Modeling Analysis (2005)	CEM	Sand	SP	0.38	Grab samples
J2	1,502,145.90	317,288.43	Modeling Analysis (2005)	CEM	Sand	SP	0.36	Grab samples
J3	1,498,231.49	317,327.04	Modeling Analysis (2005)	CEM	Sand	SP	0.36	Grab samples
J4	1,500,005.18	315,312.39	Modeling Analysis (2005)	CEM	Sand	SP	0.36	Grab samples
J5	1,501,448.31	314,867.56	Modeling Analysis (2005)	CEM	Sand	SP	0.37	Grab samples
J6	1,502,689.81	314,615.58	Modeling Analysis (2005)	CEM	Sand	SP	0.37	Grab samples
J7	1,499,176.25	313,218.41	Modeling Analysis (2005)	CEM	Sand	SP	0.38	Grab samples
J8	1,500,611.90	313,161.96	Modeling Analysis (2005)	CEM	Sand	SP	0.39	Grab samples
J9	1,503,094.60	312,724.73	Modeling Analysis (2005)	CEM	Sand	SP	0.35	Grab samples
J10	1,504,724.30	313,519.70	Modeling Analysis (2005)	CEM	Sand	SP	0.31	Grab samples
J10-DUP	1,504,724.30	313,519.70	Modeling Analysis (2005)	CEM	Sand	SP	0.32	Grab samples
J11	1,496,704.53	311,440.59	Modeling Analysis (2005)	CEM	Sand	SP	0.37	Grab samples
J11-DUP	1,496,704.53	311,440.59	Modeling Analysis (2005)	CEM	Sand	SP	0.37	Grab samples
J12	1,498,797.84	311,455.45	Modeling Analysis (2005)	CEM	Sand	SP	0.37	Grab samples
J13	1,500,686.58	311,402.24	Modeling Analysis (2005)	CEM	Sand	SP	0.36	Grab samples
J14	1,502,586.78	310,432.69	Modeling Analysis (2005)	CEM	Sand	SP	0.36	Grab samples
J15	1,504,803.14	311,231.94	Modeling Analysis (2005)	CEM	Sand	SP	0.34	Grab samples
J17	1,497,631.21	309,875.06	Modeling Analysis (2005)	CEM	Sand	SP	0.38	Grab samples

(Sheet 6 of 7)

Table A4 (Concluded)

Sample ID	X Coordinate	Y Coordinate	Study Phase	Company	Top 6-in. Classification	USCS Classification	D ₅₀ (mm)	Grain Size Description
J18	1,499,789.42	309,501.99	Modeling Analysis (2005)	CEM	Sand	SP	0.35	Grab samples
J20	1,504,039.79	308,683.06	Modeling Analysis (2005)	CEM	Sand	SP	0.33	Grab samples
J20-DUP	1,504,039.79	308,683.06	Modeling Analysis (2005)	CEM	Sand	SP	0.33	Grab samples
J21	1,499,866.44	307,408.44	Modeling Analysis (2005)	CEM	Sand	SP	0.31	Grab samples
J21-DUP	1,499,866.44	307,408.44	Modeling Analysis (2005)	CEM	Sand	SP	0.33	Grab samples
J22	1,502,419.27	306,583.18	Modeling Analysis (2005)	CEM	Sand	SP	0.18	Grab samples
J23	1,504,316.98	306,657.76	Modeling Analysis (2005)	CEM	Sand	SP	0.15	Grab samples
J24	1,496,805.45	306,603.63	Modeling Analysis (2005)	CEM	Sand	SP	0.37	Grab samples
J24-DUP	1,496,805.45	306,603.63	Modeling Analysis (2005)	CEM	Sand	SP	0.37	Grab samples
J25	1,499,945.85	305,648.75	Modeling Analysis (2005)	CEM	Sand	SP	0.34	Grab samples
J26	1,501,322.29	305,264.13	Modeling Analysis (2005)	CEM	Sand	SP	0.33	Grab samples
J27	1,498,386.49	304,265.81	Modeling Analysis (2005)	CEM	Sand	SP	0.35	Grab samples
J29	1,501,470.45	302,588.40	Modeling Analysis (2005)	CEM	Sand	SP	0.30	Grab samples
J30	1,505,767.03	304,707.89	Modeling Analysis (2005)	CEM	Sand	SP	0.32	Grab samples
J30-DUP	1,505,767.03	304,707.89	Modeling Analysis (2005)	CEM	Sand	SP	0.34	Grab samples

(Sheet 7 of 7)

Table A5
Barren Island Sample Classification Log

Sample ID	X Coordinate	Y Coordinate	Study Phase	Company	Top 6-in. Classification	USCS Classification	D ₅₀ (mm)	Grain Size Description
G-1	1,522,379.54	246,553.30	RECON (2001)	E2CR	Dark grey, wet, fine sandy clay (CL)	CL		
G-2	1,524,057.91	242,955.25	RECON (2001)	E2CR	Light brown, silty fine to coarse sand (SM)	SM		
G-3	1,525,389.96	237,897.72	RECON (2001)	E2CR	Medium to light gray, wet, silty fine to coarse sand, trace fine gravel (SP)	SP		
G-4	1,527,803.88	234,536.55	RECON (2001)	E2CR	Brownish gray, wet, fine sandy clay, trace shell frags (CL)	CL		
G-5	1,524,539.00	233,144.18	RECON (2001)	E2CR	Dark grey, wet, silty fine sand (SM)	SM		
G-6	1,523,941.32	234,304.76	RECON (2001)	E2CR	Brownish gray to orange brown, wet silty fine to med. sand, trace shell frags (SP-SM)	SP-SM		
G-7	1,520,981.28	236,047.34	RECON (2001)	E2CR	Brownish to greenish gray, wet, silty fine sand (SM)	SM	0.178	Measured at top 2 ft; overlying classification is the same
G-8	1,520,306.49	237,310.57	RECON (2001)	E2CR	Dark gray, wet, fine to med. sand (SP)	SP	0.274	Measured at top 2 ft; overlying classification is the same
G-9	1,516,828.51	241,768.80	RECON (2001)	E2CR	Medium gray, fine sand, trace silt and mica (SP-SM)	SP-SM		
G-10	1,519,862.00	247,534.75	RECON (2001)	E2CR	Black to orange brown and gray, fine sandy clay, with fine sand (CL)	CL		
G-12	1,520,360.39	240,157.76	RECON (2001)	E2CR	Dark gray, wet, silty fine sand (SM)	SM		
G-13	1,523,028.88	238,928.70	RECON (2001)	E2CR	Medium gray, wet to moist, silty clay, trace fine sand with occasional lenses of clayey sand (CL)	CL		
G-14	1,521,405.78	243,377.04	RECON (2001)	E2CR	Greenish brown, silty fine sand, trace shell frags (SM)	SM		
G-15	1,528,281.10	236,403.93	RECON (2001)	E2CR	Brownish gray, wet, fine sandy clay, trace shell frags (CL)	CL		

(Sheet 1 of 5)

Table A5 (Continued)

Sample ID	X Coordinate	Y Coordinate	Study Phase	Company	Top 6-in. Classification	USCS Classification	D ₅₀ (mm)	Grain Size Description
G-16	1,518,774.71	237,498.76	RECON (2001)	E2CR	Medium gray, wet, fine sand, trace silt (with layers of fine to med. sand) (SP-SM)	SP-SM	0.255	Measured at top 2 ft; overlying classification is the same
G-17	1,522,725.63	231,436.06	RECON (2001)	E2CR	Dark gray and brown, wet, silty fine sand (SM)	SM		
G-18	1,530,731.35	232,187.48	RECON (2001)	E2CR	Dark gray and brown, wet, silty fine sand (SC-SM)	SM		
G-103	1,527,109.94	235,174.26	FEASIBILITY (2004)	USACE	Wet, dark, gray, silty med.-fine sand w/trace of shell frags (SM)	SM	0.15	Measured at top 6 in.
G-104	1,527,831.17	235,675.89	FEASIBILITY (2004)	USACE	Wet, grayish brown, silty fine sand w/trace of shell frags (SM)	SM	0.16	Measured at top 6 in.
G-106	1,525,603.91	236,092.66	FEASIBILITY (2004)	USACE	Wet, grayish brown, poorly graded coarse to med. sand (SP)	SP		
G-108	1,521,254.28	236,796.11	FEASIBILITY (2004)	USACE	Wet, dark, gray, poorly graded sand w/silt and trace of shell frags (SP-SM)	SP-SM	0.18	Measured at top 6 in.
G-109	1,523,345.18	236,468.91	FEASIBILITY (2004)	USACE	Wet, dark, gray, poorly graded sand w/silt and trace of shell frags (SP-SM)	SP-SM		
G-11	1,519,172.22	244,688.60	FEASIBILITY (2004)	E2CR	Dark gray, silty fine to med. sand, trace shell frags (SP-SM)	SP-SM		
G-110	1,524,264.06	237,174.36	FEASIBILITY (2004)	USACE	Wet dark, gray and yellowish brown silty sand w/trace of shell frags (SM)	SM	0.16	Measured at top 6 in.
G-111	1,526,209.19	237,129.48	FEASIBILITY (2004)	USACE	Wet, grayish brown, silty, med. to coarse sand (SC)	SC		
G-112	1,522,700.75	238,304.92	FEASIBILITY (2004)	USACE	Moist, gray, soft lean clay w/sand (CL)	CL		
G-113	1,520,749.43	238,137.57	FEASIBILITY (2004)	USACE	Wet, dark, gray, poorly graded, silty, fine to med. sand (SM)	SM		
G-114	1,520,367.71	239,034.90	FEASIBILITY (2004)	USACE	Wet, dark, gray, poorly graded, fine sand w/silt and trace of shell frags (SP-SM)	SP-SM	0.18	Measured at top 6 in.
G-115	1,524,662.66	239,130.06	FEASIBILITY (2004)	USACE	Wet, light olive brown silty fine sand (SM)	SM		
G-116	1,524,255.68	240,178.88	FEASIBILITY (2004)	USACE	Wet, light olive brown, silty, very fine sand (SM)	SM		
G-117	1,522,576.11	239,932.66	FEASIBILITY (2004)	USACE	Very moist, yellowish brown and gray, soft lean clay (CL)	CL		

(Sheet 2 of 5)

Table A5 (Continued)

Sample ID	X Coordinate	Y Coordinate	Study Phase	Company	Top 6-in. Classification	USCS Classification	D ₅₀ (mm)	Grain Size Description
G-118	1,520,231.29	240,156.74	FEASIBILITY (2004)	USACE	Wet, grayish brown, silty fine sand (SM)	SM	0.16	Measured at top 6 in.
G-119	1,518,269.42	240,333.45	FEASIBILITY (2004)	USACE	Wet, dark gray, poorly graded, fine sand w/silt (SP-SM)	SP-SM	0.16	Measured at top 6 in.
G-120	1,518,729.06	241,672.43	FEASIBILITY (2004)	USACE	Wet, dark gray, poorly graded, fine sand w/silt (SP-SM)	SP-SM	0.2	Measured at top 6 in.
G-121	1,520,195.82	241,613.22	FEASIBILITY (2004)	USACE	Wet, very dark, gray, silty, fine sand (SM)	SM	0.16	Measured at top 6 in.
G-122	1,522,459.20	241,590.82	FEASIBILITY (2004)	USACE	Wet, black, clayey, fine sand (SC)	SC		
G-123	1,524,108.19	241,664.80	FEASIBILITY (2004)	USACE	Wet, very dark, gray, sandy silt(ML)	ML	0.07	Measured at top 6 in.
G-124	1,522,108.26	241,628.47	FEASIBILITY (2004)	USACE	Very moist, gray, silty, fine sand (SM)	SM		
G-125	1,519,761.63	243,107.01	FEASIBILITY (2004)	USACE	Wet, dark Grayish brown, poorly graded, fine sand w/silt (SP)	SP	0.2	Measured at top 6 in.
G-126	1,518,313.44	242,842.66	FEASIBILITY (2004)	USACE	Wet, grayish brown, poorly graded, fine silty sand (SM)	SM		
G-127	1,516,752.64	242,709.04	FEASIBILITY (2004)	USACE	Mostly empty jar with trace of sand			
G-128	1,517,716.02	243,829.38	FEASIBILITY (2004)	USACE	Wet, dark, gray, poorly graded, med. sand w/silt (SP-SM)	SP-SM	0.18	Measured at top 6 in.
G-129	1,523,348.45	243,975.33	FEASIBILITY (2004)	USACE	Wet, olive gray, silty, fine sand (SM)	SM	0.12	Measured at top 6 in.
G-130	1,522,216.64	245,008.22	FEASIBILITY (2004)	USACE	Wet, olive, silty, fine sand (SM)	SM	0.12	Measured at top 6 in.
G-131	1,521,819.31	246,866.46	FEASIBILITY (2004)	USACE	Wet, olive brown and gray, poorly graded, fine sand w/silt (SP-SM)	SP-SM		
B1	1,519,870.53	256,105.45	Modeling Analysis (2005)	CEM	Sand	SP	0.33	Grab samples
B2	1,521,959.79	256,583.40	Modeling Analysis (2005)	CEM	Sand	SP	0.31	Grab samples
B2-DUP	1,521,959.79	256,583.40	Modeling Analysis (2005)	CEM	Sand	SP	0.31	Grab samples
B3	1,521,857.50	253,244.16	Modeling Analysis (2005)	CEM	Clayey-silt	SM	0.013	Grab samples

(Sheet 3 of 5)

Table A5 (Continued)

Sample ID	X Coordinate	Y Coordinate	Study Phase	Company	Top 6-in. Classification	USCS Classification	D ₅₀ (mm)	Grain Size Description
B4	1,523,741.56	254,892.10	Modeling Analysis (2005)	CEM	Sand	SP	0.13	Grab samples
B4-DUP	1,523,741.56	254,892.10	Modeling Analysis (2005)	CEM	Sand	SP	0.13	Grab samples
B5	1,523,116.35	251,226.94	Modeling Analysis (2005)	CEM	Silty-sand	SM	0.11	Grab samples
B6	1,525,016.96	250,847.77	Modeling Analysis (2005)	CEM	Sand	SP	0.16	Grab samples
B7	1,523,132.19	249,260.43	Modeling Analysis (2005)	CEM	Silty-sand	SM	0.19	Grab samples
B8	1,525,556.05	248,624.52	Modeling Analysis (2005)	CEM	Silty-sand	SM	0.057	Grab samples
B9	1,521,639.15	247,676.36	Modeling Analysis (2005)	CEM	Sand	SP	0.32	Grab samples
B10	1,525,177.92	246,921.88	Modeling Analysis (2005)	CEM	Sandy-silt	SM	0.043	Grab samples
B10-DUP	1,525,177.92	246,921.88	Modeling Analysis (2005)	CEM	Silty-sand	SM	0.045	Grab samples
B11	1,518,899.94	246,477.05	Modeling Analysis (2005)	CEM	Sand	SP	0.38	Grab samples
B12	1,521,921.43	245,256.75	Modeling Analysis (2005)	CEM	Silty-sand	SM	0.14	Grab samples
B13	1,525,583.78	245,219.55	Modeling Analysis (2005)	CEM	Sandy-silt	ML	0.02	Grab samples
B14	1,527,470.24	247,201.62	Modeling Analysis (2005)	CEM	Sandy-silt	ML	0.017	Grab samples
B15	1,529,843.15	245,254.58	Modeling Analysis (2005)	CEM	Silty-sand	SM	0.06	Grab samples
B15-DUP	1,529,843.15	245,254.58	Modeling Analysis (2005)	CEM	Sandy-silt	ML	0.053	Grab samples
B16	1,522,457.74	243,361.18	Modeling Analysis (2005)	CEM	Sand	SW	0.38	Grab samples
B17	1,526,845.40	243,530.29	Modeling Analysis (2005)	CEM	Silty-sand	ML	0.019	Grab samples
B18	1,529,792.50	243,293.60	Modeling Analysis (2005)	CEM	Silt	SM	0.082	Grab samples

(Sheet 4 of 5)

Table A5 (Concluded)

Sample ID	X Coordinate	Y Coordinate	Study Phase	Company	Top 6-in. Classification	USCS Classification	D ₅₀ (mm)	Grain Size Description
B19	1,521,101.82	241,323.00	Modeling Analysis (2005)	CEM	Silty-sand	SP	0.33	Grab samples
B20	1,523,390.43	241,535.58	Modeling Analysis (2005)	CEM	Sand	SM	0.13	Grab samples
B21	1,527,314.12	241,761.74	Modeling Analysis (2005)	CEM	Silty-sand	ML	0.024	Grab samples
B22	1,526,087.02	240,379.90	Modeling Analysis (2005)	CEM	Sandy-silt	SP	0.17	Grab samples
B22-DUP	1,526,087.02	240,379.90	Modeling Analysis (2005)	CEM	Sand	SP	0.18	Grab samples
B23	1,529,555.09	240,214.20	Modeling Analysis (2005)	CEM	Sand	SM	0.081	Grab samples
B24	1,523,534.84	239,636.88	Modeling Analysis (2005)	CEM	Silty-sand	SP	0.38	Grab samples
B25	1,522,307.91	237,599.68	Modeling Analysis (2005)	CEM	Sand	SP	0.34	Grab samples
B26	1,524,795.55	238,074.99	Modeling Analysis (2005)	CEM	Sand	SP	0.35	Grab samples
B27	1,526,622.68	238,611.88	Modeling Analysis (2005)	CEM	Sand	SW	0.32	Grab samples
B28	1,526,641.95	236,256.93	Modeling Analysis (2005)	CEM	Sand	SP	0.29	Grab samples
B29	1,528,601.42	236,995.35	Modeling Analysis (2005)	CEM	Sand	SP	0.3	Grab samples
B30	1,530,902.35	235,770.13	Modeling Analysis (2005)	CEM	Sand	SP	0.93	Grab samples
(Sheet 5 of 5)								

Table A6**CEM Sample Sediment Characterization**

Sample ID	Percent H2O	Bulk Density	Percent Gravel	Percent Sand	Percent Silt	Percent Clay	SHEP CLASS	PEJRUP CLASS	WGHT LOSS	Percent Total	Soil Classification
B1	23.78	1.93	0.00	94.57	4.02	1.41	Sand	A,III	6.11	100.00	SP
B2	20.43	2.01	0.00	95.98	3.79	0.25	Sand	A,IV	4.73	100.02	SP
B2 DUP	18.34	2.07	0.00	96.05	2.68	1.27	Sand	A,III	1.86	100.00	SP
B3	36.73	1.67	0.00	13.45	65.53	21.02	Clayey-silt	C,III	9.73	100.00	SM
B4	21.51	1.99	0.00	86.47	11.58	1.96	Sand	B,IV	3.63	100.01	SP
B4 DUP	21.23	1.99	0.00	85.35	12.05	2.59	Sand	B,IV	2.60	99.99	SP
B5	27.19	1.85	0.43	59.53	32.78	7.26	Silty-sand	B,IV	7.33	100.00	SM
B6	27.87	1.84	0.00	80.33	16.41	2.76	Sand	B,IV	4.86	99.50	SP
B7	24.39	1.92	0.00	71.71	21.72	6.87	Silty-sand	B,III	2.09	100.30	SM
B8	32.04	1.76	0.00	48.37	42.35	9.27	Silty-sand	C,IV	8.22	99.99	SM
B9	17.57	2.09	0.00	90.84	7.40	1.76	Sand	A,IV	2.93	100.00	SP
B10	27.91	1.84	0.00	43.83	44.96	11.20	Sandy-silt	C,IV	7.33	99.99	SM
B10 DUP	26.63	1.87	0.00	44.72	43.66	11.62	Silty-sand	C,III	5.88	100.00	SM
B11	18.35	2.07	1.28	94.06	3.93	0.73	Sand	A,IV	10.07	100.00	SP
B12	27.65	1.94	0.27	61.88	31.74	6.11	Silty-sand	B,IV	6.57	100.00	SM
B13	35.09	1.70	0.00	23.16	64.76	12.08	Sandy-silt	C,IV	7.44	100.00	ML
B14	31.82	1.76	0.00	16.67	70.21	13.12	Sandy-silt	C,IV	6.53	100.00	ML
B15	30.95	1.78	0.00	49.57	45.31	5.12	Silty-sand	C,IV	6.09	100.00	SM
B15 DUP	25.67	1.89	0.00	47.00	47.01	5.99	Sandy-silt	C,IV	5.69	100.00	ML
B16	17.75	2.08	14.14	70.40	13.68	1.80	Sand	B,IV	2.59	100.02	SW
B16 DUP	18.00	2.08	9.65	64.13	22.08	4.14	Silty-sand	B,IV	3.75	100.00	SM
B17	29.14	1.81	0.00	17.79	76.14	7.08	Silt	C,IV	5.47	101.01	ML
B18	21.58	1.98	0.00	59.66	34.90	5.43	Silty-sand	B,IV	5.73	99.99	SM
B19	21.25	1.99	0.00	93.99	4.57	1.44	Sand	A,III	2.96	100.00	SP
B20	24.72	1.91	0.00	69.70	25.51	4.80	Silty-sand	B,IV	3.91	100.01	SM
B21	30.90	1.75	0.00	27.05	63.43	9.52	Sandy-silt	C,IV	5.86	100.00	ML
B22	26.37	1.87	0.00	91.23	7.28	1.50	Sand	A,IV	2.56	100.01	SP
B22 DUP	23.60	1.94	0.00	89.91	8.06	2.04	Sand	B,III	2.07	100.01	SP
B23	27.93	1.84	0.00	61.01	99.47	5.52	Silty-sand	B,IV	5.76	166.00	SM
B24	21.16	1.99	0.79	90.20	7.95	1.06	Sand	A,IV	1.43	100.00	SP
B25	18.63	2.06	0.00	94.39	3.97	1.64	Sand	A,III	2.13	100.00	SP
B26	17.51	2.09	0.00	93.61	5.24	1.14	Sand	A,IV	1.04	99.99	SP
B27	22.39	1.96	1.76	74.26	19.16	4.83	Sand	B,III	1.80	100.01	SW
B28	18.09	2.07	0.00	84.71	12.79	2.49	Sand	B,IV	2.92	99.99	SP
B29	17.82	2.08	0.99	89.43	7.82	1.76	Sand	A,IV	3.10	100.00	SP
B30	18.12	2.07	0.80	98.21	0.84	0.14	Sand	A,IV	5.44	99.99	SP
B30 DUP	18.65	2.06	0.34	97.19	1.85	0.62	Sand	A,III	2.23	100.00	SP
J1	16.76	2.11	2.28	96.84	0.26	0.63	Sand	A,II	2.24	100.01	SP
J2	18.27	2.07	0.00	98.86	0.33	0.81	Sand	A,II	12.30	100.00	SP
J3	16.70	2.11	0.00	99.34	0.28	0.38	Sand	A,II	6.69	100.00	SP

(Continued)

Table A6 (Concluded)

Sample ID	Percent H2O	Bulk Density	Percent Gravel	Percent Sand	Percent Silt	Percent Clay	SHEP CLASS	PEJRUP CLASS	WGHT LOSS	Percent Total	Soil Classification
J4	18.54	2.06	0.00	98.85	0.38	0.77	Sand	A,II	11.26	100.00	SP
J5	18.85	2.12	0.00	98.78	0.64	0.58	Sand	A,III	9.78	100.00	SP
J6	17.10	2.10	0.00	98.78	0.46	0.75	Sand	A,II	6.06	99.99	SP
J7	17.37	2.09	0.46	98.78	0.28	0.47	Sand	A,II	2.93	99.99	SP
J8	15.92	2.14	0.54	98.68	0.33	0.47	Sand	A,II	4.84	100.02	SP
J9	19.08	2.05	0.00	96.40	2.71	0.89	Sand	A,III	3.68	100.00	SP
J10	20.93	2.00	0.00	89.05	9.22	1.73	Sand	B,IV	4.43	100.00	SP
J10 DUP	21.19	1.99	0.00	93.88	5.67	0.45	Sand	A,IV	4.17	100.00	SP
J11	20.09	2.02	0.10	99.06	0.37	0.48	Sand	A,II	1.38	100.01	SP
J11 DUP	29.95	1.93	0.00	99.36	0.21	0.49	Sand	A,II	3.97	100.06	SP
J12	17.83	2.08	0.00	98.69	0.60	0.51	Sand	A,III	5.57	99.80	SP
J13	15.14	2.16	0.00	98.15	1.44	0.41	Sand	A,III	2.79	100.00	SP
J14	18.04	2.08	0.39	81.86	14.73	3.02	Sand	B,IV	4.82	100.00	SP
J15	19.89	2.09	0.00	98.00	1.27	0.74	Sand	A,III	1.78	100.01	SP
J16	36.25	1.68	0.00	34.37	55.41	10.22	Sandy-silt	C,IV	4.97	100.00	ML
J17	16.56	2.12	0.41	98.67	0.73	0.30	Sand	A,III	5.36	100.11	SP
J18	20.31	2.02	0.00	92.81	7.08	0.11	Sand	A,IV	6.24	100.00	SP
J19	41.37	1.59	0.00	14.72	70.29	14.99	Clayey-silt	C,IV	7.16	100.00	CL
J20	21.61	1.99	0.00	95.34	3.94	0.72	Sand	A,IV	4.22	100.00	SP
J20 DUP	20.90	2.00	0.00	94.86	4.46	0.68	Sand	A,IV	4.29	100.00	SP
J21	20.71	2.01	0.00	87.79	11.25	0.96	Sand	B,IV	4.15	100.00	SP
J21 DUP	22.25	1.97	0.00	93.75	5.28	0.99	Sand	A,IV	4.69	100.02	SP
J22	22.34	1.97	0.00	96.20	3.08	0.72	Sand	A,IV	3.54	100.00	SP
J23	21.96	1.87	0.00	80.10	16.59	3.32	Sand	B,IV	5.26	100.01	SP
J24	19.61	2.03	0.00	98.84	1.08	0.08	Sand	A,IV	6.81	100.00	SP
J24 DUP	19.80	2.03	0.00	98.80	0.51	0.70	Sand	A,II	5.48	100.01	SP
J25	19.25	2.04	0.00	97.68	2.14	0.18	Sand	A,IV	9.10	100.00	SP
J26	18.71	2.06	0.00	95.05	4.02	0.93	Sand	A,IV	3.70	100.00	SP
J27	19.35	2.04	0.00	97.98	1.87	0.16	Sand	A,IV	5.28	100.01	SP
J28	35.87	1.68	0.00	53.46	34.35	12.19	Silty-sand	B,III	7.35	100.00	SM
J29	19.66	2.03	0.00	96.90	2.72	0.38	Sand	A,IV	4.99	100.00	SP
J30	25.64	1.89	0.00	81.38	13.73	4.89	Sand	B,III	4.88	100.00	SP
J30 DUP	20.70	2.01	0.00	88.34	8.80	2.86	Sand	B,III	4.46	100.00	SP

Navigational channels

Two channels were identified within the vicinity of James Island and Barren Island. The Honga River Channel, located near Barren Island, is a Federal navigational channel maintained by the Baltimore District. The channel's original alignment still appears on NOAA navigational charts, although it was straightened to its new alignment in 2003, as shown in Figure A11.

A second channel was identified after discussions with local watermen in the area. This private channel is located south of James Island, between the southern-most island and the mainland of Taylors Island. Although not marked on charts and not maintained, this channel is self-sustaining and used by local watermen heading out to the bay. To better identify the location of this channel, a field visit took place on 10 August 2005 to trace the path of the local channel. A local waterman was chartered to travel through the channel so that Global Positioning System (GPS) coordinates could be obtained. The resulting alignment, with outbound and inbound paths highlighted, is shown in Figure A12.

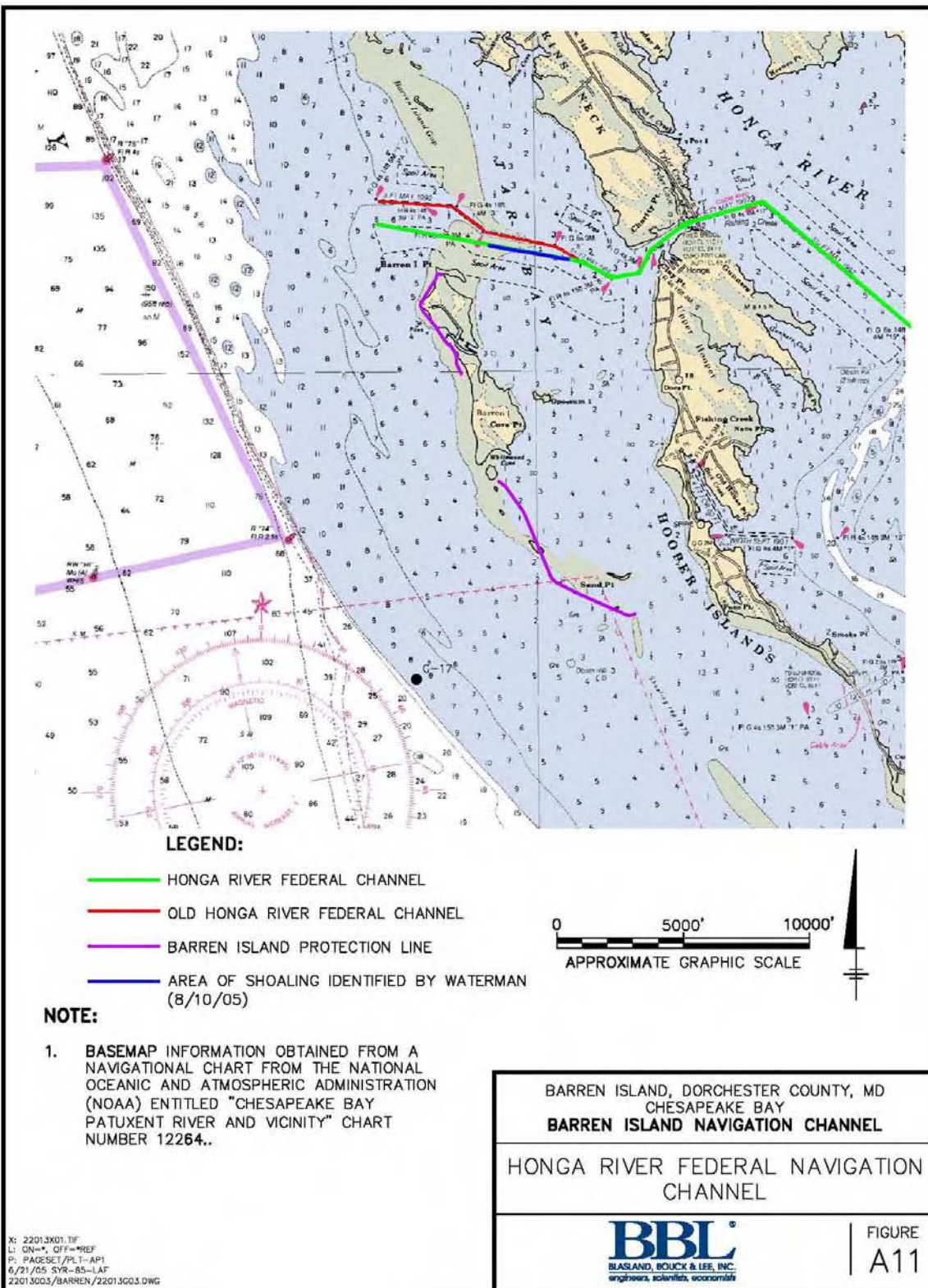


Figure A11. Honga River Federal Navigation Channel

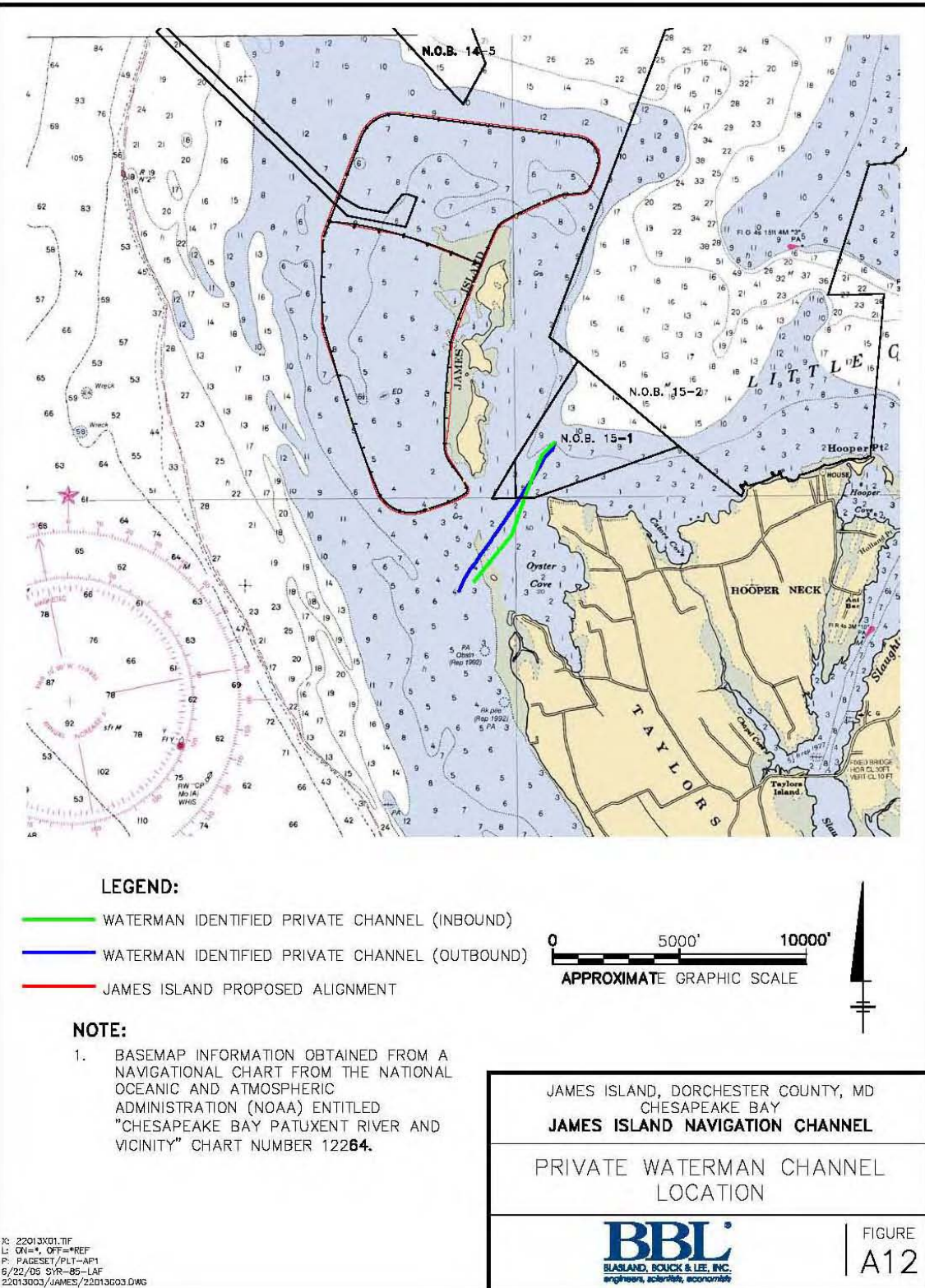


Figure A12. James Island private watermen channel

Shoaling

A shoaling analysis was performed for the Honga River Federal Navigational Channel, located near Barren Island. Data used for the shoaling study were provided by the Baltimore District on 22 August 2005 via electronic copy. Data were in three different formats: MicroStation files, AutoCAD files, and Easting, Northing, and Depth (x, y, z) files. The survey data were read into Terramodel to develop a three-dimensional (3-D) model of the survey data [Triangular Irregular Network (TIN)]. Two consecutive before-dredging or condition surveys were brought into Terramodel to determine a time line of shoaling over the given difference in time. Based on the average channel area and the volume of shoaled material, an average thickness of shoaling was then calculated.

Some data received were not applicable to the shoaling study due to contractor defaults, resulting in incomplete data sets. These periods of time were neglected from the analysis to provide the most accurate shoaling rates during periods of known change. The first analysis characterized the shoaling over the entire extent of the Honga River Channel, as seen in Figure A13 with old and current channel alignments. Table A7 follows with volume calculations done with Terramodel and shoaling rate calculations based on the amount of time passed between surveys. Surveys were taken approximately every year, with ranges of time from one-third of a year to 2.5 to 3.0 years between some surveys. Shoaling was somewhat variable, with an average of approximately 530,000 cu yd of material filling the channel, giving an average infill rate of 0.8 ft/year over the entire length of channel.

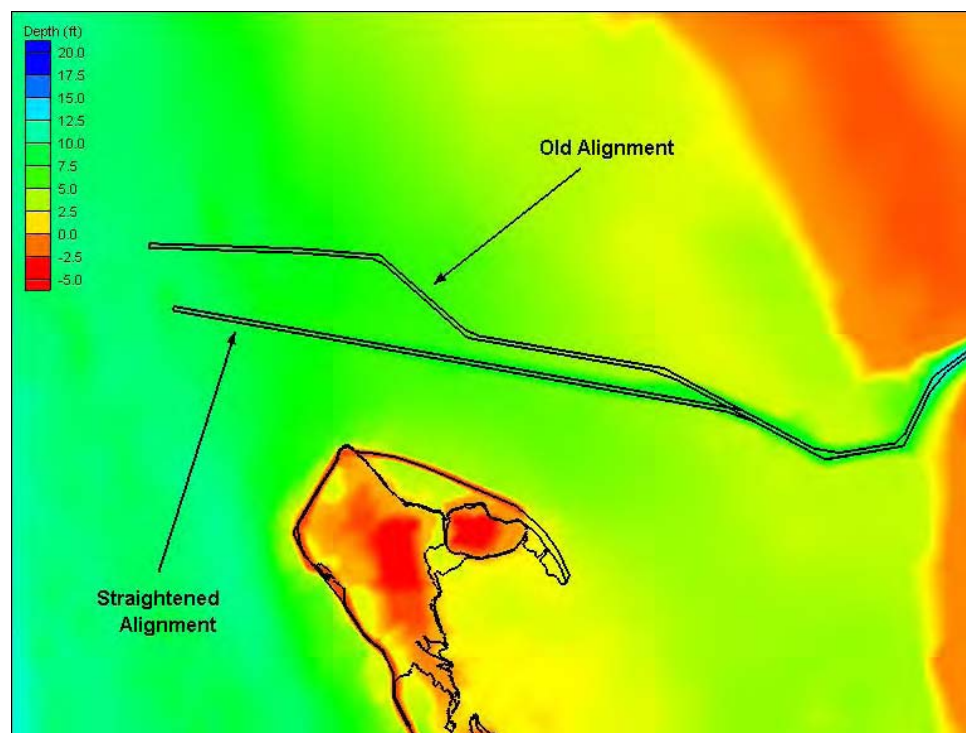


Figure A13. Honga River channel alignments

Table A7
Honga River Shoaling Analysis

Scenario	Year	Month	Day	Survey Type	Days Between Surveys	Dredging Event	Channel Area (sq ft)	Volume (cu yd)	Volume (cu ft)	Average Shoaling (ft)	Average Shoaling (ft/year)
1	1992	May	27	Condition surveys	751	No	656,238	22,604	610,308	0.93	0.45
	1994	Jun	17	Maintenance dredging							
2	1994	Jun	17	Maintenance dredging	369	No	650,245	39,748	1,073,196	1.65	1.63
	1995	Jun	21	Before dredge							
3	1996	Nov	25	After dredge	303	Yes	750,828	47,318	1,277,586	1.70	2.05
	1997	Sep	24	Condition surveys							
4	1997	Sep	24	Condition surveys	357	No	924,199	21,764	587,628	0.64	0.65
	1998	Sep	16	Before dredge							
5	1998	Sep	16	Before dredge	265	No	773,085	21,219	572,913	0.74	1.02
	1999	Jun	8	Before dredge							
6	1999	Jun	8	Before dredge	127	No	772,471	1,970	53,190	0.07	0.20
	1999	Oct	13	Before dredge							
7	1999	Oct	13	Before dredge	149	No	802,035	12,003	324,081	0.40	0.99
	2000	Mar	10	Before dredge							
8	2000	Mar	10	Before dredge	171	Yes	923,929	2,572	69,444	0.08	0.16
	2000	Aug	28	Maintenance dredging							
9	2000	Sep	27	After dredge	960	Yes	272,921	8,194	221,238	0.81	0.31
	2003	May	15	Maintenance dredging							
				Averages:	384		725,106	19,710	532,176	0.708	0.829

Notes:

- 1) Scenario 1 and 2 the survey type – maintenance dredge was an event where the contractor defaulted and no dredging occurred.
- 2) Scenarios 4, 5, 6, and 7 the survey type – before dredge was an event where several surveys were conducted in anticipation of dredging events that did not occur.

A secondary shoaling analysis was performed to more closely observe the shoaling in specific regions of the Honga River Channel, as noted during the field visit and predictions from hydrodynamic modeling performed by the U.S. Army Engineer Research and Development Center (ERDC). Two sections of the channel were studied separate from the rest of the channel for increased understanding of shoaling rates in the different portions of the channel. The two sections chosen for the detailed study are shown in Figure A14. Section 1 was noted to be in an area of high sediment movement from ERDC's modeling results (Chapter 4), whereas Section 2 was chosen due to shoaling noted in the region during the field visit. Section 2 is from the previous unstraightened alignment. Results are displayed in Tables A8 and A9 for Sections 1 and 2, respectively.

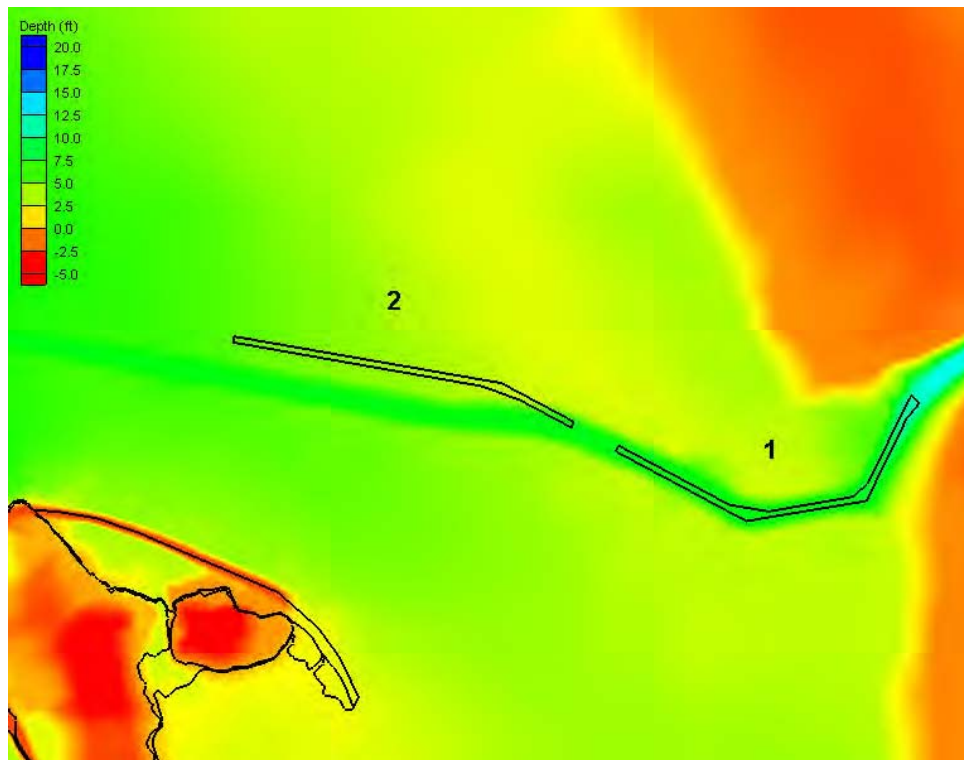


Figure A14. Honga River channel, selected shoaling study sections

Table A8 Honga River Section 1 Shoaling Analysis											
Scenario	Year	Month	Day	Survey Type	Days Between Surveys	Dredging Event	Channel Area (sq ft)	Area 1 Volume (cu yd)	Area 1 Volume (cu ft)	Average Shoaling (ft)	Average Shoaling (ft/year)
1	1992	May	27	Condition surveys	751	No	136,374	3,528	95,256	0.70	0.34
	1994	Jun	17	Maintenance dredging							
2	1994	Jun	17	Maintenance dredging	369	No	161,043	19,412	524,121	3.25	3.22
	1995	Jun	21	Before dredge							
3	1996	Nov	25	After dredge	303	Yes	226,193	13,004	351,097	1.55	1.87
	1997	Sep	24	Condition surveys							
4	1997	Sep	24	Condition surveys	357	No	229,377	7,335	198,037	0.86	0.88
	1998	Sep	16	Before dredge							
5	1998	Sep	16	Before dredge	265	No	225,265	11,621	313,759	1.39	1.92
	1999	Jun	8	Before dredge							
6	1999	Jun	8	Before dredge	127	No	225,265	1,178	31,795	0.14	0.41
	1999	Oct	13	Before dredge							
7	1999	Oct	13	Before dredge	149	No	229,377	5,469	147,652	0.64	1.58
	2000	Mar	10	Before dredge							
8	2000	Mar	10	Before dredge	171	Yes	229,376	1,375	37,125	0.16	0.35
	2000	Aug	28	Maintenance dredging							
9	2000	Sep	27	After dredge	960	Yes	218,331	7,442	200,934	0.92	0.35
	2003	May	15	Maintenance dredging							
			Averages:		384		208,956	7,818	211,086	1.070	1.212

Notes:

- 1) Scenario 1 and 2 the survey type – maintenance dredge was an event where the contractor defaulted and no dredging occurred.
- 2) Scenarios 4, 5, 6, and 7 the survey type – before dredge was an event where several surveys were conducted in anticipation of dredging events that did not occur.

Table A9
Honga River Section 2 Shoaling Analysis

Scenario	Year	Month	Day	Survey Type	Days Between Surveys	Dredging Event	Channel Area (sq ft)	Area 1 Volume (cu yd)	Area 1 Volume (cu ft)	Average Shoaling (ft)	Average Shoaling (ft/year)					
1	1992	May	27	Condition surveys	751	No	198,803	9,110	245,970	1.24	0.60					
	1994	Jun	17	Maintenance dredging												
2	1994	Jun	17	Maintenance dredging	369	No	198,804	16,065	433,755	2.18	2.16					
	1995	Jun	21	Before dredge												
3	1996	Nov	25	After dredge	303	Yes	130,104	21,074	569,001	4.37	5.27					
	1997	Sep	24	Condition surveys												
4	1997	Sep	24	Condition surveys	357	No	198,809	6,637	179,210	0.90	0.92					
	1998	Sep	16	Before dredge												
5	1998	Sep	16	Before dredge	265	No	198,809	2,576	69,549	0.35	0.48					
	1999	Jun	8	Before dredge												
6	1999	Jun	8	Before dredge	127	No	198,809	392	10,589	0.05	0.15					
	1999	Oct	13	Before dredge												
7	1999	Oct	13	Before dredge	149	No	198,809	1,465	39,542	0.20	0.49					
	2000	Mar	10	Before dredge												
8	2000	Mar	10	Before dredge	171	Yes	198,809	399	10,773	0.05	0.12					
	2000	Aug	28	Maintenance dredging												
9	2000	Sep	27	After dredge	960	Yes	Comparison Not Possible Due to Channel Realignment									
	2003	May	15	Maintenance dredging												
				Averages:	384			190,219	7,215	194,799	1.169	1.273				
<p>Notes:</p> <p>1) Scenario 1 and 2 the survey type – maintenance dredge was an event where the contractor defaulted and no dredging occurred.</p> <p>2) Scenarios 4, 5, 6, and 7 the survey type – before dredge was an event where several surveys were conducted in anticipation of dredging events that did not occur.</p>																

Hydrographic survey

Hydrographic surveys were conducted at James Island and Barren Island on 15-30 June 2005 by Hydro Data, Inc. The survey areas are shown in Figure A15 for both sites.

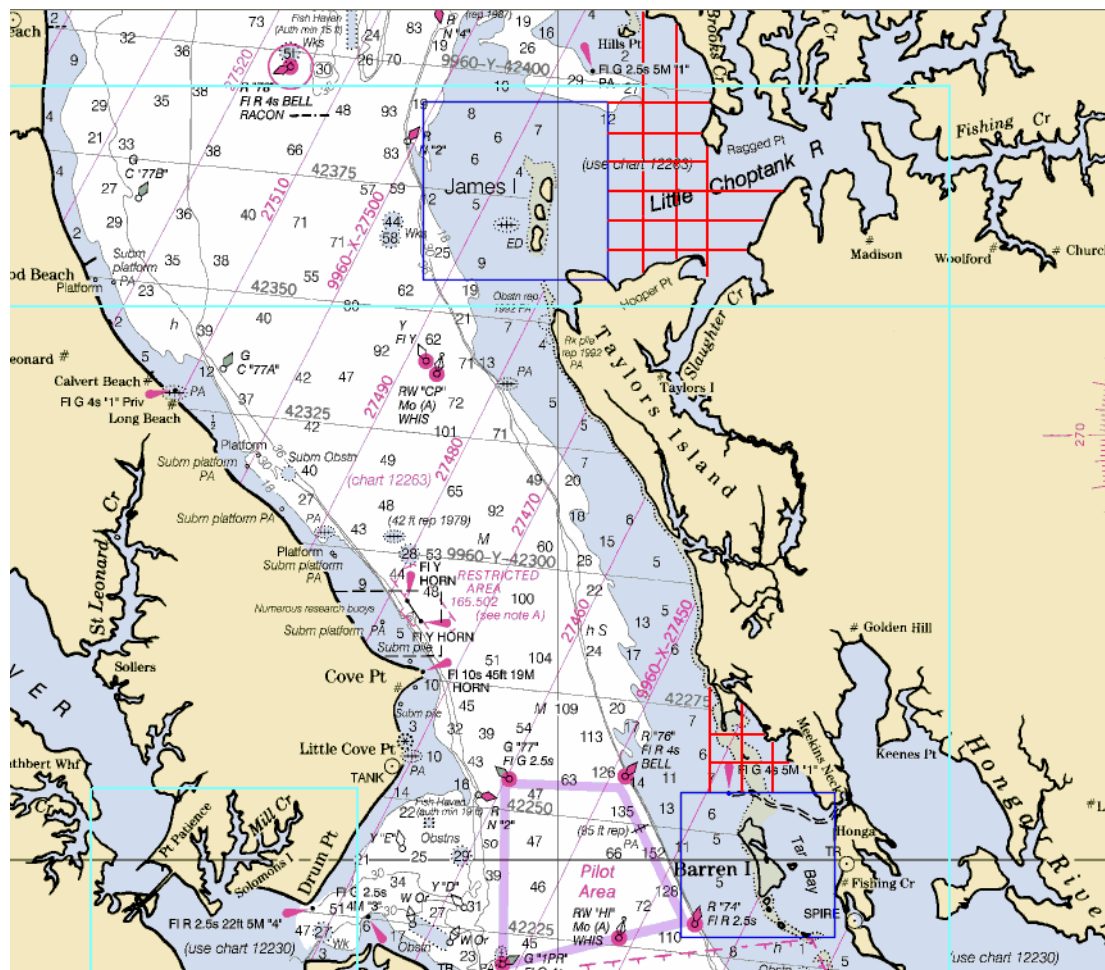


Figure A15. James Island and Barren Island hydrographic survey area, June 2005

Figure A15 shows two blue rectangles for the survey areas. The rectangle is 3 by 3 miles for James Island and 2.5 by 2.5 miles for Barren Island. The interval of survey transect lines (east to west) is every 400 ft in the rectangle. The red lines are additional transects (half mile between lines) outside the rectangle areas. Data points were collected at a rate of 18/sec, resulting in a data point every 2-4 ft.

Vertical and horizontal data are referenced to mllw based on the 1960 to 1978 tidal epoch and the Maryland State Plane, NAD83, respectively.

Historical shoreline position

Historical shoreline position data were developed for the island shorelines and mainland shorelines east of James Island and Barren Island. Available historical shoreline position data developed by the Maryland Department of Natural Resources (MDNR) and available historical aerial photography were combined with high spatial resolution imagery obtained as a part of this study. The high spatial resolution imagery was obtained following establishment of four aerial photography targets in each of the study areas and referencing the targets to the Maryland State Plane coordinate system as shown in Figure A16 and Figure A17 for James Island and Barren Island, respectively.

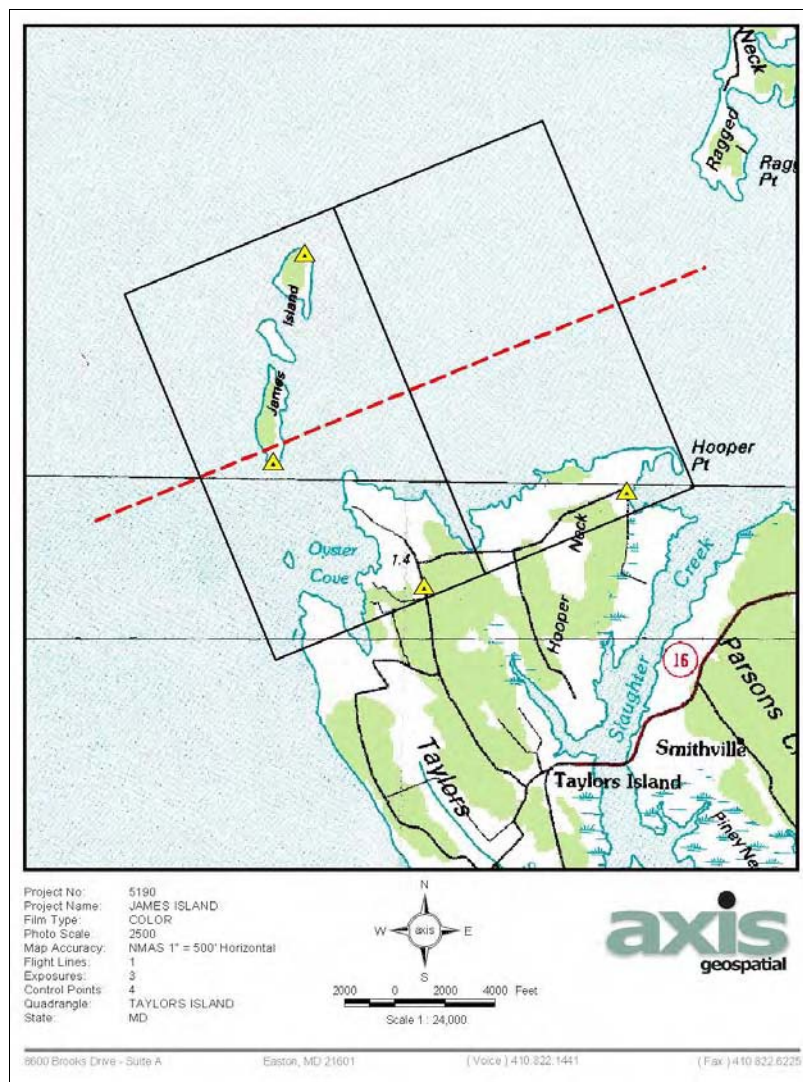


Figure A16. James Island aerial photograph coverage, 24 July 2005

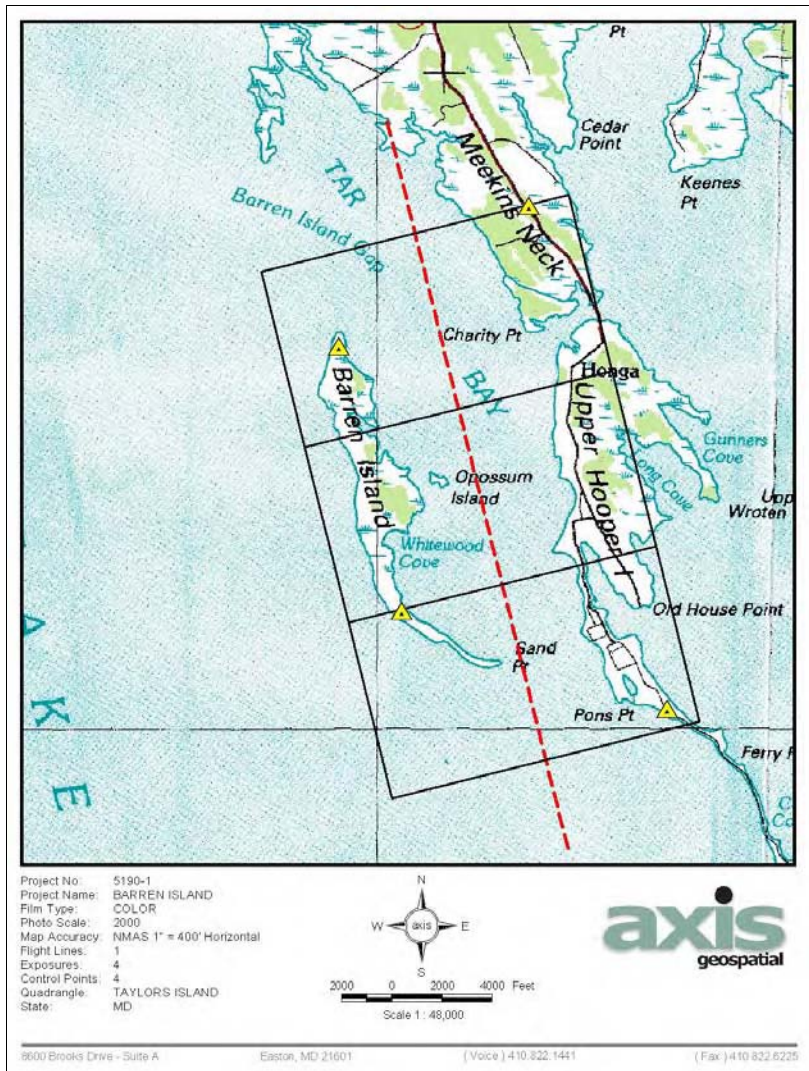


Figure A17. Barren Island aerial photograph coverage, 24 July 2005

Color infrared (CIR) film is the preferred film for shoreline mapping projects and was used for the imagery to allow best determination of shoreline location. The geo-referenced imagery was taken on 24 July 2005, at mean low water by Axis Geospatial of Easton, MD, to show the tonal differences in the exposed beach face. Stereo compilation was completed for 1 in. = 400 ft planimetrics and maps produced as AutoCAD files on CDROM. The digital ortho-processing was for 2-ft pixel CIR digital ortho Imagery in TIFF/TFW format on CDROM.

A shoreline position map was developed to determine shoreline change rates and to identify critical erosion areas, as well as be available to compare pre- and post-construction conditions to evaluate construction impacts. The shoreline position map was initially developed by overlaying three digital shorelines of the study area available from the MDNR. These shorelines were 1848, 1942, and 1994, and were georeferenced to the Maryland State Plane Grid Coordinate system.

Digital aerial photographs for 1989, 1999, and 2004 were then imported into AutoCAD Land Development Desktop along with the available 1848, 1942, and 1994 shorelines and digital planimetrics from the MDNR. Each digital photograph was registered and rectified by rotating and scaling to match the prominent features in the field. This procedure was followed for each year to result in registered and rectified tiled photographs attached to the AutoCAD coordinate drawing file.

Each of the sets of registered and rectified aerial photographs was inspected and analyzed to identify and map the mean high water (mhw) contour. This procedure consisted of locating the mhw contour based on the changes in beach sand tone, which typically denotes the mhw contour. Following this procedure, a continuous mhw contour for each of the aerial photography sets was overlaid on the earlier shorelines provided by the MDNR. The same procedure was followed with the July 2005 digital aerial photograph. The mhw contours for each of the years are shown in Figures A18 to A25.

Shoreline changes corresponding to each study area reach are also shown in Figures A18 to A25 for the following time periods:

- a. 1848 – 1942.
- b. 1942 – 1989.
- c. 1989 – 1994.
- d. 1994 – 1999.
- e. 1999 – 2004.
- f. 2004 – 2005.

Shoreline change was measured at 500-ft intervals along the baselines established for each shoreline reach. Measured annual shoreline change for each time period for each study area reach is shown in the figures. Table A10 summarizes the average annual shoreline change for each study area reach for the various time periods analyzed. Tables A11 to A16 compile the shoreline change rates along the shoreline reaches for each year for each of the time periods.

Potential sources of error in the development of the shoreline change rates include:

- a. Limited prominent features in the field available for registering and rectifying each digital photograph.
- b. Subjectivity of locating the mhw contour based on changes in beach sand tone.
- c. Subjectivity of tracing of the continuous mhw contour for each of the aerial photography sets.

Given these potential sources of error, the estimated error in measuring the differences between two shorelines of different dates is estimated to be +/-30 ft.

Analysis of the data in Table A10 indicates a continuous trend of annual shoreline erosion for the various shoreline reaches with cycles of increasing and decreasing annual erosion rates throughout the time periods analyzed. As expected, the highest erosion rates occur along the most exposed shorelines, including those of James Island, Taylors Island, and Barren Island.

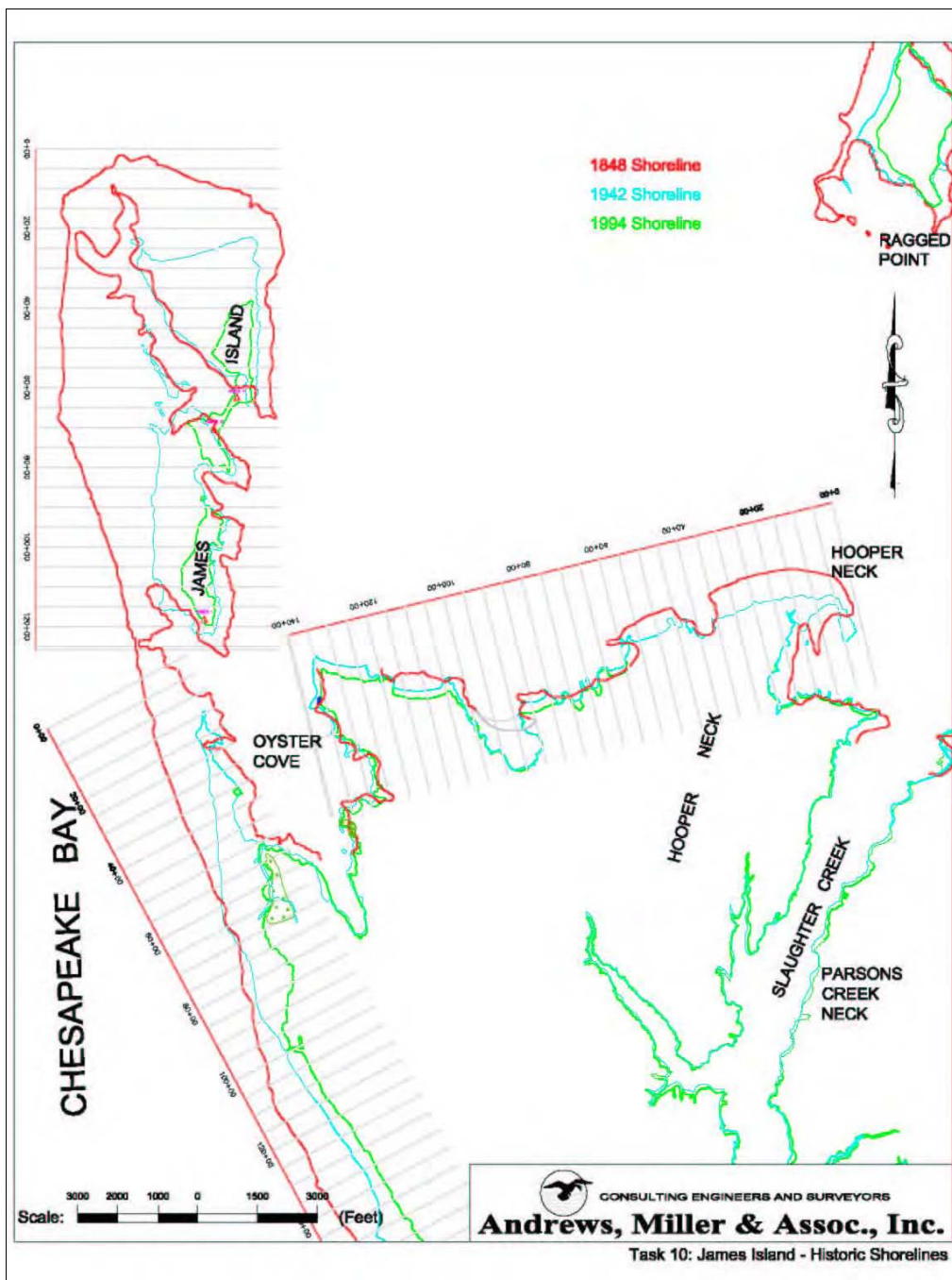


Figure A18. James Island shoreline position baselines

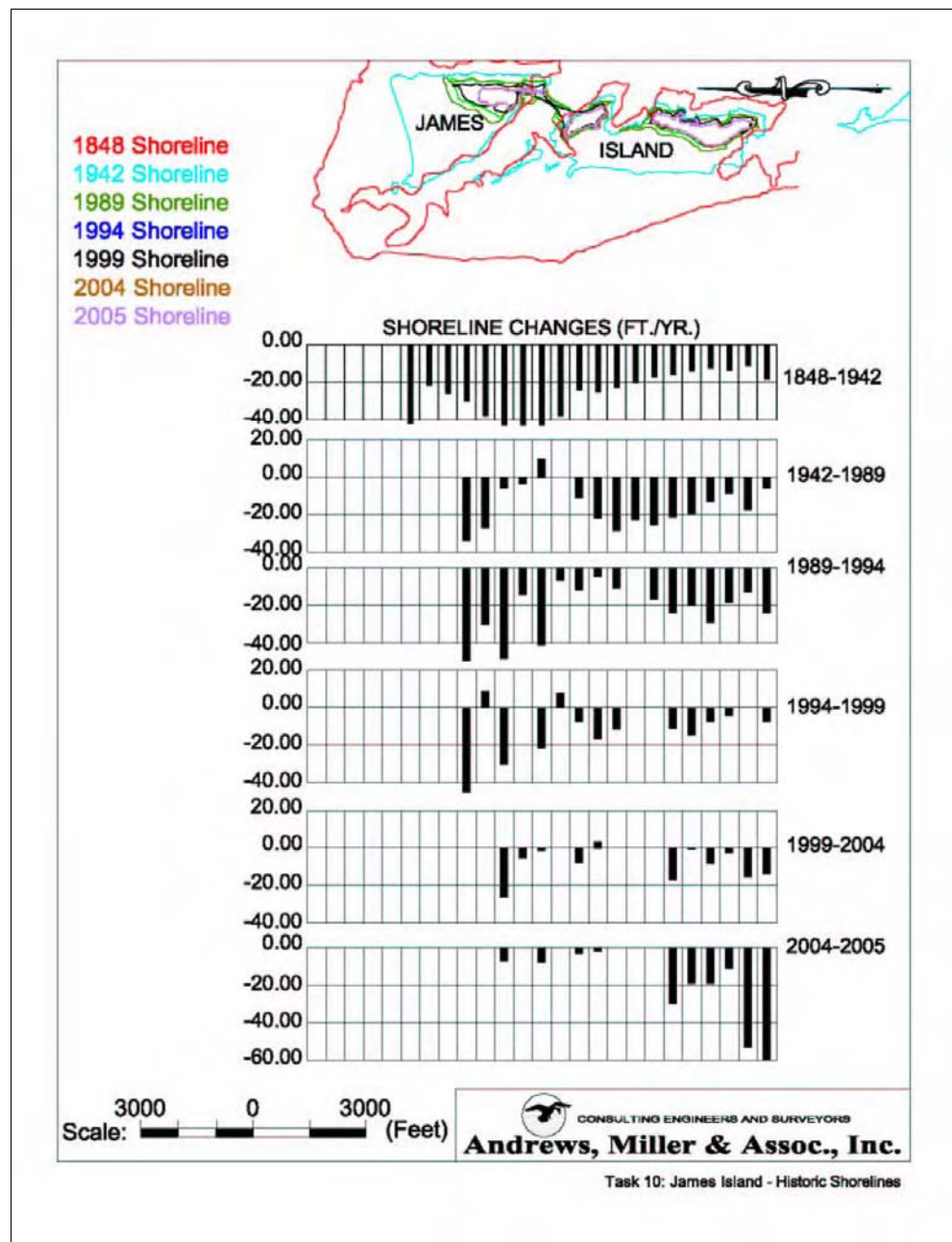


Figure A19. James Island shoreline position and change

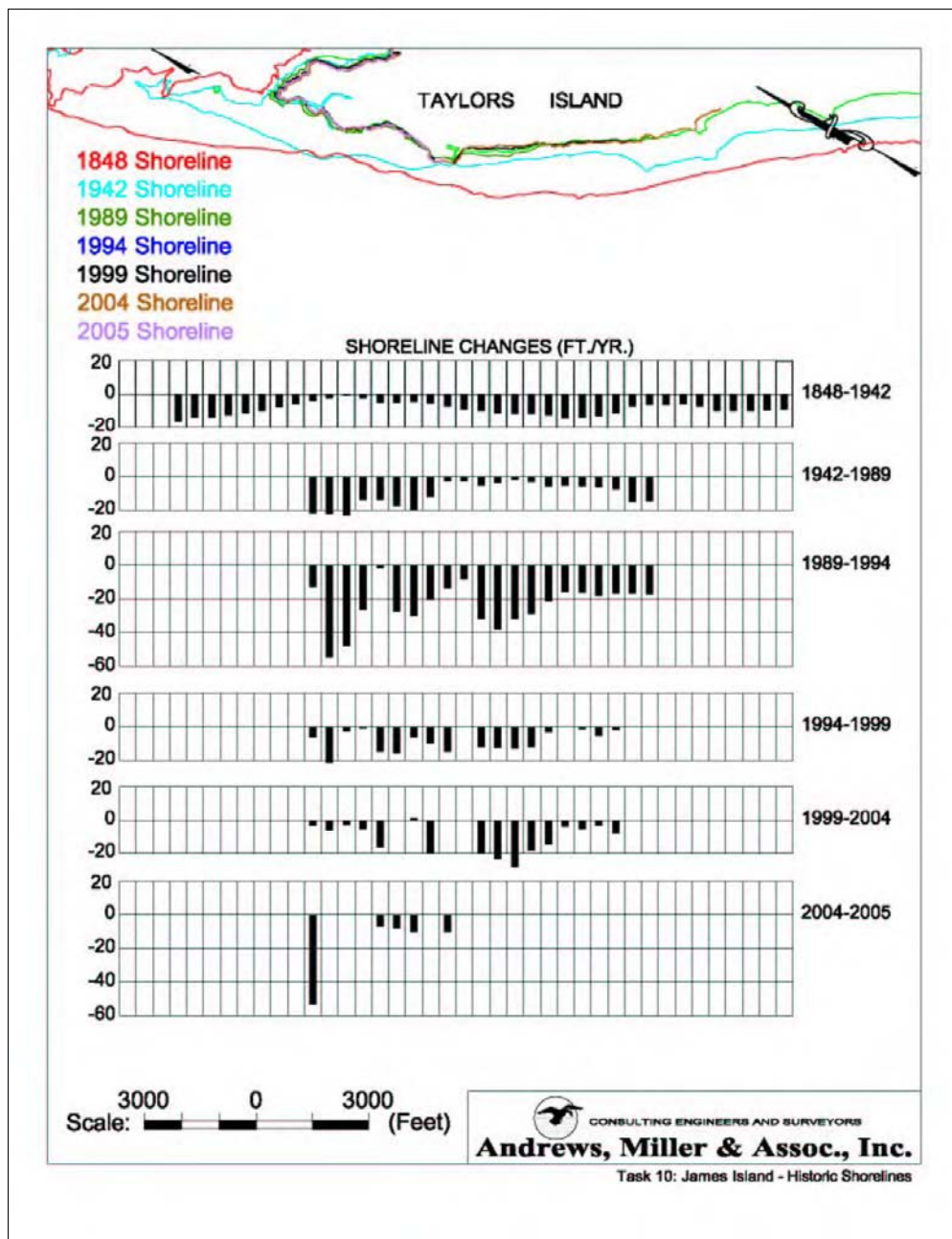


Figure A20. Taylors Island shoreline position and change

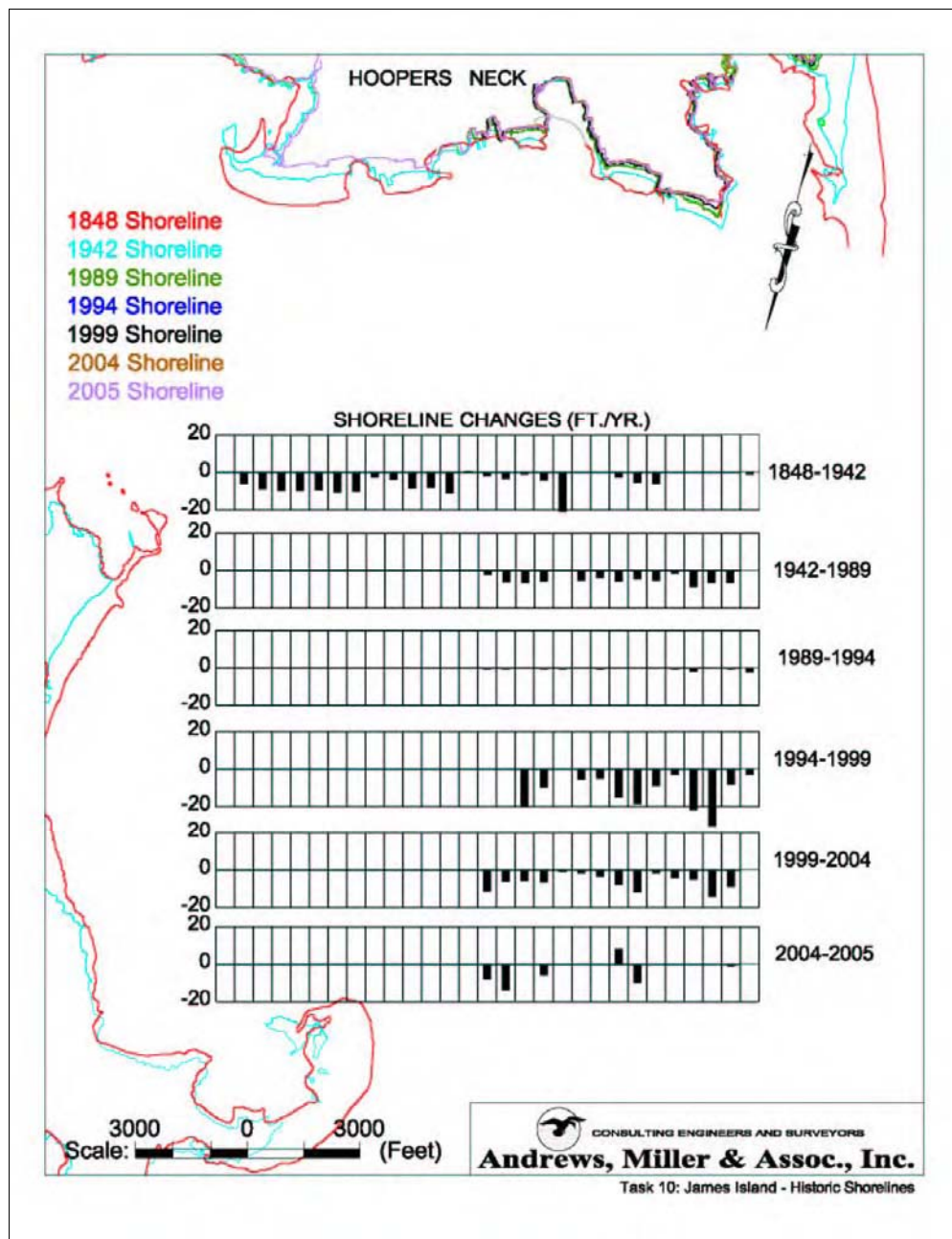


Figure A21. Hoopers Neck shoreline position and change

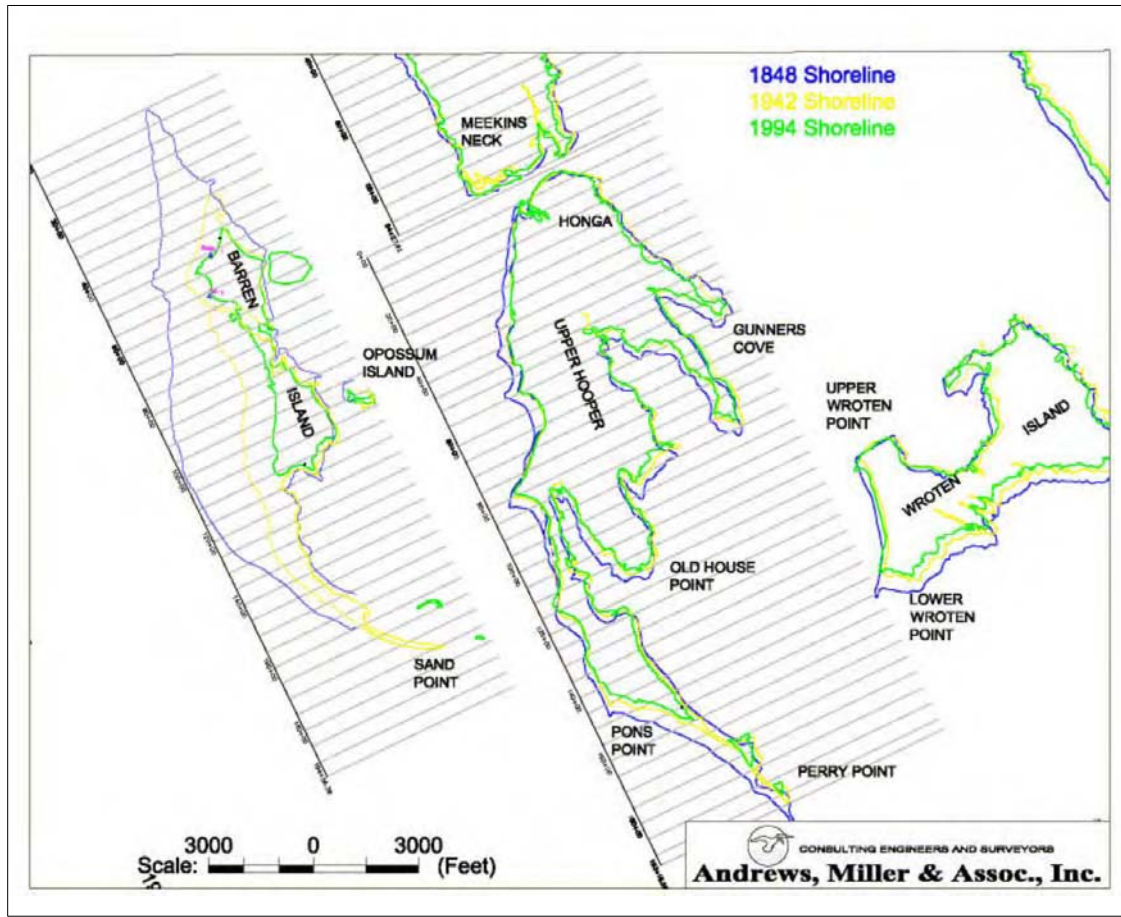


Figure A22. Barren Island shoreline position baselines

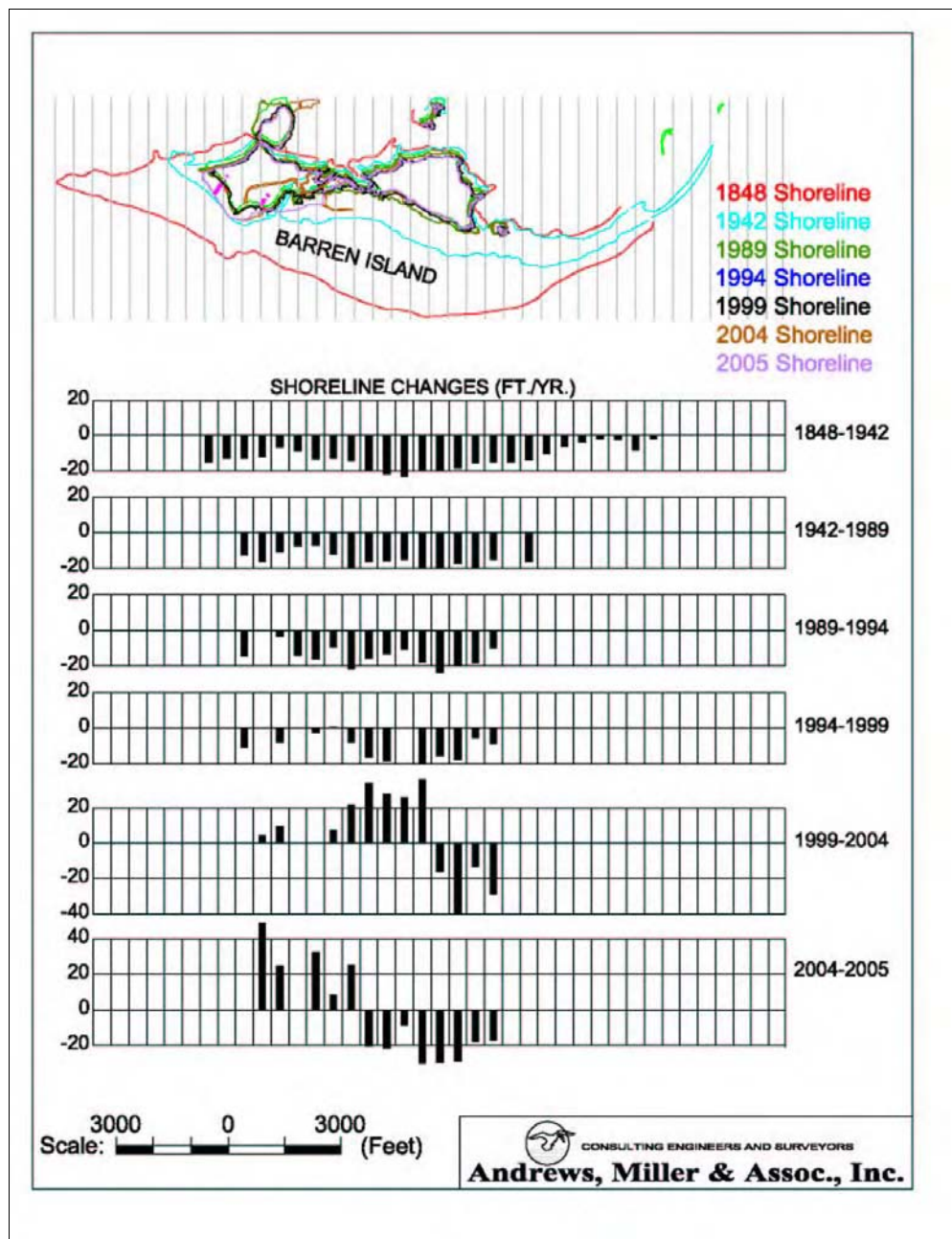


Figure A23. Barren Island shoreline position and change

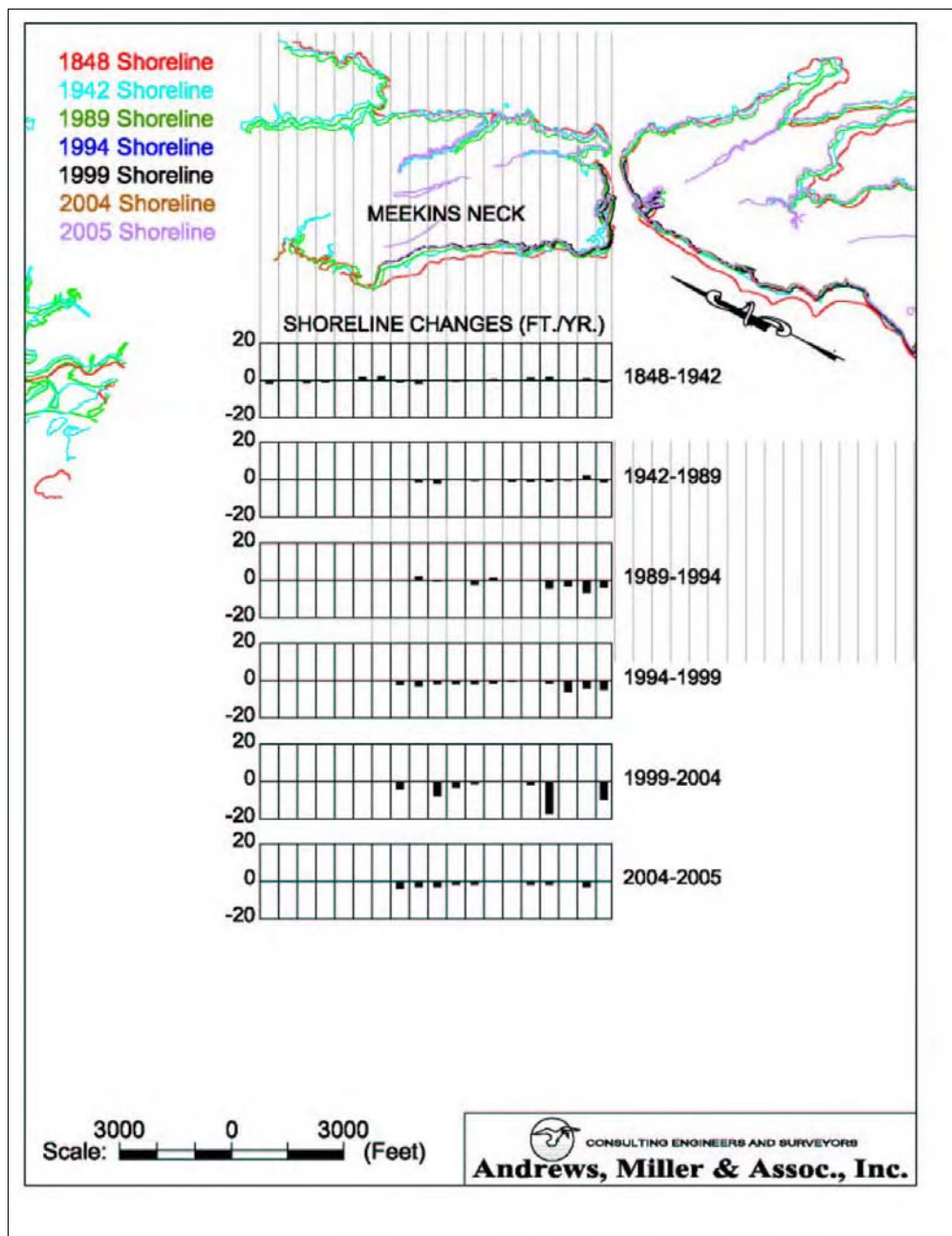


Figure A24. Meekins Neck shoreline position and change

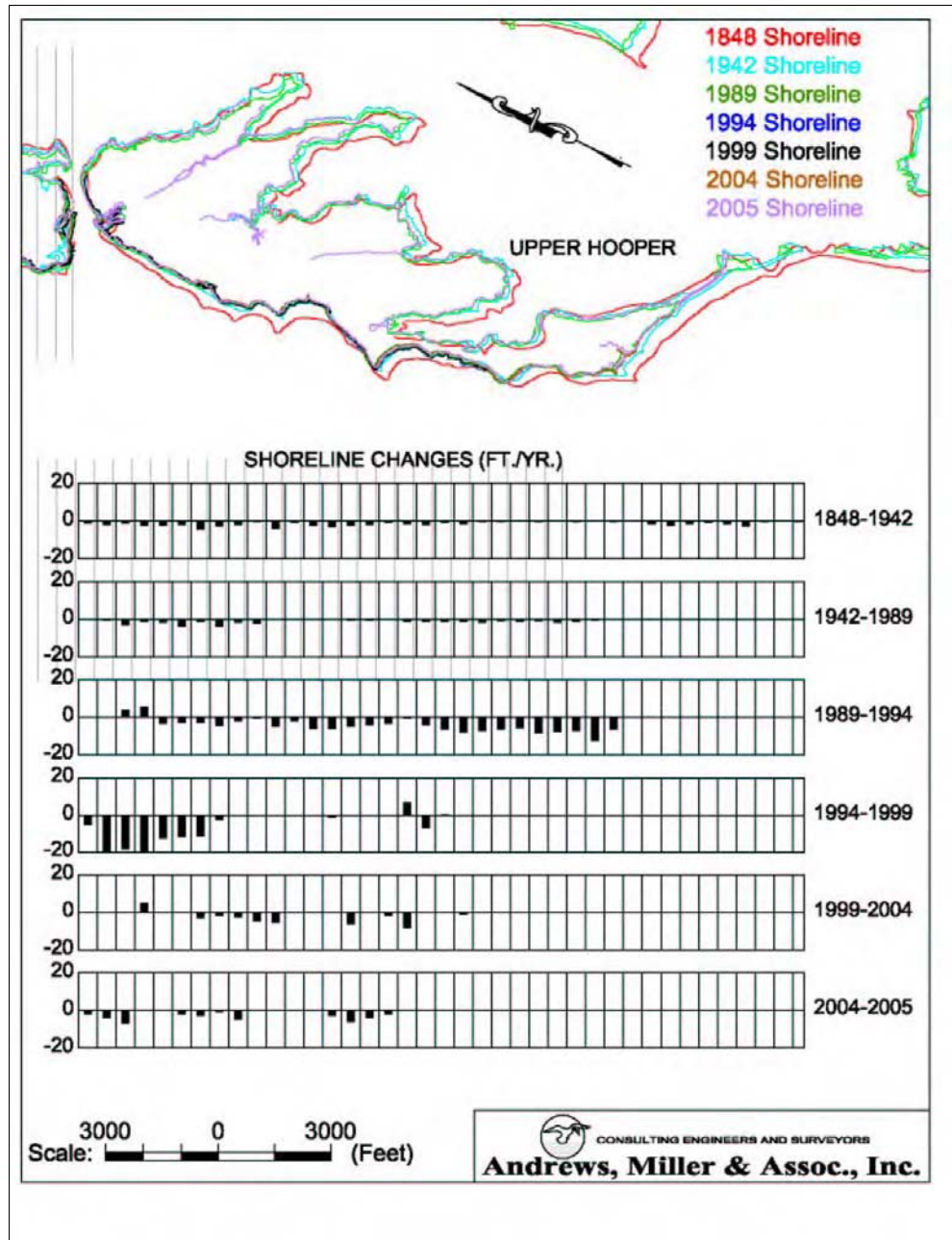


Figure A25. Upper Hoopers shoreline position and change

Table A10
**Summary of Average Annual Shoreline Change for Various Time
 Periods (ft/year)**

	1848 - 1942	1942 - 1989	1989 - 1994	1994 - 1999	1999 - 2004	2004 - 2005
James Island	-25	-14.3	-21.3	-10.6	-6.3	-14.1
Taylors Island	-8.8	-10.3	-23.4	-6.7	-8.5	-10.4
Hooper Neck	-5.9	-4.6	-0.6	-11.4	-6.5	-2.2
Barren Island	-12.3	-14.3	-31.4	-8.9	-0.2	-7.13
Meekins Neck	0	-0.4	-0.9	-2.2	-4	-1.8
Upper Hooper	-1.3	-1.3	-4.1	-5.2	-1.7	-2.3

Table A11**James Island Shoreline Change (ft)**

Station Number	1848 - 1942		1942 - 1989		1989 - 1994		1994 - 1999		1999 - 2004		2004 - 2005	
	Total Diff.	Per Year	Total Diff.	Per Year	Total Diff.	Per Year	Total Diff.	Per Year	Total Diff.	Per Year	Total Diff.	Per Year
0+00	1848 SL only											
5+00	1848 SL only											
10+00	1848 SL only											
15+00	1848 SL only											
20+00	1848 SL only											
25+00	-3,999	-42.54										
30+00	-2,048	-21.79										
35+00	-2,452	-26.09										
40+00	-2,851	-30.33	-1,585	-33.72	-247	-49.40	-225	-45.00				
45+00	-3,597	-38.27	-1,263	-26.87	-150	-30.00	-45	-9.00				
50+00	-4,062	-43.21	-263	-5.60	-240	-48.00	-151	-30.20	-131	-26.20	-7	-7.00
55+00	-4,095	-43.56	-150	-3.19	-71	-14.20		0.00	-26	-5.20	0	0.00
60+00	-4,094	-43.55	471	10.02	-205	-41.00	-108	-21.60	-7	-1.40	-8	-8.00
65+00	-3,584	-38.13	0	0.00	-32	-6.40	38	7.60		0.00	0	0.00
70+00	-2,275	-24.20	-512	-10.89	-59	-11.80	-38	-7.60	-39	-7.80	-3	-3.00
75+00	-2,381	-25.33	-1,023	-21.77	-23	-4.60	-83	-16.60	18	3.60	-2	-2.00
80+00	-2,154	-22.91	-1,337	-28.45	-53	-10.60	-58	-11.60		0.00		0.00
85+00	-1,894	-20.15	-1,056	-22.47		0.00		0.00		0.00		0.00
90+00	-1,648	-17.53	-1,184	-25.19	-82	-16.40		0.00		0.00		0.00
95+00	-1,513	-16.10	-996	-21.19	-119	-23.80	-55	-11.00	-85	-17.00	-30	-30.00
100+00	-1,319	-14.03	-928	-19.74	-99	-19.80	-74	-14.80	-3	-0.60	-19	-19.00
105+00	-1,167	-12.41	-598	-12.72	-145	-29.00	-38	-7.60	-40	-8.00	-19	-19.00
110+00	-1,297	-13.80	-393	-8.36	-91	-18.20	-22	-4.40	-12	-2.40	-11	-11.00
115+00	-1,072	-11.40	-813	-17.30	-62	-12.40	0	0.00	-76	-15.20	-53	-53.00
120+00	-1,736	-18.47	-268	-5.70	-118	-23.60	-38	-7.60	-69	-13.80	-60	-60.00
125+00	-182	-1.94	-199	-4.23	-120	-24.00		0.00		0.00		0.00
125+90												

Table A12
Taylors Island Shoreline Change (ft)

Station Number	1848 - 1942		1942 - 1989		1989 - 1994		1994 - 1999		1999 - 2004		2004 - 2005	
	Total Diff.	Per Year	Total Diff.	Per Year	Total Diff.	Per Year	Total Diff.	Per Year	Total Diff.	Per Year	Total Diff.	Per Year
0+00	1848 SL only											
5+00	1848 SL only											
10+00	1848 SL only											
15+00	-1,550	-16.49										
20+00	-1,261	-13.41										
25+00	-1,262	-13.43										
30+00	-1,147	-12.20										
35+00	-1,060	-11.28										
40+00	-900	-9.57										
45+00	-700	-7.45										
50+00	-533	-5.67										
55+00	-382	-4.06	-1,005	-21.38	-63	-12.60	-30	-6.00	-16	-3.20	-53	-53.00
60+00	-216	-2.30	-1,023	-21.77	-272	-54.40	-107	-21.40	-31	-6.20	0	0.00
65+00	-24	-0.26	-1,072	-22.81	-239	-47.80	14	2.80	13	2.60	0	0.00
70+00	-223	-2.37	-637	-13.55	-131	-26.20	5	1.00	-25	-5.00	0	0.00
75+00	-475	-5.05	-626	-13.32	-7	-1.40	-73	-14.60	-81	-16.20	-7	-7.00
80+00	-471	-5.01	-806	-17.15	-136	-27.20	-78	-15.60	0	0.00	-8	-8.00
85+00	-402	-4.28	-900	-19.15	-148	-29.60	-32	-6.40	8	1.60	-10	-10.00
90+00	-492	-5.23	-557	-11.85	-100	-20.00	-48	-9.60	-97	-19.40	0	0.00
95+00	-694	-7.38	-106	-2.26	-87	-17.40	-73	-14.60	0	0.00	-16	-16.00
100+00	-829	-8.82	-111	-2.36	-41	-8.20	0	0.00	0	0.00		
105+00	-925	-9.84	-231	-4.91	-159	-31.80	-81	-16.20	-97	-19.40		
110+00	-1,056	-11.23	-154	-3.28	-188	-37.60	-63	-12.60	-117	-23.40		
115+00	-1,082	-11.51	-77	-1.64	-159	-31.80	-64	-12.80	-139	-27.80		
120+00	-1,055	-11.22	-141	-3.00	-143	-28.60	-60	-12.00	-91	-18.20		
125+00	-1,136	-12.09	-260	-5.53	-105	-21.00	15	3.00	-73	-14.60		
130+00	-1,312	-13.96	-244	-5.19	-78	-15.60	0	0.00	17	3.40		
135+00	-1,295	-13.78	-247	-5.26	-80	-16.00	6	1.20	-26	-5.20		
140+00	-1,215	-12.93	-285	-6.06	-89	-17.80	27	5.40	-14	-2.80		
145+00	-1,064	-11.32	-333	-7.09	-82	-16.40	8	1.60	-40	-8.00		
150+00	-671	-7.14	-687	-14.62	-62	-12.40	0	0.00				
155+00	-594	-6.32	-669	-14.23	-85	-17.00	0	0.00				
160+00	-585	-6.22										
165+00	-565	-6.01										
170+00	-641	-6.82										
175+00	-930	-9.89										

Table A13
Hoopers Neck Shoreline Change (ft)

Station Number	1848 - 1942		1942 - 1989		1989 - 1994		1994 - 1999		1999 - 2004		2004 - 2005	
	Total Diff.	Per Year										
0+00												
5+00	-574	-6.11										
10+00	-832	-8.85										
15+00	-896	-9.53										
20+00	-919	-9.78										
25+00	-885	-9.41										
30+00	-981	-10.44										
35+00	-945	-10.05										
40+00	-219	-2.33										
45+00	-328	-3.49										
50+00	-780	-8.30										
55+00	-747	-7.95										
60+00	-1,037	-11.03										
65+00	69	0.73										
70+00	-149	-1.59	-103	-2.19	-31	-0.66		0.00	-58	-11.60	-8	-8.00
75+00	-297	-3.16	-289	-6.15	-24	-0.51	0	0.00	-31	-6.20	-14	-14.00
80+00	-75	-0.80	-308	-6.55	-11	-0.23	-96	-19.20	-30	-6.00	0	0.00
85+00	-401	-4.27	-257	-5.47	-35	-0.74	-49	-9.80	-34	-6.80	-6	-6.00
90+00	-1,975	-21.01	-8	-0.17	-35	-0.74	0	0.00	-6	-1.20	0	0.00
95+00	0	0.00	-244	-5.19	-10	-0.21	-27	-5.40	-10	-2.00	0	0.00
100+00	0	0.00	-164	-3.49	-34	-0.72	-25	-5.00	-17	-3.40	0	0.00
105+00	-242	-2.57	-260	-5.53	8	0.17	-75	-15.00	-40	-8.00	8	8.00
110+00	-508	-5.40	-216	-4.60	-13	-0.28	-92	-18.40	-60	-12.00	-10	-10.00
115+00	-552	-5.87	-244	-5.19	0	0.00	-44	-8.80	-9	-1.80	0	0.00
120+00	-16	-0.17	-57	-1.21	-39	-0.83	-14	-2.80	-21	-4.20	0	0.00
125+00	0	0.00	-400	-8.51	-79	-1.68	-109	-21.80	-25	-5.00	0	0.00
130+00	0	0.00	-318	-6.77	0	0.00	-152	-30.40	-71	-14.20	0	0.00
135+00	0	0.00	-317	-6.74	-28	-0.60	-41	-8.20	-46	-9.20	-1	-1.00
140+00	-76	-0.81	-41	-0.87	-11	-2.20	-14	-2.80	0	0.00	0	0.00

Table A14
Barren Island Shoreline Change (ft)

Station Number	1848 - 1942		1942 - 1989		1989 - 1994		1994 - 1999		1999 - 2004		2004 - 2005	
	Total Diff.	Per Year	Total Diff.	Per Year	Total Diff.	Per Year	Total Diff.	Per Year	Total Diff.	Per Year	Total Diff.	Per Year
0+00	1848 SL only											
5+00	1848 SL only											
10+00	1848 SL only											
15+00	1848 SL only											
20+00	1848 SL only											
25+00	1848 SL only											
30+00	-1,490	-15.85										
35+00	-1,245	-13.24										
40+00	-1,228	-13.06	-604	-12.85	-740	-148.00	-56	-11.20				
45+00	-1,146	-12.19	-777	-16.53	0	0.00	0	0.00	21	4.20	4.9	4.90
50+00	-653	-6.95	-516	-10.98	-18	-3.60	-41	-8.20	49	9.80	2.5	2.50
55+00	-830	-8.83	-367	-7.81	-710	-142.00	0	0.00	0	0.00	0	0.00
60+00	-1,301	-13.84	-338	-7.19	-82	-16.40	-14	-2.80	0	0.00	32.6	32.60
65+00	-1,251	-13.31	-573	-12.19	-47	-9.40	4	0.80	38	7.60	8.7	8.70
70+00	-1,346	-14.32	-915	-19.47	-108	-21.60	-41	-8.20	109	21.80	25.6	25.60
75+00	-1,857	-19.76	-782	-16.64	-80	-16.00	-83	-16.60	171	34.20	-20.5	-20.50
80+00	-2,057	-21.88	-754	-16.04	-66	-13.20	-94	-18.80	142	28.40	-21.7	-21.70
85+00	-2,181	-23.20	-706	-15.02	-55	-11.00	0	0.00	131	26.20	-8.5	-8.50
90+00	-1,827	-19.44	-935	-19.89	-89	-17.80	-98	-19.60	-182	-36.40	-30	-30.00
95+00	-1,826	-19.43	-923	-19.64	-120	-24.00	-78	-15.60	-82	-16.40	-29.7	-29.70
100+00	-1,752	-18.64	-819	-17.43	-100	-20.00	-90	-18.00	-198	-39.60	-28.8	-28.80
105+00	-1,477	-15.71	-937	-19.94	-92	-18.40	-29	-5.80	-68	-13.60	-17.8	-17.80
110+00	-1,451	-15.44	-709	-15.09	-46	-9.20	-44	-8.80	-144	-28.80	-17.1	-17.10
115+00	-1,428	-15.19		0.0								
120+00	-1,305	-13.88	-775	-16.49								
125+00	-1,006	-10.70										
130+00	-629	-6.69										
135+00	-361	-3.84										
140+00	-205	-2.18										
145+00	-250	-2.66										
150+00	-816	-8.68										
155+00	-197	-2.10										
160+00	-25	-0.27										
165+00	1942 SL only	0.00										
170+00	1942 SL only	0.00										
175+00	1942 SL only	0.00										
180+00		0.00										
185+00		0.00										

Table A15
Meekins Neck Shoreline Change (ft)

Station Number	1848 - 1942		1942 - 1989		1989 - 1994		1994 - 1999		1999 - 2004		2004 - 2005	
	Total Diff.	Per Year										
0+00	-190	-2.02										
5+00	-47	-0.50										
10+00	-137	-1.46										
15+00	-123	-1.31										
20+00	13	0.14										
25+00	167	1.78										
30+00	200	2.13										
35+00	-107	-1.14	-17	-0.36	0	0.00	-10	-2.00	-21	-4.20	-4	-4.00
40+00	-172	-1.83	-53	-1.13	10	2.00	-15	-3.00	0	0.00	-3	-3.00
45+00	-44	-0.47	-107	-2.28	-3	-0.60	-8	-1.60	-36	-7.20	-3	-3.00
50+00	-86	-0.91	5	0.11	0	0.00	-9	-1.80	-16	-3.20	-2	-2.00
55+00	-12	-0.13	-30	-0.64	-12	-2.40	-9	-1.80	-6	-1.20	-2	-2.00
60+00	44	0.47	0	0.00	6	1.20	-6	-1.20	0	0.00	0	0.00
65+00	-26	-0.28	-46	-0.98	0	0.00	-3	-0.60	0	0.00	0	0.00
70+00	127	1.35	-45	-0.96	0	0.00	0	0.00	-9	-1.80	-2	-2.00
75+00	153	1.63	-35	-0.74	-21	-4.20	-7	-1.40	-67	-13.40	-2	-2.00
80+00	-29	-0.31	24	0.51	-16	-3.20	-30	-6.00	0	0.00	0	0.00
85+00	70	0.74	100	2.13	-33	-6.60	-21	-4.20	0	0.00	-3	-3.00
90+00	94	1.00	-54	-1.15	20	4.00	-25	-5.00	-48	-9.60	0	0.00
94+28	95	1.01	27	0.57	0	0.00	-1	-0.20	-55	-11.00	-3	-3.00

Table A16
Upper Hoopers Shoreline Change (ft)

Station Number	1848 - 1942		1942 - 1989		1989 - 1994		1994 - 1999		1999 - 2004		2004 - 2005	
	Total Diff.	Per Year										
0+00	-101	-1.07	-19	-0.40	0	0.00	-26	-5.20	0	0.00	-2	-2.00
5+00	-183	-1.95	-31	-0.66	-1	-0.20	-101	-20.20	0	0.00	-4	-4.00
10+00	-109	-1.16	-146	-3.11	20	4.00	-92	-18.40	0	0.00	-7	-7.00
15+00	-220	-2.34	-78	-1.66	27	5.40	-102	-20.40	25	5.00	0	0.00
20+00	-218	-2.32	-89	-1.89	-17	-3.40	-64	-12.80	0	0.00	0	0.00
25+00	-194	-2.06	-174	-3.70	-14	-2.80	-60	-12.00	-1	-0.20	-2	-2.00
30+00	-412	-4.38	-60	-1.28	-14	-2.80	-57	-11.40	-15	-3.00	-3	-3.00
35+00	-254	-2.70	-174	-3.70	-22	-4.40	-11	-2.20	-9	-1.80	-1	-1.00
40+00	-177	-1.88	-82	-1.74	-10	-2.00	0	0.00	-13	-2.60	-5	-5.00
45+00	52	0.55	-116	-2.47	-3	-0.60	0	0.00	-24	-4.80	0	0.00
50+00	-369	-3.93	0	0.00	-24	-4.80	0	0.00	-28	-5.60	0	0.00
55+00	80	0.85	0	0.00	-11	-2.20	0	0.00	0	0.00	0	0.00
60+00	-244	-2.60	0	0.00	-30	-6.00	0	0.00	0	0.00	0	0.00
65+00	-285	-3.03	0	0.00	-30	-6.00	-5	-1.00	0	0.00	-3	-3.00
70+00	-232	-2.47	-29	-0.62	-24	-4.80	-2	-0.40	-31	-6.20	-6	-6.00
75+00	-203	-2.16	-29	-0.62	-21	-4.20	0	0.00	0	0.00	-4	-4.00
80+00	63	0.67	0	0.00	-16	-3.20	0	0.00	-9	-1.80	-2	-2.00
85+00	-155	-1.65	-71	-1.51	-3	-0.60	35	7.00	-41	-8.20	0	0.00
90+00	-189	-2.01	-63	-1.34	-21	-4.20	-33	-6.60	0	0.00	0	0.00
95+00	-73	-0.78	-68	-1.45	-32	-6.40	2	0.40	0	0.00	0	0.00
100+00	-136	-1.45	-74	-1.57	-41	-8.20	0	0.00	-5	-1.00	0	0.00
105+00	-53	-0.56	-82	-1.74	-36	-7.20			0	0.00	0	0.00
110+00	-55	-0.59	-53	-1.13	-33	-6.60						
115+00	18	0.19	-76	-1.62	-28	-5.60						
120+00	-52	-0.55	-52	-1.11	-42	-8.40						
125+00	-9	-0.10	-94	-2.00	-39	-7.80						
130+00	-42	-0.45	-75	-1.60	-36	-7.20						
135+00	-6	-0.06	-33	-0.70	-62	-12.40						
140+00	35	0.37	22	0.47	-32	-6.40						
145+00	16	0.17	0	0.00								
150+00	-150	-1.60										
155+00	-211	-2.24										
160+00	-139	-1.48										
165+00	-87	-0.93										
170+00	-170	-1.81										
175+00	-279	-2.97										
180+00	-42	-0.45										
185+00	-2	-0.02										

Appendix B

Evaluation of Additional James Island Alternatives

To support the screening-level evaluation of potential candidate restoration sites, Blasland, Bouck, & Lee, Inc. (BBL) assisted the U.S. Army Engineer Research and Development Center (ERDC) in the hydrodynamic modeling efforts for the Mid-Bay Island Restoration Project. As part of this coordinated effort, BBL conducted a hydrodynamic analysis for an additional three primary channel alignment alternatives to the James Island design. These additional alignments were selected by ERDC; U.S. Army Engineer District, Baltimore; Maryland Environmental Service (MES); and Maryland Port Administration (MPA) after a review of the initial model simulations, James Island Alts 1-6, as described in Chapter 1 of the main text of this report. These alternatives, combined with additional breakwater alignments analysis for the Barren Island alternatives modeled by Andrews, Miller & Associates, Inc. (AMA), were proposed to complete the investigative activities towards island restoration in the Mid-Bay region. This appendix describes the model development activities and results for these three alternatives.

James Island Alternatives

In addition to the six alignments described in Chapter 1, three primary channel alignments (Alts JI-7, JI-8, and JI-9; Figure B1) that are similar to the first six alignments (with some variations) were added to examine conditions concerning interior tidal gut configurations. The objectives of the analysis of the three additional alternatives were:

- a. Perform circulation modeling in combination with wave modeling for James Island to establish appropriate tidal gut configurations.
- b. Investigate sediment transport patterns in and around James Island, including sediment shoaling at neighboring navigation channels.
- c. Evaluate engineering merits and environmental impacts of alternative island alignments.

Screening of channel width effects, as well as the possibility of westward-facing channel entrances, was deemed sufficiently important to initiate additional

model simulations. The following three alignments were simulated to better define the impacts of typical conditions on each tidal gut configuration.

Alt JI-7. 150-ft wide “flipped y-shaped” primary channel – tidal gut entrances face westward.

Alt JI-8. 75-ft wide “y-shaped” primary channel.

Alt JI-9. 75-ft wide “c-shaped” primary channel.

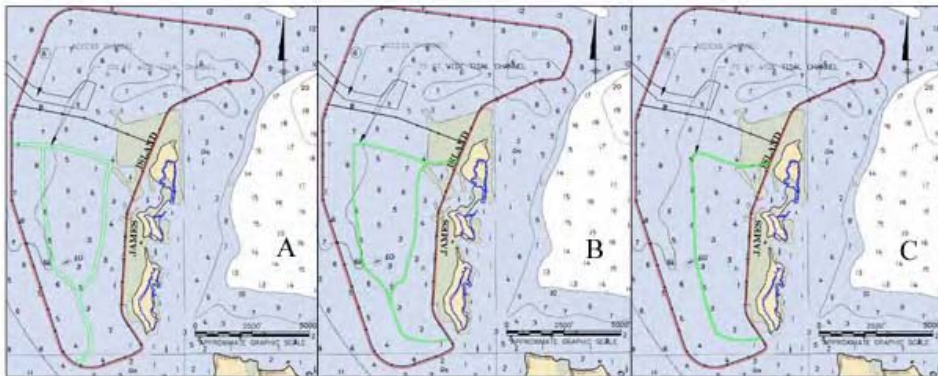


Figure B1. James Island alignment Alts 7, 8, and 9 (A, B, and C, respectively)

Suggestions by ecologists working with the Mid-Bay Island project led to the question of the natural system response to the primary channel entrances facing the open bay instead of the protected leeward side of the proposed James Island alignment. Additional concerns were expressed as the tidal channel flow exits toward the existing islands, potentially creating an increase in erosion in the existing islands and sedimentation at the tidal gut inlets.

The first additional configuration, Alt JI-7, was developed to test the potential hydrological effects of a westward-facing outlet system as a possible new design consideration. Alt JI-7 is a split “y” configuration similar to Alt JI-1 with primary channel outlets opening directly to Chesapeake Bay, rather than eastern-facing channel openings as seen in Alt JI-1.

Further comparisons with existing natural systems within Chesapeake Bay led to questions concerning the ability of different channel widths to properly flush and inundate the wetland system. To test the effectiveness of various channel widths, Alts JI-8 and JI-9 were established for comparison with the existing 150- and 300-ft channel widths. Alts JI-8 and JI-9 are configurations similar to Alts JI-1 and JI-5, respectively, with smaller 75-ft primary channels instead of 150- or 300-ft channel widths found in the other alternatives.

Wave Transformation

Additional simulations of the wave transformation effects were not conducted for James Island Alts JI7-JI9. Chapter 3 of the main text of this report describes the results of STWAVE wave transformation modeling performed for James

Island Alts J1-J6. The three additional primary channel alternatives evaluated by BBL did not alter the footprint of the island, but only the width and alignment of the interior channels. Therefore, overall effects on the wave transformation in the nearby region would be minimal compared to the six alternatives studied by ERDC. Although there would be slight differences in the bathymetry outside of the island footprint for the Alt JI-7 alternative (the alternative with the westward-facing channel openings), these differences were not considered sufficiently significant to warrant additional wave transformation modeling for this screening-level evaluation.

Hydrodynamic and Sediment Transport Modeling

The ERDC Inlet Modeling System (IMS) (Militello et al. 2004) was operated by BBL to evaluate the impacts to velocities and sediment transport patterns from the three James Island alternatives. The IMS is an integrated modeling system for calculating hydrodynamics and sediment transport for coastal projects at time scales of a tidal cycle, through a series of storms, to several years.

Hydrodynamics were evaluated with two specific models, ADCIRC and M2D, and sediment transport patterns were evaluated with only M2D. Model pre- and post-processing was done with the Surface-water Modeling System, Version 9.0 beta. This section describes the model, the model inputs, and boundary conditions.

Hydrodynamic modeling with ADCIRC

Chapter 4 of the report describes the ADCIRC model, as well as the development of the regional scale ADCIRC Chesapeake Bay model for the project. BBL modified the ADCIRC model mesh developed by ERDC to evaluate the hydrodynamics for the Alt JI-8 and JI-9 alternatives. The ERDC model mesh was modified to represent the geometry and elevations for each alternative. The ADCIRC meshes for Alts JI-1 and JI-5 were redefined within the regions of the interior channels, increasing the resolution to accurately represent the 75-ft channels of Alts JI-8 and JI-9. Figure B2 illustrates the increased resolution in the channel areas to refine the channel to 75 ft.

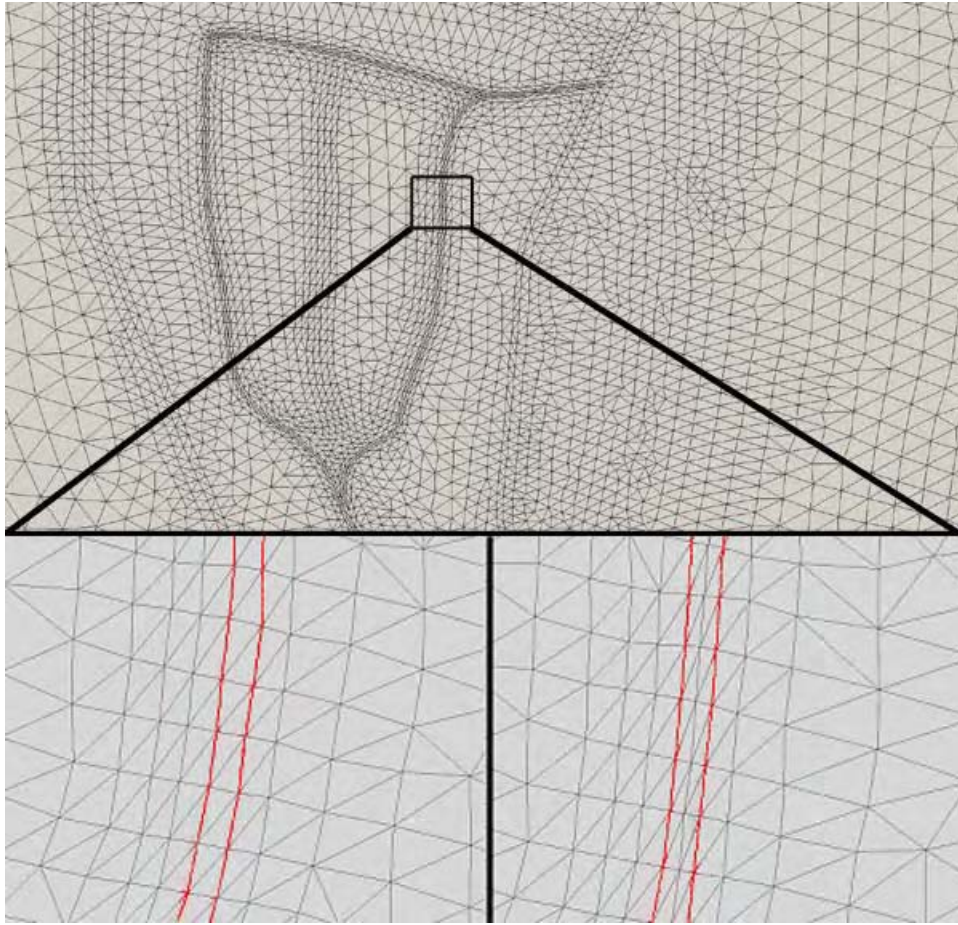


Figure B2. Example ADCIRC grid refinement in channel – bottom left is ERDC original grid, bottom right is BBL grid with increased resolution in channel area (same region highlighted in red)

Using the modified meshes for Alts JI-8 and JI-9, the spring tide was simulated with the ADCIRC model to allow for evaluation of velocities and water-surface elevations under tidal conditions. To determine the effects of varied channel widths, normal daily hydrological conditions were applied to Alts JI-8 and JI-9 for comparison to 150- and 300-ft channel widths. For each alternative, a normal tidal cycle was simulated over spring tide conditions, providing the largest range of water-level conditions within a full neap-spring tidal cycle. To allow for comparison with the other alternatives, the spring tide was chosen from the 2-week time span 1-15 January 2005 (simulated by ERDC). Figure B3 shows the predicted water level for the James Island region over the neap and spring tides modeled by ERDC; the period of modeling used for Alts JI-8 and JI-9 is highlighted in red, extending from 8-12 January 2005.

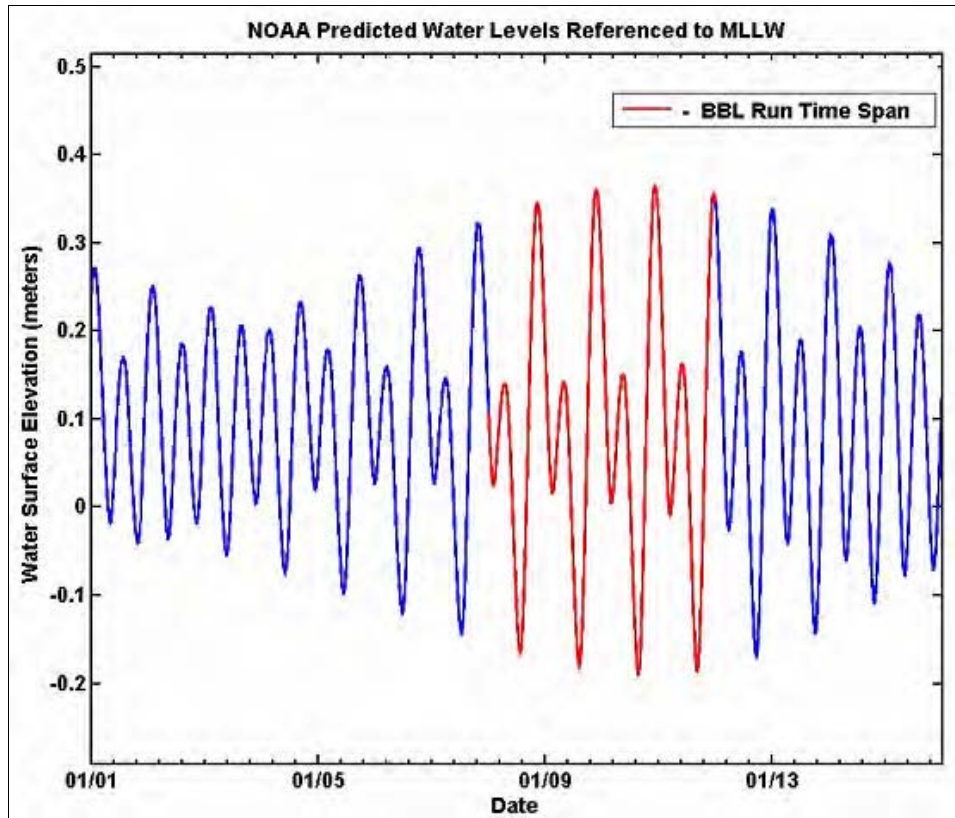


Figure B3. Predicted tidal ranges during 1-15 January in the James Island region. Red highlight indicates the time span of Alt JI-8 and JI-9 tidal conditions

Tidal circulation modeled in Alts JI-8 and JI-9 showed weak velocities in the region surrounding James Island. The private watermen channel to the southeast, between the island and the mainland, had the greatest velocity, resulting in maximum currents of 0.5 ft/sec. Interior velocities through the tidal guts for both alternatives showed an overall reduction in velocity, with velocities peaking at 0.2 to 0.3 ft/sec. Velocity differences between the two alternatives were minor, with slightly stronger currents through the southern portion of the channel in Alt JI-8, approximately 0.2 ft/sec faster than that exiting Alt JI-9. Maximum current velocity fields are shown in Figures B4 and B5.

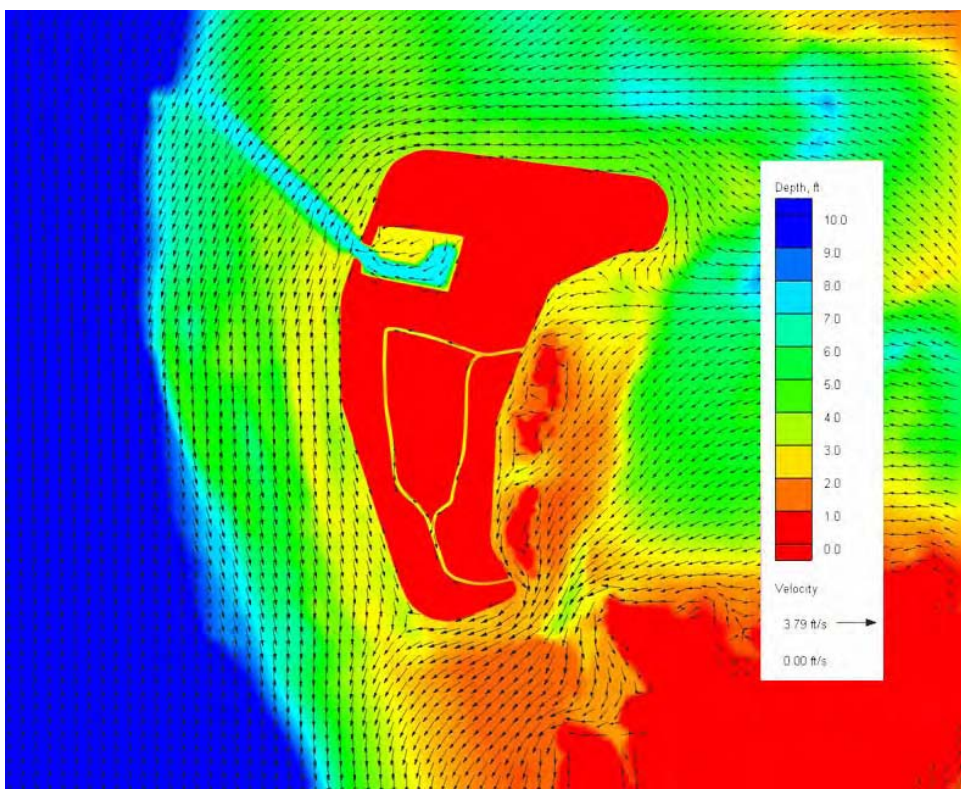


Figure B4. Alt JI-8 maximum current field, normal tide

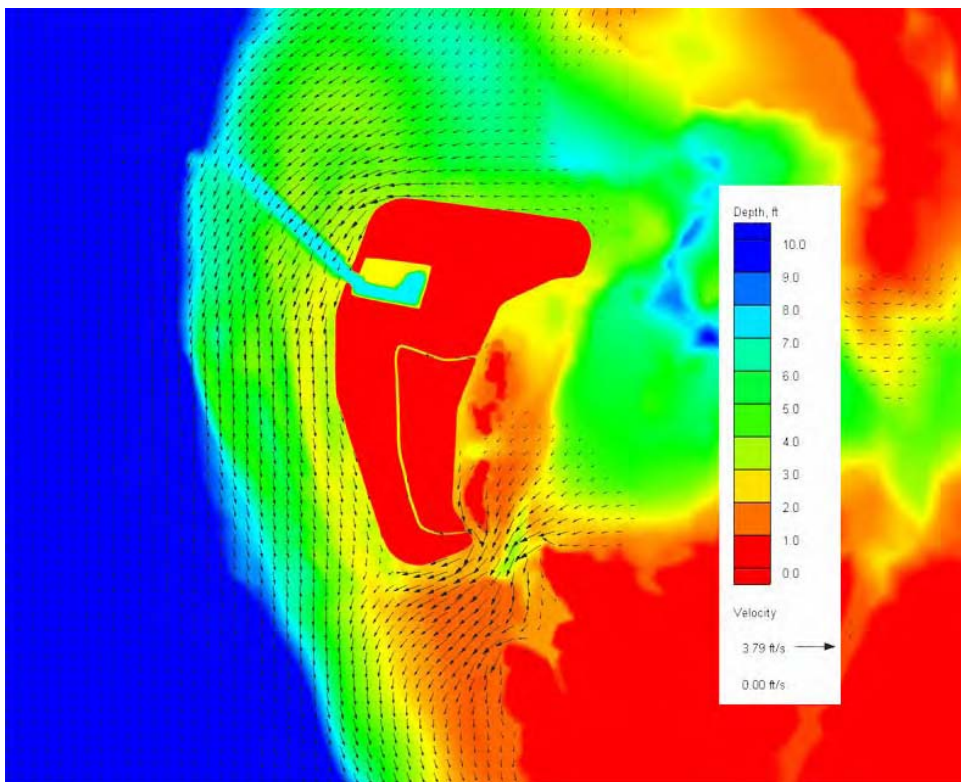


Figure B5. Alt JI-9 maximum current field, normal tide

Hydrodynamic and sediment transport modeling with M2D

The M2D model was operated to evaluate impacts to the hydrodynamics and sediment transport patterns during an extreme event for Alt JI-7. M2D is a finite-difference, two-dimensional (2-D), depth-integrated hydrological model that solves continuity and momentum equations of fluids in motion. M2D can also be coupled with wave radiation stresses provided by STWAVE to resolve changing wave conditions and their effects on local circulation. M2D was operated to simulate the effects of a northeaster (NE33) on Alt JI-7, taking advantage of the model's capabilities with wave stress coupling and sedimentation to determine storm effects on circulation and sedimentation within the westward-facing channels of Alt JI-7 (Militello et al. 2004).

Hydrodynamics

The M2D model grid was created in the SMS utilizing bathymetry data provided by ERDC, as well as data collected as part of a survey of James Island and Barren Island completed by AMA in June of 2005. Bathymetry data were interpolated into M2D using the SMS preprocessor, developing a model grid with a resolution of 20 ft in the regions of interest at the mouths and bends within the interior channel system. Land regions in excess of +4 ft elevation (model datum was developed for mean sea level) were flagged as inactive land cells because overtopping and flooding in these areas was not anticipated during the northeaster (NE). Inactive regions include portions of the mainland as well as the dike and upland systems of the island design. The M2D model grid used for the simulations is presented on Figure B6. Note that the inactive grid cells are shown with brown in A and with red in B.

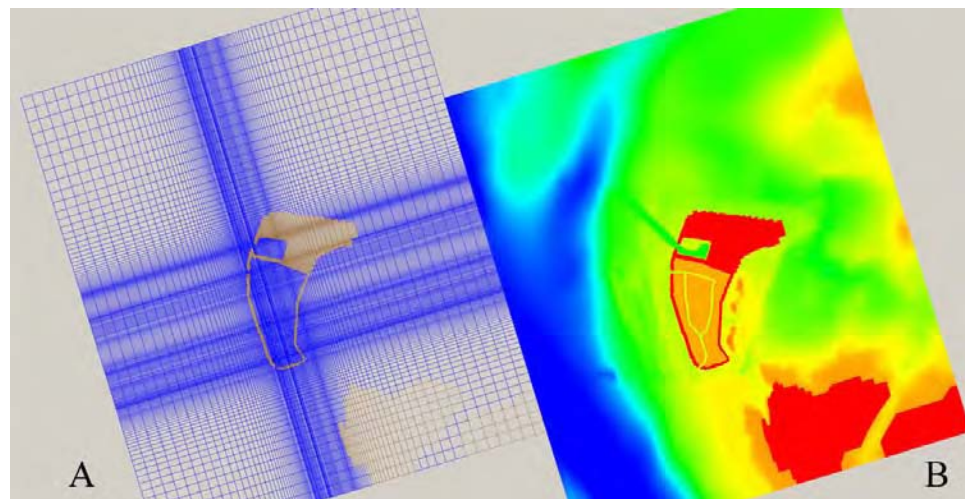


Figure B6. Alt JI-7 M2D model grid – grid cell structure visible on left in A, bathymetric view on right in B

Potential impacts of velocities at the entrances of the channel systems, as well as the potential modifications for deposition or erosion of sediments within each of the channels for the James Island alternatives, were subjects of concern for the westward-facing system. To evaluate these potential impacts, a simulation of the most commonly occurring large storm event in the Chesapeake Bay region, a northeaster, was performed. Discussions with ERDC concerning the range of historical northeaster storms, previously studied in the ERDC report by Melby et al. (2005) on the life cycle analysis of the Mid-Bay Island designs, led to the decision to force the system with a historical northeaster from 1993, identified as NE33 in Melby et al. (2005). NE33 was one of strongest historical northeasters recorded, with wind and wave effects to the north-northeast providing the most direct forcings on the westward-facing channel system. Wind files representing NE33 conditions were created from wind data provided to BBL by ERDC.

Current velocities as a result of NE33 forcing are as expected, with an overall increase in water velocity compared to normal tide. Velocities within the tidal guts are weaker as compared to those around the exterior of the island, showing maximum velocity of approximately 1.6 ft/sec. Flows outside the island are directed north and up the bay, impacting the southern channel entrance with greater effect than the northern channel entrance. Water is forced in the southern entrance and is then diverted through the two sides of the channel before exiting through the northern channel. The western interior channel receives the majority of water flow, showing increased velocities compared to the other north-south channel to the east of the island. Flow in the exterior region is altered due to the footprint of the proposed James Island alignment, creating a slight increase in flow off the southern tip of the island. Velocities through the channel between the island and the mainland are increased, resulting in the greatest velocities in the model off the tip of the island, approaching 2.7 ft/sec. The maximum current velocity field is shown in Figure B7.

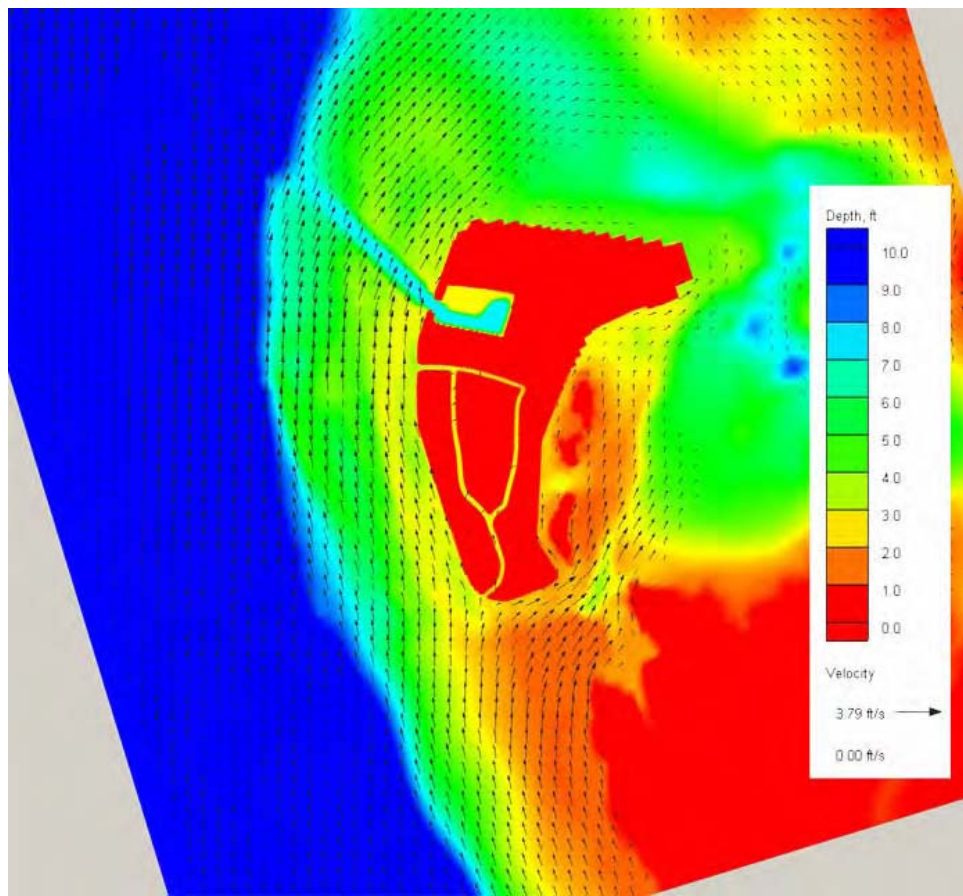


Figure B7. Alt JI-7 maximum current field, NE33

Sedimentation

A sedimentation analysis was performed for Alt JI-7 using M2D. Westward-facing channel mouths raised concerns over potential channel filling during storms. To evaluate conditions, sediment transport was enabled in the M2D model run to test northeaster effects on sediment deposition patterns. No suspended sediment forcing was included as a boundary condition, though bed-load transport was permitted across the boundary. Simulation was specified to determine sedimentation patterns throughout the James Island region as a result of the Alt JI-7 footprint. A 0.2-mm median diameter sand was specified to represent the sediment in the James Island region. Results of NE33 on sedimentation are shown in Figure B8, with the majority of material erosion or accretion from 1 to 2 cm, with maximum values exceeding 8 cm located close to the proposed access channel. Material deposition within the northern channel mouth was negligible, and the southern mouth shows approximately 1 cm of accretion. Note that maximum values of deposition and erosion occurred within regions of limitations in M2D that may affect the actual deposition pattern and rate. These limitations are described in the subsequent paragraph.

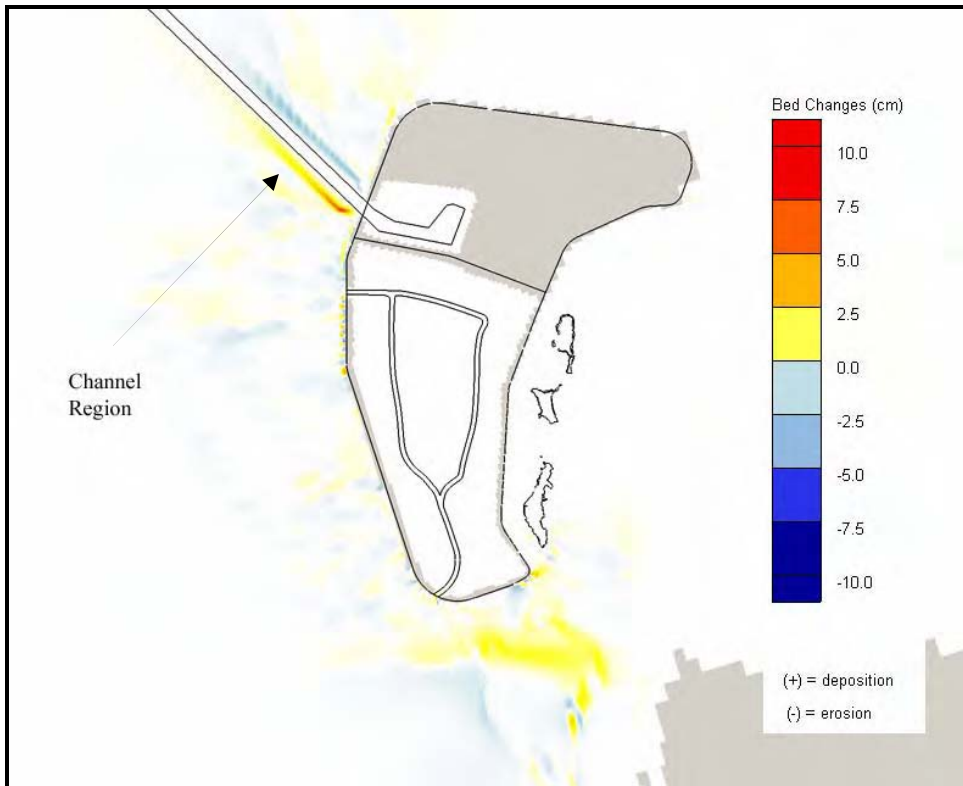


Figure B8. Alt JI-7 M2D sedimentation results

As described by ERDC as part of project training provided at the Mid-Bay Modeling Study Workshop, held 9-11 August 2005 in Baltimore, MD, this total-load version of M2D code (which allows most rapid simulations to be run) does not account for infilling of deep channels, as noted in the channel region indicated in Figure B8. Thus, the navigation channel leading to the turning basin within the upland part of the James Island alignment is not properly filled in, and no accretion is calculated within that channel toe. Sediment is calculated as removed from one channel side and deposited on the other, as noted in the figure with the north side of the channel eroding and depositing on the southern side of the channel. As a result, interpretation of sedimentation results must be made with care, observing patterns of deposition over the area surrounding James Island to determine regions of relative deposition or erosion.

Evaluation of Alternatives

For comparison, key locations established by ERDC were used to save data on maximum current speed and erosion/accretion in the modeled region of James Island. Table B1 lists the location of Points 1-16 in Maryland State Plane NAV83 Easting and Northing feet. Points 1-16 were chosen to provide an understanding of conditions surrounding the island, with additional detail in areas of concern at the tidal gut entrances, around the existing islands and within the interior of the island in the channel system. The key locations are shown in Figure B9.

Table B1
James Island Model Run Save Locations

Location	Easting, ft	Northing, ft
1	1,503,685.827	304,923.294
2	1,508,416.896	312,049.5079
3	1,500,881.824	320,596.2927
4	1,502,676.969	309,755.1837
5	1,501,389.862	304,992.7822
6	1,498,119.882	303,393.7336
7	1,498,537.27	306,209.4816
8	1,501,737.73	312,605.6759
9	1,498,258.99	313,127.0997
10	1,495,058.53	313,439.9606
11	1,495,291.995	316,450.1312
12	1,500,916.47	303,225.9514
13	1,501,402.231	304,382.5459
14	1,501,761.549	305,303.0184
15	1,500,937.008	304,818.5696
16	1,500,618.438	305,018.0446

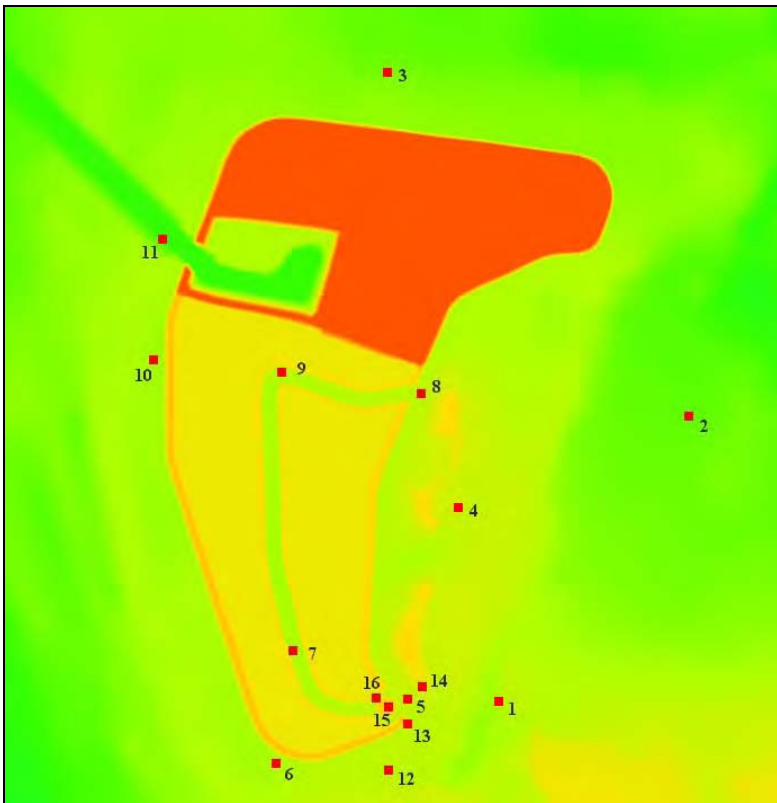


Figure B9. James Island key locations

Current Velocity Comparison

The behavior of the current for each alternative was as expected, with reasonable velocities for conditions in the nearby regions. Velocities were shown to have increased in the channel region to the southeast of the tip of James Island as a result of a narrower channel through which flow is diverted by the presence of the island. Velocity increases in other regions surrounding the island were slight, with no excessive changes as a result of the presence of the island. Table B2 presents the calculated maximum current speed at each of the 16 save key locations for each alternative modeled. Additional notes on individual configurations are as follows:

Alt JI-7. During NE33, current velocities within the mouths of the westward facing tidal guts were slightly greater than velocities in the mouths of the eastward-facing channel entrances in JI-8 and JI-9. Velocities quickly dissipated within the primary channel, showing only a 0.2-ft/sec increase over that of normal tidal velocities.

Alt JI-8. Similar to conditions found in JI-9; the only noticeable difference is a slight increase in velocity at the interior data collection locations, Points 7 and 9. Velocities differed by less than 0.1-ft/sec throughout the tidal gut.

Alt JI-9. Similar in comparison to JI-8; slight differences in velocities within the tidal gut, seen at Points 7 and 9, with a reduced channel velocity in comparison to that of JI-8.

Table B2 Calculated Maximum Current Speed (m/sec) at James Island			
Location	JI-7 - (NE33)	JI-8 - (Tide)	JI-9 - (Tide)
1	0.79	0.47	0.48
2	0.14	0.04	0.04
3	0.24	0.16	0.17
4	0.37	0.09	0.10
5	0.52	0.33	0.35
6	0.27	0.17	0.17
7	0.39	0.14	0.03
8	0.31	0.08	0.08
9	0.12	0.06	0.00
10	0.67	0.30	0.32
11	0.45	0.15	0.16
12	0.82	0.55	0.57
13	0.77	0.52	0.54
14	0.18	0.00	0.00
15	0.00	0.25	0.23
16	0.00	0.00	0.00

NOTE: A '0' velocity magnitude indicates the 'no-current' (dry) condition.

Sedimentation

Sedimentation was only calculated for Alt JI-7, modeled in M2D. Sediment transport was calculated over the span of time of the northeaster, determining typical conditions for the frequent strong storms that impact the Chesapeake region. Table B3 presents the bed elevation change at each of the 16 key locations for each alternative scenario modeled.

Alt JI-7. Small pockets of greater deposition or erosion are visible, although no excessive movement of material appeared to occur. Sedimentation patterns do not appear to show a tendency to deposit or erode material at channel entrances or along channel lengths.

Alt JI-8. Sedimentation was not calculated within the ADCIRC model for Alt JI-8.

Alt JI-9. Sedimentation was not calculated within the ADCIRC model for Alt JI-9.

Table B3
Calculated Bed Elevation Change (cm) at James Island

Location	JI-7 - (NE33)	JI-8 - (Tide)	JI-9 - (Tide)
1	2.38	N/A	N/A
2	5.68	N/A	N/A
3	4.81	N/A	N/A
4	1.00	N/A	N/A
5	1.40	N/A	N/A
6	2.31	N/A	N/A
7	2.15	N/A	N/A
8	1.73	N/A	N/A
9	1.57	N/A	N/A
10	3.16	N/A	N/A
11	7.46	N/A	N/A
12	1.66	N/A	N/A
13	1.63	N/A	N/A
14	-0.54	N/A	N/A
15	-0.77	N/A	N/A
16	-0.73	N/A	N/A

NOTE: Positive values indicate accretion, negative values indicate erosion.

Summary

In summary, modeling of the three additional alternatives determined the feasibility and performance of a westward-facing tidal gut configuration, as well as the probable effects of varying channel width. Results from the Alt JI-7 test conditions under a strong northeaster did not show adverse hydrodynamic or sedimentation impacts. Deposition patterns did not suggest a tendency to deposit or erode material at the entrances to the tidal guts – the primary concern of such an arrangement. Storm effects were seen to be reduced in the interior regions of the island, placing only a small section at risk of the increased current and wave effects, compared to the eastward-facing equivalents. Results from Alts JI-8 and JI-9 configurations show little difference in velocities in comparison to the similar Alts JI-1, JI-4, JI-5, and JI-6 configurations. The difference in channel width at this scale does not seem to significantly impact the channel velocities of each design. Additional testing would be required to verify the volumetric flow capacities of each design and determine the appropriate flow to flush the system.

Appendix C

Evaluation of Additional Barren Island Alternatives

During preparation of the “Mid-Chesapeake Bay Island Ecosystem Restoration Integrated Feasibility Report and Environmental Impact Statement,” the functional performance of the proposed breakwater south of the existing Barren Island was evaluated in terms of its capability to reduce wave heights to levels tolerable for submerged aquatic vegetation (SAV). An overtopping analysis was performed to determine the crest elevation for the breakwater structure required to reduce wave heights. Crest heights of 2, 4, 6, and 8 ft were evaluated. Available literature on SAV indicated that the tolerable wave height for SAV ranges from 0-2 m (0-6.6 ft) with an average of 1 m (3.3 ft). The preliminary results for the overtopping analysis indicate that a crest height of +4 ft mean lower low water (mllw) would provide SAV protection to the limiting tolerable wave height of 3.3 ft for just over a 30-year return period storm. A structure of +6 ft mllw would reduce wave height to tolerable levels for up to a 50-year return period event. These preliminary results were based solely on an analysis of overtopping, which is considered to be the dominant factor controlling the transmitted wave for submerged structures, as well as local waves generated on the eastern side of the project.

To further evaluate the performance of the southern breakwater alternatives, a preliminary investigation of wave transmission through the proposed structures and gaps in proposed segmented structures was conducted. Six alternative designs, Alts BI-1 through BI-6, for restoration and modification of Barren Island were defined in close coordination with the Maryland Port Administration (MPA) and the U.S. Army Engineer District, Baltimore. Numerical models were then applied by the U.S. Army Engineer Research and Development Center (ERDC), Coastal and Hydraulics Laboratory (CHL), and the results analyzed for preliminary evaluation of alternative designs and their impacts on the mainland shoreline, adjacent Federal and private navigation channels, and neighboring SAV.

Study Approach

ERDC-CHL conducted the numerical modeling and evaluation of six alternative alignments at the Barren Island restoration site (see main text of this report). Their study had the following goals, with emphasis on storm conditions that would produce the maximum change in physical environmental conditions at the sites:

- a. Perform wave modeling for Barren Island.
- b. Perform circulation modeling in combination with wave modeling for Barren Island to assess alternatives.
- c. Investigate sediment transport patterns at and around Barren Island, including sediment shoaling at neighboring navigation channels.
- d. Evaluate engineering merits on environmental impacts of alternative island alignments.

Andrews, Miller & Associates, Inc. (AMA) reviewed the results of the modeling conducted by ERDC with the objective of developing two additional alternatives and then conducting circulation and wave modeling for those alternatives for comparison with Alts BI-1 through BI-6. Of particular interest is an evaluation of the proposed breakwater south of the existing island in terms of the capability to reduce wave heights and tidal currents to levels tolerable for survivability of SAV.

Evaluation of Barren Island Alts BI-1 to BI-6

The proposed Barren Island restoration emphasizes protection of the existing island and SAV east and south of the island though the construction of new breakwaters and raising of the existing shore protection structure. The design for the protection of the existing island includes a new northern breakwater or sill at + 4 ft mllw (3,840 ft long), a raised existing northwestern breakwater at +4 ft mllw (4,900 ft long), and a new western breakwater at +4 ft mllw (5,915 ft long).

The design for additional protection of SAV includes a new southern breakwater that extends southeastward from the Island into the bay. The restoration is expected to provide improved sheltering to the Honga River Channel that is located to the north and northeast of Barren Island. Six alternatives with four southern breakwater configurations and two different southern breakwater crest elevations were investigated by ERDC in the present study (Table C1).

This chapter focuses on an evaluation of the proposed breakwater south of the existing island for each alternative in terms of the capability to reduce wave heights and tidal currents to levels tolerable for SAV.

Table C1
Barren Island Alternatives

Alternative	Description
BI-1	8,166-ft-long south breakwater at +6 ft mllw.
BI-2	5,915-ft-long south breakwater at +6 ft mllw.
BI-3	8,166-ft-long south breakwater at +4 ft mllw.
BI-4	5,915-ft-long south breakwater at +4 ft mllw.
BI-5	8,166-ft-long south breakwater at +4 ft mllw with 400-ft segments and 200-ft gaps.
BI-6	8,166-ft-long south breakwater at +6 ft mllw with 500-ft segments and 100-ft gaps.

SAV History at Barren Island

SAV has been present in the Barren Island area, particularly east of the island between the island and the mainland. There has been considerable fluctuation in the areal extent of the SAV in recent years, as shown in Figure C1. The data in Figure C1 were provided by the Virginia Institute of Marine Science (VIMS) from their annual SAV surveys in which they map the area of SAV by U.S. Geological Survey quadrangle map. Comparison of Figures C2 to C4 shows the most recent fluctuation in SAV in the Barren Island area with the greatest area of higher density SAV occurring in 2002 and the least area in 2004.

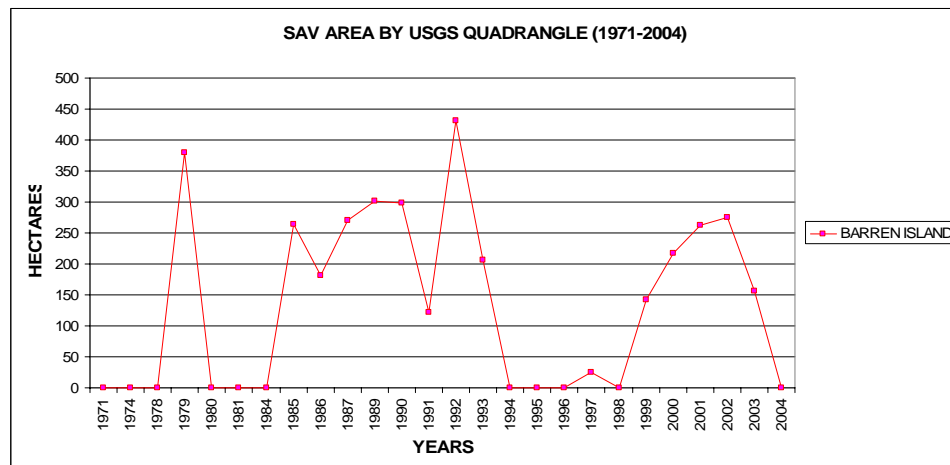


Figure C1. Estimated Barren Island SAV areal extent 1971–2004

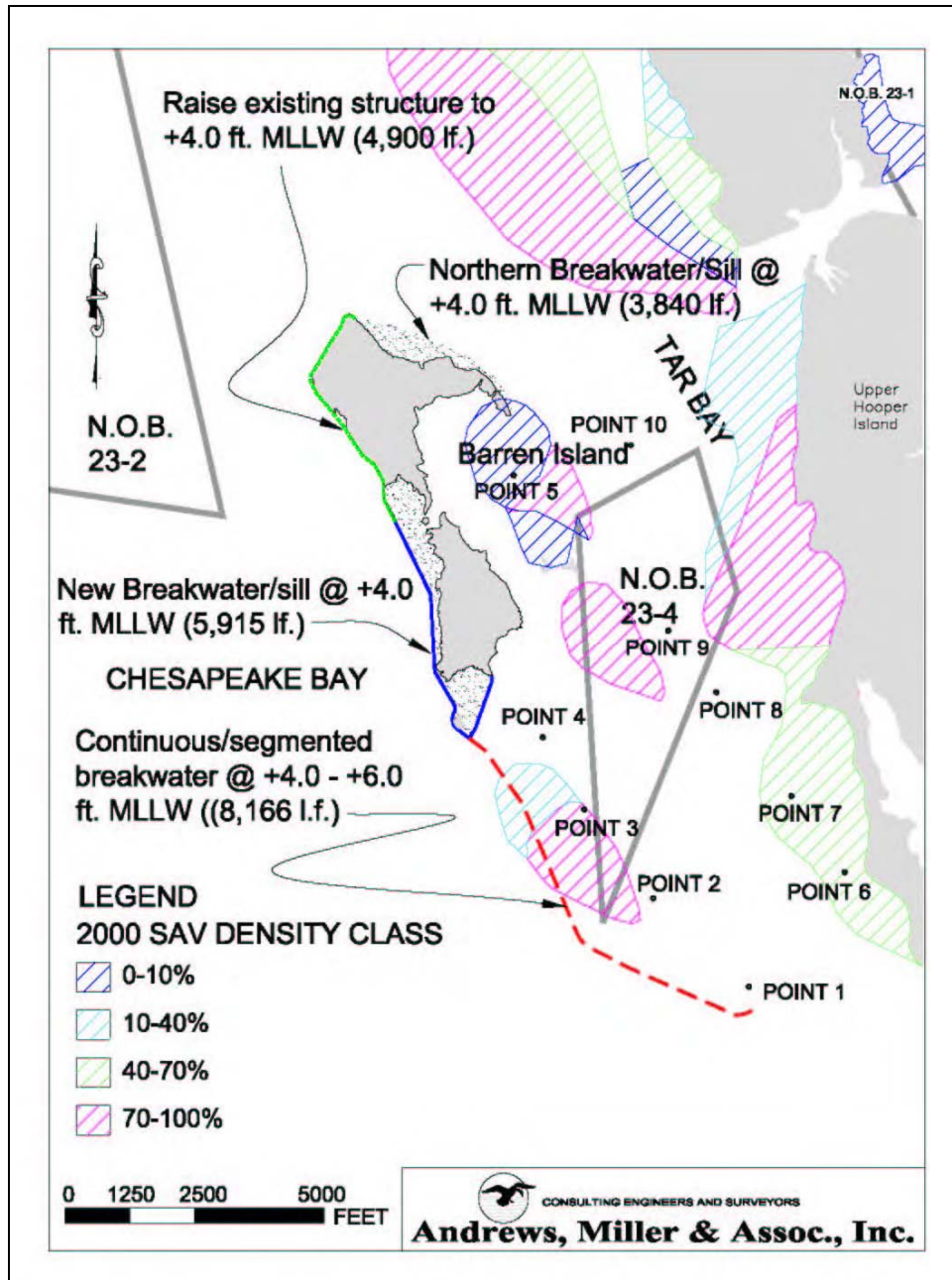


Figure C2. Barren Island SAV in 2000 (VIMS)

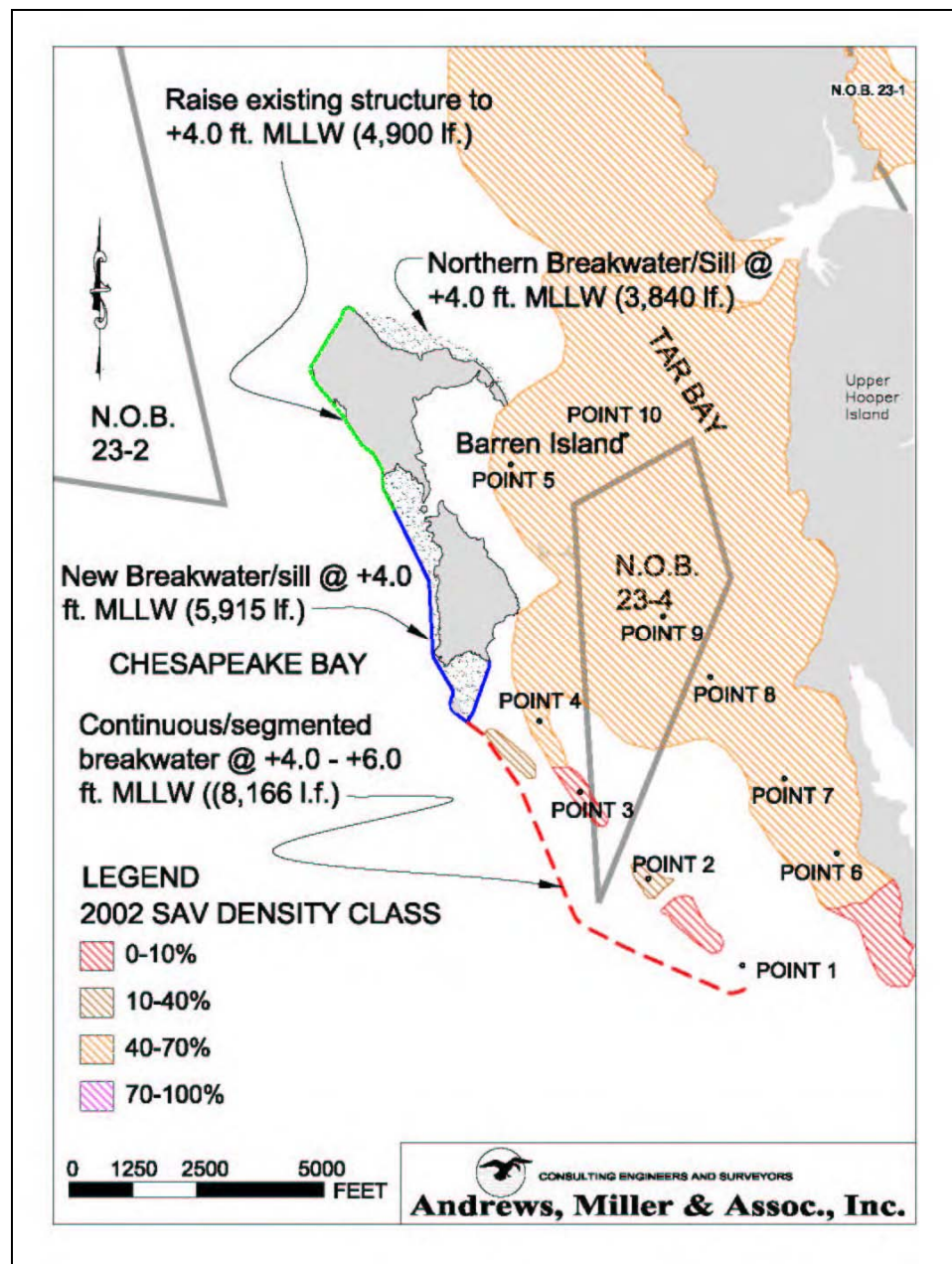


Figure C3. Barren Island SAV in 2002 (VIMS)

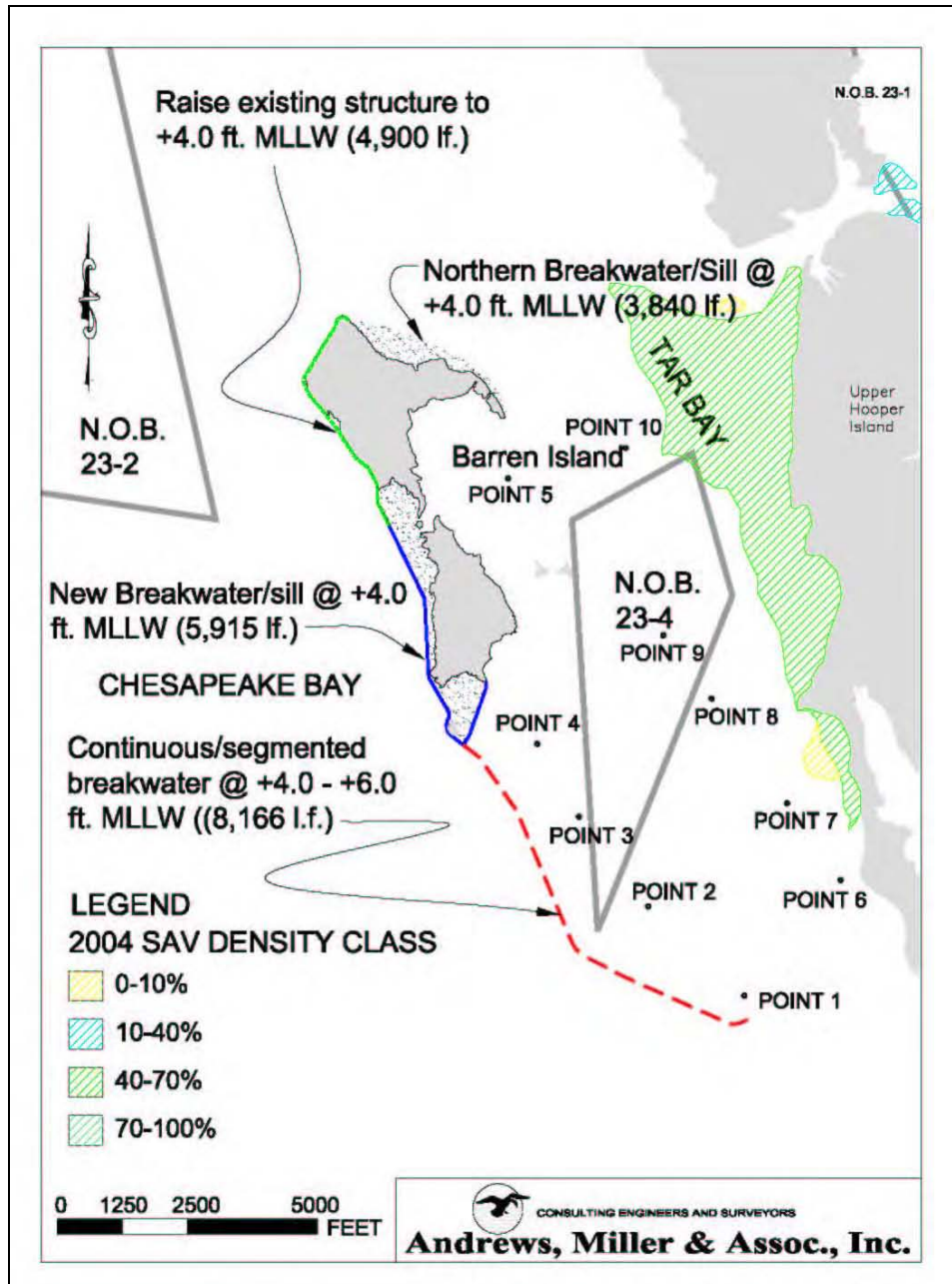


Figure C4. Barren Island SAV in 2004 (VIMS)

SAV Tolerance

One of the objectives of the Barren Island project is to enhance the conditions for SAV survivability east of the island. Research has indicated that SAV is affected by a number of environmental factors. Perhaps one of the most important parameters to SAV success is the provision of an area that limits the amount of tidal current velocity, wave height, and sedimentation to tolerable levels. These factors are discussed next. Quantitative data on the tolerable levels of these parameters are limited, and only general guidelines exist. Selected guidelines are discussed in the following paragraphs.

Literature search

A literature search was conducted to find available guidelines for the hydrodynamic threshold for SAV tolerance in Chesapeake Bay to wave energy and tidal current velocity. The most pertinent information is presented here.

A discussion of parameters, other than the established SAV light requirements, addressed waves, currents, tides, sediment organic content, grain size and contaminants and their influence on the presence or absence of SAV in a certain area (Chesapeake Bay Program 2000)¹.

Excerpts from this discussion (Chesapeake Bay Program 2000) are as follows:

“Current Velocity SAV Habitat Requirements. From the positive and negative effects of the reduced current velocities found in SAV beds, it can be concluded that these plants could benefit from intermediate current velocities (Boeger 1992; Koch and Gust 1999; Merrell 1996; Koch 1999). Extremely low water flows could increase the blade diffusion boundary layer thickness as well as the accumulation of organic matter in the sediment leading to carbon starvation or death due to high phytotoxin concentrations in the sediment, respectively. In contrast, extremely high water flow has the potential to 1) increase drag above a critical value where erosion of the sediment and plants occurs, 2) reduce light availability through resuspension of sediment and self-shading and 3) decrease the accumulation of organic matter, leading to reduced nutrient concentration in the sediments. A literature review revealed that 1) the range of current velocities tolerated by marine SAV species lies between approximately 0.2 ft/sec. (5 cm s^{-1}) and 3.3 ft/sec (100 cm s^{-1}).

Survival of SAV in high current velocity environments may be possible if the development of seedlings occurred under conditions of slow current velocity in space (e.g., a protected cove) or time (e.g., a low water discharge period). Once a bed is established under such conditions, it can expand into adjacent areas with higher currents due to the reduced currents at the edge of the bed or persist during times of higher water flow. Therefore, the stage of the plants (for example, seeds, seedlings, vegetative shoots, reproductive shoots) also needs to be taken into account when considering if current velocity is above or below the

¹ References cited in this appendix are contained in the reference section of the main text of this report.

established requirement for growth and distribution. Based on the literature review presented here, no data are available on the current velocity requirements of plants other than those found in well-established beds. In summary, intermediate current velocities between 0.3 ft/sec (10 cm s^{-1}) and 3.3 ft/sec (100 cm s^{-1}) are needed to support the growth and distribution of healthy marine SAV beds. If currents are above or below these critical levels, the feedback mechanisms in the system may become imbalanced and possibly lead to the decline or even complete loss of the vegetation. Although some of the feedback mechanisms between SAV beds and current velocity involve light availability through the effects of resuspension of sediments, selfshading, and epiphytic growth, extreme currents alone can limit the growth of SAV. Therefore, current velocity should be considered as a key SAV habitat requirement.

TABLE VI-1. Minimum and maximum current velocities required for SAV growth and distribution.

Minimum current velocities required to saturate photosynthesis		
Current	Species	Source
$> 0.04 \text{ cm s}^{-1}$	<i>Potamogeton pectinatus</i> *	Madsen and Sondergaard 1983
$> 0.08 \text{ cm s}^{-1}$	<i>Callitricha stagnalis</i>	Westlake 1967
$> 0.5 \text{ cm s}^{-1}$	<i>Ranunculus pseudofluitans</i>	Westlake 1967
$> 3 \text{ cm s}^{-1}$	<i>Zostera marina</i>	Koehl and Worcester 1991
$> 5 \text{ cm s}^{-1}$	<i>Ranunculus perriculatus</i>	Werner and Wise 1982
$> 5 \text{ cm s}^{-1}$	<i>Thalassia testudinum</i>	Koch 1994
$> 13 \text{ cm s}^{-1}$	<i>Cymodocea nodosa</i>	Koch 1994
$> 16 \text{ cm s}^{-1}$	<i>Z. marina</i>	Fonseca and Kenworthy 1987

Maximum currents at which the following species occur		
Current	Species	Source
$< 7 \text{ cm s}^{-1}$	<i>Vallisneria americana</i>	Merrell 1996
$< 45 \text{ cm s}^{-1}$	<i>Ranunculus perriculatus</i>	Werner and Wise 1982
$< 50 \text{ cm s}^{-1}$	<i>Zannichellia palustris</i>	Sculthorpe 1967
$< 50 \text{ cm s}^{-1}$	<i>Z. marina</i>	Conover 1964
$< 120 \text{ cm s}^{-1}$	<i>Z. marina</i>	Scoffin 1970
$< 150 \text{ cm s}^{-1}$	<i>Z. marina</i>	Fonseca <i>et al.</i> 1982
$< 180 \text{ cm s}^{-1}$	<i>Z. marina</i>	Phillips 1974

* Indicates species for which leaf polarity has been confirmed.

Effects of High Wave Energy. The impact of high wave energy on SAV can be direct or indirect. The direct impact of waves on SAV can be seen when waves (in combination with currents) erode the edges of an SAV bed (Clarke 1987) or when portions of the plants are removed by storm-generated (Thomas *et al.* 1961; Eleuterius and Miller 1976;

Rodriguez et al. 1994; Dan et al. 1998) or boat generated waves (Stewart et al. 1997).

Indirect consequences of wave energy in SAV beds include sediment resuspension, changes in sediment grain size, mixing of the water column and epiphytic growth. If the capacity of an SAV bed to attenuate waves is reduced, for example, due to a reduction in shoot density because of clam dredging or eutrophication, the underlying sediment will become more vulnerable to erosion, and higher concentrations of suspended sediment particles can be expected in the water. Wave attenuation and sediment resuspension in vegetated areas depend on the water levels above the plants.

In areas of high wave exposure, sediments are coarser, which leads to lower nutrient concentration in the sediment and, consequently, lower root biomass (Idestam-Almquist and Kautsky 1995). By contrast, the above-ground biomass of *Potamogeton pectinatus* depends directly on wave exposure; shoots are shorter in areas with high wave exposure than in areas with low wave exposure (Idestam-Almquist and Kautsky 1995). In Chesapeake Bay, shore erosion (caused by wave action) contributes 13 percent of the total suspended matter in the upper Bay and 52 percent in the middle Bay (Biggs 1970). Perhaps, before the decline of SAV in this area, SAV protected the coastlines from the direct impact of waves.

In high wave exposure areas, where sediments are constantly being shifted and grain size may be skewed toward coarser particles, SAV may not be able to become established due to the balance between the anchoring capacity of the roots and the drag exerted on the leaves. High wave exposure also leads to reduced light availability due to increased sediment resuspension.”

A summary of quantitative and qualitative descriptions of wave tolerance for various species is shown in the following two tables (Chesapeake Bay Program 2000):

TABLE VI-3. Quantitative and qualitative descriptions of wave tolerance for Chesapeake Bay species.

Species	Wave Tolerance	Source
Canopy formers		
<i>Myriophyllum spicatum</i>	Wave limited	Rawls (1975), Stewart <i>et al.</i> 1997
<i>Zannichellia palustris</i>	Wave limited	Stevenson and Confer 1978
Flowering structures of <i>Ruppia maritima</i>	Wave sensitive	Joanen and Glasgow 1965
Meadow formers		
<i>Zostera marina</i>	2 m waves	Dan <i>et al.</i> 1998
<i>Potamogeton pectinatus</i>	Wave tolerant	Hannan 1967
<i>Vallisneria americana</i>	More wave tolerant than <i>Myriophyllum</i>	Stewart <i>et al.</i> 1997

TABLE 2. Summary of physical and chemical factors defining habitat constraints for submersed aquatic plants.

Factor	Description	Constraint	Submersed Plants
Water Movement	Minimum velocities (cm s ⁻¹)	0.04-5	Freshwater plants
		3-16	Seagrasses
	Maximum velocities (cm s ⁻¹)	7-50	Freshwater plants
		50-180	Seagrasses
Wave Tolerance	Waves 0-1 m	Limited growth	Canopy formers (e.g., <i>Myriophyllum spicatum</i> , <i>Ruppia maritima</i> flowers)
	Waves >2 m	Tolerant growth	Meadow formers (e.g., <i>Zostera marina</i> , <i>Vallisneria americana</i>)
Sediments	Grain size (% fines, <64 µm)	2-62	Freshwater plants
		0.4-30	Seagrasses
	Organic matter (%)	0.4-12	Seagrasses and freshwater plants
Porewater Sulfide	(mM)	<1	Healthy plants
		>1	Reduced growth

UMCES coordination

The University of Maryland Center for Environmental Studies (UMCES) at Horn Point, Cambridge, MD, has conducted studies regarding the restoration of SAV in Chesapeake Bay. Dr. Evamaria Koch of UMCES has been investigating the impacts of waves and currents on SAV. Although absolute wave and current exposure limits for eelgrass have not yet been established, Dr. Koch indicated that based on her field and laboratory experience, she estimated the threshold for SAV tolerance would be a wave height ranging from 1.3 to 2.0 ft with a wave period of about 3.0 sec, and tidal current velocities of about 2.5 to 3.0 ft/sec during typical conditions. However, Dr. Koch indicated that waves and currents may not adversely affect SAV until the sediment in which the SAV is rooted starts to erode. Consequently, higher waves and stronger currents may be tolerated in areas where the bed material is coarser and more resistant to erosion. Dr. Koch also indicated that higher water temperature can adversely impact SAV in areas that have restricted tidal circulation. Dr. Koch is actively investigating the tolerance of SAV to tidal currents and waves. Her investigations include

physical modeling (tidal flumes) and field experiments. Additional investigations to evaluate the effect of wave period and duration on SAV are necessary.

Additional investigation is required to quantify the conditions (and combinations of conditions) tolerated by SAV. Based on a literature search and coordination with UM CES, a summary of preliminary guidelines for the thresholds for SAV tolerance is presented in Table C2. Based on this information, the preliminary SAV tolerance threshold is estimated to be 1 m (3.28 ft).

Table C2
SAV Tolerances

	Literature	UMCES
Tidal Current (ft/sec)	0.3 – 3.3	2.5 – 3.0
Wave Height (ft)	0 – 6.4	1.3 – 2.0

Alts BI-1 to BI-6 Performance

To evaluate the conditions provided by each of the proposed alternative plans, a comparison of the modeling data compiled by ERDC for Alts BI-1 through BI-6 was conducted, with focus on current velocity and wave height. To facilitate this comparison, 10 points were selected for output data from the modeling, as shown in Figure C5. These points are located throughout the SAV areas as well as the natural oyster bar east of Barren Island.

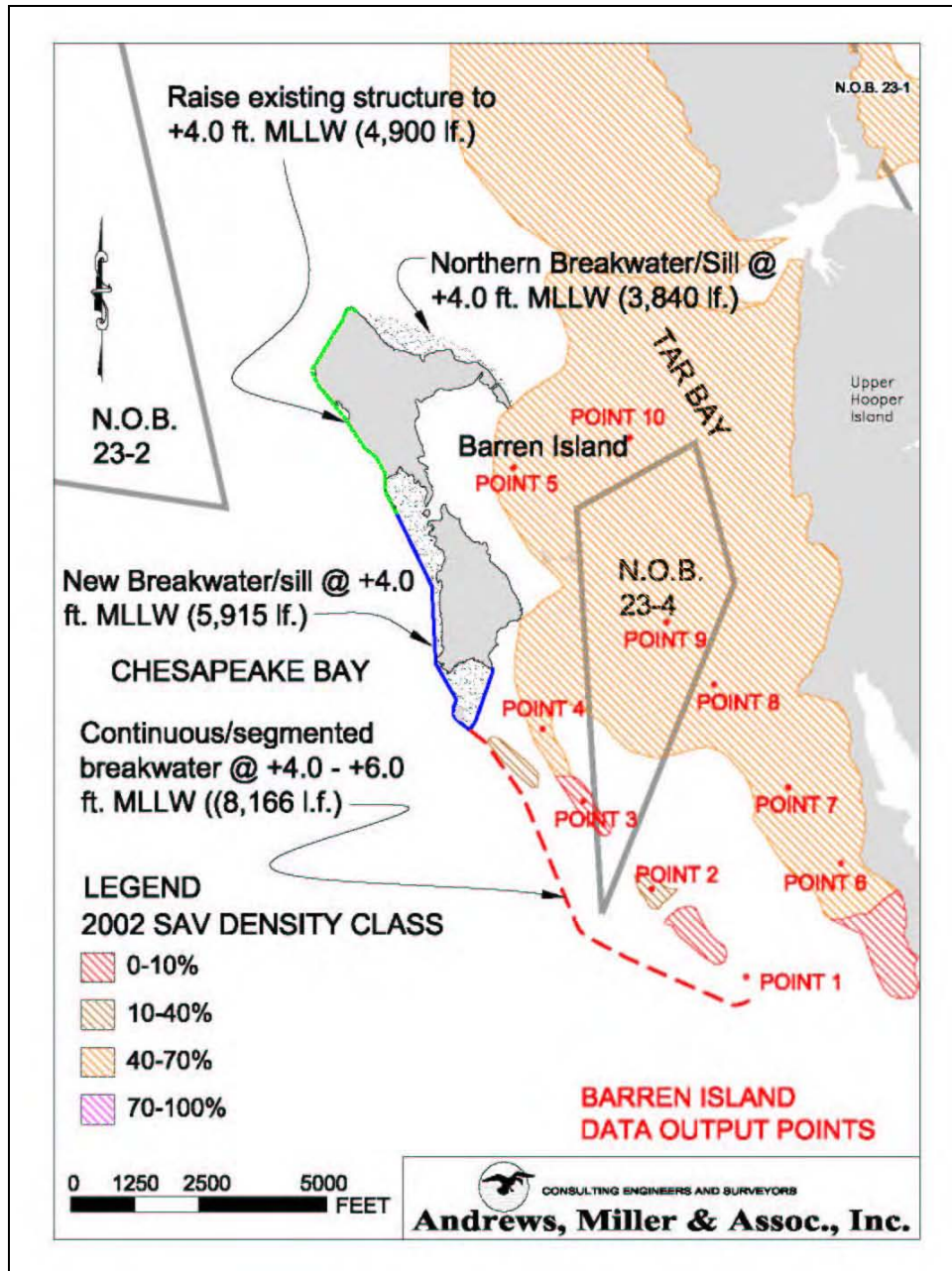


Figure C5. Modeling data output points

The results of the modeling by ERDC for Alts BI-1 through BI-6, as described in Table C3, were compiled into an alternatives evaluation matrix. This matrix is presented in Table C4 and shows the maximum tidal current velocity, V_{max} , and the maximum wave height, H_{max} , for each alternative, existing conditions and future conditions for each of the four storms at each of the 10 data output points.

Table C3
Barren Island Alternatives

Alternative	Description
BI-1	8,166-ft-long south breakwater at +6 ft mllw.
BI-2	5,915-ft-long south breakwater at +6 ft mllw.
BI-3	8,166-ft-long south breakwater at +4 ft mllw.
BI-4	5,915-ft-long south breakwater at +4 ft mllw.
BI-5	8,166-ft-long south breakwater at +4 ft mllw with 400 ft segments and 200 ft gaps.
BI-6	8,166-ft-long south breakwater at +4 ft mllw with 500 ft segments and 100 ft gaps.

The data in Table C4 indicate that the maximum current velocities generally were produced during Hurricane Hazel, followed closely by Hurricane Isabel, and then NE20 and NE33. The maximum wave heights were produced during Hurricane Isabel, followed closely by Hurricane Hazel, and then NE20 and NE33. For the evaluation of the performance of the proposed alternative plans, Hurricane Hazel and NE20 were selected because these events on average appear to have produced the most significant hydrodynamic conditions.

Table C4
Barren Island Alternative Plan Evaluation Matrix

	Point 1		Point 2		Point 3		Point 4		Point 5		Point 6		Point 7		Point 8		Point 9		Point 10	
	H _{max} (ft)	V _{max} (ft/sec)																		
Alternative BI-1																				
NE20	0.8	1.9	1.3	1.1	1.3	1.1	1.0	0.9	0.4	0.8	1.3	1.4	1.1	1.3	1.0	1.3	0.8	1.5	1.5	1.1
NE33	0.4	2.3	0.5	1.3	0.3	1.2	0.1	0.8	0.4	0.9	0.3	0.9	0.4	1.3	0.5	1.4	0.6	1.2	1.2	1.4
Isabel	1.8	3.0	1.9	1.9	1.7	2.4	1.7	2.5	1.3	3.0	2.3	3.1	1.9	3.2	1.6	2.8	1.6	2.7	1.3	3.1
Hazel	1.4	3.3	1.2	3.2	1.2	3.3	1.2	3.3	0.9	3.3	1.8	3.4	1.4	3.3	1.2	3.3	1.1	3.3	0.9	3.3
Alternative BI-2																				
NE20	2.8	1.1	2.3	1.1	1.4	1.0	1.0	0.7	0.4	1.0	2.4	1.5	2.5	1.1	1.6	1.2	1.2	1.5	1.5	1.3
NE33	2.4	0.8	0.8	1.4	0.3	1.1	0.1	0.7	0.4	0.5	1.7	0.9	1.2	1.3	0.5	1.0	0.6	1.5	1.2	1.4
Isabel	4.5	3.1	4.1	2.4	1.9	2.6	1.7	2.5	1.4	3.0	3.8	3.0	4.3	3.0	3.1	2.8	2.4	2.7	1.7	3.2
Hazel	4.1	3.3	3.5	3.3	1.5	3.3	1.2	3.3	1.1	3.3	3.5	3.4	3.7	3.3	2.7	3.3	2.0	3.3	1.3	3.3
Alternative BI-3																				
NE20	0.9	1.8	1.0	1.0	1.0	1.0	0.9	0.8	0.4	0.8	1.0	1.4	0.9	1.3	0.8	1.2	0.9	1.5	1.5	1.1
NE33	0.4	1.0	0.5	0.5	0.4	0.5	0.5	0.4	0.4	0.5	0.4	0.7	0.5	0.5	0.5	0.6	0.6	0.6	1.2	0.7
Isabel	2.4	3.3	2.5	2.7	2.3	2.7	2.2	2.5	1.4	3.1	2.5	3.1	2.3	3.2	2.2	2.9	2.2	2.7	1.5	3.1
Hazel	1.8	3.3	2.0	2.9	1.8	3.3	1.7	3.2	1.1	3.3	2.0	3.4	1.8	3.3	1.7	3.3	1.7	3.3	1.2	3.3
Alternative BI-4																				
NE20	2.8	1.2	2.4	1.4	1.0	1.3	0.9	0.9	0.5	0.9	2.3	1.5	2.6	1.5	1.6	1.5	1.2	1.7	1.5	1.2
NE33	2.4	0.8	0.8	1.5	0.4	1.2	0.5	0.8	0.4	0.5	1.8	0.9	1.2	1.3	0.5	1.0	0.6	1.5	1.2	1.4
Isabel	4.5	3.2	4.2	2.9	2.4	2.7	2.2	2.4	1.5	2.9	3.7	3.1	4.4	3.1	3.3	2.8	2.7	2.7	1.8	3.1
Hazel	4.1	3.3	3.7	3.3	1.9	3.3	1.7	3.3	1.1	3.3	3.5	3.4	3.8	3.3	2.8	3.3	2.3	3.3	1.4	3.3
Alternative BI-5																				
NE20	1.2	1.3	1.6	1.1	1.5	1.2	1.3	1.3	0.4	1.0	1.4	1.3	1.5	1.4	1.4	1.5	1.3	1.8	1.7	1.3
NE33	0.7	1.1	1.0	1.3	0.9	1.6	0.8	1.8	0.3	0.6	0.8	0.8	0.9	1.2	0.7	2.1	0.7	1.5	1.3	1.4
Isabel	2.3	2.7	2.9	2.9	3.0	2.7	2.6	2.5	0.5	2.9	2.7	2.7	2.8	3.0	2.6	2.7	2.5	2.7	1.6	3.1
Hazel	1.8	3.3	2.4	3.3	2.6	3.3	2.2	3.3	0.4	3.3	2.3	3.3	2.4	3.3	2.2	3.3	2.1	3.3	1.4	3.3
Alternative BI-6																				
NE20	1.0	1.4	1.4	1.0	1.6	1.2	1.5	1.3	0.6	1.0	1.2	1.5	1.3	1.5	1.3	1.8	1.7	1.3	1.3	
NE33	0.7	1.4	1.1	1.4	0.9	1.7	0.8	1.7	0.5	0.8	0.9	1.0	0.9	1.5	0.7	2.1	0.7	1.6	1.3	1.3
Isabel	2.5	2.8	2.9	1.8	3.0	2.0	2.9	3.3	0.5	3.1	2.7	2.7	3.0	2.7	2.6	2.6	2.6	2.6	1.6	3.3
Hazel	2.0	3.2	2.3	2.3	2.6	2.5	2.5	3.3	0.4	3.3	2.3	3.4	2.3	3.3	2.2	3.3	2.2	3.3	1.3	3.3
Existing																				
NE20	3.1	1.1	3.3	1.3	3.0	1.4	2.8	1.7	0.6	1.0	2.5	2.1	2.8	1.4	2.8	1.6	2.6	1.9	1.6	1.3
NE33	2.7	0.7	2.9	0.9	2.7	1.2	2.4	1.4	0.6	0.5	2.2	1.3	2.4	1.0	1.9	1.3	1.6	1.9	1.3	1.5
Isabel	4.6	3.3	5.1	3.3	4.8	3.1	4.7	2.8	0.6	2.9	3.7	3.1	4.5	3.2	4.7	2.9	4.5	2.7	2.4	2.9
Hazel	4.1	3.3	4.5	3.3	4.3	3.3	4.1	3.3	0.6	3.3	3.5	3.4	4.1	3.3	4.1	3.3	3.9	3.3	2.2	3.3
Future																				
NE20	3.2	1.1	3.4	1.2	3.1	1.3	2.8	1.3	2.5	1.3	2.5	1.3	2.8	1.4	2.8	1.3	2.7	1.6	2.4	1.1

For evaluation, the average of the maximum current velocities and the wave heights for Points 6-9, which are located in the historic SAV growth area, were compared with the existing condition and Alts BI-1 - BI-6 as shown in Figure C6 and Figure C7, respectively.

As shown in Figure C6, the average of the current velocities at Points 6-9 during NE20 for existing conditions is 1.7 ft/sec as compared to approximately 1.3 ft/sec for Alts BI-1 - BI-3, and 1.5 ft/sec for Alts BI-4 - BI-6. With reference to the preliminary current velocity guidelines for SAV tolerance, the existing conditions velocities and the velocities with the alternative plans for NE20 would not be expected to exceed the SAV tolerable conditions.

For Hurricane Hazel, the average of the current velocities at Points 6-9 during the storm for existing conditions as well as for Alts BI-1 - BI-6 is 3.3 ft/sec. During this level of storm, it is apparent that the alternative plans have a negligible impact on the current velocities. These existing-conditions velocities and the velocities with the alternative plans for the Hurricane Hazel event are at the upper limit of the SAV tolerable conditions.

As shown in Figure C7, the average of the wave heights at Points 6-9 during NE20 for existing conditions is 2.7 ft as compared to approximately 1.0 ft for Alts BI-1 and BI-3; 1.9 ft for Alts BI-2 and BI-4; and 1.4 ft for Alts BI-5 and BI-6. Given the preliminary wave height guidelines for SAV tolerance, the existing conditions wave heights exceed the upper limit of the SAV tolerant conditions. The wave heights with the alternative plans for NE20 do not exceed the SAV tolerable conditions. Alts BI-1 and BI-3 result in the lowest wave heights with Alts BI-2 and BI-4 with the shortened south breakwater result in the highest wave heights for NE20. The wave heights with Alts BI-5 and BI-6 with the segmented south breakwater are about midway between the other alternatives.

The average of the wave heights at Points 6-9 during Hurricane Hazel for the existing condition is 3.9 ft as compared to approximately 1.6 ft for Alts BI-1 and BI-3; 3.0 ft for Alts BI-2 and BI-4; and 2.2 ft for Alts BI-5 and BI-6. With reference to the preliminary wave height guidelines, the existing conditions wave heights exceed the threshold of the SAV tolerable conditions and the wave heights with all of the alternative plans for the storm event are below the SAV tolerance conditions; particularly for Alts BI-1, BI-2, BI-5, and BI-6.

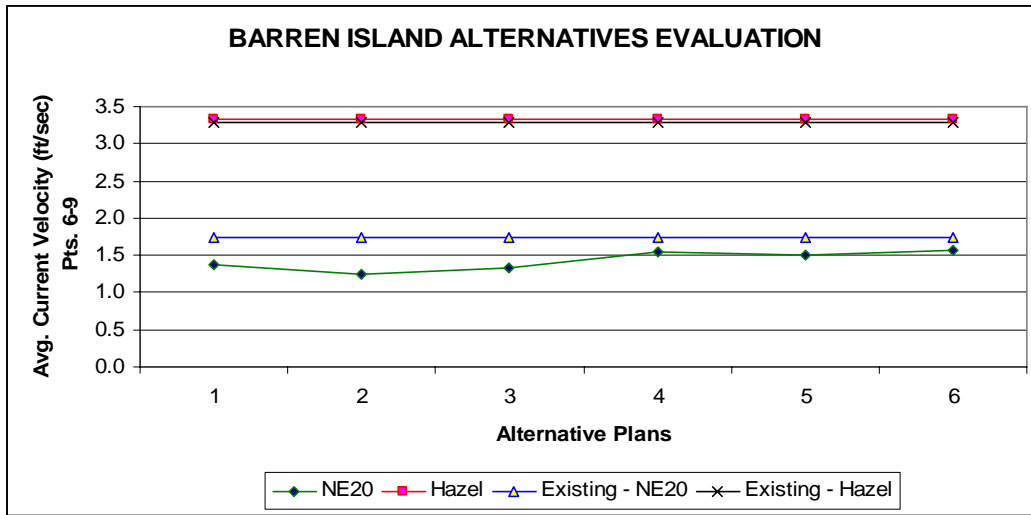


Figure C6. Average calculated maximum current velocity in SAV area (Points 6-9)

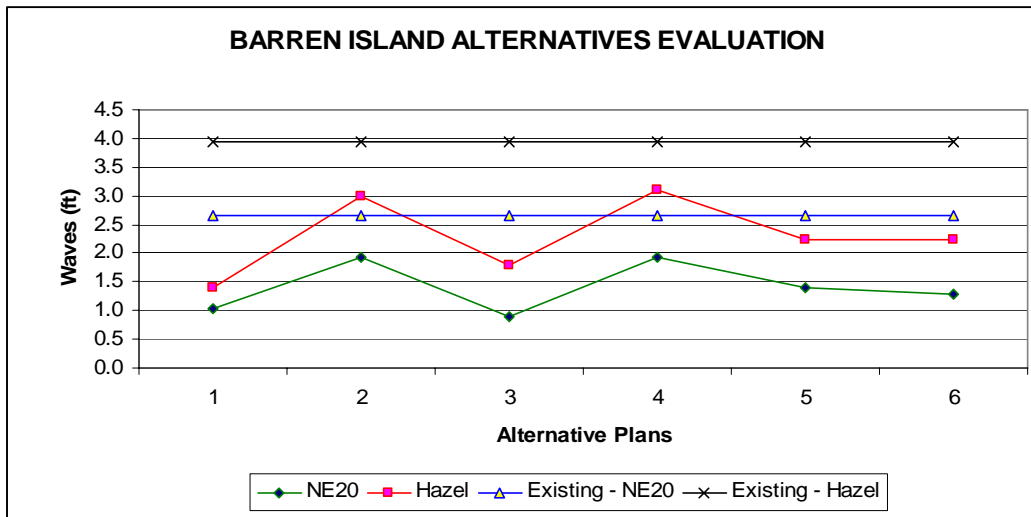


Figure C7. Average calculated maximum wave height in SAV area (Points 6-9)

In general, there appears to be little difference in the maximum current velocities between alternatives and the existing-condition velocities. Based on the preliminary guidelines for SAV tolerance, the maximum velocities for the evaluated alternatives are not sufficient to adversely impact the SAV in the area.

Because neither the maximum current velocities nor the maximum wave heights during the representative extreme storms evaluated appear to be significant enough in magnitude for Alt BI-5 and Alt BI-6 (with a segmented south breakwater) to adversely impact SAV in the primary SAV area, Points 6-10, (based on the preliminary tolerance guidelines), further consideration should be given to segmented breakwater alternatives; including evaluation of the wave and current conditions closer to the breakwater gaps. Segmented breakwaters could result in substantial construction cost savings as opposed to a continuous breakwater. The segmented breakwaters would also promote circulation in the SAV area and a reduced potential for adverse water temperature increases in that area.

Accordingly, two additional alternatives were developed to further investigate the impacts of segment lengths and gap widths between the segments, discussed next.

Development and Modeling of Alts BI-7 and BI-8

Based on the evaluation of the performance of Alts BI-1 through BI-6, it was decided that further consideration should be given to segmented breakwater alternatives because substantial construction cost savings could be realized in comparison with a continuous breakwater, as well as other potential environmental benefits including enhanced current circulation and reduced water temperature in the SAV area. Two of the initial modeling simulations incorporated segmented breakwaters, Alt BI-5 (segment length = 400 ft and gap width = 200 ft) and Alt BI-6 (segment length = 500 ft and gap width = 100 ft). To further investigate the impacts of segment lengths and gap widths between the segments, two additional alternatives were developed. These alternatives are described in Table C5 and shown in Figures C8 and C9.

Table C5
Barren Island Alternatives

Alternative	Description
BI-7	8,166-ft-long south breakwater at +4 ft mllw with 600-ft segments and 300-ft gaps.
BI-8	8,166-ft-long south breakwater at +4 ft mllw with 600-ft segments and 200-ft gaps.

Alt BI-7. This alternative was developed to evaluate the impact of increased breakwater segment lengths (600 ft) and larger gaps between the segments (300 ft).

Alt BI-8. This alternative was developed to evaluate the impact of the longer breakwater segment lengths (600 ft) combined with smaller gaps between the segments (200 ft).

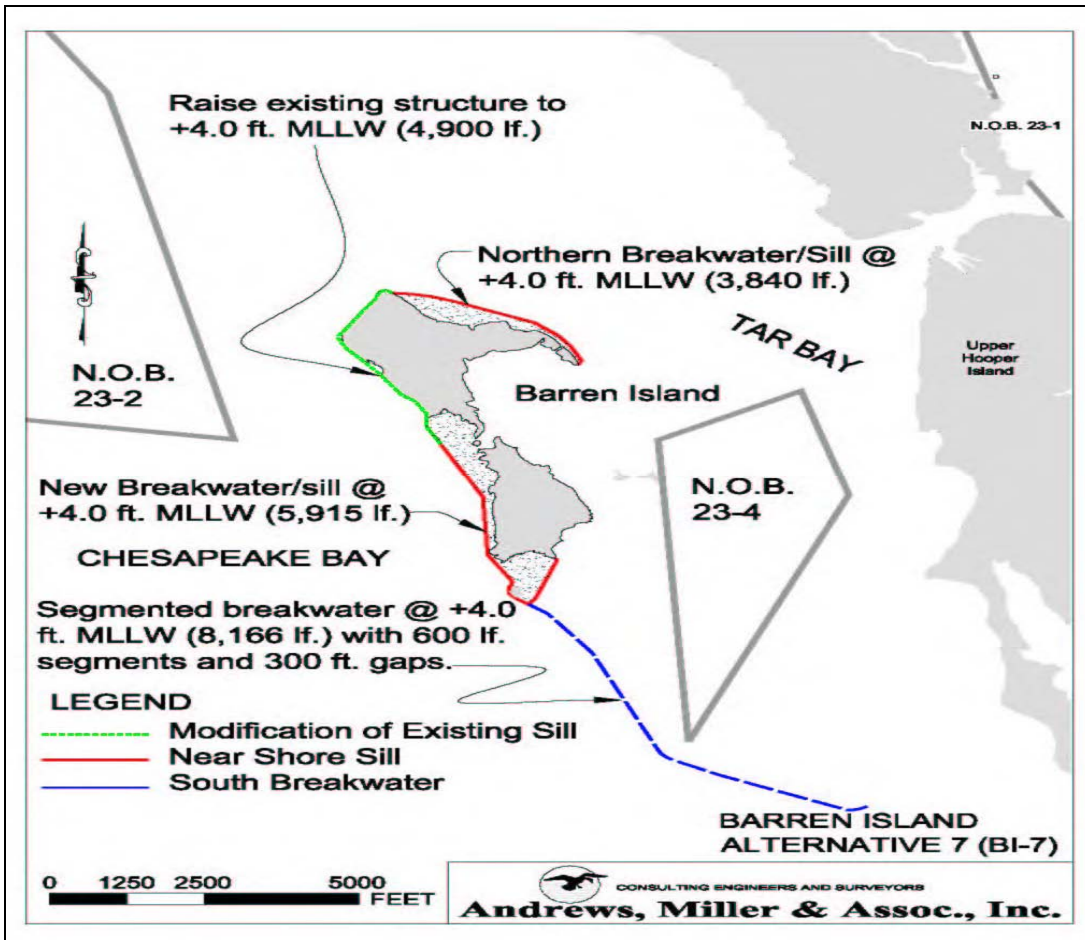


Figure C8. Barren Island Alt BI-7

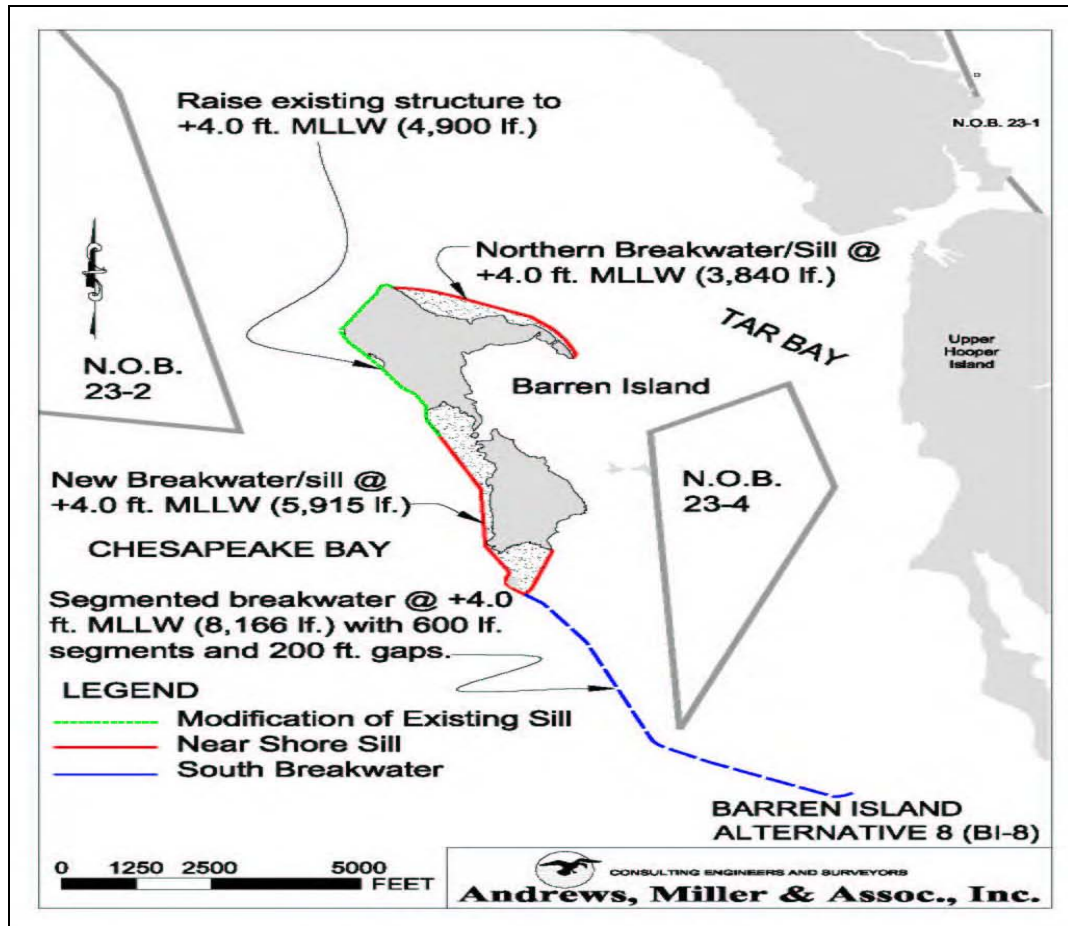


Figure C9. Barren Island Alt BI-8

Modeling of Barren Island Alts BI-7 and BI-8

Hydrodynamic and wave modeling was conducted for Alts BI-7 and BI-8 to investigate the environmental impact of these alignments; particularly in the SAV growth area.

The USACE's Inlet Modeling System (IMS) (Militello et al. 2004) was operated to evaluate the impacts to velocities for the two additional Barren Island alternatives. The IMS is an integrated modeling system for calculating hydrodynamics for coastal projects at time scales of a tidal cycle, through a series of storms, to several years. The model used for the hydrodynamic calculation is a depth-integrated, two-dimensional (2-D) finite-difference circulation model, M2D. The model M2D was developed under the Coastal Inlets Research Program conducted at ERDC, CHL. M2D is a finite-difference numerical representation of the 2-D depth-integrated continuity and momentum equations of water motion. Model pre- and post-processing was done with the Surface-water Modeling System, Version 9.0 beta.

Wave transformation modeling was performed to assess impacts of Alts BI-7 and BI-8 on adjacent SAV areas, natural oyster bars, and shorelines. The wave transformation model used was STWAVE. The model was forced with directional wave spectra based on typical wave height, period, and direction combinations. The stand-alone STWAVE model simulations include representative wave and tidal levels from two storms, Hurricane Hazel and NE20.

Hydrodynamic Modeling

The simulations for Alts BI-7 and BI-8 include representative wave and tidal levels from two storms, Hurricane Hazel (14-16 October 1954) and one northeaster, NE20 (28-31 March 1984).

The regional scale ADCIRC mesh developed by ERDC was adopted for the M2D simulations. This mesh was refined for the local Barren Island area. The M2D Cartesian grid that was generated to cover the local Barren Island area was 4,650 m by 5,800 m and consisted of 25-m square cells. The same M2D grid was used in all runs with different bathymetries and storms. The bathymetries (geometries, layouts) for the Alt BI-7 and Alt BI-8 were generated utilizing scatter sets of the mesh data associated with the ADCIRC model for Alt BI-5, provided by the respective fort.14, and (*.dep) and (*.end) files. The new bathymetries were generated by modifying the locations and elevations of the appropriate points of the scatter set, and interpolating them during the generation of the M2D grids. Figures C10 and C11 show the regional bathymetry and local scale bathymetry grid for the Barren Island area.

The water-surface elevation and velocity data were forced at the boundaries of the M2D grid through the fort.63 and fort.64 files provided by ERDC based on the regional ADCIRC runs. The IMS-M2D model control parameters that were implemented during the steered STWAVE and M2D runs included the use of the wind data for the specific storm and the location (Barren Island) and the executables for the M2D program, which were provided by ERDC.

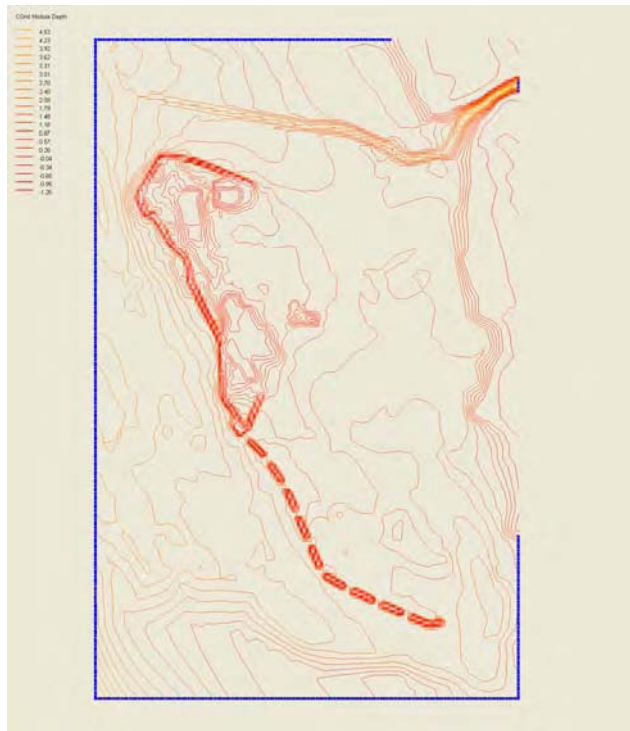


Figure C10. Alt BI-7 M2D bathymetry



Figure C11. Alt BI-7 M2D grid

The hydrodynamic simulations were conducted for each of the alternative island alignments, Alts BI-7 and BI-8. Two storms were selected for the hydrodynamic modeling, Hurricane Hazel and one moderate northeaster which occurred in March 1984 (NE20). For this hurricane and northeaster, both surface wind and pressure fields developed from the previous hydrodynamic simulations (Alts BI-1 through BI-6) were input, together with the surface wave forcing and tidal potentials at the local boundary, to the hydrodynamic model. Maximum current velocities for Alt BI-7 for NE20 and Alt BI-8 for Hurricane Hazel are shown in Figures C12 and C13, respectively.

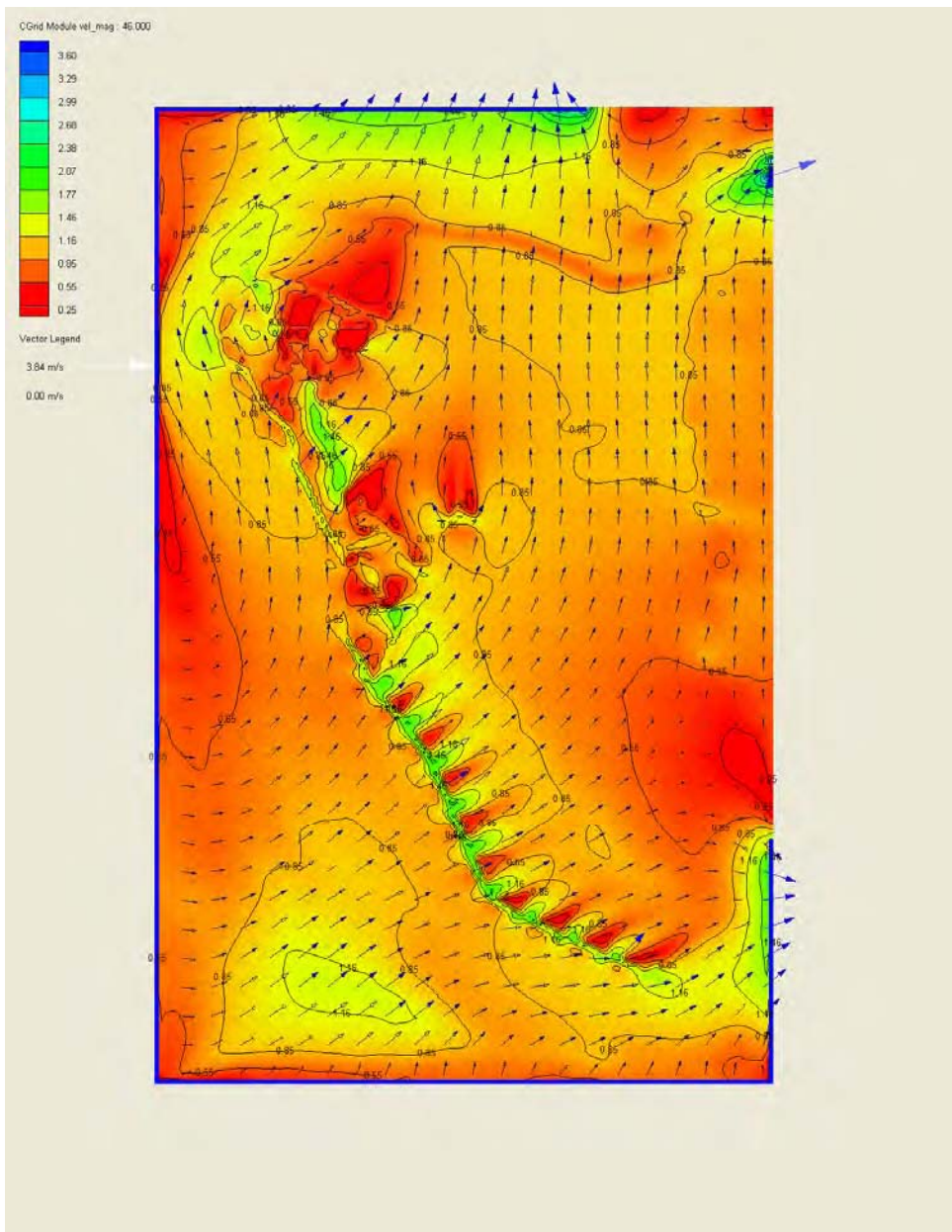


Figure C12. Alt BI-7 NE20 time-step 45 (maximum current)

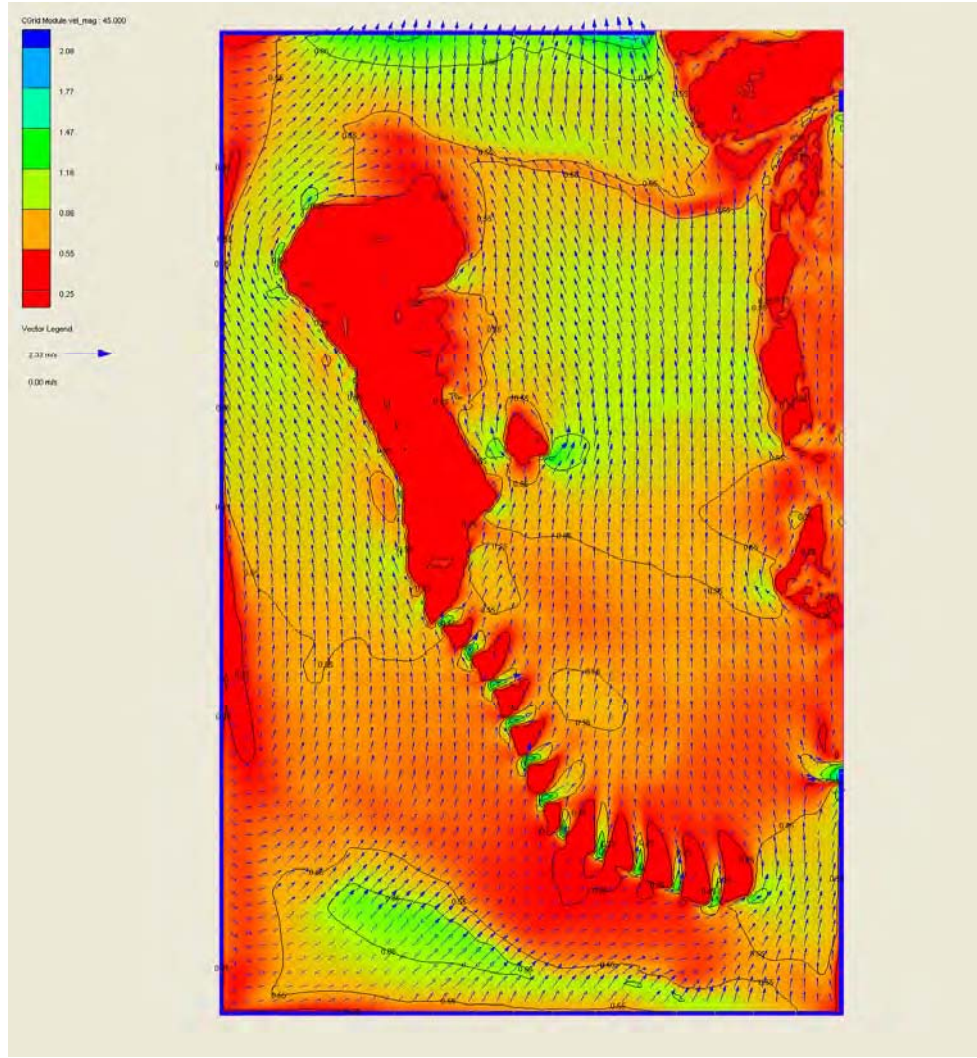


Figure C13. Alt BI-8-Hazel time-step 45 (near-maximum current)

Current Velocity Comparison

The current velocity was evaluated at several key locations selected to identify the impact on environmental resources including oyster bed and SAV areas. For Barren Island, Points 1-10 are located in the SAV area. Points 9 and 10 are located in the oyster bed. Point 1 is located in the south local channel. Figure C14 shows these key locations for Barren Island (Alt BI-6 serves as the background bottom topography). Tables C6 and C7 summarize of the maximum current velocity at Points 1-10 for the two different storms and the individual Barren Island Alts BI-7 and BI-8.

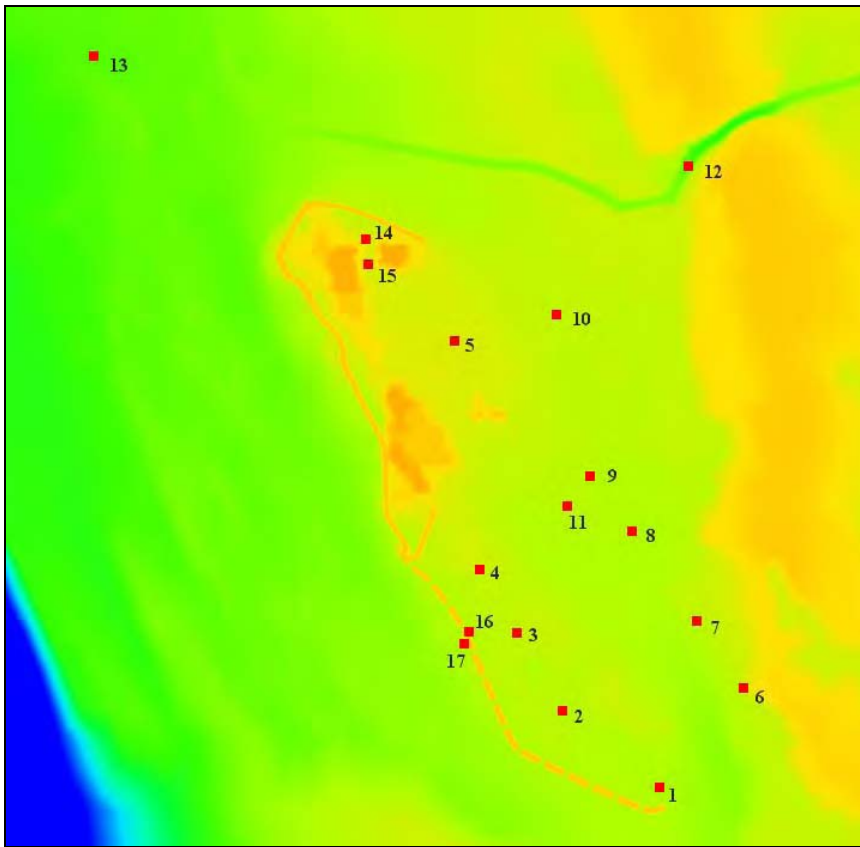


Figure C14. Barren Island output data locations

Table C6
Calculated Maximum Current Speed (ft/sec) at Barren Island During Hurricane Hazel

Location	BI-1	BI-2	BI-3	BI-4	BI-5	BI-6	BI-7	BI-8
1	3.3	3.3	3.3	3.3	3.3	3.2	2.1	1.1
2	3.2	3.3	2.9	3.3	3.3	2.3	2.8	2.0
3	3.3	3.3	3.3	3.3	3.3	2.5	2.9	2.2
4	3.3	3.3	3.2	3.3	3.3	3.3	3.7	2.0
5	3.3	3.3	3.3	3.3	3.3	3.3	2.3	2.3
6	3.4	3.4	3.4	3.4	3.3	3.4	2.7	1.5
7	3.3	3.3	3.3	3.3	3.3	3.3	1.1	1.4
8	3.3	3.3	3.3	3.3	3.3	3.3	2.0	2.1
9	3.3	3.3	3.3	3.3	3.3	3.3	2.4	2.2
10	3.3	3.3	3.3	3.3	3.3	3.3	2.7	2.9

Table C7
Calculated Maximum Current Speed (ft/sec) at Barren Island during NE20

Location	BI-1	BI-2	BI-3	BI-4	BI-5	BI-6	BI-7	BI-8
1	1.9	1.1	1.8	1.2	1.3	1.4	2.1	1.2
2	1.1	1.1	1.0	1.4	1.1	1.0	2.8	2.1
3	1.1	1.0	1.0	1.3	1.2	1.2	2.9	2.3
4	0.9	0.7	0.8	0.9	1.3	1.3	3.7	2.3
5	0.8	1.0	0.8	0.9	1.0	1.0	2.3	1.8
6	1.4	1.5	1.4	1.5	1.3	1.5	2.7	1.2
7	1.3	1.1	1.3	1.5	1.4	1.5	1.1	1.3
8	1.3	1.2	1.2	1.5	1.5	1.5	2.0	1.8
9	1.5	1.2	1.5	1.7	1.8	1.8	2.4	2.0
10	1.1	1.3	1.1	1.2	1.3	1.3	2.7	2.8

Alt BI-7. Analysis of the data in Table C6 indicates that the computed maximum current velocities for Alt BI-7 for Hurricane Hazel are similar in magnitude to Alts BI-5 and BI-6 for some of the points, but significantly lower for some of the other points. Preliminary review of the run files did not identify any specific reason for the discrepancy at these points. Further evaluation is required, to determine if there should be any differences expected when comparing computed maximum velocities from M2D/STWAVE simulations (Alts BI-7 and BI-8) with computed maximum velocities from ADCIRC simulations (Alts BI-1 through BI-6).

Analysis of the data in Table C7 indicates that the computed maximum current velocities for Alt BI-7 for NE20 are significantly greater than the computed velocities for Alts BI-5 and BI-6 for almost all of the points. Similar to the Hurricane Hazel data, preliminary review of the run files for NE20 did not identify any specific reason for the discrepancy at these points and further evaluation is required.

Alt BI-8. Analysis of the data in Table C6 indicates that the computed maximum current velocities for Alt BI-8 for Hurricane Hazel are weaker than Alts BI-5 and BI-6 for all of the points, but significantly weaker for some of the other points.

Analysis of the data in Table C7 indicates that the computed maximum current velocities for Alt BI-8 for NE20 are weaker than Alt BI-7 and similar to Alts BI-5 and BI-6 for the majority of the points, but significantly stronger for a few of the other points.

Wave Modeling

The STWAVE model was used to simulate the wave conditions for Alts BI-7 and BI-8 for two storms (Hurricane Hazel and NE20). The STWAVE grid which

was provided by ERDC utilized a 50-ft-square cell size. This cell size was maintained during the interpolation for Alt BI-7 and Alt BI-8 bathymetries.

Wave Height Comparison

Tables C8 and C9 summarize the calculated maximum wave heights at Points 1-10 for the two different storms and the individual Barren Island Alts BI-7 and BI-8.

Table C8
Calculated Maximum Wave Heights (ft) at Barren Island During Hurricane Hazel

Location	BI-1	BI-2	BI-3	BI-4	BI-5	BI-6	BI-7	BI-8
1	1.4	4.1	1.8	4.1	1.8	2.0	2.7	2.6
2	1.2	3.5	2.0	3.7	2.4	2.3	3.1	3.2
3	1.2	1.5	1.8	1.9	2.6	2.6	3.1	2.4
4	1.2	1.2	1.7	1.7	2.2	2.5	3.1	3.0
5	0.9	1.1	1.1	1.1	0.4	0.4	2.9	2.9
6	1.8	3.5	2.0	3.5	2.3	2.3	3.0	3.0
7	1.4	3.7	1.8	3.8	2.4	2.3	2.7	2.8
8	1.2	2.7	1.7	2.8	2.2	2.2	2.8	2.8
9	1.1	2.0	1.7	2.3	2.1	2.2	2.3	2.3
10	0.9	1.3	1.2	1.4	1.4	1.3	2.4	2.3

Table C9
Calculated Maximum Wave Heights (ft) at Barren Island During NE20

Location	BI-1	BI-2	BI-3	BI-4	BI-5	BI-6	BI-7	BI-8
1	0.8	2.8	0.9	2.8	1.2	1.0	1.6	1.6
2	1.3	2.3	1.0	2.4	1.6	1.4	1.7	1.7
3	1.3	1.4	1.0	1.0	1.5	1.6	1.3	0.9
4	1.0	1.0	0.9	0.9	1.3	1.5	1.2	0.9
5	0.4	0.4	0.4	0.5	0.4	0.6	0.9	0.8
6	1.3	2.4	1.0	2.3	1.4	1.2	0.9	0.8
7	1.1	2.5	0.9	2.6	1.5	1.3	1.4	1.2
8	1.0	1.6	0.8	1.6	1.4	1.3	1.0	0.9
9	0.8	1.2	0.9	1.2	1.3	1.3	0.9	0.8
10	1.5	1.5	1.5	1.5	1.7	1.7	1.1	0.8

Alt BI-7. Analysis of the data in Table C8 indicates that the computed maximum wave heights for Hurricane Hazel for Alt B-7 (with 300-ft gaps) are higher than the maximum wave heights for Alts B-5 (with 200-ft gaps) and B-6 (with 100-ft gaps) for all points. A preliminary conclusion might be that the higher wave heights could be a result of wider gaps between the breakwater segments in Alt BI-7. However, comparison of the maximum wave heights for Alt BI-5 (with 200-ft gaps) and BI-6 (with 100-ft gaps) does not show a decrease in wave height with the smaller gaps in Alt BI-6. An explanation that maximum wave heights for Alt BI-5 with 200-ft gaps are not greater than BI-6 with 100-ft gaps could be that BI-5 has a 4-ft crest elevation, whereas BI-6 has a 6-ft crest elevation. Further evaluation is required to better define the impact of the breakwater gaps and to consider the variation in breakwater segment length. In any event, it is noted that the computed maximum wave heights for Alt BI-7 for Hurricane Hazel are lower than the preliminary 1-m (3.28-ft) SAV tolerance threshold.

Analysis of the data in Table C9 indicates that the computed maximum wave heights for NE20 for Alt BI-7 (with 300-ft gaps) are lower than Alts BI-5 (with 200-ft gaps) and BI-6 (with 100-ft gaps) for the majority of the points. Longer breakwater segments in Alt BI-7 (600 ft vs. 400 ft and 500 ft in Alt BI-5 and Alt BI-6, respectively) may be the reason for the lower wave heights; particularly during NE20 with a lower storm surge, which would possibly result in lower wave heights with longer breakwater segments. It is noted that the computed wave heights for Alt BI-7 for NE20 are significantly lower than the 1-m (3.28-ft) SAV tolerance threshold.

Alt BI-8. Analysis of the data in Table C8 indicates that the computed maximum wave heights for Hurricane Hazel for Alt BI-8 (with longer, 600-ft segments and 200-ft gaps) are higher than Alts BI-5 (with 400-ft segments and 200-ft gaps) and BI-6 (with 500-ft segments and 100-ft gaps) for essentially all of the points. The computed maximum wave heights for Alt BI-8 are generally lower than Alt BI-7 (with 600-ft segments and 300-ft gaps), which would be expected. Further evaluation is required to better define the impact of the breakwater segment lengths and gaps combinations and to verify that the modeling procedures are consistent. However, it is also noted that the computed wave heights for Alt BI-8 for Hurricane Hazel are lower than the preliminary 1-m (3.28-ft) SAV tolerance threshold.

Analysis of the data in Table C9 indicates that the computed maximum wave heights for NE20 for Alt BI-8 are lower than Alts BI-5 (with 400-ft segments and 200-ft gaps) and BI-6 (with 500-ft segments and 100-ft gaps) for the majority of the points as well as lower than Alt BI-7. The computed maximum wave heights for Alt BI-8 for NE20 are significantly lower than the 1-m (3.28-ft) SAV tolerance threshold.

Summary

Results from the wave and hydrodynamic models were analyzed to evaluate the performance of the Barren Island alternatives listed in Table C10.

Table C10
Barren Island Alternatives

Alternative	Description
BI-1	8,166-ft-long south breakwater at +6 ft mllw.
BI-2	5,915-ft-long south breakwater at +6 ft mllw.
BI-3	8,166-ft-long south breakwater at +4 ft mllw.
BI-4	5,915-ft-long south breakwater at +4 ft mllw.
BI-5	8,166-ft-long south breakwater at +4 ft mllw with 400-ft segments and 200-ft gaps.
BI-6	8,166-ft-long south breakwater at +4 ft mllw with 500-ft segments and 100-ft gaps.
BI-7	8,166-ft-long south breakwater at +4 ft mllw with 600-ft segments and 300-ft gaps.
BI-8	8,166-ft-long south breakwater at +4 ft mllw with 600-ft segments and 200-ft gaps.

As discussed in the main text, for the Barren Island alternatives, Alts BI-1 and BI-3 with a longer southern breakwater, show the best wave height reduction by 2 to 3 ft in the lee of the island for the four storms. Alts BI-3 and BI-4 with the low-crest southern breakwater are likely to create large current velocity, causing strong bottom erosion at the breakwater. Segmented breakwater (Alts BI-5 and BI-6) can create a similar condition with strong current velocity around the segmented breakwater element, causing more sediment deposition and erosion at the breakwater.

From an SAV tolerance perspective, there does not appear to be a significant difference in the current velocities in the SAV areas (Points 6–9) for the various alternatives during the storms simulated. The current velocities for all of the alternatives appear to be less than the preliminary 1 m/sec (3.3 ft/sec) SAV tolerance threshold. Further evaluation at points closer to the breakwaters is required to evaluate potential impacts on intermittent SAV in those areas.

There is a significant difference in wave height in the SAV areas for the various alternatives, with the continuous southern breakwater alternatives (Alts BI-1 and BI-3) providing lower wave height in the SAV area than the segmented southern breakwater alternatives (Alts BI-5 - BI-8). However, the wave heights for all of the alternatives appear to be less than the preliminary 1-m (3.28-ft) SAV tolerance threshold.

Conclusions and Recommendations

Based on the evaluation of the hydrodynamic modeling and the wave modeling results conducted in this study, it appears that segmented breakwaters should be considered further for the southern breakwater during the preconstruction and engineering design process. Substantial construction cost savings could be realized in comparison with a continuous breakwater, as well as other potential environmental benefits such as enhanced current circulation and reduced water temperature in the SAV area. Wave transmission through overtopping, transmission through the breakwaters, and diffraction need to be evaluated in more detail. Rigorous tidal current, wave transmission, and sedimentation modeling should be conducted to evaluate the impacts of various breakwater segment lengths, crest elevation, and gap widths between the segments.

to establish the optimum design to reduce currents, waves, and sedimentation to tolerable levels for SAV.

A more comprehensive investigation to determine the tolerance of SAV to tidal currents, waves, and sedimentation should be conducted based on ongoing research and physical modeling similar to the modeling conducted by UM CES.

REPORT DOCUMENTATION PAGE

*Form Approved
OMB No. 0704-0188*

Public reporting burden for this collection of information is estimated to average 1 hour per response, including the time for reviewing instructions, searching existing data sources, gathering and maintaining the data needed, and completing and reviewing this collection of information. Send comments regarding this burden estimate or any other aspect of this collection of information, including suggestions for reducing this burden to Department of Defense, Washington Headquarters Services, Directorate for Information Operations and Reports (0704-0188), 1215 Jefferson Davis Highway, Suite 1204, Arlington, VA 22202-4302. Respondents should be aware that notwithstanding any other provision of law, no person shall be subject to any penalty for failing to comply with a collection of information if it does not display a currently valid OMB control number. **PLEASE DO NOT RETURN YOUR FORM TO THE ABOVE ADDRESS.**

1. REPORT DATE (DD-MM-YYYY) August 2006			2. REPORT TYPE Final report			3. DATES COVERED (From - To)		
4. TITLE AND SUBTITLE Mid-Bay Islands Hydrodynamics and Sedimentation Modeling Study, Chesapeake Bay			5a. CONTRACT NUMBER					
			5b. GRANT NUMBER					
			5c. PROGRAM ELEMENT NUMBER					
6. AUTHOR(S) Walter J. Dinicola, Edward T. Fulford, Mathew R. Henderson, Nicholas C. Kraus, Lihwa Lin, Ram K. Mohan, Mark Reemts, Ann R. Sherlock, Jane M. Smith, and Oner Yucel Editor Nicholas C. Kraus			5d. PROJECT NUMBER					
			5e. TASK NUMBER					
			5f. WORK UNIT NUMBER					
7. PERFORMING ORGANIZATION NAME(S) AND ADDRESS(ES) Coastal and Hydraulics Laboratory, U.S. Army Engineer Research and Development Center, 3909 Halls Ferry Road, Vicksburg, MS 39180-6199; Andrews, Miller, and Associates, Inc., 508 Maryland Avenue, Cambridge, MD 21613; Blasland, Bouck & Lee, Inc., 326 First Street, Suite 200, Annapolis, MD 21403			8. PERFORMING ORGANIZATION REPORT NUMBER ERDC/CHL TR-06-10					
9. SPONSORING / MONITORING AGENCY NAME(S) AND ADDRESS(ES) U.S. Army Engineer District, Baltimore, 10 South Howard Street, Baltimore, MD 21201; Maryland Port Administration, 2310 Broening Highway, Baltimore, MD 21224			10. SPONSOR/MONITOR'S ACRONYM(S)					
			11. SPONSOR/MONITOR'S REPORT NUMBER(S)					
12. DISTRIBUTION / AVAILABILITY STATEMENT Approved for public release; distribution is unlimited.								
13. SUPPLEMENTARY NOTES								
14. ABSTRACT James Island and Barren Island, in Maryland waters, are among the few remaining eastern shore islands in mid-Chesapeake Bay. Both islands are eroding at a rapid rate due to wave and storm action, as well as to relative sea level rise. These two islands are considered as potential candidate restoration sites as a beneficial use of clean dredged material from the Baltimore Harbor and Channels Federal Navigation Project. The island restoration project requires the construction of protective dikes to contain the dredged material. The restoration work should provide efficient protection to the existing islands, shelter sandy beaches and the shoreline from severe erosion, and improve water quality and surrounding environment for submerged aquatic vegetation. This report describes establishment and operation of a suite of numerical models to evaluate alternative designs as an initial study for restoration and modification of James Island and Barren Island. The predicted wave climate along the mainland shore was also estimated for the alternatives. Both typical and storm hydrodynamic conditions were assessed. In support of the numerical modeling, sediment samples were taken and bathymetric surveys made in key areas, together with assemblage of relevant data sets such as aerial photographs of the shoreline, wind, and presence and vulnerability of submerged aquatic vegetation. Data from the modeling and other data sets assembled and collected were compiled on a DVD.								
15. SUBJECT TERMS Baltimore Harbor Barren Island			Beneficial uses of dredged material Chesapeake Bay James Island			Maryland Numerical modeling		
16. SECURITY CLASSIFICATION OF:			17. LIMITATION OF ABSTRACT	18. NUMBER OF PAGES	19a. NAME OF RESPONSIBLE PERSON			
a. REPORT UNCLASSIFIED	b. ABSTRACT UNCLASSIFIED	c. THIS PAGE UNCLASSIFIED			19b. TELEPHONE NUMBER (include area code)			
				186				